EXAMINING HOW STAPHYLOCOCCUS AUREUS ENGAGES THE SULFUR REGULON TO MEET NUTRITIONAL DEMANDS

By

Paige Jennifer Kies

A DISSERTATION

Submitted to
Michigan State University
in partial fulfillment of the requirements
for the degree of

Microbiology and Molecular Genetics – Doctor of Philosophy

2023

ABSTRACT

The age of antimicrobial resistance has driven a sharp demand for new routes that inhibit opportunistic pathogens such as *Staphylococcus aureus*. In response to this has been a steady rise in research characterizing pathways essential to pathogen proliferation, such as those relating to essential nutrient acquisition and metabolism. *S. aureus* employs a flexible metabolism that promotes colonization throughout most mammalian tissues. This characteristic, combined with an ability to develop antibiotic resistance, incites nosocomial infections that range from skin and soft tissue infection to osteomyelitis. Regarding essential nutrients, the foundation for *S. aureus* metabolism for the critical element sulfur is still being molded. The current thesis provides a series of investigations that expand our understanding of how *S. aureus* engages sulfur metabolism to meet nutritional demands.

Expression of the machinery involved with sulfur acquisition and catabolism is under control of the transcriptional repressor, CymR. We investigate the transcriptional response of *S. aureus* to varying states of sulfur supplementation *in vitro* with a special focus on the sulfur regulon. We note that during sulfur starvation there is both a CymR-dependent and -independent response that occurs; notably, the majority of differentially expressed genes during sulfur depletion are influenced by the presence of CymR. Found within the sulfur starvation response is the upregulation of iron metabolism and oxidative stress response genes. Glutathione was used to exemplify this observed connection between sulfur, iron, and oxidative stress—the *S. aureus* sulfur source also protects against toxic levels of heme (iron source) and the oxidative stressor, H_2O_2. We further show that *S. aureus* expresses unique responses when exposed to organic (cysteine, reduced and oxidized glutathione) and inorganic (thiosulfate) sulfur sources. With this

series of transcriptomics, the **t**hio**s**ulfate **u**ptake protein **A** (TsuA) is shown as the sole importer associated with growth on thiosulfate as a sulfur source. Interestingly, each sulfur source induced upregulation of sulfur-associated transporters, suggesting that regulatory actions within the sulfur regulon are more complex than previously appreciated.

Upon examination of the sulfur regulon, we next focused on the redundancy surrounding transportation mechanisms of *S. aureus* sulfur sources. Glutathione is one example, having at least two associated transporters in this pathogen. We identify that the di-tripeptide transporter, DtpT, supports proliferation of *S. aureus* on nutritional glutathione. This line of inquiry also describes cysteinyl-glycine, the glutathione breakdown product, as a DtpT-mediated sulfur source for *S. aureus*. DtpT contributions to *S. aureus* physiology is likewise demonstrated through its impact on colonization of the murine liver.

We also initiated a new field of study that characterizes the distribution of host sulfur sources using matrix-assisted laser desorption/ionization imaging mass spectrometry. With this technique we confirm the presence of several known sulfur sources during *S. aureus* infection of the murine kidney, including reduced and oxidize glutathione as well as cysteinyl-glycine. An additional metabolite, cysteine-glutathione mixed disulfide, was found to be highly abundant in the *S. aureus*-infected kidney. We establish that this compound is a sulfur source for this organism and that growth on cysteine-glutathione disulfide is associated with three transporters: the glutathione import system (GisABCD) as well as the cysteine/cystine transporters, TcyABC and TcyP. This work is concluded with thoughts surrounding future research which, alongside the data presented here, will further enhance our understanding of the nutritional sulfur interface between the host and pathogen during *S. aureus* infection.

This thesis is dedicated to those who have supported me.
Thank you for helping me make dreams a reality.

ACKNOWLEDGMENTS

I would like to begin by expressing my heartfelt gratitude to my mentor, Dr. Neal Hammer. His exceptional guidance and the nurturing environment he provided have been instrumental in fostering my confidence and honing my skills as a scientist. I am immensely thankful for his unwavering support and encouragement to challenge myself! My committee members, Drs. Sean Crosson, Robert Quinn, Gemma Reguera, and Chris Waters, have also made fundamental contributions to my development as a scientist. I am thankful for all of their invaluable insights over the years, which have nurtured my critical thinking skills and overall scientific abilities. I also want to extend my appreciation to all the members of the Hammer laboratory, both current and past. Nick, Jessica, and Gabby have not only been fantastic colleagues but have also contributed to creating a relaxed and enjoyable lab atmosphere. I'd like to offer special recognition to the undergraduates I've had the privilege of working with during my time at Michigan State University: Abigail Kuplicki, Emily Cleary, Jessica Liu, and Rosemary Northcote. Learning how to be an effective mentor is an ongoing process that demands time, patience, understanding, and open communication from all parties involved. I'm truly thankful to each undergraduate who has assisted me in my journey toward becoming a better mentor. A special mention goes to Rosemary for her dedicated benchwork assistance during the crucial period leading up to my defense. She's an exceptional individual with a bright future ahead in her own graduate career, and I wish her nothing but the best!

My fellow graduate students and post-doc in the lab provided a support and camaraderie which was indispensable throughout my graduate school journey. Joelis Lama Díaz, with boundless energy and a gift for bringing out the best in everyone, played

a crucial role in helping our lab break out of its shell. I am especially grateful to Joelis for generously allowing me to include her *S*-lactoylglutathione data in Figure 4.3 of this dissertation. Troy Burtchett, a true embodiment of the term “cool as a cucumber”, remained unflappable under all circumstances and kept the lab entertained with his reservoir of dad jokes. Cristina Kraemer Zimpel, an amazing post-doc in the lab, has been a constant source of guidance as I wrap up my tenure at MSU. I can't express enough how much I value her assistance, from training me on RNAseq analysis for Chapter 2 to creating a phylogenetic tree for Chapter 3. Rajab Curtis, a former PhD student in the lab who joined the program alongside me, has been an incredible peer on this journey. We've faced numerous challenges together, and I couldn't have asked for a better bench buddy during the pandemic. I've always enjoyed our discussions, whether they revolved around scientific theories or the playlists on Rajab's Spotify. Lastly, Beth Ottosen...she's simply the best, or should I say the 'be(th)st'? While Beth only rotated in the lab, she became my closest friend here in Michigan and has stood by me through every obstacle, often with a pop-tart in hand.

The Department of Microbiology and Molecular Genetics at MSU is home to a remarkable group of individuals who consistently provide unwavering support for one another. I must extend my gratitude to Roseann Bills from the MMG office, who has been instrumental in guiding me through the intricacies of graduate school's technical aspects. I would have undoubtedly found myself lost on numerous occasions if it weren't for her irreplaceable help. The fifth floor of BPS holds a special place in my heart. I cannot begin to express how many times someone on this floor came to my aid, whether it was by providing a much-needed reagent, lending a friendly ear for scientific discussions, or

simply stopping for a quick chat. I consider myself incredibly fortunate to have pursued my graduate studies within this department.

I additionally want to thank my family and friends. They always say it takes a village and I firmly believe in that sentiment. My extended family members, who have checked in on me throughout the years, always brought a warm smile to my face and provided the encouragement I needed during tough times. I also want to acknowledge the incredible support I've received from two dear friends, Emily Baldwin and Akshaya Warrier, who have remained with me over many years, reaching out and forever encouraging me during our many video chats. My sister, Lily, played a crucial role in reminding me that life exists beyond graduate school, often through phone calls and conversations about topics unrelated to my work! She too is one of my oldest supporters and I cannot thank her enough for that. I would also like to recognize my brother Ben and his wife, Kami, for all their efforts in helping me set up the next chapter of my life in Minnesota.

Above all, I want to express my deepest gratitude to my parents. No words can adequately capture the depth of my love for them. They both worked tirelessly to ensure that I had the opportunity to attend college, setting me on a life path that has consistently exceeded my expectations. My parents offered unwavering support throughout my journey. I can't fathom where I would be without them.

TABLE OF CONTENTS

CHAPTER 1: A resourceful race: bacterial scavenging of host sulfur metabolism during colonization

Work presented within this chapter has been published as: Kies PJ, Hammer ND. 2022. A Resourceful Race: Bacterial Scavenging of Host Sulfur Metabolism during Colonization. Infect Immun 90:e00579-21.

ABSTRACT

Sulfur is a requirement for life. Therefore, both the host and colonizing bacteria must regulate sulfur metabolism in a coordinated fashion to meet cellular demands. The host environment is a rich source of organic and inorganic sulfur metabolites that are utilized in critical physiological processes such as redox homeostasis and cellular signaling. As such, modulating enzymes dedicated to sulfur metabolite biosynthesis plays a vital role in host fitness. This is exemplified from a molecular standpoint through layered regulation of this machinery at the transcriptional, translational, and posttranslational levels. With such a diverse metabolite pool available, pathogens and symbionts have evolved multiple mechanisms to exploit sulfur reservoirs to ensure propagation within the host. Indeed, characterization of sulfur transporters has revealed that bacteria employ multiple tactics to acquire ideal sulfur sources, such as cysteine and its derivatives. However, bacteria that employ acquisition strategies targeting multiple sulfur sources complicate *in vivo* studies that investigate how specific sulfur metabolites support proliferation. Furthermore, regulatory systems controlling the bacterial sulfur regulon are also multifaceted. This too creates an interesting challenge for *in vivo* work focused on bacterial regulation of sulfur metabolism in response to the host. This Chapter examines the importance of sulfur at the host-bacterium interface and the elegant studies conducted to define this interaction.

INTRODUCTION

Bacteria impact the health of complex, multicellular organisms such as humans. This concept is well recognized and remains an area of intense scientific study. One focal point within this domain is understanding the nutritional relationship between the host and colonizing bacteria (i.e., pathogens or symbionts). Over the past few decades, there has been exceptional progress in describing the dynamic host-bacterium interplay surrounding essential nutrients such as iron, magnesium, manganese, zinc, and carbon (1–3). Sulfur is another such essential nutrient that has started to receive more attention regarding its impact on bacteria during colonization.

Within biological systems, sulfur is largely stored as a thiol group (R-SH) within organosulfur compounds. Due to the reactive property of sulfur, thiols partake in numerous cellular reactions, a characteristic that demands cells maintain an optimal supply of this nutrient (4). At the center of sulfur metabolism and distribution within a cell is the amino acid cysteine (Cys). In fact, intracellular Cys concentrations indicate whether a cell has sufficient quantities of sulfur. When Cys levels are below the threshold, cells import exogenous sulfur-containing metabolites and assimilate them to Cys. From there, Cys contributes to cellular processes such as maintenance of protein structure or ion coordination, synthesis of critical metabolic cofactors (e.g., coenzyme A, biotin), and redox balance (5–9). Here, we will discuss the diverse nutritional sulfur reservoir generated through host sulfur metabolism and the strategies bacteria utilize to exploit this diversity to meet the sulfur requirement during colonization.

HOST SULFUR METABOLISM

Given the essential nature of sulfur, it can be hypothesized that the host modulates sulfur metabolism in response to bacterial colonization. However, to our knowledge there are no investigations that directly support this hypothesis. Thus, to address whether and how the host alters sulfur metabolism during infection, it becomes pertinent to first understand metabolism of this element from the perspective of a healthy host. As more information is presented regarding the host-pathogen nutritional sulfur interface, models then can be developed that reflect how these pathways operate during various types of infections. Furthermore, understanding how the host controls flux of sulfur during infection will require investigating alterations of enzymatic expression or activity within sulfur metabolism pathways, generating further interest for discussion of the proteins involved in sulfur distribution. Consequently, we will (i) briefly describe enzymatic pathways involved in generating sulfur-containing metabolites that are known sources of nutrient sulfur for bacteria and illustrate their diverse regulatory systems, (ii) address the contribution of pathways or enzymes to host physiology, and (iii) consider the consequences that arise from dysfunction of the major enzymes within these pathways.

Transmethylation and reverse transsulfuration pathways. As the fulcrum of sulfur metabolism, free Cys can be synthesized from methionine via the transmethylation pathway (Fig. 1.1, orange) (10). The product of transmethylation, homocysteine, is subsequently used as a substrate in the reverse transsulfuration pathway, which requires the critical enzymes cystathionine β-synthase (CBS) and cystathionine γ-synthase (CSE; Fig. 1.1, green) (11–13). In animals this pathway is irreversible, meaning neither methionine nor homocysteine is produced from Cys. As the final product, Cys can

autoxidize to cystine (CSSC) or be acetylated, forming *N*-acetylcysteine (NAC) (Fig. 1.1, asterisk). Furthermore, reverse transsulfuration may flux such that Cys undergoes CBS- or CSE-mediated desulfhydration, resulting in production of hydrogen sulfide (H_2S) and, in the case of CBS, a net loss of homocysteine (11). A common thread is that the enzymes participating in these two pathways are widely distributed, if not ubiquitous, throughout mammalian tissues (Table 1.1). In general, though, the pathways are predominantly active in the liver or kidney. In keeping with their importance to host physiology, products and substrates of the trans-methylation and reverse transsulfuration pathways are established sources of nutrient sulfur for symbiotic and pathogenic bacteria (14) (Figure 1.1, boldface, underlined).

As a consequence of their expansive tissue localization, CBS and CSE regulation is complex. These two proteins are constitutively expressed in most cell types with a layered regulation system, from gene expression to posttranslational modifications, that determines enzyme concentrations throughout the host (15–18). As a result, CBS is abundant in the liver, brain, kidney, and pancreas compared to moderate expression in the muscles, endocrine, heart, or lungs. CSE also displays higher expression in the liver and kidney. In contrast to CBS, CSE is more prevalent in the cardiovascular system as well as the lungs and in the brain (15–18). Transmethylation and reverse transsulfuration enzymes as a whole localize to the cytosol of cells under normal conditions. However, some of the enzymes may move to other organelles under specific circumstances. CBS and CSE, for instance, can both be relocated to the mitochondria under conditions such as hypoxia (CBS) or an increase of intracellular Ca^{2+} (CSE) (19).

Dysfunction within either pathway leads to serious host impairments, another overarching theme of host sulfur metabolism. For example, *S*-adenosylmethionine (SAM) accumulation from disrupted methionine adenosyltransferase (MAT) in the transmethylation pathway contributes to an array of ailments such as methionine accumulation in the blood (i.e., hypermethioninemia), neurodegenerative diseases (e.g., Parkinson), and cancer (20). Dysfunction of CBS and CSE are also associated with disease (15–17). CBS is known to be upregulated in Down syndrome and in breast, colon, or liver cancers. Additionally, some naturally occurring mutations in CBS render the host incapable of metabolizing methionine, a disease known as homocystinuria. This leads to a buildup of homocysteine, leading to a condition known as hyperhomocysteinemia. Continuing this trend, decreased CSE activity contributes to a variety of host maladies, including those with diabetes, asthma, or chronic kidney disease. On the other hand, increased CSE activity also causes hyperhomocysteinemia.

The γ-glutamyl cycle. Cys can be stored within the stable tripeptide, glutathione (GSH). This versatile low-molecular-weight thiol consists of γ-glutamate-cysteine-glycine and can reach millimolar concentrations within a cell (12, 21). The γ-peptide bond between glutamate and Cys can only be cleaved by select enzymes such as γ-glutamyl transpeptidase (GGT) to ensure a controlled Cys repository within the host (12, 22–24).One benefit from this strategy is increased control over the generation of reactive oxygen species (ROS) that result when Cys autoxidizes to CSSC. However, if Cys must be replenished, GSH can be catabolized via the γ-glutamyl cycle (Figure 1.1, blue) (25–27). Interestingly, the dipeptide formed in this pathway, cysteinyl-glycine (Cys-Gly), is not solely dedicated to the γ-glutamyl cycle, as it is thought to impact the redox status of the

plasma (28–30). This supports the notion that thiol-containing compounds participate in multiple aspects of host physiology.

Given the impact of this cycle (discussed below), the presence of GSH catabolism enzymes in most or all host tissues is unsurprising (Table 1.1). As described above with the reverse transsulfuration enzymes CBS and CSE, the host exerts a complex regulation system for expression of proteins in this aspect of the γ-glutamyl cycle. GGT, a well-studied example, is constitutively expressed with transcriptional control exerted through the use of multiple promoters for the corresponding gene; this encourages selective expression throughout different host-tissue environments (31, 32). Furthermore, translational regulation at the mRNA 5' end acts as a second layer of management for GGT production across different tissues (31). Within mammalian hosts, this results in GGT being highly expressed in regions such as the kidney (particularly the proximal tubule), pancreas, intestine, brain capillaries, or various types of white blood cells (33, 34). As expected, GGT expression is comparably low in the liver, given that this organ is the main site for GSH production (33, 34). As is typical of any enzyme with major contributions to host physiology, dysregulation of GGT imposes health disorders. In fact, alterations to GGT concentrations have long been associated with increased cardiovascular disease (35–39). GGT levels in the liver are also used as a marker for one of the most common ailments for the organ, nonalcoholic fatty liver disease (NAFD) (40, 41). Synthesis of GSH from Cys and/or NAC precursors completes the γ-glutamyl cycle (Figure 1.1, blue) (42, 43). Continuing the concept of multifactorial expression, production of glutamate-cysteine ligase (GCL) and GSH synthase is influenced at the posttranscriptional and translational levels. As this is a well-reviewed area, information regarding GSH synthesis enzyme

expression and dysfunction is provided from the following review (42). As a select example, we consider the similar features of GCL and GSH synthase expression. Gene activity for both increases in response to a variety of compounds, such as tumor necrosis factor (TNF-alpha) or hepatocyte growth factor (HGF), in cultured rat hepatocytes. Furthermore, expression of both GCL and GSH synthase partially involves activator protein (AP-1), whose activity is induced by TNF-alpha. However, bear in mind that there are a number of other transcription factor binding sites located at the promoters of these genes, such as an ARE consensus sequence (GCL) or nuclear factor erythroid 2 motif (GSH synthase). Additionally, it is noteworthy that hydrogen peroxide (H_2O_2)-induced oxidative stress increases GCL transcription as well. Although GSH synthesis occurs in most host tissues (e.g., kidney, pancreas, lungs, plasma, or brain), its production is highest in the liver, indicating robust activity of GSH synthase, GCL, or even GSH reductase (GR), which reduces oxidized GSH (GSSG) (Figure 1.1, blue) (44–46). Dysfunction of GSH biosynthesis enzymes contributes to a number of host diseases (42). Polymorphisms in GCL can contribute to decreased cardiovascular health or asthma; decreased expression of this protein complex is known to contribute to disorders such as cystic fibrosis or alcoholic liver injury. Additionally, buildup of γ-glutamylcysteine in those with GSH synthase deficiency can have impacts on the central nervous system or result in conditions such as hemolytic anemia. Given that GSH contributes immensely to host physiology beyond the role of Cys storage, it is important to discuss some of its additional roles. Importantly, GSH is a major detoxification metabolite. GSH combats ROS stress, particularly H_2O_2, through its own oxidation via GSH peroxidase (Figure 1.1, blue, GP) (47). This is an important reaction given that H_2O_2 endogenously results from

mitochondrial respiration and can lead to hydroxy radical formation (48). Furthermore, GSH is the substrate for GSH *S*-transferases, which detoxify electrophilic xenobiotics by conjugating GSH to the harmful metabolite (12, 22, 48). These enzymes are also greatly expressed in the liver compared to other tissues, making the organ a critical site of GSH metabolism. Changes to protein activity can also result from the process of glutathionylation (49). In this instance, the GSH reduced-to-oxidized ratio influences *S*-glutathionylation of protein Cys residues. Considering this, it is easy to see how malfunction of GSH synthesis and catabolism enzymes result in a variety of host disorders, epitomizing the vital impact of the γ-glutamyl cycle on host physiology.

Taurine and sulfate biosynthesis. Aside from GSH, Cys is also a precursor for synthesis of the nonproteinogenic amino acid taurine and inorganic sulfate (Figure 1.1, pink) (18, 50–54). Note that in this pathway, glutamate oxaloacetate transaminase (GOT) is also known as cysteine aminotransferase (CAT) or aspartate aminotransferase (AST) due to its ability to bind cysteinsulfinate, cysteine, and aspartate. Typically GOT nomenclature is associated with taurine or sulfate biosynthesis, whereas CAT is linked to H_2S synthesis (see below). As such, this protein will be denoted GOT/CAT. Taurine, though it does not directly contribute to protein synthesis, is one of the most abundant amino acids throughout host organs and has a multitude of functions. For example, it is known for its participation in bile acid formation and controls intracellular Ca^{2+} levels as well as alleviating glutamate toxicity in the brain (50). Sulfate also contributes to important cellular reactions within the host. Similar to GSH, sulfate conjugation is an important step in the activation/detoxification of exogenous and endogenous compounds, such as steroids or xenobiotics (55). Maintenance of cysteine dioxygenase (CDO) is imperative,

as it contributes to the balance of Cys levels and ensures production of taurine and sulfate as the first synthetic step of these two metabolites. Unlike other enzymes discussed, CDO is unique in that the prevalence of this enzyme is more heavily influenced by diet than gene expression: when Cys from ingested protein is abundant, CDO is as well (56). This compares to increased CDO ubiquitination and degradation when Cys is scarce (i.e., in a lower protein diet). The CDO-deficient murine line underscores the impact of this protein on host physiology, as these mice have a high postnatal mortality rate, growth impairment, and connective tissue pathology (57). With this in mind, it is interesting to speculate how the scavenging of Cys by a colonizing bacterium might adversely affect CDO abundance and the resulting effects on taurine and sulfate biosynthesis.

H_2S production and oxidation. Cys also contributes to formation of H_2S (Figure 1.1, black) (58–61). It is noteworthy that CBS and CSE activity within cells are also major sources of H_2S production during Cys desulfhydration (11, 62). H_2S is an increasingly studied gaseous signaling molecule. It is a neurotransmitter with implicated roles in vasorelaxation, angiogenesis, inflammation, oxygen sensing, and cytoprotection (63–70). However, H_2S can also be toxic to mammals, perhaps being most infamously known for its inhibitory effects on mitochondrial cytochrome *c* oxidase (71). With this assorted influence on host physiology, regulation of H_2S is critical. Thus, H_2S concentrations are tightly controlled and as a result become a hub for thiosulfate and sulfate production, which are also known inorganic sulfur sources for colonizing bacteria. Both of these sulfur compounds may be generated as a result of H_2S oxidation in the mitochondria (Figure 1.1, purple) (72–74). Interestingly, the oxidation product thiosulfate can replenish this H_2S pool (Figure 1.1, red) (75–77). Therefore, thiosulfate plays an integral role in production and

break-down of H_2S within the host. Thiosulfate also detoxifies cyanide, underscoring its importance to management of volatile compounds (78). Due to this activity, thiosulfate is commonly administered to those with acute cyanide poisoning (75). H_2S toxicity necessitates that its production is strictly controlled; this is demonstrated best by the previously described layered regulation of CBS, CSE, and other enzymes involved in H_2S production. Naturally, H_2S catabolism is a notable step of regulation for sulfur metabolism. Sulfide-quinone oxidoreductase (SQR) represents the first enzymatic step in H_2S oxidation in the mitochondria, and activity of this enzyme contributes to normal function of this organelle in the model eukaryotic organism *Schizosaccharomyces pombe* (79). In vertebrates, SQR has been identified in the kidney, liver, heart, colon, podocytes, and even leukocytes (Table 1.1) (80). Although less is known about the regulation of SQR, it has been demonstrated that H_2S increases expression of this enzyme (80, 81). On the other hand, Cys reduces transcriptional levels of SQR, which emphasizes its involvement in host sulfur metabolism (79). As with CDO, it is interesting to consider whether scavenging of Cys by bacterial colonizers influences SQR expression in the host. It has recently been reported that deleting SQR results in mitochondrial dysfunction due to cysteine deficiency in *S. pombe* (79). Given the importance of SQR in yeast, it is somewhat unsurprising that studies are beginning to link defects in this enzyme to mammalian disease as well. It has been proposed that altered SQR activity contributes to reduced H_2S concentrations observed in people afflicted with Alzheimer's disease or ethylmalonic encephalopathy (80, 82, 83). Furthermore, an association between SQR overexpression and postmenopausal osteoporosis has been implicated (84, 85). Collectively, these facts illustrate the vital nature of sulfur metabolism enzymes and the diverse ways in which they

impact the host. Additionally, determining whether and how sulfur scavenging by a colonizing bacterium encourages or exacerbates host diseases associated with dysfunctional sulfur metabolism will be of immense value to the health care system.

COLONIZING BACTERIA EMPLOY MULTIPLE STRATEGIES TO ACCESS THE DIVERSEHOST SULFUR RESERVOIR.

A colonizing bacterium must acquire essential nutrients using metabolites available in a dynamic environment. This point is emphasized in a previous review that discusses the wide range of sulfur acquisition strategies employed by bacterial pathogens (14). However, different host tissues present various concentrations or types of sulfur metabolites that bacteria are capable of catabolizing (Figure 1.1, boldfaced and underlined). This poses a unique challenge that a colonizer can surmount by employing multiple acquisition strategies for various sulfur metabolites. Here, we provide an update on implicated *in vivo* mechanisms employed by colonizing bacteria to exploit physiological sulfur reservoirs.

Advances in pathogen sulfur acquisition: *Staphylococcus aureus* and *Francisella tularensis*. *S. aureus* is a Gram-positive bacterium and leading cause of hospital-acquired infections in the United States (86, 87). *S. aureus* persistently colonizes 20% of humans as a commensal on areas such as the skin or nasopharynx. However, the pathogenic potential of this organism greatly stems from an ability to propagate in most host tissues, indicating that *S. aureus* encounters most host sulfur metabolism compounds. Remarkably, *S. aureus* does not encode various enzymes required in sulfate, sulfonate, or taurine assimilation and is not capable of *de novo* methionine or Cys synthesis. As such, from a nutritional sulfur standpoint, import of compounds such as Cys

and its derivatives, γ-glutamyl cycle intermediates, thiosulfate, and H_2S, represent the host metabolites that this organism may capitalize on *in vivo*. In support of this, one critical study describes Cys, CSSC, thiosulfate, sulfide, and GSH as viable nutritional sulfur sources for *S. aureus in vitro* (88). A more recent study has also demonstrated GSSG as a source of nutrient sulfur for this opportunistic pathogen (89). Interestingly, a novel ABC-transporter (glutathione import system ABCD) was implicated as the major GSH and GSSG importer in *S. aureus*. As is typical for ABC transporters, this system hydrolyzes ATP as a source of energy for substrate import. GisABCD seems to be conserved within close relatives of the pathogen, excluding *Staphylococcus epidermidis*. In consideration of the individuals who mare persistently colonized with *S. aureus*, it has been proposed that GisABCD-dependent GSH acquisition is an evolutionary development to compete for sulfur resources in the presence of *S. epidermidis*. Employing this transporter during infection could then greatly affect the host GSH-to-GSSG thiol balance. Such a disruption could have considerable impacts both on the production of downstream host sulfur metabolites as well as other important physiological aspects, like ROS management. However, a *gisBCD*-deficient mutant displays no overt virulence defect during murine systemic infection. It is postulated that *S. aureus* expresses an alternative GSH transporter and that the activity of this theoretical protein masks overt phenotypes during infection. Should this be the case, encoding multiple GSH transporters would underscore the importance of GSH acquisition to *S. aureus* propagation within host tissues. It is well established that a number of colonizing bacteria encode multiple Cys/CSSC transporters, again emphasizing the importance organisms have placed on these organic compounds throughout evolution. Transportation of these metabolites in *S. aureus* has recently been

elucidated and investigated in a biological context (90). In this study, it was also determined that both NAC and homocystine, the oxidized form of homocysteine, are viable sulfur sources for *S. aureus*. The transporters implicated in their collective acquisition, TcyABC and TcyP, were further demonstrated to have biological impacts on *S. aureus* propagation *in vivo*. TcyABC is an ABC transporter, while TcyP belongs to the sodium-dicarboxylate symporter family (91). The latter family of proteins is widely distributed throughout eukaryotes and prokaryotes; members include those that import dicarboxylic acids and some amino acids, including those that are small, nonpolar, and neutral, such as Cys (92). Notably, *S. aureus* TcyABC and TcyP function similarly to their *Bacillus subtilis* homologs, which have been previously characterized (93). In *S. aureus*, TcyABC and TcyP are necessary for maximal fitness in colonization of the murine host for both the methicillin-sensitive strain Newman and resistant strain LAC. Specifically, the Newman *tcyABC tcyP* double mutant displayed significantly reduced colony forming units (CFU) numbers in the heart when in competition against the wild type (WT). However, in the liver in activation of only *tcyP* results in impaired Newman colonization. Additionally, TcyP of LAC was found to be required for maximal competitive fitness in the murine heart and liver. In addition to increasing foundational knowledge, this study accentuates the fact that intraspecies variance exists for how some bacteria meet the sulfur nutritional requirement in the host. Identification of NAC and homocystine as sources of nutrient sulfur for *S. aureus* warrants a brief discussion regarding their distribution and impact within a healthy host. Both metabolites have been detected in human plasma, a location where thiols are commonly found in their oxidized form (21, 43, 94, 95). It is noteworthy that the balance between reduced and oxidized homocysteine has long been associated with

cardiovascular disease (e.g., forms of atherothrombotic disease) (96, 97). Thus, future *in vivo* data implicating the use of homocysteine or homocystine by a pathogen could have interesting implications regarding how the bacterium affects the cardiovascular system of mammalian hosts. In addition to being part of the plasma redox pool, NAC is known to be a GSH precursor within mammals, either through its own deacetylation or by its role in reducing CSSC to Cys; due to this, NAC is a clinically relevant supplement used to increase GSH levels within the host (43, 98). It is clear from these studies that the flexible nature of *S. aureus* sulfur metabolism and the burden this plasticity enforces on the host is just beginning to emerge. Sulfur acquisition and metabolism of the Gram-negative, facultative intracellular pathogen *F. tularensis* has also seen advances in recent years. This organism is the etiological agent of tularemia, a disease with various clinical manifestations depending on the route of entry (99). As a Cys auxotroph, *F. tularensis* depends on GSH as a source of Cys for successful intramacrophage survival (100). However, *F. tularensis* Ggt periplasmic localization implies that GSH catabolism initiates in this subcellular environment, resulting in Cys-Gly being transported into the cytosol as the nutrient sulfur source. In support of this notion, a Tn-Seq screen for genes required for replication in J774A.1 murine macrophage-like cells revealed a proton-dependent oligopeptide transporter (POT) family gene, *dptA*, as a top hit (101). This observation was validated through monoinfection of J774 macrophages with a *dptA* mutant. Furthermore, in a murine model of pulmonary infection, DptA significantly impacts the ability of *F. tularensis* to colonize the lungs and spleen. Reduced accumulation of radiolabeled GSH was also observed with a *dptA* mutant, supporting its function as a Cys-Gly transporter. Carbonyl cyanidem-chlorophenyl hydrazone (CCCP) abolition of WT *F. tularensis* cell

membrane potential also reduced intracellular radiolabeled GSH abundance to that of a *dptA* mutant, exemplifying this protein as a POT family member. Overall, these findings are the first to demonstrate Cys-Gly as a viable nutrient sulfur source to bacteria within multiple host environments.

Progress regarding symbiotic sulfur acquisition: *Staphylococcus hominis* and *Vibrio fischeri*. Like *S. aureus*, *S. hominis* is a commensal of the human underarm skin (axilla) microbiome and has pathogenic potential, albeit to a lesser extent than *S. aureus* (102). Though little is known regarding sulfur metabolism in this species of staphylococci, one can predict capabilities similar to those of *S. aureus*. A current study clearly demonstrates the ability of *S. hominis* to import a sulfur-containing metabolite as well as accentuating another physiological role for Cys-Gly in the host (103). Here, the γ-glutamyl cycle is highlighted for its participation in the production of an axilla malodor precursor, *S*-[1-(2-hydroxyethyl)-1methylbutyl]-L-cysteinylglycine (S-Cys-Gly-3M3SH). This pathway begins when glutathione *S*-transferase preforms a conjugation reaction, forming glutathione 3-methyl-3-sulfanylhexanol (SG-3M3SH) (104). From there, host GGT generates S-Cys-Gly-3M3SH. At this point it is postulated that *S. hominis* imports S-Cys-Gly-3M3SH through the POT family protein, PepT. Once in the cytoplasm, 3-methyl-3-sulfanylhexan-1-ol (3M3SH) is liberated and released back into extracellular milieu, which produces malodor. Although it has not been demonstrated, it is tempting to speculate that release of Cys during this process aids in the maintenance of nutrient sulfur demands in *S. hominis*. In light of the fact that host-bacterium interactions are not limited to mammals, the Gram-negative marine bacterium *V. fischeri* serves as a growing model of sulfur metabolism for nonmammalian symbionts. *V. fischeri* is a bioluminescent symbiont located

in the light organ of the bobtail squid, *Euprymna scolopes* (105). Both organic (Cys, CSSC, and GSH) and inorganic (sulfate and thiosulfate) sulfur sources are capable of supporting *V. fischeri* proliferation *in vitro*, and pioneering efforts have defined the nutritional sulfur interface between *E. scolopes* and this bacterium (105).In the first study, various mutants of the sulfur regulon regulator, CysB, were utilized (105). The authors determined that symbiosis of a *cysB* mutant is not dependent upon the ability of *V. fischeri* to assimilate sulfate in the squid light organ. Furthermore, a *cysB* variant grows similarly to the WT when CSSC was present *in vitro* and *in vivo*. However, due to redundancy of encoded CSSC transporters, the authors could not completely determine how *V. fischeri* acquires this nutrient from the host. As mentioned above, this could be a strong indication of the importance CSSC has to *V. fischeri* colonization. To that end, when the CSSC transporter TcyP is ectopically expressed in a *cysB* mutant, the strain establishes WT-like symbiosis (106). Additionally, expression of *tcyJ*, which encodes a CSSC-specific periplasmic binding protein, is highly upregulated in a mutant defective for sulfate assimilation (106). Collectively these data indicate an association between CSSC utilization as a sulfur source and *V. fischeri* symbiosis. In this environment, CSSC is predicted to arise as a result of Cys oxidation upon degradation of host proteins in the light organ crypt space (105). The importance of sulfate acquisition to establishment of symbiosis was further elucidated (106). Sulfate is a dominant sulfur source in seawater. Given the prevalence of seawater in the squid light organ, it is a substantial supplier of sulfate in this environment. Therefore, bacteria that colonize this host organ likely utilize sulfate as a nutrient sulfur source. Wasilko *et al*. identified that a sulfate assimilation mutant displays lower numbers of CFU per milliliter than the WT, suggesting that sulfate is an impactful sulfur source during

symbiosis. To examine this concept from another angle, the authors identified that *V. fischeri* encodes a novel sulfate transporter, YfbS (106). YfbS belongs to the solute carrier 13 (SLC13) protein family, which consists of sodium-coupled anion symporters with substrates such as sulfate, thiosulfate, or dicarboxylates (107). A *yfbS* mutant exhibits lower bioluminescence and number of CFU in the light organ compared to the WT, emphasizing the importance of sulfate acquisition to *V. fischeri* symbiosis. Overall, it is predicted that in this location the abundant sulfate pool provides ample sulfur to an expanding population.

Bacterial regulation of sulfur acquisition and assimilation machinery. To meet its nutritional requirement, a colonizing bacterium must employ sulfur acquisition and assimilation systems in dynamic host environments. However, importing too much sulfur can be toxic due to the involvement of intracellular Cys in Fenton chemistry (i.e., production of hydroxyl radical formation) (108, 109). Therefore, it is critical for bacteria to regulate sulfur metabolism genes such that ideal propagation conditions are maintained within the host. For simplicity, this review will discuss two models of regulation that have been tested *in vivo*, recognizing that other influencing factors have also been described (110–112). Collectively, genes dedicated to achieving the nutritional sulfur requirement are largely collected within the sulfur regulon. Depending on the Gram status of a bacterium, expression of this regulon will depend on either a positive or negative transcriptional regulator (Figure 1.2). However, in both models the Cys status of the cell is indirectly communicated to a transcriptional regulator through *O*-acetylserine (OAS). Regulation of sulfur metabolism in Gram-negatives has been thoroughly characterized (Figure 1.2, A and B). In this system, there are two key enzymes: the positive LysR-family

transcriptional regulator CysB and serine transacetylase (CysE). CysE is the product of a gene that is constitutively expressed (113, 114). The catalytic activity of CysE is responsible for providing the critical metabolite, OAS. To do so, CysE binds to L-serine and acetyl-coenzyme A substrates, and the resulting acetyl group transfer produces OAS and CoA (115). OAS may then act either as an intermediate in sulfate or thiosulfate assimilation to Cys or as a signaling molecule. It is noteworthy that OAS spontaneously converts to *N*-acetylserine (NAS) (115). As such, this pool will be denoted O/NAS. Furthermore, CysE activity is directly controlled by concentrations of intracellular Cys (115, 116). Abundant Cys inhibits CysE activity, and the diminished O/NAS pool renders CysB inactive, repressing sulfur regulon genes (Figure 1.2, A) (115). Alternatively, during Cys limitation O/NAS concentration grows as a result of increased CysE activity (Figure 1.2, B). O/NAS association with CysB fosters binding to promoters, allowing expression of nutrient sulfur acquisition strategies, and Cys production ensues (114). While work regarding effects of CysB on bacterial colonization is relatively sparse, the aforementioned *V. fischeri* study underscores the significance of this protein during colonization of the bobtail squid light organ (105). Monitoring green fluorescent protein (GFP) production from the promoter of a CysB-responsive gene revealed that CysB activity varies throughout the colonizing population within select locations of the *E. scolopes* light organ. It is suggested that this reflects the preference of *V. fischeri* to utilize sulfate where CysB activity is greater than CSSC acquisition in regions with lower regulator action. In other words, this work exemplifies the ability of a colonizing organism to modulate its sulfur regulon in response to available host sulfur sources. Gram-positive bacteria employ negative transcriptional regulation through the cysteine metabolism repressor, CymR (Figure 1.2, C and D) (117).

Although less studied than CysB, there is a good understanding of how this regulator functions in *S. aureus* (118). OAS-thiol-lyase B (CysM; also known as *O*-acetylserine sulfhydrylase B) also plays an impactful role in addition to CysE and CymR. When CysE activity is inhibited due to replete intracellular Cys concentrations, CysM associates with CymR. In this complex, CymR is then proposed to bind DNA, repressing expression of the sulfur regulon (Figure 1.2, C). As Cys becomes limiting, O/NAS binds to CysM, destabilizing the CysM-CymR complex or reducing the complex's affinity for DNA (118, 119). The former is a more plausible outcome given that CysM also functions in thiosulfate assimilation to Cys. At this point CymR is inactive and releases from the DNA, promoting transcription of sulfur acquisition and assimilation genes (Figure 1.2, D). It should be noted that in *B. subtilis*, OAS-thiol-lyase A (CysK) has been shown to interact with CymR rather than CysM (119, 120). However, it is unclear why this occurs or what subgroups of Gram-positive species utilize CysM or CysK for this regulatory process. CymR is also rendered inactive upon oxidation of its sole Cys residue (Cys25), suggesting that this regulator also senses the oxidation state of the cell (e.g., Cys levels) to regulate Cys metabolism (121). It would be of interest for future work to characterize how oxidation of $CymR^{C25}$ affects binding of CysM or CysK. Interestingly, a *S. aureus cymR* deletion mutant is more resistant to macrophage oxidative stress and yet is less virulent in a murine intraperitoneal or bacteremia infection model (122). Further investigation deter-mined that inactivation of *cymR* resulted in reduced δ-hemolysin activity, which was pro-posed to be the factor contributing to the virulence defect. These investigations clearly illustrate the complex nature of CymR, from the factors that regulate its activity within the sulfur regulon to its connections with virulence. Recently another LysR-family protein, GigC, was described in

Acinetobacter baumannii (123). Through transposon sequencing, GigC was first noted as being critical for colonization of *Galleria mellonella* (124). *lacZ* reporter assays further determined that this protein acts as both an activator and repressor for several sulfur assimilation genes. Specifically, promoters for *cysI* and the *cysDN* operon showed increased expression in a *gigC* deletion mutant, whereas activity of *cysH* and *cysQ* promoters was decreased. The authors demonstrated that GigC binds to the *cysI* promoter and proposed that it binds other sulfur regulon genes, such as *cysDN*, *cysH*, and *cysQ*. Considering this information, one could speculate that the bifunctional nature of this regulator serves to fortify *A. baumannii* sulfur preference throughout the host. Consistent with this, a *gigC* mutant shows decreased virulence in murine models of intraperitoneal and peritoneal infection. Future work on the model of GigC function and assessments of its sulfur regulation activity in other bacterial species will undoubtedly exemplify the diverse control that can be exerted over this critical regulon. In doing so, questions such as why these distinct regulatory factors have evolved can be more aptly addressed.

OUTLOOK

It is clear from this collective body of literature that colonizing bacteria interact with the host to procure a variety of sulfur sources. However, there remains a pivotal knowledge gap regarding whether the host actively redistributes or limits sulfur as a result of bacterial colonization and whether bacterial sulfur acquisition systems are an evolutionary response to this action. To that end, the nutrient sulfur status (i.e., excess or limited) of bacteria during various stages of colonization is currently at a nascent stage. Defining *in vivo* importance of transporters to bacterial propagation within the host, however, helps clarify the relative nutrient sulfur source hierarchy for colonization. Furthermore, expanding our

view of how import and assimilation mechanisms are regulated assist in explaining bacterial responses to the host environment during colonization. Specifically relating to pathogens, expanding our knowledge regarding these sulfur acquisition and assimilation pathways serves to broaden the list of possible therapeutic targets in the age of multidrug resistance. However, a holistic under-standing of these bacterial studies is incomplete without considering the host perspective. As can be seen above, there is currently little to no characterization of how host pathways respond to bacterial colonization. This represents unexplored territory within the nutrient sulfur relationship at the host-bacterium interface.

ACKNOWLEDGMENTS

We thank members of the Hammer laboratory for their insightful input and discussions. We sincerely apologize to the colleagues we were unable to cite due to space limitations. This work was supported by National Institutes of Health no. R01AI139074 and R21AI142517.

TABLES

Table 1.1. Localization of sulfur metabolism enzymes in mammalian tissues.

Pathway	Enzyme	Host	Example tissue localization	References
γ-glutamyl cycle	γ-glutamyl transpeptidase (GGT)	human	kidney, pancreas, intestine, liver	(12, 22–24, 31–34)
	dipeptidase (DP)	porcine, rat	wide tissue distribution, largely expressed as brush boarder enzyme (kidney, small intestine) and in cytosol of liver	(22–27)
	glutamate-cysteine ligase (GCL)	mouse	liver, kidney, pancreas, lungs, plasma, brain	(44–46)
	GSH synthetase	rat	kidney, liver, heart, lungs	(46)
Transmethylation pathway	methionine-adenosyltransferase (MAT)	rat	liver, pancreas, kidney, lungs	(11)
	methyltransferase (MT)	n.d.	n.d., likely same tissues as MAT	(11)
	SAH hydrolase	human, mammals	all tissues, plasma	(11, 13)
Transsulfuration pathway	cystathionine β-synthase (CBS)	human	liver, brain, kidney, pancreas, heart, lungs, muscles, endocrine	(15, 16, 18)
	cystathionine γ-synthase (CSE)	human, mouse, rat	cytosol; liver, kidney, heart, lungs, brain	(16–18)
Taurine & sulfate production	cysteine dioxygenase (CDO)	rat, mouse	liver, adipose, kidney, brain, lung, pancreas, colon	(18, 50–52)
	cysteinesulfinate decarboxylase (CSD)	rat, mouse	liver, kidney, brain, adipose, lung, pancreas, colon	(18, 50, 51)

Table 1.1 (cont'd)

	glutamate oxaloacetate transaminase (GOT); aka cysteine aminotransferase (CAT)	rat	liver, arterioles, lymphocytes, kidney, arteriolar endothelium, anterior pituitary (cytosolic and mitochondrial); two isoforms	(50, 51, 53, 54)
	sulfite oxidase (SO)	human, mouse	intermembrane space of mitochondria, largely found in liver, kidney	(51, 74)
H_2S production from cysteine	3-mercaptopyruvate sulfurtransferase (3-MST)	mouse	widespread (high expression in liver, intestine, kidney), mostly localized in mitochondria	(50, 58, 60)
	thioredoxin	mammals	ubiquitous; depending on isoform will be found in cytosol (Trx-1) or mitochondria (Trx-2)	(61)
H_2S oxidation	sulfide-quinone oxidoreductase (SQR)	mammals	ubiquitous, matrix of inner mitochondrial membrane	(51, 73)
	sulfide dioxygenase (SDO)	mammals	ubiquitous, mitochondrial matrix	(51)
	thiosulfate sulfurtransferase (TST)	mammals	mitochondrial matrix, mostly found in liver, stomach/intestines	(51)

n.d. = not discussed

FIGURES

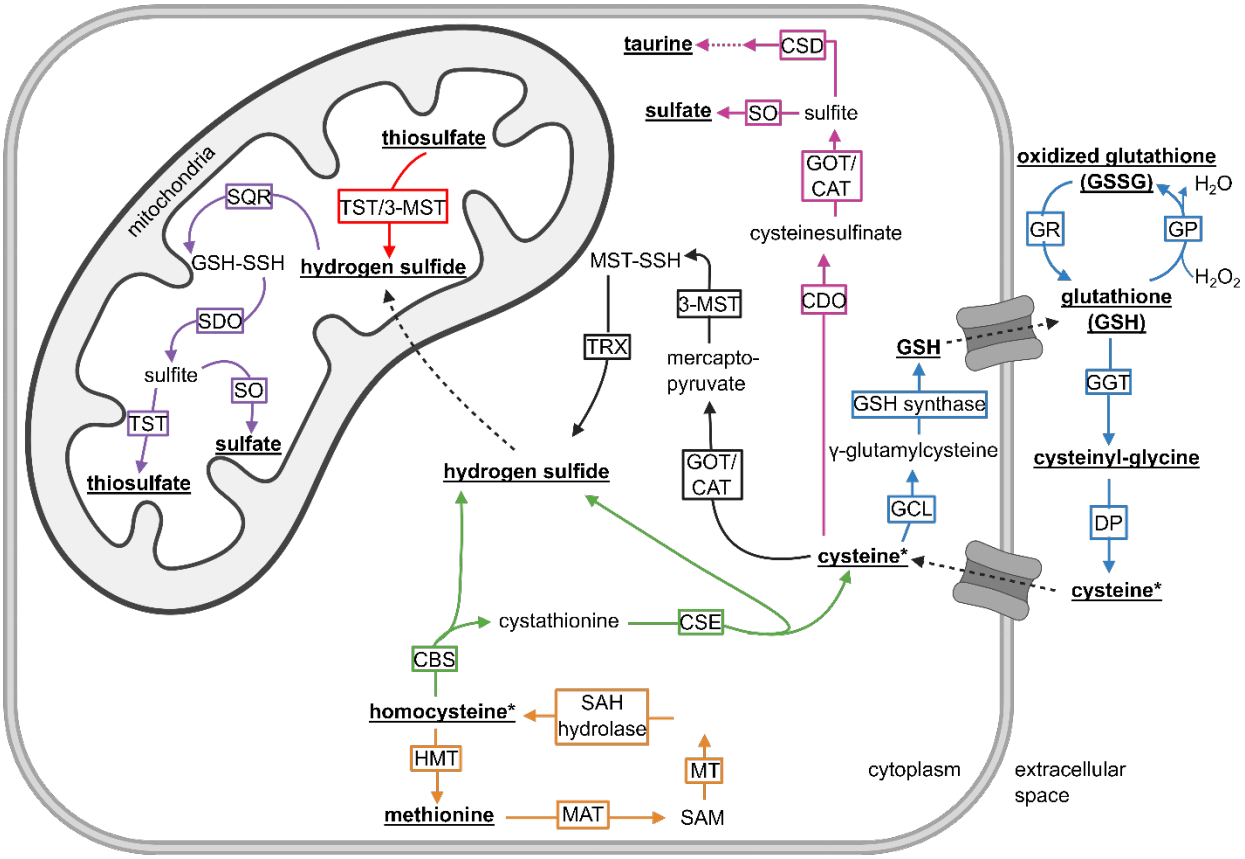

Figure 1.1. The host environment is rich with sulfur-containing metabolites. Cys and H_2S influence production of other sulfur-containing metabolites through their interconnected participation in several metabolic pathways (denoted by colored arrows) within a eukaryotic cell. Note that these pathways are simplified versions of enzymatic reactions (i.e., only the sulfur-containing enzymatic substrates and products are shown). Known sulfur sources for colonizing bacteria are boldfaced and underlined. Biosynthesis of Cys results from the transmethylation and reverse transsulfuration pathways (orange and green, respectively) involves methionine adenosyltransferase (MAT), *S*-adenosylmethionine (SAM), methyltransferase (MT), *S*-adenosyhomocysteine (SAH), SAH hydrolase, cystathionine β-synthase (CBS), cystathionine γ-synthase (CSE), and homocysteine *S*-methyltransferase (HMT). An asterisk denotes the ability of (i) Cys to oxidize to CSSC or methylate to form NAC and (ii) for homocysteine to oxidize to homocystine. Free Cys can be released from GSH via the γ-glutamyl cycle (blue), consisting of glutathione reductase (GR), glutathione peroxidase (GP), γ-glutamyl transpeptidase (GGT), and dipeptidase (DP) enzymes. This cycle may also result in production of GSH from Cys with the use of glutamate-cysteine ligase (GCL) and glutathione synthase (GSH synthase). Factors involved in the formation of sulfate and taurine (pink) include cysteine dioxygenase (CDO), cysteinesulfinate decarboxylase (CSD), nonenzymatic oxidation (dashed arrow), glutamate oxaloacetate transaminase, also known as Cys aminotransferase (GOT/CAT), and sulfite oxidase (SO). Cys can also

Figure 1.1 (cont'd)

be directly metabolized to form H_2S (black) with the activities of GOT/CAT, 3-mercaptopyruvate sulfurtransferase (3-MST), and thioredoxin (TRX). H_2S can be oxidized to sulfate or thiosulfate (purple) using sulfide-quinone oxidoreductase (SQR), sulfur dioxygenease, also known as ETHE1 (SDO), and thiosulfate sulfurtransferase (TST). Thiosulfate is also a source of H_2S as a result of TST or 3-MST activity (red). Image created with BioRender.com.

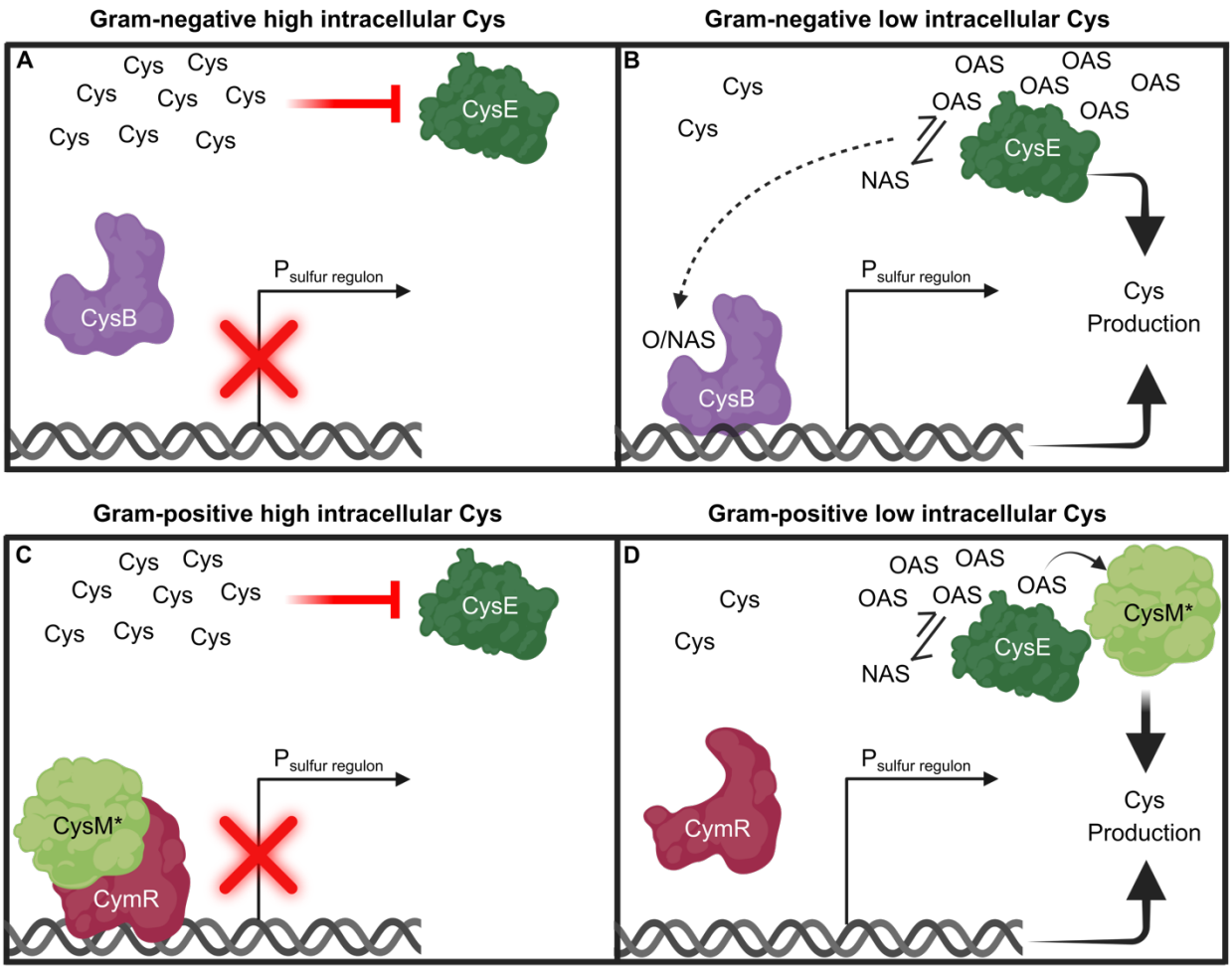

Figure 1.2. Intracellular cysteine modulates the bacterial sulfur regulon. (**A** to **D**) Regulation of the sulfur regulon in Gram-negative (**A** and **B**) and Gram-positive bacteria (**C** and **D**) under high (**A** and **C**) or low (**B** and **D**) intracellular Cys concentrations. (**A**) When abundant in a Gram-negative bacterium, intracellular Cys inhibits activity of serine transacetylase (CysE). *O*-acetylserine (OAS) production is reduced and cannot facilitate CysB binding to DNA. Consequently, CysB fails to induce expression of the sulfur regulon. (**B**) Upon depletion of Cys, CysE produces OAS, which spontaneously converts to *N*-acetylserine (NAS). Either NAS or OAS binds to CysB (denoted O/NAS), allowing the positive regulator to induce expression of the sulfur regulon. (**C**) Sulfur-replete conditions in Gram-positive bacteria inhibit CysE, which leads to decreased OAS levels and promotes CysM or CysK (denoted CysM*) interaction with CymR. CymR functions as a negative regulator that binds DNA and inhibits expression of the sulfur regulon. (**D**) Limited intracellular sulfur leads to increased CysE-mediated OAS generation, destabilizing the CysM*-CymR complex and promoting transcription of sulfur acquisition systems. Oxidation of $CymR^{C25}$ during oxidative stress conditions also contributes to an inactive state. In the inactive state, CymR no longer binds DNA, allowing expression of sulfur acquisition and Cys biosynthesis genes. Image created with BioRender.com.

CHAPTER 2: Defining the transcriptional adaptation of *Staphylococcus aureus* to a range of nutritional sulfur supplementation

ABSTRACT

Bacterial pathogens must adapt to dynamic environments to proliferate within host tissues. Accordingly, elegant regulatory systems evolved to combat the immune response, coordinate virulence factor production, and satisfy nutritional requirements. Sulfur is an essential macronutrient and Gram-positive bacteria such as *Staphylococcus aureus* balance this nutritional requirement by employing the transcriptional repressor, CymR. Previous investigations defined the *S. aureus* CymR regulon by comparing transcriptional changes of a *cymR* mutant cultured in cystine replete, rich medium to wild type cells. This study defines the *S. aureus* CymR-dependent and -independent sulfur-starvation response in chemically defined growth conditions. Notably, these results expand the set of genes within the sulfur starvation regulon and support previously noted connections between iron acquisition, oxidative stress, and sulfur metabolism. Validation of results is highlighted by the ability of sulfur-containing glutathione (GSH) to mitigate heme and peroxide toxicity in *S. aureus*. Since a variety of compounds fulfill the *S. aureus* sulfur requirement, we monitored transcriptional profiles in response to organic (cysteine, cystine, reduced and oxidized GSH) or inorganic (thiosulfate) metabolites. This analysis reveals sulfur source-specific mRNA alterations, with thiosulfate inducing the largest transcriptional shift. Consequently, the sole thiosulfate transporter (SAUSA300_RS10985) has been established as it is essential for *S. aureus* growth when thiosulfate is the nutritional sulfur source. Furthermore, we demonstrate that a hypothetical protein operonic with SAUSA300_RS10985, SAUSA300_RS10980, supports maximal growth of this bacterium on thiosulfate. Collectively, a resourceful

transcriptomics framework is provided which underscores the versatile nature of *S. aureus* sulfur metabolism.

IMPORTANCE

The opportunistic pathogen *Staphylococcus aureus* proliferates within numerous host environments and consequently is a leading cause of hospital-acquired infections. During colonization *S. aureus* must acquire essential nutrients like sulfur to survive. Regulation of machinery to procure host-derived metabolites occurs to satisfy nutritional requirements and maintain homeostasis to circumvent detrimental impacts on bacterial physiology. This report investigates the *S. aureus* regulatory response during various states of sulfur supplementation *in vitro*, enhancing our knowledge of staphylococcal sulfur metabolism and represents a repository of information that will guide future research surrounding *S. aureus* sulfur acquisition and metabolism.

INTRODUCTION

Staphylococcus aureus harbors considerable pathogenic potential given it adapts to and proliferates within most vertebrate organs (86, 125). Such capabilities demand bacteria sense and respond to the extracellular milieu to procure essential nutrients from the host. For example, regulatory mechanisms that control *S. aureus* transition metal acquisition and homeostasis are well defined (126). The transcriptional repressors Fur, Zur, and MntR modulate genes involved in acquisition and utilization of iron, zinc, and manganese, respectively. Each regulator has dedicated binding pockets for their cognate metal ion (i.e., Fe^{2+}, Zn^{2+}, and Mn^{2+}) which senses intracellular concentrations, allowing the regulator to switch to an active, repressive conformation in replete environments (126). Activity of these metalloregulators is tightly coordinated given that transition metals, though essential, are detrimental when in excess (126–128).

Sulfur represents another essential nutrient whose coordinated acquisition by *S. aureus* involves similar regulation. Within cells sulfur is stored in the form of cysteine (Cys) which partakes in numerous cellular reactions such as protein and co-factor synthesis or redox balance (4, 5, 7, 8, 129–132). Given this amino acid is the crux of sulfur distribution within a cell, all metabolites used to meet this nutritional requirement must be catabolized (organosulfur) or assimilated (inorganic) to Cys. As with iron, in *Escherichia coli* it has been demonstrated that an overabundance of intracellular Cys contributes to Fenton chemistry (108). Thus, stringent management of this element in coordination with iron is needed to accommodate proliferation (133). The major regulatory factor influencing *S. aureus* sulfur homeostasis is the cysteine metabolism repressor, CymR (117, 118, 134). In contrast to the metalloregulators, CymR indirectly senses Cys levels to modulate DNA

binding activity via two methods (Fig. 2.1). Intracellular Cys levels are communicated through the sulfur assimilation intermediate *O*-acetylserine (OAS) whose abundance will drop under high Cys concentrations. OAS-thiol-lyase B (CysM, aka MccA) responds to this OAS depletion by complexing with CymR, activating repression (Fig. 2.1A). Alternatively, CymR is also known to respond to the oxidation state of *S. aureus* through its sole Cys residue at position 25 (Fig. 2.1B).

To maintain intracellular sulfur, metabolites—including Cys, cystine (CSSC), *N*-acetylcysteine, homocysteine, reduced and oxidized glutathione (GSH and GSSG, respectively), thiosulfate (TS), and hydrogen sulfide— are acquired by *S. aureus* and converted to Cys (88–90). These compounds participate in host sulfur metabolism across numerous tissues (134). However, even with advances in our understanding of sulfur metabolism in this pathogen, how *S. aureus* synchronizes internal demands for this element throughout the host and the mechanisms by which *S. aureus* prioritizes sulfur metabolite utilization remain outstanding questions.

This study defines how *S. aureus* responds to sulfur starvation by establishing sulfur replete and deplete transcriptional profiles that emerge in a CymR-dependent and -independent manner. Using a chemically defined medium (CDM) supplemented with various sulfur sources, our findings expand upon work performed by Soutourina *et al*. who describe a CymR-dependent transcriptional response of *S. aureus* cultured in rich medium supplemented with 2 mM CSSC (118, 122). Like the previous study, we observe a CymR-independent upregulation of iron transport and oxidative stress genes when *S. aureus* is sulfur starved (122). The importance of connected regulation is established by showing that *S. aureus* scavenging exogenous nutrient sulfur in the form of glutathione

(GSH) combats heme-induced oxidative stress as well as enhancing survival in response to hydrogen peroxide (H_2O_2). Additionally, growth on inorganic TS elicited the greatest number of differentially expressed genes compared to proliferation on organic metabolites (Cys, CSSC, GSH, and GSSG). The RNAseq was substantiated by addressing the role of upregulated genes in response to TS. This investigation confirms that SAUSA300_RS10985, a YeeE/YedE family transporter, is required for *S. aureus* growth on TS along with a protein of unknown function, SAUSA300_RS10980. Together with their high degree of homology to the *E. coli* **t**hio**s**ulfate **u**ptake proteins A and B (TsuAB), these findings suggest the reannotation of SAUSA300_RS10985 and SAUSA300_RS10980 to *tsuA* and *tsuB*, respectively (135). Overall, this work validates the importance of transcriptional links between sulfur starvation, iron homeostasis, and oxidative stress responses as well as accentuating intricacies within the *S. aureus* sulfur regulon.

RESULTS

***Staphylococcus aureus* sulfur starvation response includes altered transcription within the CymR regulon.** A direct assessment of the *S. aureus* sulfur starvation response has not been established. Previous work defined the CymR regulon using a *cymR* deletion mutant (Δ*cymR*), an isogenic SH1000 wild type (WT) strain, and microarray hybridization (118). Both strains were cultured in rich medium (tryptic soy broth; TSB) supplemented with 2 mM cystine (CSSC). We sought to compare the sulfur starved transcriptome of WT *S. aureus* with a sulfur deprived *cymR* transposon mutant (*cymR*::Tn) to define the CymR-dependent and -independent response. This assessment required growth conditions distinct from those employed previously (118). WT JE2, a

derivative of the current endemic USA300 LAC strain, and an isogenic *cymR*::Tn were cultured in CDM supplemented with 25 μM CSSC to mid-exponential phase. Cells were washed, resuspended into CDM supplemented with or without 25 μM CSSC, and cultured for an additional 2 h prior to isolating RNA and performing RNAseq (Fig. 2.2). The use of WT and *cymR*::Tn provides a robust methodology to discern between the respective *S. aureus* CymR-dependent and -independent responses to sulfur starvation. Comparisons between culture conditions and the total number of differentially regulated genes (>2-fold) are outlined in Table 2.1.

Overall, the WT sulfur starvation response included 425 upregulated and 142 downregulated genes, resulting in a total of 567 differentially expressed transcripts (Table 2.1a and Table A-1). The number of genes responding to sulfur starvation (*n*=567) is far greater than the previously described CymR regulon (*n*=79), supporting the hypothesis that sulfur starvation induces CymR-dependent and -independent responses (118, 122). To define CymR-dependent transcripts, we compared the sulfur replete CymR regulon to the previously reported CymR regulon, which was also generated in sulfur-replete culture conditions (18,22). Specifically, genes differentially expressed in *cymR*::Tn when cultured in CSSC-supplemented CDM were identified and compared to WT grown in the same condition (Table A-2). This analysis revealed that *cymR* inactivation altered the expression of 67 genes, 45 upregulated and 22 downregulated (Table 2.1b). For comparison, 79 genes were upregulated when Δ*cymR* was cultured in CSSC-supplemented TSB (118, 122). With the WT sulfur starvation and CymR regulons in hand, we sought to compare upregulated sulfur metabolism genes across the three conditions (118). Notably, 15 out of the 16 published sulfur acquisition and metabolism genes are

shared between sulfur starved WT (Table A-1) and the previously reported CymR regulon (118, 122) with a total of 28 common genes between the two Tables overall (Table 2.2 and Fig. 2.3A). Adding upregulated genes from the sulfur-replete *cymR*::Tn condition (Table 2.3) transcriptome to this comparison reveals 10 total shared genes (Fig. 2.3A), eight of which are published sulfur metabolism genes (Table 2.2c) while the remaining two, SAUSA300_RS01875 and SAUSA300_RS15260, are described as cell wall associated by Soutourina *et al*. (118).

To more strictly define sulfur metabolism associated genes within our conditions, cluster of orthologous groups (COGs) were assigned to the WT sulfur starvation and *cymR*::Tn sulfur replete Tables and then reassessed against Soutourina *et al.* (118). Sulfur-metabolism associated genes within the sulfur-deplete WT (*n*=26), sulfur-replete *cymR*::Tn (*n*=14), and the Soutourina *et al*. published (*n*=16) Tables were compared, revealing eight shared genes (Fig. 2.3B, Table 2.2) (118). Soutourina *et al*. also identified cell-wall associated genes in the CymR regulon and therefore COG assigned cell-wall associated genes were also isolated and analyzed; however, cell-wall associated genes were not shared across the three Tables (Fig. 2.3C). A direct comparison of the WT sulfur starvation and *cymR*::Tn sulfur replete conditions reveals 35 shared genes (Fig. 2.3D), 16 of which are sulfur metabolism associated (Fig. 2.3D, asterisk). This suggests that CymR influences expression of these 35 genes.

The disparity between the total number of genes differentially regulated in response to sulfur starvation (*n*=567) and the sulfur replete CymR regulons (*n*=79 and *n*=67) underscores the importance of accounting for the sulfur status of cells. We surmise that CymR-dependent and -independent transcriptional alterations comprise the WT

sulfur starvation response. Therefore, identifying differentially expressed transcripts that are similar between sulfur starved WT and *cymR*::Tn will define transcripts regulated independently of CymR as those transcripts change in abundance regardless of whether CymR is present. Induction of sulfur starvation in *cymR*::Tn cells results in the differential expression of 344 genes, with 169 and 175 being up- and downregulated, respectively (Table 2.1c and Table A-3). Of those 344 genes, 138 are also differentially regulated in sulfur starved WT cells (Fig. 2.4A, Tables A-1 and A-3). These genes contribute to several cellular pathways with amino acid transport and metabolism, inorganic ion transport and metabolism, and genes of unknown function being most represented (Fig. 2.4B). Two transcriptional regulators are also differentially expressed in this CymR-independent sulfur starvation response (Tables A-1 and A-3). SbnI is a heme-responsive regulator for staphyloferrin B synthesis (136) while Fur is the master iron regulator.

While these 138 genes represent the CymR-independent transcriptional response to sulfur starvation the remaining 429 genes are CymR-dependent, underscoring the importance of CymR in the sulfur starvation response. In keeping with this, a range of cellular processes were described with the COG analysis such as energy production and conversion, amino acid transport and metabolism, transcription, as well as carbohydrate transport and metabolism (Fig. 2.4C). Lastly, a subset of genes are differentially expressed solely in the *cymR*::Tn sulfur starvation response (*n*=117). Though these genes are considered CymR-independent, their differential expression is more likely a compensatory response to the loss of CymR. Within this subset of genes there are only three COG categories that have more than 10 genes represented: those with unknown function, amino acid transport and metabolism, and inorganic transport and metabolism

(Fig. 2.4D). Together, these comparisons reveal an intricate *S. aureus* starvation response that engages transcriptional alterations within and beyond the sulfur regulon.

Sulfur starvation induces changes in numerous *S. aureus* transcriptional regulators and the upregulation of iron acquisition and oxidative stress response genes. In addition to their initial report of genes differentially expressed in a Δ*cymR* mutant cultured in TSB + 2mM CSSC (118), Soutourina *et al*. observed 18 upregulated genes involved with oxidative stress and metal ion homeostasis (122). Genes associated with oxidative stress and iron metabolism are also upregulated in response to sulfur deprivation in this study (Table A-1). Of the 567 differentially expressed genes in sulfur starved WT, 34 encode transcriptional regulators, of which 28 are upregulated while 6 are downregulated (Table 2.4). Notably, *cymR*, *fur*, and *perR* (major peroxide sensor) were upregulated (Table 2.4). Increased *fur* and *perR* expression were also observed in Soutourina *et al*. (122). Interestingly, *fur* upregulation occurred in both of our sulfur starvation Tables despite iron supplementation (Tables A-1 and A-3). Consistent with activation of the Fur and PerR regulons, both the WT and *cymR*::Tn sulfur starvation responses include an upregulation of seven oxidative stress genes as well as 29 iron acquisition and Fe-S cluster assembly genes (Table 2.5). Some iron acquisition genes are upregulated in both the WT and *cymR*::Tn sulfur starvation conditions, indicating that their expression is CymR-independent (Table 2.5, asterisk). Within these shared genes are those found to be upregulated by Soutourina *et al*. such as alkyl hydroperoxide reductase subunits C and F as well as *ftnA* (122).

Some genes are uniquely upregulated only during WT sulfur starvation (e.g., *fhuB*, *fhuG*) which would suggest differential expression in response to the presence of CymR

(Table 2.5). Fourteen genes, largely involved in Fur-regulated siderophore biosynthesis and Fe-S cluster assembly, are unique to the *cymR*::Tn starvation condition as well as a regulator of redox-stress, HypR (137) (Table 2.5). Upregulation of *hypR* solely during *cymR*::Tn sulfur starvation led us to question whether other transcriptional regulators are altered in this condition. Two such regulatory systems were found: *sarR* (SAUSA300_RS12390), which modulates the virulence regulatory *sar* system (91, 138), is downregulated while SAUSA300_RS11905 (MerR family of metal sensing regulators) is upregulated (91, 139).

Several of the CymR-independent upregulated genes belong to the Isd system (iron-regulated surface determinant) which promotes the release of iron from heme (140). The observed interconnection between sulfur, iron, and oxidative stress should benefit *S. aureus* because numerous enzymes require Fe-S clusters to function and homeostasis of these two nutrients is crucial given their contributions to Fenton chemistry (108, 141, 142). Additionally, GSH (a sulfur-containing metabolite with a free thiol) protects *Streptococcus* species against oxidative damage upon exposure to copper or paraquat (143, 144). These facts support the hypothesis that *S. aureus* employs a similar method of GSH scavenging to manage oxidative stress (144). Given the Isd system is important for heme-mediated iron acquisition and the fact that erythrocytes contain approximately 21 μM of free heme and 1-2 mM GSH (145, 146), we explored *S. aureus* sensitivity to hemin (oxidized form of heme) upon supplementation with reduced or oxidized GSH. WT and a *hrtA*::Tn mutant—which is hypersensitive to heme due to impaired efflux (147, 148)—display identical growth profiles when cultured in CDM with 50 μM GSH (Fig. 2.5A). However, toxicity is observed as an increased lag phase upon supplementation of the WT

culture with 10 μM hemin while the *hrtA*::Tn mutant fails to proliferate (Fig. 2.5A). To reflect GSH levels *S. aureus* likely encounters during infection, GSH was increased to a more physiologically relevant concentration (42); supplementation with 750 μM GSH abolishes any impact of hemin on WT propagation (Fig. 2.5B). The *hrtA* deficient strain experiences a longer lag phase, but eventually reaches a WT-like OD_{600} (Fig. 2.5B), indicating an alleviation of heme toxicity. To assess whether this protection is specific to the free thiol, reduced GSH was replaced with oxidized GSH (GSSG) using equimolar concentrations of sulfur. Exposing S. *aureus* supplemented with low (25 μM) or high (375 μM) concentrations of GSSG to hemin inhibited growth of both WT and the *hrtA* deficient strain (Fig. 2.5C, D respectively). Taken together, this indicates that S. *aureus* scavenging of GSH sufficiently combats hemin-mediate oxidative stress. To further demonstrate that GSH protects against ROS, we quantified the viability of *S. aureus* cells that were preincubated with GSH or GSSG and subsequently exposed to H_2O_2 (Fig. 2.5E). WT cultured in 750 μM GSH exhibited significantly increased viability upon H_2O_2 challenge compared to WT grown in 50 μM GSH or 375 μM GSSG. Collectively, these data indicate that sulfur starvation and iron homeostasis coordination protect *S. aureus* from oxidative stress (122).

Adaptation of *S. aureus* to distinct nutrient sulfur sources induces unique transcriptional responses. Given that the absence of sulfur drives transcriptional changes, we hypothesized that discrete *S. aureus* transcriptome alterations occur when cultured in the presence of organic or inorganic sulfur sources. To test this, *S. aureus* was grown in CDM supplemented with 50 μM Cys, 25 μM GSSG, 50 μM GSH, or 50 μM sodium thiosulfate (sTS) and differentially expressed genes were identified (Table B-1,

B-2, B-3, and B-4, respectively). CSSC was used as the comparator because it is typically supplemented as the sulfur source in CDM (149, 150). In total, 776 genes alter expression when *S. aureus* proliferates in the presence of Cys, GSSG, GSH, or sTS when compared to CSSC (Tables B-1 to B-4). Only six genes were differentially expressed in WT supplemented with Cys (Table B-1). One of the two downregulated genes in this condition, SAUSA300_RS04580, encodes a putative pyridine nucleotide disulfide oxidoreductase (91), suggesting a role in reducing CSSC. However, inactivation of SAUSA300_RS04580 does not impact the ability of *S. aureus* to utilize CSSC as a sulfur source (Fig. 2.6).

In stark contrast to Cys supplementation, sTS led to the greatest shift in differentially expressed genes. In this condition, a total of 231 genes were upregulated and 175 downregulated (Fig. 2.7A); compared to growth in GSH and GSSG, 135 upregulated and 83 downregulated genes are unique to growth on sTS (Fig. 2.7B, C). Supplementation with GSH or GSSG results in a total of 193 upregulated and 177 downregulated genes (Fig. 2.7A); 19 of these genes had unique differential expression when GSH was the provided sulfur source whereas 26 were specific to GSSG (Fig. 2.7B, C). An explanation for this disproportional transcript abundance across sulfur sources is variant transcriptional regulator expression. In total, 21 regulators experienced altered expression in the presence of sTS, GSH, and GSSG. Twelve of these regulators were solely altered in sTS while three were found to have differential expression in GSSG (Fig. 2.7D). Four regulators were differentially expressed in both GSH and sTS while one regulator was shared between GSSG and sTS (Fig. 2.7D). Only one regulator, *vraR*, shared differentially expression across all three sulfur sources (Fig. 2.7D). The 12

regulators uniquely expressed in sTS support the notion that altered gene expression in the presence of this sulfur source is related to transcriptional regulation. Consequently, we hypothesize that sTS supplementation leads to altered nutritional requirements which manifest through increased expression of transporters compared to GSH and GSSG. Consistent with this, 53 differentially transporters across all the sulfur conditions were found (Table B-5). Seventeen were specifically upregulated in sTS compared to the eight and four transporters uniquely upregulated in GSSG and GSH, respectively (Table B-5). Several transporters in Table B-5 are differentially expressed in just two sulfur sources—GSH and GSSG (*n*=1), GSH and sTS (*n*=5), or GSSG and sTS (*n*=1)—while 15 experience transcriptional alterations in all three conditions. Of these 15 genes, 12 are upregulated (Fig. 2.8 "+" symbols), six of which are were also upregulated in the previously described CymR regulon (Fig. 2.8, bold) (118). The remaining three shared transporters (i.e., SAUSA300_RS01625, SAUSA300_RS13340, and SAUSA300_RS13345) are downregulated (Table B-5). Collectively, these observations indicate that growth on inorganic sulfur sources alters *S. aureus* physiology to a greater extent than when this organism proliferates on organic sulfur sources.

To substantiate these Table, we further assessed the sTS condition given that supplementation with this metabolite led to the largest transcriptional shift. SAUSA300_RS10985 and SAUSA300_RS10980 encode for a YedE/YeeE family transporter and oxidoreductase, respectively (91, 118, 151). Recently, *E. coli* homologs of SAUSA300_RS10985 and SAUSA300_RS10980 were found to import TS (TsuA, SAUSA300_RS10985 homolog, referred to as 985) and support its assimilation to Cys (TsuB, SAUSA300_RS10980 homolog, referred to as 980) (135, 152). This is in

accordance with previous predictions that 985 is the *S. aureus* TS transporter (118). To investigate whether 985 supports *S. aureus* utilization of TS as a source of nutrient sulfur, a 985::Tn mutant was employed. The Tn insertion likely has polar effects on the downstream 980 gene (Fig. 2.9A). As such, complementation was performed using the pKK22 vector (153). Both genes were cloned, under native promoter control, into pKK22 individually or as an operon. The resulting strains were then cultured in CDM supplemented with either 50 μM sTS or 25 μM CSSC (Fig. 2.9B, C respectively). In comparison to WT harboring an empty vector (EV), the 985::Tn EV mutant is incapable of proliferation when TS is the sulfur source (Fig. 2.9B). Expression of 985 *in trans* partially restores propagation of the mutant while complementation with the entire operon completely rescues the observed growth defect. Ectopic expression of 980 does not restore proliferation of the mutant in CDM supplemented with sTS. These results demonstrate that 985 is necessary, but not sufficient for maximal growth of *S. aureus* on sTS while 980 is sufficient, but not necessary. Each phenotype is sulfur specific given that strains demonstrate WT-like growth on the control sulfur source, CSSC (Fig. 2.9C). In accordance with the nomenclature proposed by Morigasaki *et. al*. (135) we propose to rename 985 and 980 to thiosulfate uptake proteins A and B (TsuA, TsuB), respectively.

DISCUSSION

As knowledge regarding *S. aureus* sulfur acquisition and assimilation mechanisms grow, it is vital to understand how these strategies are regulated during infection (89, 90). Initial observations defined the *S. aureus* CymR regulon using an isogenic mutant cultured in sulfur replete media (118, 122). Here, we examine how the CymR-dependent and -independent transcriptome fluctuates under sulfur replete and deplete conditions. To do

so, RNAseq was employed due to its increased sensitivity over the microarray technology applied by Soutourina *et al*. Additionally, WT and *cymR*::Tn cells were cultured in a defined medium in the presence or absence of CSSC allowing us determine the sulfur starvation transcriptome. Our study also assessed a methicillin resistant, USA300 LAC derivative (JE2) which is reflective of the current endemic strain, whereas previous work utilized the methicillin susceptible SH1000 strain. Comparing our WT sulfur starvation and *cymR*::Tn sulfur replete transcriptomes to the ∆*cymR* sulfur replete transcriptome generated by Soutourina *et al*. (118), we observe a greater number of differentially regulated genes related to sulfur metabolism and fewer cell-envelope associated genes (Fig. S2B and S2C). These differences are likely due to increased sensitivity, contrasting growth conditions, and variations in cell wall composition and structure given that different *S. aureus* strains were assessed (154, 155).

Querying sulfur-starved WT (Table A-1), a CSSC-supplemented *cymR*::Tn mutant (Table A-2; Table 2.3), and the sulfur replete Δ*cymR* strain described in Soutourina *et al*. (118, 122) reveals overlap in upregulated sulfur-associated transporters. Notably, *S. aureus* encodes two Cys and CSSC transporters, TcyP and TcyABC (90). Upregulation of *tcyP* was consistent across all three Tables as was *tcyA*, the gene encoding the TcyABC substrate binding protein. However, the remaining *tcyB*-encoded permease and ATPase encoded by *tcyC* are upregulated in WT sulfur starvation and Soutourina *et al*., but not in the CSSC replete *cymR*::Tn mutant. Heightened expression of a recently described glutathione import system (*gisABCD-ggt*; SAUSA300_RS01055-RS01075) was also observed across the three analyses (89). The ABC transporter is encoded by divergently transcribed *gisA* and *gisBCD*. The terminal gene of the *gisBCD* operon is *ggt*,

which encodes a γ-glutamyl transpeptidase. All five genes exhibit increased expression in sulfur starved WT. Both *gisA* and *gisB* are expressed in CSSC supplemented *cymR*::Tn while Soutourina *et al*. observe upregulation of *gisA* (118, 122). The genes encoding for a predicted sulfate/sulfonate transport system, *ssuABC*, were also upregulated in both the CSSC supplemented *cymR*::Tn and WT sulfur starvation conditions; however only *ssuB* was upregulated in Soutourina *et al*. Despite these subtle inconsistencies across presumably operonic genes, expression of the *gisABCD-ggt* and *ssuABC* loci further solidifies the overlap within the compared Tables. Lastly, upregulation of *tsuA*, the verified TS transporter, occurred across all three Tables.

A portion of the sulfur starvation response involves genes outside of the CymR regulon (Fig. 2.4) such as those involved in iron metabolism and oxidative stress (Table 2.5 and Table B-1). A potential link between iron and sulfur regulons seems intuitive considering the number of enzymes that require Fe-S clusters. In *Pseudomonas aeruginosa* the sulfur regulon transcriptional regulator, CysB, directly promotes expression of *pvdS*, an alternative sigma factor involved in the iron response (156), suggesting beneficial effects of balancing iron and sulfur levels. This coordination is further exemplified in *E. coli* where Fur binds an [2Fe-2S] cluster to sense intracellular free iron (133) though, whether Fur is also responsive to CysB in this organism is currently unknown. The fact that iron and sulfur potentiate Fenton chemistry also underscores a link between sulfur acquisition, iron acquisition, and oxidative stress.

Scavenging host GSH, a low molecular weight thiol antioxidant, to satisfy the nutritional sulfur requirement may also offset toxicity associated with iron or heme-iron acquisition. We demonstrate that GSH protects *S. aureus* from hemin toxicity, supporting

propagation in an otherwise inhibitory environment (Fig. 2.5). Though not fully understood, heme can induce bactericidal effects at high enough concentrations. To combat heme accumulation, *S. aureus* employs the heme-regulated ABC transporter, HrtAB, which effluxes heme from the cell. Therefore, genetic inactivation of *hrtA* or *hrtB* results in heme hypersensitivity (147, 148). Here we observe that GSH scavenging promotes proliferation of both WT and a *hrtA*::Tn mutant in the presence of hemin. The free thiol of GSH is a crucial aspect of this protection given that GSSG is not sufficient to alleviate the toxicity. Additionally, we demonstrate that toxicity of another stressor, H_2O_2, is decreased upon culturing *S. aureus* in the presence of physiologically relevant GSH concentrations. This supports the notion that the restored growth observed in response to heme is likely due to management of cell-associated stress induced by heme rather than a direct, extracellular GSH-heme interaction (157, 158). The relevance of these results towards *S. aureus* management of heme-induced stress during bacteremia stem from the facts that the pathogen is hemolytic, and erythrocytes harbor abundant concentrations of GSH and heme (159, 160). Thus, coordination of the sulfur, iron, and oxidative stress regulons should benefit *S. aureus*.

Due to the numerous metabolites that satisfy the *S. aureus* sulfur requirement, it is unknown whether this pathogen encounters sulfur-limited environments during infection. Nonetheless, *S. aureus* has evolved several elegant mechanisms to pillage host-derived sulfur reservoirs (134). Sulfur-containing metabolites vary in abundance or composition depending on tissue types and sub-cellular localization (134). Given this, it is accordingly plausible that *S. aureus* adapts to the local sulfur milieu by altering its sulfur acquisition and metabolism transcriptome. Growth of *S. aureus* on four different sulfur

sources (Cys, GSH, GSSG, and sTS) reflects this. In comparison to the CSSC condition, each sulfur source resulted in at least six (Cys) and a maximum of 248 (sTS) differentially expressed genes.

The function of CymR when *S. aureus* meets threshold intracellular Cys levels provokes the thought that providing CSSC, Cys, GSH, GSSG, or TS to *S. aureus* would cause CymR to repress target genes. However, we observe upregulation of sulfur regulon genes in each condition, save Cys (Tables B-2 to B-4). This finding suggests that the provided sulfur concentration is sufficient for growth *in vitro* but does not maintain sufficient intracellular Cys concentrations that would result in CysE inhibition (Fig. 2.1). Quantifying kinetic expression of target genes while monitoring OAS levels throughout *S. aureus* growth will address this. Alternatively, CymR might respond to stimuli not currently appreciated. In fact, CymR has two defined inputs that affects its DNA binding capacity, OAS-thiol-lyase B (CysM) and oxidation of the Cys residue at the position 25 (Fig. 2.1) (118, 121). Another possibility is the influence of coordinated regulation on the sulfur regulon. Indeed, our Tables demonstrate upregulation of transcriptional regulators in both sulfur-limited and -replete environments, implicating connections between sulfur metabolism and other metabolic processes (e.g., iron, oxidative stress). Finally, the Δ*cymR* mutant used in the Soutourina *et al*. study exhibited decreased hemolytic activity and virulence though differential expression of virulence factors was not reported (118, 122). Similarly, our conditions did not reveal altered expression of virulence genes. We attribute this to harvesting RNA from mid-exponential cells when Agr, the major virulence regulator, activity is low.

Collectively, our investigation into the *S. aureu*s sulfur response reveals intricacy surrounding CymR and the sulfur regulon. This manifests when examining the molecular mechanisms of TS assimilation. Extensive characterization of TS assimilation in *E. coli* and *Salmonella typhimurium* has generated a model where an ABC transporter, CysPUWA, imports TS into the cell (161–163). *S. aureus* does not encode a CysPUWA homolog (91). Here we demonstrate that *S. aureus* employs TsuA to support growth on TS (Fig. 2.9B). Additionally, TsuB is thought to be produced from the gene operonic with *tsuA* and contributes to the efficient assimilation of TS (Fig. 2.9B). Given that TsuB belongs to the TusA family of proteins, we predict that it is involved in guiding TS from TsuA to the first enzyme in assimilation, CysM. These observations mirror recent work in *E. coli* and, together, are reshaping our understanding of how bacteria use this inorganic metabolite to meet the nutritional sulfur requirement (135, 152). Most importantly, however, is that these data support the RNAseq by demonstrating that upregulated genes with predicted sulfur metabolism function indeed contribute to meeting this nutritional requirement. Overall, this work provides compelling Tables that highlight the *S. aureus* response to various states of sulfur supplementation and can be utilized to probe the nuances of sulfur metabolism to better understand this persistent threat to global health.

ACKNOWLEDGEMENTS

We thank Jeffery Bose for supplying the pKK22 vector. Transposon mutants were acquired from the Network on Antimicrobial Resistance in *Staphylococcus aureus* (NARSA) for distribution by BEI Resources, NIAID, NIH, and the Nebraska Transposon Mutant Library (NTML) Screening Array NR-48501. This work is funded by the National Institutes of Health R01 AI139074 and R21 AI142517.

MATERIALS AND METHODS

Strains and Primers. A complete list of strains and plasmids as well as primers used in this study can be found in Tables 2.6, 2.7, and 2.8 respectively. JE2, a derivative of the community acquired USA300 LAC, is the WT *S. aureus* strain used in these studies (164). *Bursa aurealis* Tn inactivated strains were generated by transducing the Tn inactivated gene from the Nebraska Transposon Mutant Library into JE2 using a previously described protocol (164–166). Tn insertions and chromosomal deletions were verified using PCR. Plasmids were confirmed using Sanger sequencing (58, 59). Complementation studies were done with the pKK22 vector (153). All pKK22 vector derivatives were generated via Gibson assembly in the *E. coli* DH5α strain and then transformed into *S. aureus* RN4220, an intermediate strain, before JE2.

Media and growth conditions. All strains were cultured overnight in 5 mL tryptic soy broth (TSB; Remel) at 37°C, shaking at 225 rpm. A base chemically defined medium (CDM) was prepared using a previously described recipe with slight modifications (149, 150). Base CDM included the following salts: K_2HPO_4 (7 mg mL^{-1}), KH_2PO_4 (2 mg mL^{-1}), $(NH_4)_2SO_4$ (1 mg mL^{-1}); amino acids: Phe (0.04 mg mL^{-1}), Iso (0.03 mg mL^{-1}), Tyr (0.05 mg mL^{-1}), Glu (0.1 mg mL^{-1}), Lys (0.01 mg mL^{-1}), Met (0.07 mg mL^{-1}), His (0.03 mg mL^{-1}), Trp (0.01 mg mL^{-1}), Leu (0.09 mg mL^{-1}), Asp (0.09 mg mL^{-1}), Arg (0.07 mg mL^{-1}), Ser (0.03 mg mL^{-1}), Ala (0.06 mg mL^{-1}), Thr (0.03 mg mL^{-1}), Gly (0.05 mg mL^{-1}), Val (0.08 mg mL^{-1}), Pro (0.01 mg mL^{-1}); nucleotides: adenosine (0.005 mg mL^{-1}), cytosine, guanine (0.005 mg mL^{-1}), thymine (0.02 mg mL^{-1}), uracil (0.005 mg mL^{-1}); vitamins: thiamine (0.001 mg mL^{-1}), nicotinic acid (0.0012 mg mL^{-1}), biotin ($5e^{-6}$ mg mL^{-1}), calcium pantothenate ($2.5e^{-4}$ mg mL^{-1}); $MgSO_4$ (0.1024 mg mL^{-1}); and $FeCl_3$ (0.008 mg mL^{-1}). This

medium lacks CSSC, asparagine, and glutamine. Freshly prepared D-glucose (5 mg mL^{-1}) was supplemented into the base medium and, depending on the condition, either no sulfur source, 25 μM cystine (CSSC), 50 μM cysteine (Cys), 25 μM reduced glutathione (GSH), 50 μM oxidized glutathione (GSSG), or 50 μM sodium thiosulfate (sTS) prior to inoculation. CSSC and Cys stocks were dissolved in 1 N HCl. Stocks of GSH, GSSG, and sTS were made fresh by dissolving in ddH_2O prior to filter sterilization.

Cultures for biological duplicates for each RNAseq experiment were conducted on independent days. Sulfur starvation was induced by washing WT or *cymR*::Tn *S. aureus* overnight cultures in 1X phosphate buffered saline (PBS) to a normalized optical density at 600 nm (OD_{600}) of 1. Cells were then sub-cultured 1:100 (i.e., OD_{600} equal to 0.01) into two 250 mL Erlenmeyer flasks containing 50 mL CDM supplemented with 25 μM CSSC. Flasks were incubated at 37°C, shaking at 225 rpm, for 4 h (Fig. 2.2). The duplicate flasks were then combined, centrifuged at 4°C, 4700 rpm for 10 min, washed with PBS, centrifuged again, and resuspended in 100 mL CDM harboring no sulfur source. The resulting resuspension was separated by pipetting 50 mL into two 250 mL Erlenmeyer flasks. One flask of WT and *cymR*::Tn was supplemented with 25 μM CSSC while the other remained sulfur deplete. Flasks were incubated at 37°C, shaking at 225 rpm, for 2 h prior to RNA isolation. To assess transcriptional changes between organic (Cys, CSSC, GSH, and GSSG) or inorganic (sTS) sulfur sources, WT cells were prepared identically as described above up to OD_{600} normalization. Cells were then subcultured 1:100 in CDM supplemented with either 50 μM Cys, 25 μM CSSC, 25 μM GSSG, 50 μM GSH, or 50 μM sTS. Flasks were incubated at 37°C, 225 rpm, for 4 h prior to RNA isolation.

Cells were prepared for growth analyses in 96-well plates growth curves as follows: overnight cultures were washed in 5 mL PBS and normalized to an OD_{600} equal to 1. Cells were diluted 1:100 into 150 µL CDM supplemented with 25 µM CSSC, 50 µM sTS, 50 µM GSH, 750 µM GSH, 25 µM GSSG, 375 µM GSSG, or without a source of sulfur. Where described, a 30 mM hemin stock (dissolved in 1.4 M NH_4OH) was diluted into the CDM at a final concentration of 10 µM. OD_{600} was monitored every hour for 24 h using a 96-well round bottom plate in an Epoch2 Biotek microplate spectrophotometer (Agilent, Santa Clara, CA) at 37°C, shaking continuously. For each strain, growth curves were conducted in technical triplicate with the average of the triplicates constituting a single biological replicate. Growth curves were conducted three independent times.

RNA isolation and sequencing. 50 mL cultures from the respective growth conditions were centrifuged at 4°C for 10 min at 4700 rpm. RNA was isolated from the resulting pellet as previously described (90). The RNA was then treated with Turbo DNase following manufacturer's instructions (ThermoFisher, Waltham, MA). Total RNA was sent to Genewiz Inc. (South Plainfield, NJ) who conducted rRNA depletion with Illumina Ribo-Zero Plus (Illumina, Inc., San Diego, CA) and then generated libraries using stranded total RNA kit and sequenced using Illumina HiSeq (Illumina, Inc.) with 2x 150 bp paired-end read technology.

RNA-seq data processing and visualization. Raw reads for this project were submitted under bioproject number PRJNA989516. Gene expression was analyzed using Geneious Prime 2022.0.2 (Dotmanics, Boston, MA). Briefly, paired end fastq files were trimmed using Bbduk plugin, and mapped and annotated against the reference genome *S. aureus* USA300_FRP3757 (NC_007793.1) using Geneious mapper with default settings. The

expression levels were calculated within the software using default parameters, and DESeq2 was implemented to determine the differential expression with the comparisons listed in figure legends (167). Data was filtered using a $\log_2$ ratio greater than or equal to 1 and less than or equal to -1 representing a 2-fold change and an adjusted *P*-value of less than 0.05. Differential expression analysis was conducted using transcripts per million (TPM). Low TPM values (<10) were manually removed to eliminate bias. Variance was then controlled for by either discarding replicates with TPM differences >5 and/or if the TPM values between conditions were to close (≤5). Cluster of orthologous groups (COG) categories were determined using eggNOG-mapper v2 (168, 169). Briefly, protein sequences from USA300_FPR3757 (NC_007793.1) were used as input for eggNOG-mapper v2 to assign functional annotations. Protein sequences that were recognized by eggNOG-mapper but had no resulting COG assignment were denoted as “not classified”. The protein sequences that were not recognized by eggNOG-mapper and were double checked for any COG assignments as follows: the USA300_FPR3757 locus tag was used to identify the corresponding homolog in *S. aureus* NCTC8325 using Aureowiki (91). The NCTC8325 homolog locus tag was then queried against EggNOG v6.0 (170). When this did not return any COG assignment the gene was denoted as “no homolog found”.

H_2O_2 peroxide killing assay. This assay was modified from a previously defined protocol (171). Overnight WT TSB cultures were washed in PBS and normalized to an OD_{600} of 1. Cells were then sub-cultured 1:100 into two 250 mL Erlenmeyer flasks containing 50 mL CDM supplemented with either 50 μM GSH, 750 μM GSH, or 375 μM GSSG. Cultures were incubated at 37°C, shaking at 225 rpm, for 4 h. Cells were then transferred to a 50 mL falcon tube and spun at 4000 rpm and then resuspended in 50 mL PBS. 1 mL of the

resuspension was utilized to obtain the OD_{600} while the remaining cells were spun at 4000 rpm. After decanting the supernatant cells were gently resuspended in residual PBS. One falcon tube for each growth condition was then resuspended in PBS to a final OD_{600} of 0.7. The other tube was resuspended to the same OD_{600} with PBS containing 1 M H_2O_2 (freshly made). Tubes were then placed at 37°C**,** static, for 20 min. Afterwards 3x 50 µL aliquots (i.e., 3 technical replicates) from each condition were resuspended in 950 µL PBS containing approximately 2,000-5,000 units mg^{-1} catalase (Sigma-Aldrich Cat No: C9322-5G; resuspended at 1 mg mL^{-1} and not filter sterilized). Samples were then incubated at 37°C**,** static, for 5 min. For each strain, three technical replicates were then serial diluted in PBS and 10 µL was spot plated onto TSA to enumerate for CFU**.** Note that the average of these technical triplicates is considered as one biological replicate. Plates were incubated overnight at 37°C**.** Each assay was performed in biological triplicate.

Data visualization. Growth curves, heat maps, and bar graphs were generated using GraphPad Prism software version 10.0.0 (153). All finalized figures were generated using the open source Inkscape 1.2.2 (b0a8486, 2022-12-01). Available at: https://inkscape.org.

TABLES

Table 2.1. Transcriptional changes resulting from sulfur starvation and CymR regulation.

Culture condition	Comparator	Total DE genes	Upregulated genes	Downregulated genes
WT no sulfur supplementation[a]	WT + CSSC	567	425	142
cymR::Tn + CSSC[b]	WT + CSSC	67	45	22
cymR::Tn no sulfur supplementation[c]	*cymR*::Tn + CSSC	255	170	85

Genes were differentially expressed (DE) with a Log_2 fold change at least equal to +/-1 with a *P* value <0.05 from DESeq2 output.

[a]Sulfur starvation response

[b]CymR sulfur-replete regulon

[c]Starvation-induced changes independent of CymR

Table 2.2. Previously identified sulfur metabolism genes identified within the upregulated sulfur starvation transcriptome and the CymR regulon.

Locus[a]	Gene	WT -S Log_2 FC	WT -S Adjusted *P*-value[b]	*cymR* +S Log_2 FC	*cymR* +S Adjusted *P*-value[b]
SAUSA300_RS00910[c]		5.396	6.368E-33	3.430	1.335E-06
SAUSA300_RS00915[d]	*ssuB*	4.636	5.563E-24		
SAUSA300_RS00930[c]		5.543	1.586E-27	3.059	5.169E-07
SAUSA300_RS00935[e]		2.108	4.827E-07		
SAUSA300_RS00940[e]	*fdh*	1.617	1.017E-03		
SAUSA300_RS01055[c]	*gisA*	4.815	1.637E-19	2.266	3.735E-03
SAUSA300_RS02035[c]	*tcyP*	2.679	1.024E-06	2.699	1.428E-04
SAUSA300_RS02320[d]	*mccA*	3.664	6.023E-15		
SAUSA300_RS02325[c]	*mccB*	2.907	5.072E-08	1.988	2.250E-02
SAUSA300_RS02330[c]	*gmpA*	4.815	9.671E-27	1.904	1.135E-02
SAUSA300_RS02635[f]	*cysK*			2.035	1.199E-02
SAUSA300_RS10985[c]		6.339	1.132E-52	3.435	5.131E-07
SAUSA300_RS12345[d]	*ydbM*	1.676	2.724E-03		
SAUSA300_RS13015[d]	*tcyC*	2.063	7.411E-06		
SAUSA300_RS13020[d]	*tcyB*	1.681	1.932E-03		
SAUSA300_RS13025[c]	*tcyA*	2.083	5.380E-06	1.693	2.663E-02

[a]All 16 sulfur metabolism genes from Table 1 of (118) represented as the respective JE2 homologs. that are shared between Soutourina *et al*.
[b]Adjusted *P*-value from DESeq2 output from the WT sulfur starvation (denoted as WT -S, Table 1) and *cymR*::Tn sulfur replete (represented as *cymR* +S, Table 2) conditions.
[c]Shared between the published CymR regulon (118), WT -S, and *cymR* +S
[d]Genes that are downregulated in *cymR* +S and does not meet the adjusted *P*-value cutoff of <0.05 (data not shown).
[e]Denotes genes that are upregulated in *cymR* +S but does not have a Log_2 ratio ≥1 and/or does not meet the adjusted *P*-value cutoff of <0.05 (data not shown).
[f]Represents the gene that is upregulated in WT -S but does not have a Log_2 ratio ≥1 and/or does not meet the adjusted *P*-value cutoff of <0.05 (data not shown).

Table 2.3. *cymR* mutant upregulated genes under sulfur replete conditions.

Locus	Gene	Product	Log2 FC[a]	Adjusted *P*-value[b]	COG[c]
SAUSA300_RS10985		YeeE/YedE family protein	3.435	5.131E-07	S
SAUSA300_RS00910		DUF4242 domain-containing protein	3.430	1.335E-06	S
SAUSA300_RS10980		sulfurtransferase TusA family protein	3.325	9.084E-07	O
SAUSA300_RS00925	*ssuC*	ABC transporter permease	3.109	2.476E-06	P
SAUSA300_RS00930		acyl-CoA/acyl-ACP dehydrogenase	3.059	5.169E-07	I
SAUSA300_RS13915	*isaA*	lytic transglycosylase IsaA	2.807	1.255E-03	M
SAUSA300_RS02035	*tcyP*	L-cystine transporter	2.699	1.428E-04	U
SAUSA300_RS05050		DoxX family protein	2.369	6.815E-04	S
SAUSA300_RS02045		hypothetical protein	2.290	2.041E-04	A
SAUSA300_RS01055	*gisA*	ABC transporter ATP-binding protein	2.266	3.735E-03	P
SAUSA300_RS02340	*gmpC*	dipeptide ABC transporter glycylmethionine-binding lipoprotein	2.194	6.966E-03	P
SAUSA300_RS12610	*sdpC*	CPBP family intramembrane glutamic endopeptidase SdpC	2.104	2.280E-03	S
SAUSA300_RS00915		ABC transporter ATP-binding protein	2.053	1.266E-02	P
SAUSA300_RS05345		YkyA family protein	2.048	1.382E-02	L
SAUSA300_RS02635	*cysK*	cysteine synthase A	2.035	1.199E-02	E
SAUSA300_RS09430		hypothetical protein	2.020	1.388E-02	not classified
SAUSA300_RS02325	*mccB*	bifunctional cystathionine γ-lyase/homocysteine desulfhydrase	1.988	2.250E-02	E
SAUSA300_RS02335	*gmpB*	methionine ABC transporter permease	1.977	2.036E-02	P
SAUSA300_RS09440	*crcB2*	CrcB family protein	1.976	9.513E-03	D

Table 2.3 (cont'd)

SAUSA300_RS01875		low temperature requirement protein A	1.933	1.404E-02	S
SAUSA300_RS13605		ATP-binding cassette domain-containing protein	1.906	1.654E-02	V
SAUSA300_RS00920	*ssuA*	ABC transporter substrate-binding protein	1.904	2.249E-02	P
SAUSA300_RS02330	*gmpA*	methionine ABC transporter ATP-binding protein	1.904	1.135E-02	P
SAUSA300_RS12685		alpha/beta hydrolase	1.878	3.211E-02	I
SAUSA300_RS01060	*gisB*	ABC transporter permease	1.834	3.649E-02	EP
SAUSA300_RS13940		DUF896 domain-containing protein	1.825	4.623E-02	S
SAUSA300_RS04485		DUF3055 domain-containing protein	1.822	1.364E-02	S
SAUSA300_RS02855		M20 family metallopeptidase	1.785	2.250E-02	E
SAUSA300_RS07460		hypothetical protein	1.725	2.352E-02	no homolog found
SAUSA300_RS13025	*tcyA*	transporter substrate-binding domain-containing protein	1.693	2.663E-02	ET
SAUSA300_RS13320	*lnsB*	CPBP family lipoprotein N-acylation protein LnsB	1.654	3.853E-02	S
SAUSA300_RS10230		hypothetical protein	1.646	3.008E-02	not classified
SAUSA300_RS05540	*isdA*	LPXTG-anchored heme-scavenging protein IsdA	1.646	3.382E-02	M
SAUSA300_RS12705		TetR/AcrR family transcriptional regulator	1.620	4.532E-02	K
SAUSA300_RS11450		DUF2529 domain-containing protein	1.618	2.554E-02	S
SAUSA300_RS00605	*sirA*	staphyloferrin B ABC transporter substrate-binding protein SirA	1.608	2.782E-02	P
SAUSA300_RS12440		CHAP domain-containing protein	1.588	3.896E-02	S
SAUSA300_RS03340	*tagA*	N-acetylglucosaminyldiphosphoundecaprenol N-acetyl-β -D-mannosaminyltransferase TarA	1.532	3.008E-02	M

Table 2.3 (cont'd)

SAUSA300_RS07465	*cmk*	(d)CMP kinase	1.530	2.784E-02	F
SAUSA300_RS04060	*clpP*	ATP-dependent Clp endopeptidase proteolytic subunit ClpP	1.525	4.532E-02	OU
SAUSA300_RS00985	*brnQ1*	branched-chain amino acid transport system II carrier protein	1.503	4.983E-02	E
SAUSA300_RS04205	*lnsA*	lipoprotein N-acylation protein LnsA	1.498	3.766E-02	not classified
SAUSA300_RS07075	*brnQ3*	branched-chain amino acid transport system II carrier protein	1.469	4.532E-02	E
SAUSA300_RS15260		hypothetical protein	1.454	4.532E-02	no homolog found
SAUSA300_RS09900		PTS transporter subunit IIC	1.454	4.532E-02	S

[a]Fold change (FC) expression of *cymR*::Tn grown in medium containing CSSC relative to WT grown in same medium.
[b]Adjusted *P*-value from DESeq2 output.
[c]COG assignments using eggNOG-mapper. A: RNA processing and modification; D: cell cycle control and mitosis; E: amino acid metabolism and transport; F: nucleotide metabolism and transport; I: lipid metabolism; K: transcription; L: replication and repair; M: cell wall/membrane/ envelope biogenesis; O: post-translational modification, protein turnover, chaperone function; P: inorganic ion transport and metabolism; S: function unknown; T: signal transduction; U: intracellular trafficking and secretion; V: defense mechanisms . Not classified: genes with an eggNOG-mapper homolog, but no associated COG. No homologs found: neither eggNOG-mapper nor Eggnog v6 could find a homolog for these proteins.
Genes highlighted in grey indicate overlap with Soutourina *et al*. (118).

Table 2.4. *S. aureus* sulfur starvation induces differential expression of genes encoding transcriptional regulators.

Locus	Gene	Description	Log_2 FC[a]	Adjusted *P*-value[b]
Upregulated				
SAUSA300_RS00650	*sbnI*	bifunctional transcriptional regulator/O-phospho-L-serine synthase SbnI	2.787	4.361E-11
SAUSA300_RS04840	*spxA*	transcriptional regulator SpxA	2.710	2.553E-09
SAUSA300_RS07905	*fur*	Fur family transcriptional regulator	2.692	9.202E-11
SAUSA300_RS05125		MarR family transcriptional regulator	2.488	6.488E-06
SAUSA300_RS08020	*argR*	transcriptional regulator ArgR	2.348	2.264E-07
SAUSA300_RS12240	*sarV*	HTH-type transcriptional regulator SarV	2.319	6.725E-06
SAUSA300_RS03710	*saeR*	response regulator transcription factor SaeR	2.241	2.563E-06
SAUSA300_RS13930		TetR/AcrR family transcriptional regulator	2.009	8.284E-06
SAUSA300_RS03330		metal-dependent transcriptional regulator	1.998	4.804E-06
SAUSA300_RS12705		TetR/AcrR family transcriptional regulator	1.954	5.729E-05
SAUSA300_RS10810		XRE family transcriptional regulator	1.937	5.507E-06
SAUSA300_RS13640		MarR family transcriptional regulator	1.908	1.274E-04
SAUSA300_RS00590	*sarS*	HTH-type transcriptional regulator SarS	1.798	1.302E-04
SAUSA300_RS10675		transcriptional activator RinB	1.720	1.793E-03
SAUSA300_RS13480	*scrA*	SaeRS system activator ScrA	1.647	1.974E-03
SAUSA300_RS09835		helix-turn-helix transcriptional regulator	1.627	3.238E-03
SAUSA300_RS12900		MerR family transcriptional regulator	1.516	3.018E-03
SAUSA300_RS12510		MurR/RpiR family transcriptional regulator	1.506	2.981E-04
SAUSA300_RS01375		GntR family transcriptional regulator	1.481	5.905E-04

Table 2.4 (cont'd)

SAUSA300_RS08625	*cymR*	Rrf2 family transcriptional regulator	1.466	1.744E-03
SAUSA300_RS08905	*nrdR*	transcriptional regulator NrdR	1.432	1.425E-03
SAUSA300_RS06710	*lexA*	transcriptional repressor LexA	1.360	1.701E-03
SAUSA300_RS03605	*mgrA*	HTH-type transcriptional regulator MgrA	1.227	9.413E-03
SAUSA300_RS10805		transcriptional regulator	1.224	1.972E-02
SAUSA300_RS10800		helix-turn-helix transcriptional regulator	1.179	2.229E-02
SAUSA300_RS10060	*perR*	peroxide-responsive transcriptional repressor PerR	1.134	2.713E-02
SAUSA300_RS14275		Crp/Fnr family transcriptional regulator	1.131	1.960E-02
SAUSA300_RS12730		MarR family transcriptional regulator	1.032	2.767E-02
Downregulated				
SAUSA300_RS06210	*codY*	GTP-sensing pleiotropic transcriptional regulator CodY	-3.183	3.373E-12
SAUSA300_RS03665		DeoR/GlpR family DNA-binding transcription regulator	-2.413	5.295E-08
SAUSA300_RS10935	*agrB*	accessory gene regulator AgrB	-2.386	4.644E-09
SAUSA300_RS03250	*sarA*	global transcriptional regulator SarA	-2.301	1.061E-06
SAUSA300_RS13560		MerR family transcriptional regulator	-1.867	4.348E-05
SAUSA300_RS02550		septation regulator SpoVG	-1.696	2.131E-04

[a]Fold change (FC) expression of WT grown in sulfur deplete conditions relative to WT grown in sulfur replete conditions.
[b]Adjusted *P*-value from DESeq2 output.

Table 2.5. *S. aureus* sulfur starvation induces expression of iron acquisition and oxidative stress genes.

Locus	Gene	Product	Log_2 FC[a]	Adjusted *P*-value[b]
Iron acquisition and metabolism				
SAUSA300_RS10250*	*ftnA*	H-type ferritin FtnA	4.859	8.351E-36
SAUSA300_RS07500*	*fer*	ferredoxin	3.830	1.039E-20
SAUSA300_RS12340*	*fhuD2*	ABC transporter substrate-binding protein	3.640	3.636E-14
SAUSA300_RS05570*	*isdG*	staphylobilin-forming heme oxygenase IsdG	3.569	2.570E-13
SAUSA300_RS03395*	*fhuA*	ABC transporter ATP-binding protein	2.842	7.910E-10
SAUSA300_RS00650*	*sbnI*	bifunctional transcriptional regulator/O-phospho-L-serine synthase SbnI	2.787	4.361E-11
SAUSA300_RS00885*	*isdI*	staphylobilin-forming heme oxygenase IsdI	2.708	1.950E-09
SAUSA300_RS07905*	*fur*	Fur family transcriptional regulator	2.692	9.202E-11
SAUSA300_RS03880*	*sstD*	siderophore ABC transporter substrate-binding protein	2.494	1.217E-08
SAUSA300_RS03400	*fhuB*	iron ABC transporter permease	2.401	6.004E-09
SAUSA300_RS11755*	*htsB*	iron ABC transporter permease	2.288	3.617E-08
SAUSA300_RS11750*	*htsD*	iron chelate uptake ABC transporter family permease subunit	1.805	1.631E-05
SAUSA300_RS13050		cation diffusion facilitator family transporter	1.699	7.185E-05
SAUSA300_RS11760	*htsA*	Fe(3+) dicitrate ABC transporter substrate-binding protein	1.683	3.142E-04
SAUSA300_RS04430	*sufB*	Fe-S cluster assembly protein SufB	1.592	2.898E-04
SAUSA300_RS03405	*fhuG*	iron ABC transporter permease	1.079	1.426E-02
Oxidative stress				
SAUSA300_RS02020*	*ahpF*	alkyl hydroperoxide reductase subunit F	2.890	6.579E-11
SAUSA300_RS02025*	*ahpC*	alkyl hydroperoxide reductase subunit C	2.847	2.870E-12

Table 2.5 (cont'd)

SAUSA300_RS06680*	*katA*	catalase	2.170	7.710E-08
SAUSA300_RS14205	*gpxA2*	glutathione peroxidase	2.025	1.969E-05
SAUSA300_RS13655	*frp*	NAD(P)H-dependent oxidoreductase	1.909	2.779E-05
SAUSA300_RS06465	*bsaA*	glutathione peroxidase	1.228	7.125E-03
SAUSA300_RS10060	*perR*	peroxide-responsive transcriptional repressor PerR	1.134	2.713E-02
Genes unique to sulfur depleted *cymR*::Tn				
SAUSA300_RS03085	*hypR*	redox-sensitive transcriptional regulator HypR	4.455	9.670E-19
SAUSA300_RS11770	*sfnaC*	staphyloferrin A biosynthesis protein SfaC	2.994	3.400E-09
SAUSA300_RS11780	*sfnaA*	staphyloferrin A export MFS transporter	2.994	4.050E-06
SAUSA300_RS00625	*sbnD*	staphyloferrin B export MFS transporter	2.922	2.110E-07
SAUSA300_RS05560	*isdF*	hemin ABC transporter permease protein IsdF	2.816	6.940E-06
SAUSA300_RS11775	*sfnaB*	staphyloferrin A synthetase SfaB	2.728	2.970E-07
SAUSA300_RS14545		ABC transporter ATP-binding protein	2.710	1.190E-05
SAUSA300_RS03875	*sstC*	ABC transporter ATP-binding protein	2.679	2.990E-06
SAUSA300_RS05555	*isdE*	heme ABC transporter substrate-binding protein IsdE	2.249	2.651E-03
SAUSA300_RS04425	*sufU*	SUF system NifU family Fe-S cluster assembly protein	2.109	5.562E-04
SAUSA300_RS03865	*sstA*	ABC transporter permease	2.090	1.951E-04
SAUSA300_RS04410	*sufC*	Fe-S cluster assembly ATPase SufC	1.661	2.513E-03
SAUSA300_RS04420	*sufS*	cysteine desulfurase	1.581	1.014E-02
SAUSA300_RS04415	*sufD*	Fe-S cluster assembly protein SufD	1.534	1.325E-02

[a]Fold change (FC) expression of WT grown in sulfur deplete condition relative to WT grown in sulfur replete condition (Table A-1). The *cymR*::Tn unique genes are the expression ratio of *cymR*::Tn grown in sulfur deplete conditions relative to *cymR*::Tn grown in sulfur replete conditions (Table A-3).
[b]Adjusted *P*-value from DESeq2 output.

Table 2.5 (cont'd)

*Also upregulated in sulfur starved *cymR*::Tn.

Table 2.6. Strains used in this study.

Strain	Description	Reference
wild type	USA300 LAC derivative JE2	(164, 166)
cymR::Tn	Erythromycin resistant (Erm^r) *Bursa* Tn insertion at JE2 chromosome position 1733227	(164, 166)
hrtA::Tn	Erm^r *Bursa* Tn insertion at JE2 chromosome position 2479408	(164, 166)
tsuA::Tn	Erm^r *Bursa* Tn insertion at JE2 chromosome position 2156268	(164, 166)
SAUSA300_RS04580::Tn	Erm^r *Bursa* Tn insertion at JE2 chromosome position 927895	(164, 166)

Table 2.7. Plasmids used in this study.

Plasmid	Description	Reference
pKK22	Derivative of the naturally occurring *S. aureus* plasmid LAC-p01. Maintains stability in *S. aureus* without antibiotics. Linearized for Gibson assembly using primers PK85 & PK86.	(153)
pKK22-*tsuAB*	pKK22 expressing *tsuA* (SAUSA300_RS10985) and *tsuB* (SAUSA300_RS10980) under native promoter expression. Insert generated with following primers: PK5 & PK8	This study
pKK22-*tsuA*	pKK22 expressing *tsuA* (SAUSA300_RS10985) under native promoter expression. Generated insert with following primers: PK5 & PK10	This study
pKK22-*tsuB*	pKK22 expressing *tsuB* (SAUSA300_RS10980) under native promoter expression. Insert generated as follows: PK5 & PK6 (promoter), PK7 & PK8 (*tsuB*); PK5 & PK8 used to sew promoter and *tsuB* fragments together before Gibson assembly.	This study

Table 2.8. Primers utilized to generate strains in Table 1.

Primer	Description	Sequence (5' → 3')
PK85	pKK22 amplification/linearization for Gibson assembly	GCGGCCGCTAGCCTAGGAGC
PK86	pKK22 amplification/linearization for Gibson assembly	ATCGCCTGTCACTTTGCTTGATATATGA
NE Martn-ermR*	Used to confirm Tn insertions on plus strand	CTCGATTCTATTAACAAGGG
NE Buster*	Used to confirm Tn insertions on minus strand	GCTTTTTCTAAATGTTTTTTAAGTAAATCAAGTAC
HL246	Confirming *Bursa* Tn insertion in *cymR*	CTAATAACAAGATAACTTGACCAGAC
PK110	Confirming *Bursa* Tn insertion in *hrtA*	AGAACTTAATGTCCCAGCC
HL267	Confirming *Bursa* Tn insertion in *tsuA*	TCCCATACATATGCCACC
PK5	Amplify *tsuAB* promoter and operon for Gibson assembly	CAAGCAAAGTGACAGGCGATTAGATGTTGTGATTCTAACTAC
PK6	Amplify *tsuAB* promoter for Gibson assembly	CGTGTATCATAATCTTAACCTCTCATTTCC
PK7	Amplify *tsuB* for Gibson assembly	GGTTAAGATTATGATACACGAATTAGGTAC
PK8	Amplify *tsuB* for Gibson assembly	GCTCCTAGGCTAGCGGCCGCTTAAACTTTTTGAATTGTAATTGTC
PK10	Amplify promoter and *tsuA* operon for Gibson assembly	GCTCCTAGGCTAGCGGCCGCCTATACTATTTGCGTTTGC

*Reference: (164, 166)

FIGURES

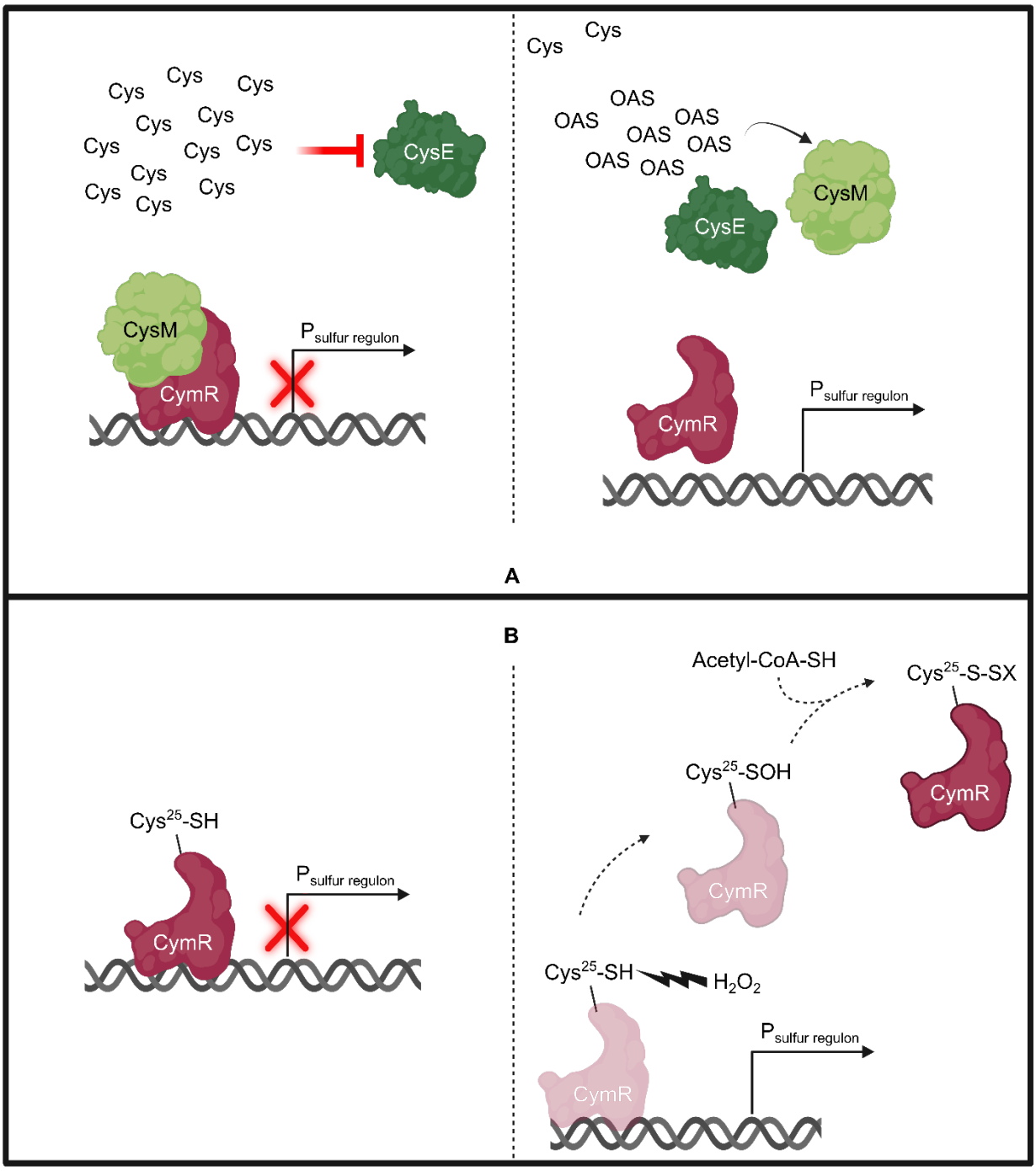

Figure 2.1. *S. aureus* CymR responds to at least two different stimuli. A) Model of CymR function described by Soutourina *et al* (118). CymR senses the intracellular Cys pool through the product of serine transacetylase (CysE), *O*-acetylserine (OAS), Top Left: CysE forms a complex with OAS-thiol-lyase B (CysM, aka MccA) and, under low intracellular Cys levels, produces OAS which is then consumed by CysM for use in

Figure 2.1 (cont'd)

inorganic sulfur assimilation. CymR is inactive in this condition and transcription of sulfur acquisition and metabolism systems proceed. Top Right: CysE is inhibited by Cys when the amino acid is present at threshold concentrations. In this situation, CysM is released and interacts with CymR. The CysM-CymR complex then binds target DNA and inhibits expression of the sulfur regulon (118, 134). B) Model of CymR activity as described by Ji *et al.* Bottom Left: CymR additionally senses the oxidation state of *S. aureus* via its sole Cys residue at position 25. When the Cys is in the reduced stated (i.e., has the -SH thiol group), CymR will bind to DNA. Bottom Right: When this residue is oxidized by H_2O_2, the thiol group will form a sulfinic acid (-SOH) intermediate. The low molecular weight thiol, Acetyl CoA, can then form a disulfide bond with CymR, decreasing the affinity of this regulator for DNA (right) (121). Made with BioRender.

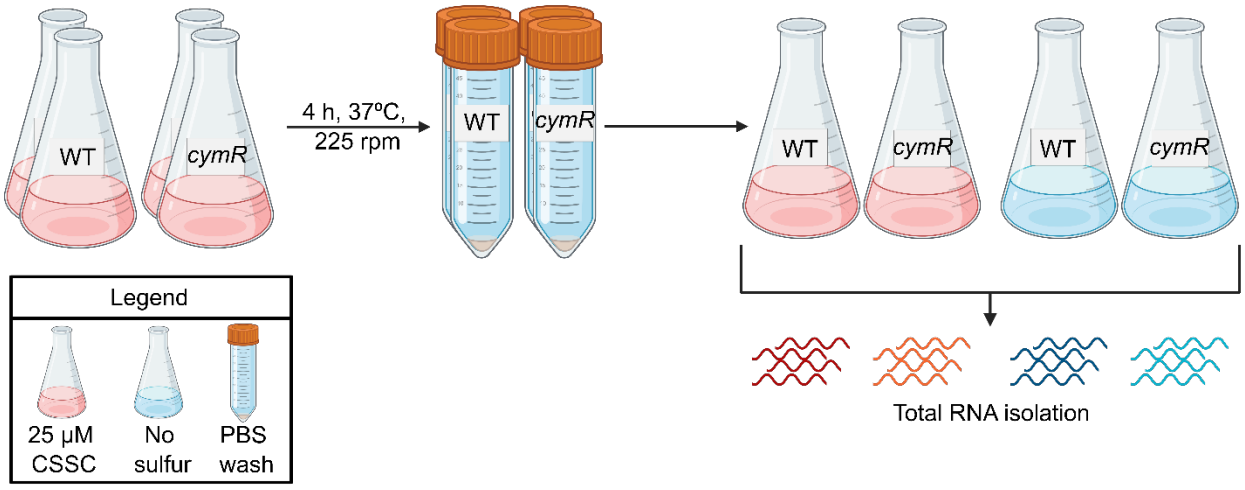

Figure 2.2. Experimental design employed to define the CymR-dependent and –independent responses to sulfur starvation in *S. aureus*. WT or *cymR*::Tn *S. aureus* were sub-cultured from normalized overnights into CDM supplemented with 25 µM CSSC and grown to mid-exponential phase (4 h). Cultures were pelleted, washed, and resuspended to the same cell density in medium with 25 µM CSSC or no viable sulfur source. Cells were grown for an additional 2 h prior to RNA isolation. Image generated with BioRender.com.

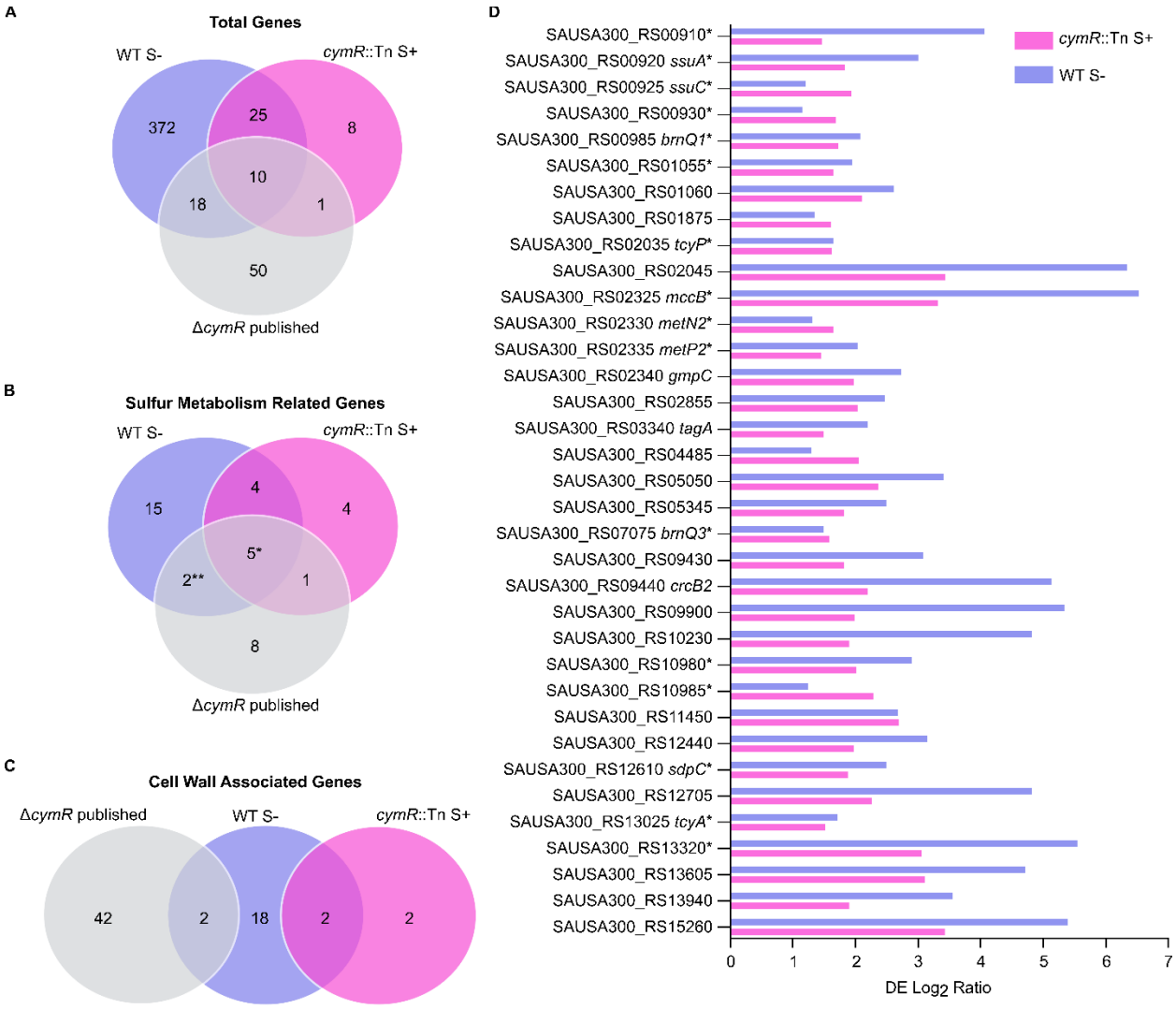

Figure 2.3. Comparison of the *S. aureus* sulfur starvation transcriptional response to the CymR regulon. A-C) Venn diagrams comparing genes upregulated in sulfur starved WT (WT -S; purple), *cymR*::Tn cultured in CSSC (*cymR*::Tn +S, pink), and the previously published Δ*cymR* mutant sulfur Table (Δ*cymR* published, grey). The previously defined Δ*cymR* transcriptome was generated from using Table 2 and Table 4 from (118) as well as Table 1 from (122). **A**) The total number of genes upregulated in all three Tables. **B**) Sulfur metabolism associated genes differentially regulated between the three Tables. Table 2 from Soutourina *et al*. (118) was used for this assessment. Functional annotation of genes identified in the current study were defined using eggNOG-mapper (168, 169). The COG Database was then used to identify COGs associated with the terms "sulf", "methionine", "cysteine", "cystine", "glutathione", and "γ-glutamyl-transpeptidase" (172, 173); these genes were classified as sulfur metabolism related. *Note that the genes shared between Δ*cymR* published, WT -S, and *cymR*::Tn +S should be eight. One gene, SAUSA300_RS13025 (*tcyA*), was assigned COG0834 (ABC-type amino acid transport/signal transduction system, periplasmic component/domain) and was thus not identified within the abovementioned parameters.

Figure 2.3 (cont'd)

However, *tcyA* is known to participate in cyst(e)ine transport in *S. aureus* (90). Of the remaining two genes, SAUSA300_RS00910 is a hypothetical protein assigned the COG category of unknown function (S) under CymR regulon control (91); SAUSA300_RS00930 was designated COG "I" for lipid transport and metabolism but is part of the SfnB family of sulfur acquisition oxidoreductases (91). **Additionally, genes shared between WT -S and Δ*cymR* published should be four: *tcyC* (SAUSA300_RS13015) was assigned to COG1126, and *tcyB* (SAUSA300_RS13020) was assigned to COG0765; neither of these COGs were found with the search parameters for sulfur metabolism genes described above. However, these genes encode subunits of the TcyABC complex (90). **C**) Cell wall associated genes differentially regulated between the three Tables. Table 4 from Soutourina *et al*. (118) was used to generate this Venn diagram. Genes for the current study were defined as cell wall associated if eggNOG-mapper assigned the gene to COG category M (cell wall/membrane/envelope biogenesis). No genes were found to be common amongst all three Tables using this method. However, upon comparing Table 4 from Soutourina *et al*. to the total upregulated genes for sulfur starved WT (WT -S) and CSSC supplemented *cymR*::Tn (*cymR*::Tn +S) revealed two common genes, SAUSA300_RS01875, which was assigned as COG S (unknown function), and SAUSA300_RS15260 (no homolog found). **D**) Comparison of the Log_2 ratio of genes upregulated in either *cymR*::Tn supplemented with CSSC (Table 2; pink) or sulfur depleted WT (Table 1; purple). *denotes genes that were shared with WT -S and *cymR*::Tn +S sulfur metabolism genes in B, including genes *tcyA*, SAUSA300_RS00910, and SAUSA300_RS00930.

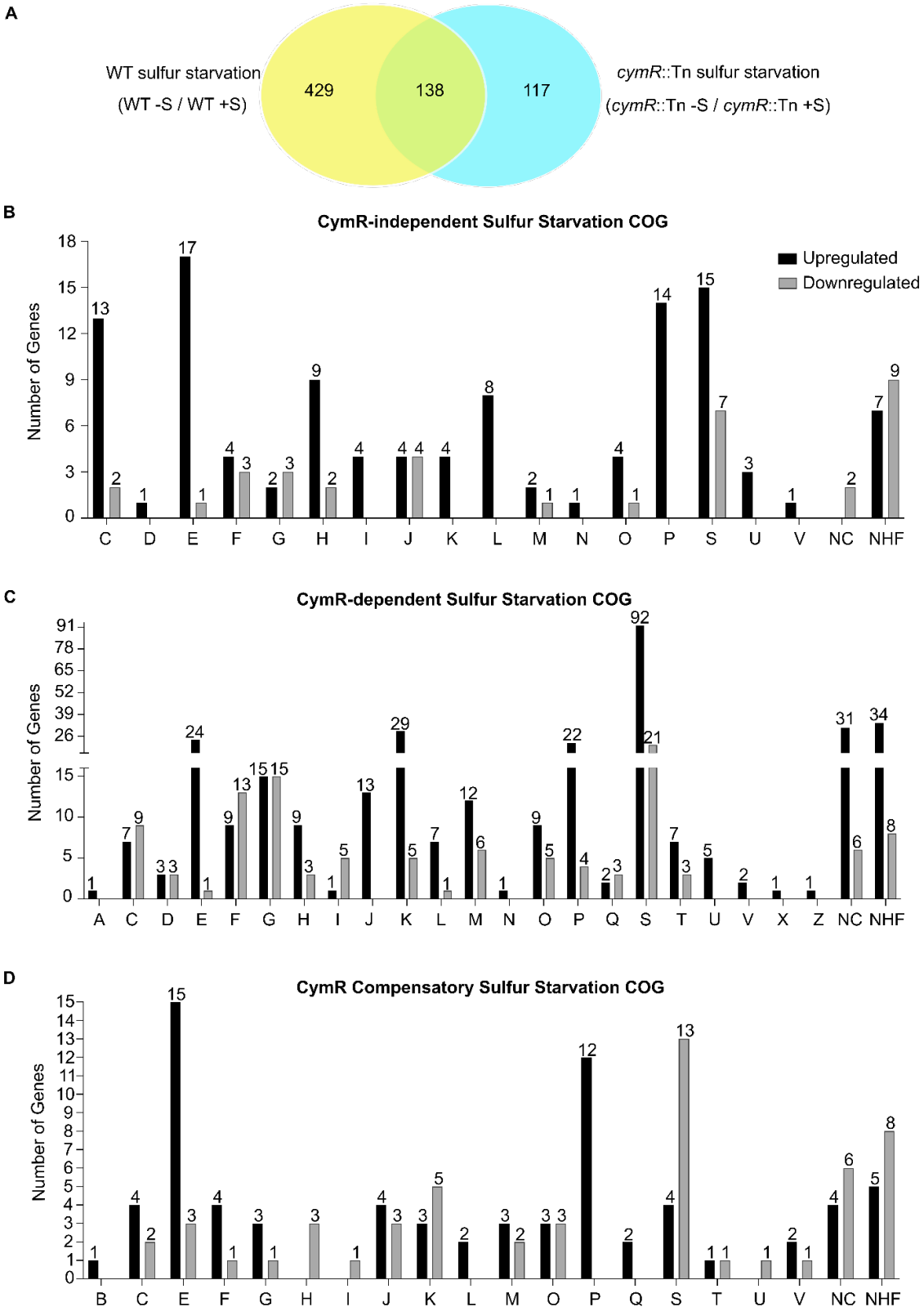

Figure 2.4. The *S. aureus* sulfur starvation response is not fully dependent on CymR. A) WT sulfur starvation response loci from Table 1a (*n*=567; yellow) were

Fgiure 2.4 (cont'd)

compared against the starvation response when CymR is absent (Table 1c; *n*=255; cyan). Genes that shared between WT and the *cymR*::Tn mutant are considered to CymR-independent (*n*=138). CymR independent genes are those genes unique to the WT sulfur starvation condition (*n*=429). Additionally, genes unqiue to the *cymR*::Tn condition (*n*=117) are likely differentially expressed to compensate for the loss of CymR during sulfur starvation. Figure created in Biorender. **B-D)** Genes that shared between the WT and *cymR*::Tn sulfur starvation (**B**) or are unique to WT or *cymR*::Tn sulfur starvation (**C** and **D**, respectively) conditions catagorized by COG assignment. COG assignments are as follows: A (RNA processing and modification), B (chromatin structure and dynamics), C (energy production and conversion), D (cell cycle control, cell division, chromosome partitioning), E (amino acid transport and metabolism), F (nucleotide transporter and metabolism), G (carbohydrate transport and metabolism), H (coenzyme transport and metabolism), I (lipid transport and metabolism), J (translation, ribosomal structure and biogenesis), K (transcription), L (replication, recombination and repair), M (cell wall/membrane/envelope biogenesis), N (cell motility), O (posttranslational modification, protein turnover, chaperones), P (inorgnaic ion trasnport and metabolism), Q (secondary metabolites biosynthesis, transport and catabolism), S (function unknown), T (signal trasnduction mechanisms), U (intracellular trafficking, secretion, and vesicular transport), V (defense mechanisms), Z (cytoskeleton) not classified (NC). In some instances no homologs were found (NHF). Values above each bar represents the number of genes for each COG category.

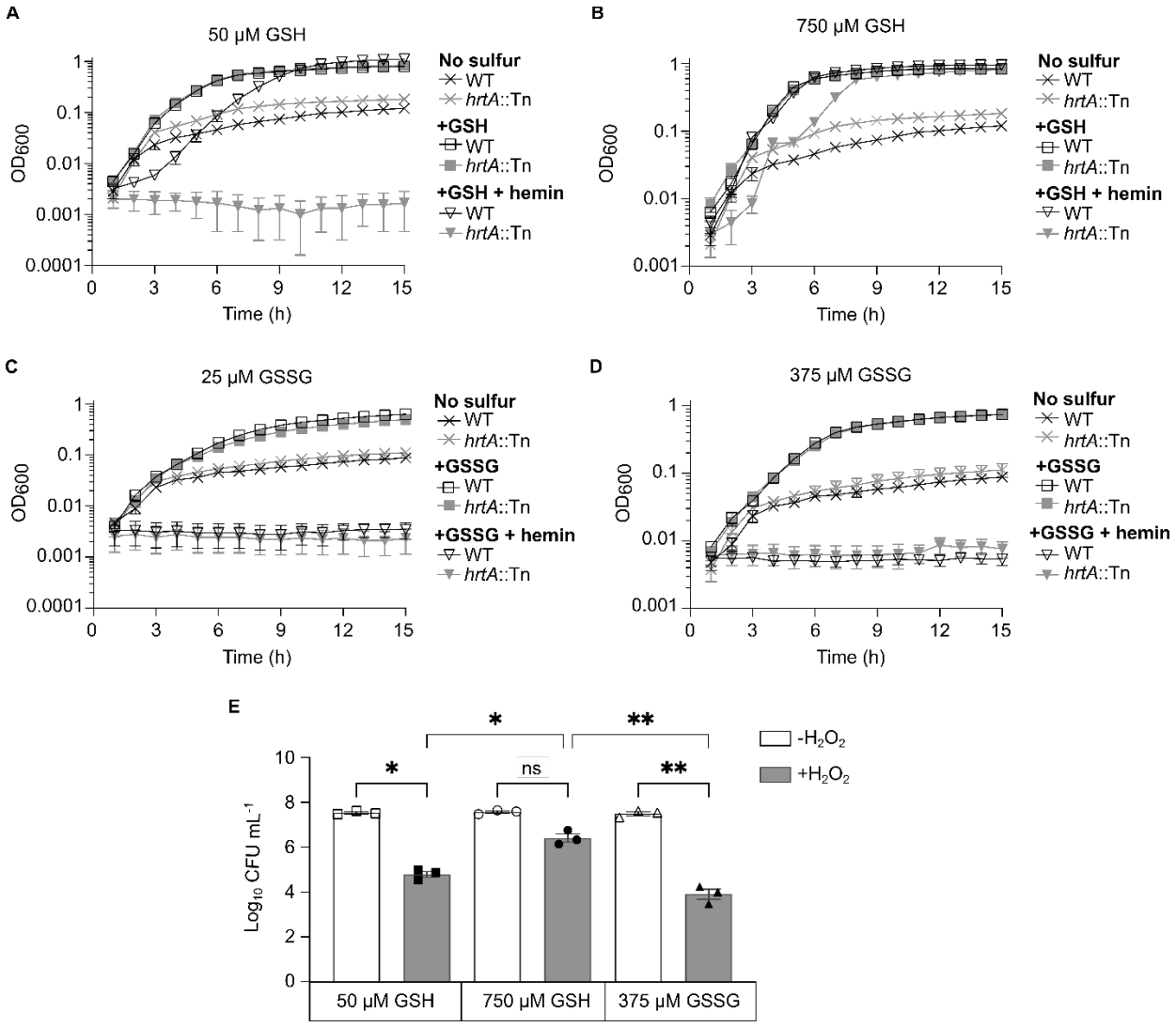

Figure 2.5. GSH alleviates oxidative stress in *S. aureus*. *S. aureus* WT and *hrtA*::Tn were cultured in chemically defined medium (CDM) in the absence of a sulfur source or supplemented with 50 μM or 750 μM reduced glutathione (GSH) (**A** and **B**, respectively) as well as 25 μM or 375 μM oxidized glutathione (GSSG) (**C** and **D**, respectively) in the presence or absence of 10 □M hemin. Curves are the mean of three independent trials and the error bars represent ±1 standard error of the mean. **E**) WT preloaded with either 50 □M GSH (squares), 750 □M GSH (circles), or 375 □M GSSG (triangles) were left untreated (open symbols) or exposed to 1 M H_2O_2 (closed symbols) before enumeration for CFU. Presented are the average of three independent trials ±1 standard error of the mean. Statistical significance represents Brown-Forsythe and Welch ANOVA tests. * Represents *P*-values <0.05 while ** are for *P*-values <0.005. “Not significant” indicates a *P*-value >0.05. Any comparisons not represented are not significant.

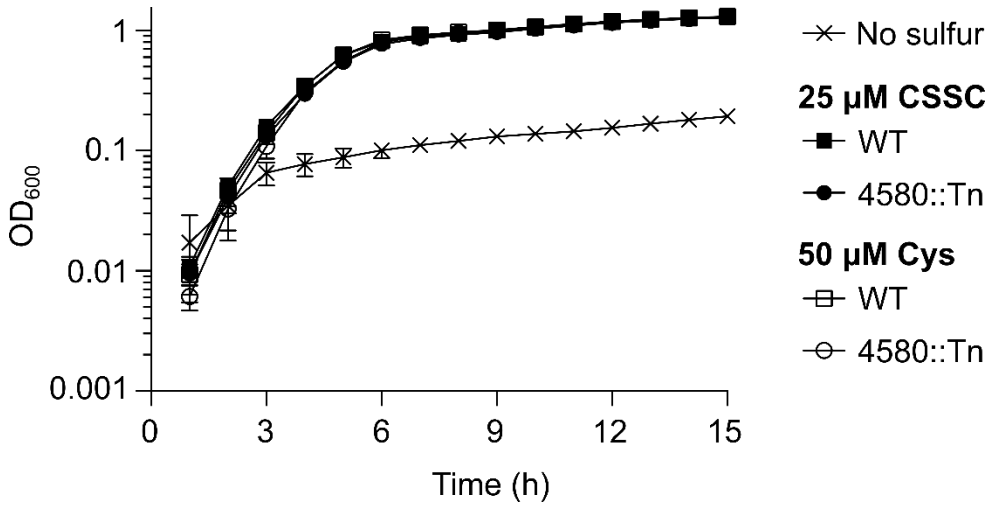

Figure 2.6. SAUSA300_RS04580 does not contribute to *S. aureus* proliferation on CSSC as a source of nutritional sulfur. WT and SAUSA300_RS04580::Tn (denoted 4580::Tn) were cultured in chemically defined medium (CDM) supplemented with either 25 µM cystine (CSSC; closed symbols) or 50 µM cysteine (Cys; open symbols). Curves are the mean of three independent trials and the error bars depict ±1 standard error of the mean.

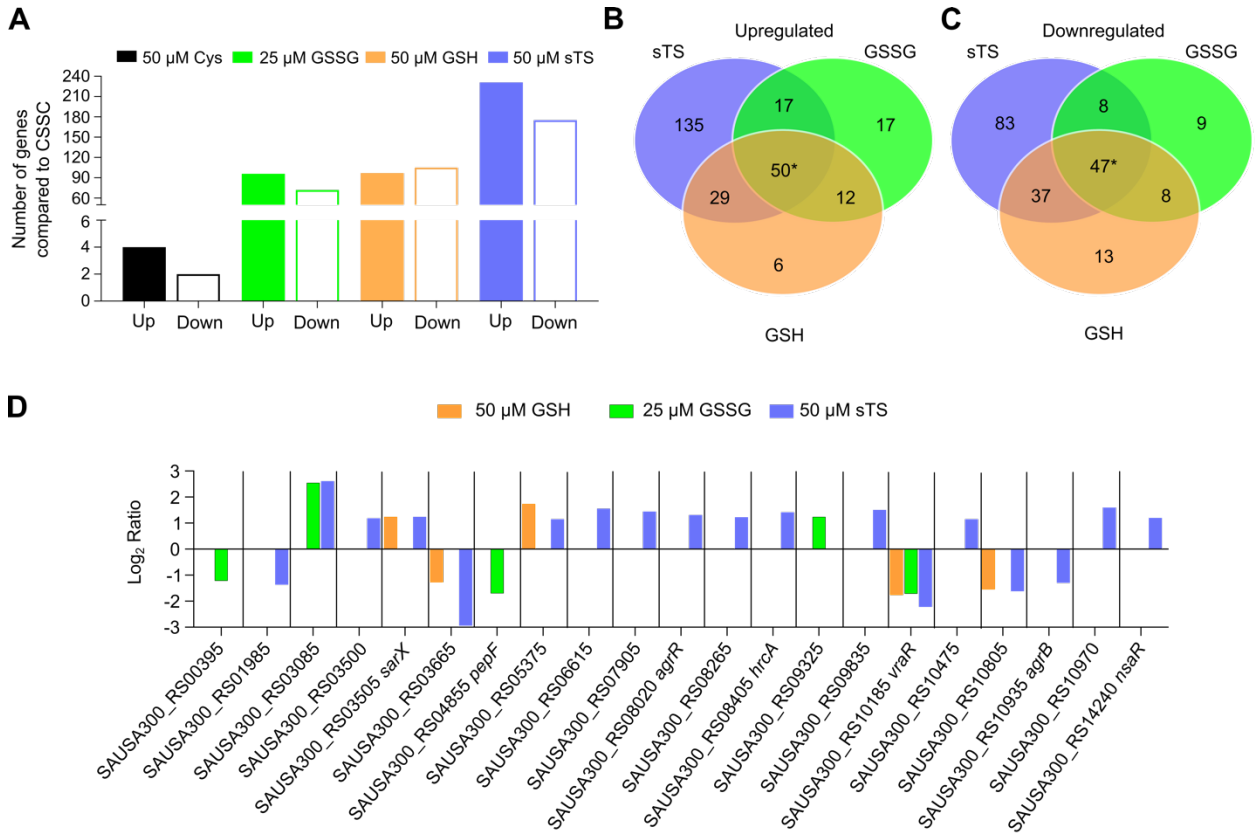

Figure 2.7. Supplementation with sodium thiosulfate induces considerable transcriptional changes in *S. aureus*. Differential expression in WT cells was determined by comparing cells cultured in chemically defined medium (CDM) supplemented with cysteine (Cys; black), oxidized glutathione (GSSG; green), reduced glutathione (GSH; orange), or sodium thiosulfate (sTS; purple) to the CDM supplemented with cystine (CSSC). Only a single gene is differential expressed (downregulated) in *S. aureus* grown in Cys compared to CSSC and is therefore not presented in these comparisons. **A**) Total number of genes that are differentially expressed in response to distinct sources of nutrient sulfur. **B**) Venn diagram comparing genes upregulated when *S. aureus* is cultured in GSSG-, GSH- or sTS-supplemented medium. *The four upregulated genes in CSSC (SAUSA300_RS15735, SAUSA300_RS15740, SAUSA300_15090, SAUSA300_RS15730) were not shared with GSSG, GSH, or sTS and were thus excluded from the Venn Diagram. **C**) Genes that are downregulated between the GSSG, GSH, and sTS. *The two downregulated genes in CSSC (SAUSA300_04580 and SAUSA300_06690) were both shared with GSSG, GSH, or sTS and are represented within the total shared genes in the Venn Diagram. **D**) Transcriptional regulators differentially expressed when *S. aureus* is grown on GSH, GSSG or sTS.

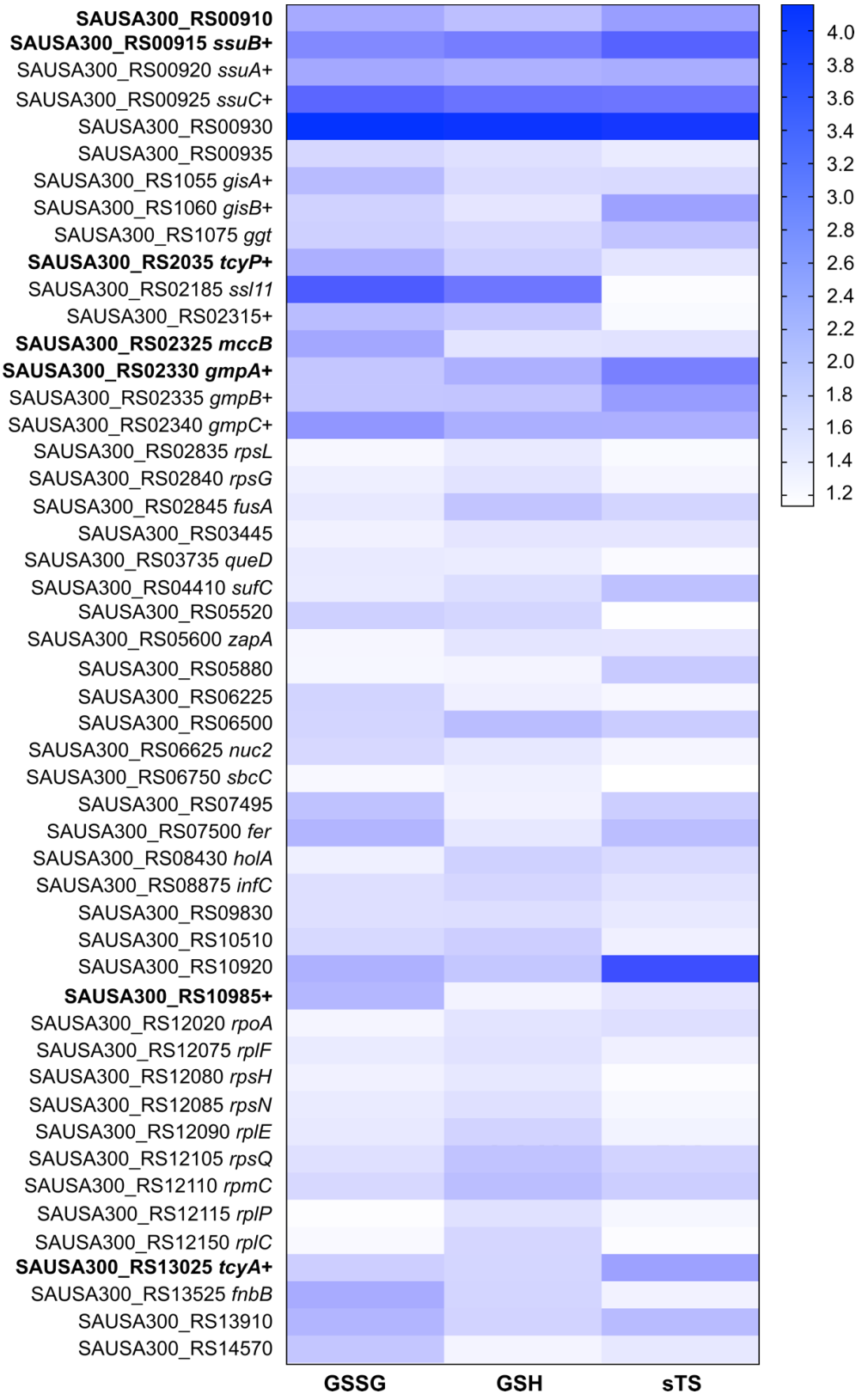

Figure 2.8. The *S. aureus* transcriptome is influenced by different metabolites utilized to meet the nutritional sulfur requirement. Heat map of the shared

Figure 2.8 (cont'd)

upregulated genes in *S. aureus* cultured in medium supplemented with 50 μM sodium thiosulfate (sTS), 25 μM oxidized glutathione (GSSG), and 50 μM reduced glutathione (GSH) compared medium supplemented with cystine (CSSC). Genes included are at least 2-fold upregulated with an adjusted *P*-value <0.05. The color of the boxes indicates the $\log_2$ expression ratio. Genes labeled in bold text were also found to be upregulated in the published CymR regulon (118). A "+" indicates the gene encodes a putative transporter or a protein with a transporter -associated function.

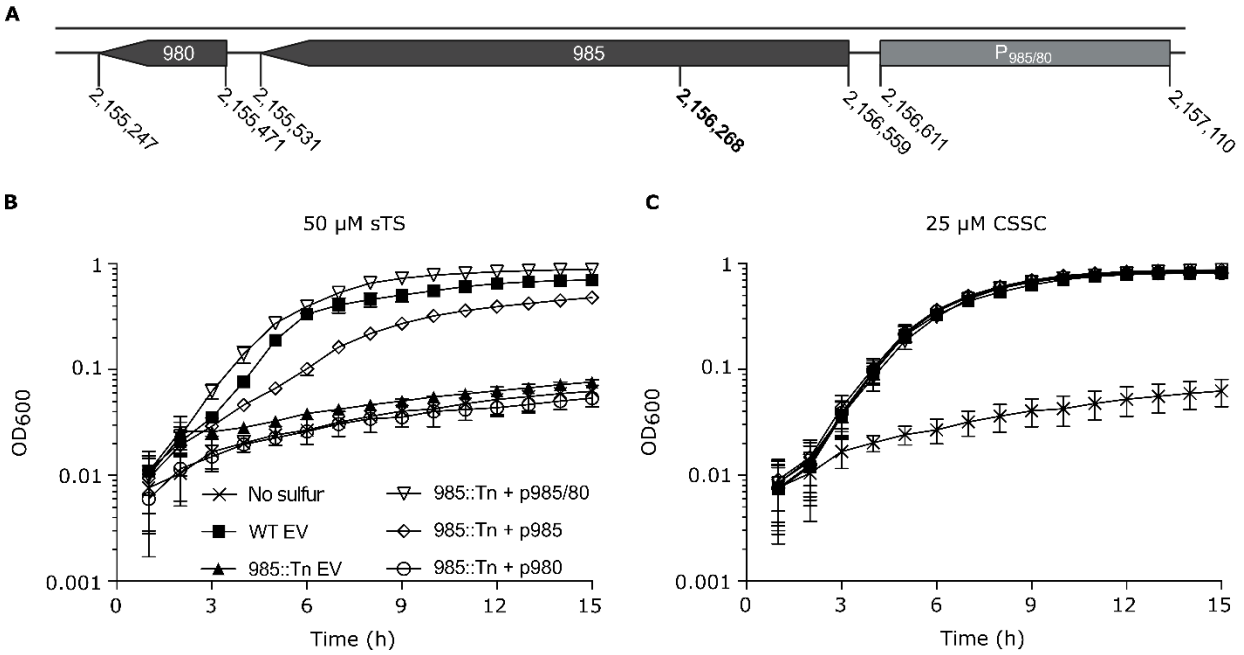

Figure 2.9. *Staphylococcus aureus* employs the TsuAB thiosulfate import system to utilize thiosulfate as a source of nutrient sulfur. A) An illustration of the 985 (SAUSA300_RS10985) and 980 (SAUSA300_RS10980) operon and location of the Tn insertion (position 2,156,268, bold) (164, 166). P_{985} (position 2,156,611-2,157,110) denotes the genetic region used in complementation studied that includes the native promoter region. Image generated using BioRender. **B-C**) Resulting growth kinetics of strains cultured in chemically defined medium (CDM) supplemented with either 50 µM sodium thiosulfate (sTS) (**B**) or 25 µM cystine (CSSC) (**C**) or as the sole sulfur source. WT *S. aureus* harboring an empty pKK22 vector (EV) cultured in medium lacking a viable sulfur source represents the no sulfur control. The mean of three independent trials is presented and the error bars represent ±1 standard error of the mean.

CHAPTER 3: *Staphylococcus aureus* DtpT supports nutrient sulfur acquisition of γ-glutamyl cycle intermediates

ABSTRACT

Staphylococcus aureus is an opportunistic pathogen that incites a range of infections such as osteomyelitis, pneumonia, or bacteremia. Proliferation within the host, however, demands the ability to procure local nutrients. Sulfur is one such nutrient *S. aureus* must acquire but the metabolites obtained, and the machinery employed to do so remain incomplete areas of study. Glutathione is the most abundant non-protein thiol in mammals and previous work has demonstrated that *S. aureus* engages the glutathione import system and at least one other importer to sustain growth on this nutrient as a sulfur source. The current study establishes that the di-tripeptide transporter, DtpT, supports *S. aureus* proliferation on glutathione. Furthermore, we identify that *S. aureus* utilization of cysteinyl-glycine (the glutathione breakdown product) as a sulfur source involves DtpT activity. A systemic infection study underscores the relevance of *dtpT*, as harboring this gene drives maximal colonization of *S. aureus* in the murine liver. Our investigations additionally illustrate the exploitable nature of sulfur metabolism pathways by characterizing the DtpT-dependent susceptibility of *S. aureus* to the peptide antibiotic, bialaphos. Bialaphos was also used to ascertain the *Staphylococcus epidermidis* DtpT homolog, B4U56_10070. The contributions of this gene to *S. epidermidis* propagation on both glutathione and cysteinyl-glycine is additionally highlighted. In summary, this investigation expands our knowledge regarding staphylococcal sulfur acquisition systems by accentuating the strategic redundancy engaged by *S. aureus* and *S. epidermidis* to acquire sulfur sources.

INTRODUCTION

The opportunistic pathogen *Staphylococcus aureus* represents a major cause of nosocomial infections and its burden on society is exacerbated by the rise in community-acquired methicillin-resistant *S. aureus* (MRSA) (86, 125, 174). Infections range from infective endocarditis to skin lesions and even sepsis, making *S. aureus* the most common cause of fatally acquired invasive infections (86, 175–181). As MRSA becomes increasingly treatment-recalcitrant, a better understanding of its essential pathways is needed. The host-pathogen interface for macronutrients such as iron are well defined for this pathogen (3, 182–186). In comparison, how *S. aureus* engages sulfur metabolism to acquire the equally important nutrient sulfur is not fully defined (14, 89, 90, 134).

Within all cells, sulfur is stored in carbon-containing organosulfur compounds that contain reactive sulfhydryl groups, called thiols (R-SH). This element partakes in numerous critical cellular reactions, demanding high prioritization to meet the sulfur requirement. For example, proteins harbor cysteine (Cys) residues that coordinate ions and form disulfide bonds to maintain tertiary structure (4, 5). Furthermore, Cys is the precursor to several cellular cofactors. Fe-S clusters are involved in redox reactions while coenzyme A and biotin contribute to general metabolism via the citric acid cycle or fatty acid biosynthesis; therefore, proper cofactor maintenance influences proliferation of a pathogen during infection (6–8, 129, 130). Redox balance is also managed by organosulfur compounds such as Cys and glutathione (GSH) that contain thiol groups (4, 131, 132, 187). Thus, there is potential to expand *S. aureus* therapeutic strategies by targeting its sulfur acquisition and utilization pathways.

GSH is the most abundant non-protein thiol in mammals (42). This tripeptide is composed of glutamate, Cys, and glycine. Glutamate forms a unique γ-peptide bond with Cys through interaction of its γ-carboxyl group and the Cys amide while Cys and glycine are linked via a typical α-carboxyl peptide bond. The γ-peptide bond in GSH is considered stable as it can only be cleaved by specialized enzymes such as γ-glutamyl transpeptidase (aka γ-glutamyl transferase). Given its stability and reactive thiol group, GSH is vital to the maintenance of host physiology—it acts as a major antioxidant by reducing reactive oxygen species (ROS) such as hydrogen peroxide (H_2O_2), a process that results in the formation of oxidized glutathione (GSSG) (12). Additionally, GSH acts as a Cys reservoir through the γ-glutamyl cycle (12, 22, 23, 188, 189). The γ-glutamyl cycle begins when transporters export intracellular GSH from the cell. The γ-peptide bond is then cleaved by γ-glutamyl transpeptidase 1 (GGT1), which is peripherally anchored to the cell membrane. GGT1 produces γ-glutamate and the dipeptide cysteinyl-glycine (CysGly). From there, the CysGly peptide bond is cleaved by dipeptidases, allowing Cys to be transported into cells for incorporation into various cellular components or stored once again in GSH. Given the abundance of host GSH, it is unsurprising that pathogens have evolved mechanisms to exploit the metabolite as a source of nutrient sulfur. Indeed, *Francisella tularensis*, *Haemophilus influenzae*, *Streptococcus mutans*, and *Streptococcus pneumonia* are known to consume host GSH to meet the sulfur requirement (100, 144, 190, 191). *F. tularensis*, interestingly, imports GSH by first cleaving its γ-peptide bond in the periplasm with Ggt and then importing CysGly through a di-tripeptide transporter, DptA (101).

Recently, we have shown that *S. aureus* encodes a specialized glutathione import system (GisABCD) to import GSH and GSSG into the cytoplasm where Ggt then begins catabolism of these metabolites for use as nutritional sulfur (89). However, the complexity of *S. aureus* GSH acquisition was discovered when deletion of the *gisABCD-ggt* system failed to abolish *S. aureus* propagation on physiologically relevant concentrations of GSH *in vitro*. Furthermore, a Δ*gisABCD-ggt* mutant does not impact the ability of *S. aureus* to colonize during systemic infection. In the current study, we expand upon our previous work by demonstrating that the di-tripeptide transporter, DtpT, supports *S. aureus* growth on GSH. Our investigations also reveal that CysGly is a source of nutritional sulfur for *S. aureus* in a DtpT-mediated manner. Phylogenetic studies indicate that homologs for this protein are found across a number of other Gram-positive bacteria. Assessing colonization of a MRSA strain during systemic infection, we further corroborate earlier findings that DtpT promotes maximal *S. aureus* proliferation *in vivo*. Finally, we determine that *S. aureus* sulfur acquisition machinery can be taken advantage of by delivering a toxic tripeptide, bialaphos, via DtpT. This proof-of-concept is extended into another clinically relevant species, *Staphylococcus epidermidis*. Collectively, these data expand our knowledge regarding Staphylococcus sulfur acquisition strategies and provide evidence that *S. aureus* sulfur metabolism pathways can yield new avenues to combat this threat to societal health.

RESULTS

***Staphylococcus aureus* employs redundant strategies to support utilization of GSH and CysGly as sources of nutritional sulfur.** Prior investigations in our lab demonstrate the presence of at least two GSH transporters (89). Given that GisABCD was defined as

a putative nickel-peptide ABC transporter, we surmised that another oligopeptide transporter encoded by *S. aureus* would associate with this metabolite. These potential systems include the NiKA & NikBCDF importer, CntABCD, Opp3BCDFA, Opp4ADFB, and OppACME-ABCDF, and DtpT (192, 193). Within this list, the proton-dependent oligopeptide transporter (POT) family protein DtpT has been implicated in the uptake of both di- and tripeptides in *S. aureus* (91, 192). Given that GSH is a tripeptide, we hypothesized that DtpT would play a role in use of this nutrient as a sulfur source.

To test this, a clean *dtpT* deletion was generated in the WT and isogenic Δ*gisABCD-ggt* backgrounds (denoted Δ*dtpT* and Δ*gis* Δ*dtpT*, respectively). The growth profile of these strains on CDM supplemented with GSH was assessed (Fig. 3.1). When low a concentration (i.e., 50 μM) of GSH is supplied as the sulfur source, the Δ*gis* EV mutant exhibits drastically reduced optical density at 600 nm (OD_{600}) values compared to WT (Fig. 3.1A). This is in accordance with previous observations (89). A Δ*dtpT* EV propagates like WT while the Δ*gis* Δ*dtpT* EV mutant phenocopies growth kinetics of the Δ*gis* EV strain. Complementation of Δ*gis* Δ*dtpT* with the WT *dtpT* allele *in trans* allows for marginally improved growth compared to the EV counterpart.

While 50 μM GSH is sufficient for *S. aureus* to meet the sulfur requirement *in vitro*, this concentration does not reflect what the pathogen might encounter *in vivo*. Indeed, GSH is the most abundant non-protein thiol in mammals and can reach millimolar concentrations (42); thus, the strains were cultured in CDM containing 750 μM GSH (Fig. 3.1B). As seen previously, this condition supports WT-like proliferation of the Δ*gis* EV mutant (89). In fact, the only strain with an impairment is the Δ*gis* Δ*dtpT* EV mutant whose proliferation is restored upon complementation with WT *dtpT*. However, the appreciable

growth of Δ*gis* Δ*dtpT* EV on 750 μM GSH suggests the presence of at least one more active transporter in this condition. Furthermore, it is important to note that these phenotypes are sulfur specific given all strains propagate like WT when provided with a control sulfur source such as cystine (CSSC) or in the rich medium, tryptic soy broth (TSB; Fig. 3.1C and 3.1D, respectively).

GisABCD is an ABC-transporter while DtpT is a POT family member (89, 192). With such a difference in protein families, we predicted that there would be subtle variations in how each transporter correlates with GSH. Thus, we sought to investigate which properties of GSH influence the ability of DtpT and GisABCD to support *S. aureus* proliferation on this metabolite. To do so, a GSH analog was supplemented in the CDM (Fig. 3.2). In this analog the γ-peptide bond shared between the glutamyl and cysteinyl residues of GSH was replaced with an α-peptide bond; this glutamyl-cysteinyl-glycine peptide is denoted as ECG for short. Notably, ECG is a sulfur source for WT and the Δ*gis* mutant displays no growth defect regardless of the concentration supplied (Fig. 3.2A-C). However, deleting *dtpT* severely impacts growth compared to WT at 50 μM ECG (Fig. 3.2A). The severity of this phenotype is not compounded upon inactivation of both transporters. Interestingly, increasing ECG concentration in the CDM restores the ability of the Δ*dtpT* and Δ*gis* Δ*dtpT* strains to proliferate (Fig. 3.2B and 3.2C). These observations stand in stark contrast compared to what is observed with 50 μM GSH where strains harboring a Δ*gis* mutation struggle to propagate and the Δ*dtpT* has WT-like growth (Fig. 3.2D). As expected, no growth defects are observed when CSSC is the sulfur source (Fig. 3.2E). These data imply that the γ-peptide bond of GSH is important for GisABCD

and while its tripeptide nature is what DtpT relates to when assisting *S. aureus* proliferation on this nutrient.

Given that DtpT also imports dipeptides we postulated that this transporter would also sustain the use of CysGly (the GSH breakdown product) as a sulfur source for *S. aureus*. Importantly, WT EV is capable of robust proliferation in CDM supplemented with 25 μM CysGly, demonstrating the sufficiency of this dipeptide for meeting the *S. aureus* nutritional sulfur requirement (Fig. 3.3A). Deletion of DtpT reduces, but does not abolish, the ability of *S. aureus* to grow in this condition. Notably, this phenotype can be complemented. GisABCD does not contribute to propagation on CysGly as the Δ*gis* Δ*dtpT* EV strain growth kinetics mimic those of Δ*dtpT* EV. However, these are the assessments of a laboratory strain. To evaluate whether clinical *S. aureus* isolates retain the ability to utilize CysGly for nutritional sulfur needs, six isolates from cystic fibrosis (CF) patients were cultured in the presence of CysGly. After 24 h each strain showed at least a 225% increase in OD_{600} when compared to being cultured the absence of a viable sulfur source (Fig. 3.3B). Collectively, these data indirectly suggest that DtpT is both a GSH and CysGly transporter in *S. aureus* and that at least one additional importer is contributing to propagation on these nutrients.

DtpT is broadly conserved among Gram-positive bacteria. Phylogenetic analyses were employed to look at the conservation of DtpT across bacteria. First homologs that retained ≥80% coverage and 40% identity were isolated. All returned strains belonged to the *Staphylococcaceae* family, with the majority being *S. aureus* isolates and the second most represented species *S. epidermidis*. Considering that some hits were only classified as *Staphylococcus*, we sought to expand the selection of bacteria

that might contain a protein with lower homology to *S. aureus* DtpT. Thus, a tree was generated for homologs that had a least ≥50% coverage and 40% identity (Fig. 3.4). There are 14 families containing at least 50 representatives that harbor a DtpT homolog. The top three most abundant families are *Bacillaeceae, Staphylococcaceae* (including *S. aureus* and *Staphylococcus epidermidis*), and *Lactobacillaceae*. When looking at all the families, four clades are observed (Fig. 3.4B, upper left). Clade 1 largely constitutes the *Staphylococcaceae*, but also contains *Listeriaceae*. *Bacillaceae*, *Caryophanaceae*, and *Paenibacillaceae*. Clade 2, in addition to those families in Clade 1, represent the homologs with the closest relation to *S. aureus* DtpT given they share the same common ancestor. Found within Clade 3 are *Leuconostocaceae*, *Micrococcaceae*, *Pseudonocardiaceae*, *Streptomycetaceae*, and bacteria that had <50 representatives (i.e., Others) while Clade 4 constitutes *Enterococcaceae*, *Lactobacillaceae*, and *Streptococcaceae*. This information reveals that DtpT-like proteins are selectively found within a Gram-positive bacterial group that includes pathogens, commensals, and environmental isolates.

Maximal *S. aureus* colonization of the murine liver requires functional DtpT. In addition to previously defined di-tripeptides (192), *in vitro* work above demonstrates two new, sulfur containing peptides associated with DtpT. Given this, we sought to identify the impact this transporter has on *S. aureus* proliferation during infection. Earlier studies employing signature tagged transposon (Tn) mutant pools suggested that a *dtpT*::Tn mutant negatively impacts *S. aureus* strain RN6390 in murine abscess, wound, and systemic bacteremia infection models (194). Individual assessment of a *dtpT*::Tn mutant in rabbit endocarditis and murine abscess or wound models demonstrate attenuated

mutant phenotypes (194). Furthermore, inactivating *dtpT* led to increased survival of mice in a median lethal dose (LD_{50}) challenge. However, RN6390 is a derivative of the methicillin sensitive *S. aureus* (MSSA) laboratory strain NCTC8325 and contains a deletion in the critical stress response regulator, *rsbU* (195). To better understand the impact of *dtpT* on a strain that represents the current epidemic *S. aureus* lineage, we utilized the methicillin resistant USA300 LAC derivative, JE2. Using a systemic model of infection, mice were inoculated with either WT or a *dtpT*::Tn mutant. Mice infected with *dtpT*::Tn tend to exhibit lower bacterial burdens in the heart or kidneys, along with having significantly reduced CFUs in the liver (Fig. 3.5). This data therefore extends the biological impact of DtpT to include both MRSA and MSSA isolates.

DtpT is a relevant model to assess exploitation of sulfur metabolism for delivery of a lethal substance into *S. aureus*. Given the demonstrated impact of DtpT on *S. aureus* proliferation *in vivo*, this transporter was employed to investigate the potential for inhibiting pathogen proliferation by exploiting sulfur transportation pathways. Bialaphos is a tripeptide produced by *Streptomyces viridochromogenes* as well as *Streptomyces hydroscopius* and is used commercially as a non-selective herbicide (196, 197). This peptide antibiotic consists of glufosinate-alanyl-alanyl residues. Glufosinate (aka phosphoinothricin) is a toxic glutamate analog harboring a phosphinate moiety that mimics the tetrahedral intermediate of glutamine synthetase (196, 197). Characterizing this peptide with *Escherichia coli* and *Bacillus subtilis* indicates that, upon import, glufosinate is cleaved from the alanyl residues before inhibiting glutamine synthetase. If the cell cannot import exogenous glutamine to compensate for the loss of glutamine synthetase then cellular death ensues. Interestingly, oligopeptide transporters in *E. coli*

(Opp; (198)), *B. subtilis* (OppABCD; (199, 200)), *Salmonella typhimurium* (Opp, Tpp, Dpp; (201)) and *Listeria monocytogenes* (OppA; (202)) are associated with bialaphos import. However, bialaphos sensitivity in staphylococcal species has not yet been explored.

We hypothesized that *S. aureus* would be sensitive to bialaphos in both a glutamine and transportation-dependent manner. Conducting a bialaphos Kirby Bauer on a rich medium (trypic soy agar, TSA) did not result in a zone of inhibition (Fig. 3.6A and B). However, plating cells on a CDM agar plate that lacks glutamine (Gln) resulted in WT EV sensitivity to bialaphos which could be mitigated by adding 500 μM Gln to the CDM. Most importantly, the deletion of *dtpT* confers complete resistance to bialaphos regardless of the presence of Gln in the medium, and sensitivity can be reintroduced through complementation (Fig. 3.6A and B). It was noted that the WT and D*dtpT* p*dtpT* strains develop bialaphos resistant colonies (RCs) in the CDM + 0 mM Gln condition (Fig. 3.6A and C). Nine of these RCs were isolated from the WT plates and were challenged with bialaphos (Fig. 3.7). Six out of nine RC strains were completely resistant to the peptide antibiotic and the remaining three displayed significantly increased resistance (Fig. 3.7A and B). These strains displaying reduced zones of inhibition also developed resistant colonies like WT (Fig. 3.7C). Whole genome sequencing of the nine RCs reveals several genes being mutated (Table 3.1). Importantly, there is only one gene, *dtpT*, that is uniquely mutated in all the bialaphos RC strains (Table 3.1, Fig. 3.7D). As such, it is concluded that DtpT is both sufficient and necessary for *S. aureus* import of bialaphos.

Bialaphos is a tool to identify sulfur metabolism machinery in *S. epidermidis*. While *S. aureus* is the most notorious of the Staphylococcal species, *S. epidermidis* is another clinically relevant organism known for causing skin, mucosa membrane, and

prosthetic join infections (203, 204). Thus, it is equally pertinent to understand what sulfur metabolism pathways help this organism meet the nutritional sulfur requirement. Our work has indicated that *S. epidermidis* utilizes GSH as a source of nutritional sulfur but does not encode GisB nor GisD homologs of the GisABCD-Ggt system (89). Since DtpT is associated with both GSH and bialaphos import in *S. aureus*, we hypothesized that bialaphos could serve as an effective means to discern the GSH transporter in *S. epidermidis*.

Kirby Bauer assays reveal that, like *S. aureus*, WT *S. epidermidis* 1457 is only sensitive to bialaphos when plated on CDM that does not contain Gln and develops resistant colonies (Fig. 3.8A-C). Selecting nine RCs and challenging them against bialaphos demonstrates that each strain has either complete or near complete resistance to the peptide antibiotic (Fig. 3.8A-C). Strikingly, these bialaphos RCs only share mutations in one common gene, B4U56_10070, which encodes for a peptide MFS peptide (Table 3.2, Fig. 3.8D). BlastP alignment of B4U56_10070 and DtpT from *S. aureus* results in 100% coverage and 82.83% identity. This observation is consistent with the phylogenetic studies where many *S. epidermidis* isolates were found to harbor a DtpT homolog (Fig. 3.4).

To further assess B4U56_10070 as a DtpT homolog, *S. epidermidis* 1457 bialaphos RCs were cultured in a modified CDM that does not contain Met or sulfate (CDM_{mod}), given they support the nutritional sulfur requirement in this species (89). In comparison to WT, each of the B4U56_10070 mutated strains display reduced growth in CDM_{mod} supplemented with 750 μM GSH (Fig. 3.8E). We next tested the ability of *S. epidermidis* 1457 to utilize CysGly as a sulfur source (Fig. 3.8F). Here the WT strain

shows robust proliferation on CDM_{mod} supplied with 75 μM CysGly while the bialaphos resistant colonies demonstrate poor propagation. These phenotypes are sulfur specific given the ability of all strains to grow to WT-like levels in the presence of CSSC (Fig. 3.8G). Collectively, these data strongly suggest that B4U56_10070 is a DtpT homolog and represents the major transporter associated with *S. epidermidis* 1457 growth on both GSH and CysGly as sources of nutrient sulfur.

DISCUSSION

This investigation increases our knowledge of GSH acquisition strategies employed by *S. aureus* in addition to identifying CysGly, the breakdown product of GSH, as a nutrient that satisfies the nutritional sulfur requirement for this pathogen. Data for both peptides highlight the fact that *S. aureus* employs redundant strategies to procure select nutritional sulfur sources. Previous work with *S. aureus* has revealed the involvement of multiple transporters (i.e., TcyABC and TcyP) in the utilization of Cys and CSSC (90). In contrast, only one transporter associates with *S. aureus* proliferation on thiosulfate (see Chapter 2). It would seem, then, that there is an evolutionary strategy for *S. aureus* to encode multiple acquisition systems for what might be considered preferred sulfur sources. The current study underscores this notion by demonstrating that presence of at least three importers driving *S. aureus* proliferation on physiologically relevant concentrations of GSH *in vitro* (Fig. 1B). To that end, our work is the first to associate the di-tripeptide transporter, DtpT, with GSH import. Indeed, results from Fig. 3.1A and 3.1B suggest that DtpT contributes to *S. aureus* growth on physiologically relevant concentrations of GSH. This comes as little surprise given that DtpT has been associated with the import of glutamate or glycine containing di-tripeptides as sources of nitrogen (192). However, the

contribution of DtpT toward GSH uptake is not to the same extent as the GisABCD-Ggt system given its WT-like growth at 50 μM (Fig. 3.1A). This may be because GisD harbors a solute-binding protein family 5 domain, known for its high substrate specificity; in contrast, transporters from the POT family such as DtpT identify substrates through specificity pockets that establish substrate affinity based on peptide charge (91, 205–208).

Our work additionally investigates the properties involved with GSH substrate identification for both DtpT and GisABCD using an ECG analog (Fig. 3.2). Employing ECG has indirectly implied that DtpT recognizes GSH due to its tripeptide nature given the growth defect of a *dtpT* mutant on low concentrations of this metabolite (Fig. 3.3A). This stands in contrast to the GisABCD-Ggt system which did not display any growth impairments in ECG (Fig. 3.2A-C) or the dipeptide CysGly (Fig. 3.3A); this signifies that GisABCD requires the γ-peptide bond of GSH and perhaps the tripeptide aspect as well in order to support growth of *S. aureus* on this nutrient. However, to solidify whether GisABCD identifies with dipeptides, growth kinetics using the GSH precursor, γ-glutamyl-cysteine would be needed. Furthermore, binding assays with purified protein or uptake of radiolabeled GSH and/or CysGly will provide direct insight into substrate binding for these two transporters. Future investigations are also necessary to elucidate the complete set of transporters involved with growth of CDM supplemented with GSH. Given that both GisABCD and DtpT are peptide importers, we predicted that another oligopeptide transporter is responsible for the growth of the Δ*gis* Δ*dtpT* on physiologically relevant concentrations of tripeptides such as GSH or ECG. Opp3BCDFA is associated with import of tripeptides and represents an ideal candidate for future studies (192, 193).

CysGly has also been uncovered as a sulfur source for *S. aureus* (Fig. 3.3). Interestingly, other groups have shown the capacity of bacteria to utilize oligopeptide transporters to bring CysGly into the cytoplasm. One study demonstrates that another opportunistic pathogen, *Campylobacter jejuni*, employs an oligopeptide transporter family protein (OPT), CptA, to import CysGly as a source of nutrient sulfur (209). The *F. tularensis* di-tripeptide transporter DptA is also known to import a CysGly into the cytosol; DtpA also strongly impacts the survival of *F. tularensis* during macrophage infection (101). Perhaps even more significant are the structural studies that confirm a *Staphylococcus hominis* POT family protein, PepT, as an importer for the malodor precursor called cysteinyl-glycine 3-methyl-3-sulfanylhexanol (S-CysGly-3M3SH) (103). PepT and other proteins denoted as S-CysGly-3M3SH transporters were found within the *Staphylococcaceae* family when conducting phylogenetic analyses on DtpT (Fig. 3.4). This reinforces the notion that *S. aureus* DtpT is likely a CysGly transporter. In total, the DtpT-mediated utilization of CysGly to meet *S. aureus* nutritional sulfur demands adds to our knowledge surrounding the use of CysGly by microbial residents of the mammalian host.

This study not only expands our understanding of *S. aureus* sulfur metabolism but defines the biological relevance of the involved pathways. This was done by confirming the ability of several *S. aureus* CF isolates to proliferate on CysGly as a source of nutrient sulfur (Fig. 3.3B). Though some strains have a higher capacity to growth on CysGly than others, this overall suggests that the pathways needed for import of this dipeptide are actively maintained in the CF lung environment. Furthermore, we find that DtpT helps drive successful colonization of *S. aureus* JE2 to in the murine liver (Fig 3.5). Whether

the biological relevance of DtpT during infection lies within the import of GSH and/or CysGly will need to be assessed.

How *S. aureus* sulfur metabolism pathways can be exploited to inhibit proliferation of this prevalent threat to societal health is also explored. Some prior investigations in this have focused on the *O*-acetylserine sulfhydrylase isomers, which are involved in thiosulfate and sulfate assimilation to Cys (14). Inhibitors for *O*-acetylserine sulfhydrylase in *Salmonella typhimurium*, *Haemophilus influenzae*, and the protozoan *Entamoeba histolytica* have been identified (210–212), illustrating that inhibition of sulfur metabolism could be an effective treatment strategy across multiple phyla**.** Another aspect to consider for therapeutics is sulfur transportation. However, the data presented here suggest that sulfur transporters are not ideal candidates for inhibition because *S. aureus* can acquire multiple sulfur sources, and there is extensive transporter redundancy for some of these metabolites. While targeting the transporter may not effectively inhibit *S. aureus* proliferation, these proteins can still be utilized in a Trojan horse approach for delivering toxic substances through the system of interest. Here we conduct a proof-of-concept investigation, where the sensitivity of *S. aureus* to bialaphos is DtpT-dependent. Directed genetics by deleting the transporter and indirectly through mutations occurring within this gene in bialaphos RCs demonstrate this (Figs. 3.7 and 3.8). Together this suggests that, for *S. aureus*, DtpT is the route of bialaphos import. Bialaphos sensitivity of another clinically relevant Staphylococcal species, *S. epidermidis*, which depends on the activity of a DtpT homolog, B4U56_10070 reinforces the *S. aureus* data (Fig. 3.8). This protein is also involved in *S. epidermidis* sulfur metabolism—B4U56_10070 is established as a main factor in *S. epidermidis* growth on the previously characterized sulfur source, GSH.

CysGly also supports nutritional sulfur needs in *S. epidermidis*, a process that largely hinges on B4U56_10070. Because of this, we propose to rename this gene as DtpT (**d**i-**t**ri**p**eptide **t**ransporter). It is worth noting that the consistent correlation between DtpT and the growth of staphylococcal species on GSH and CysGly suggests that this transporter likely recognizes these metabolites as substrates. However, the absence of direct experiments is a limitation to that assertion. Collectively, this study reveals new GSH and CysGly import routes for *S. aureus* and *S. epidermidis*, highlighting an evolutionary strategy of sulfur acquisition redundancy that enables these staphylococcal species to access multiple host sulfur sources.

ACKNOWLEDGEMENTS

Transposon mutants were provided by the Network on Antimicrobial Resistance in *Staphylococcus aureus* (NARSA) for distribution by BEI Resources, NIAID, NIH, and the Nebraska Transposon Mutant Library (NTML) Screening Array NR-48501. We thank Vinai Chittezham Thomas for donating the WT *S. epidermidis* 1457 strain. Our gratitude to the Hammer laboratory members for their insights into this manuscript. This work is funded by the National Institutes of Health R01 AI139074 and R21 AI142517.

MATERIALS AND METHODS

Strains and Primers. All strains, plasmids, and primers used throughout the course of this study can be found in **Tables 3.3**, **3.4**, and **3.5**, respectively. JE2, a derivative of the community acquired USA300 LAC, is the WT *S. aureus* strain used in these studies (164). Generation of *Bursa aurealis* transposon (Tn) inactivated strains were done by transducing the inactivated gene from the Nebraska Transposon Mutant Library into JE2 (164, 165). Correct Tn location and deletions were determined using PCR. The pKK22

plasmid was generated via Gibson assembly in the *Escherichia coli* DH5α strain before being transferred to *S. aureus* RN4220 to obtain appropriate vector methylation patterns that would permit transformation into the appropriate JE2 background strain. The pKOR1 plasmid was generated as follows using restriction digestion: first the 1kb upstream and 1kb downstream of *dtpT* was amplified. Then these fragments were PCR sewn before blunt end cloning into pJET1.2 (ThermoFisher). From there, the 2kb up/downstream fragment was removed from pJET1.2 using NotI and KpnI restriction digestion enzymes for cloning into pKOR1. The resulting pKOR1-dtpT plasmid was transformed into E. coli DH5α before being transferred into *S. aureus* RN4220 and then JE2. Note that all plasmids were confirmed using Plasmidsaurus whole plasmid sequencing. Complementation vectors were generated using the pKK22 expression vector (153). Deletion of the *dtpT* gene was performed following a well-defined allelic exchange protocol using the pKOR1-mcs plasmid donated from the laboratory of Taeok Bae (213).

Media and growth conditions. Each strain was cultured overnight in 5 mL tryptic soy broth (TSB) at 37°C, shaking at 225 rpm. Strains harboring a pKOR1-based plasmid were supplemented with 10 µg/mL of chloramphenicol unless otherwise noted during the allelic exchange protocol (213). pKK22-based plasmids were supplemented with 10 µg/mL of trimethoprim except for during growth curve assays. A base chemically defined medium (CDM) was prepared using a previously described recipe with slight modifications (149, 150). Please refer to Chapter 2 Materials and Methods for the complete CDM recipe. 5 mg mL^{-1} of freshly prepared glucose was supplemented into the base medium and, depending on the condition, either no sulfur source, 25 mM of CSSC, 50 mM of GSH, or 25 mM of CysGly was added into the CDM prior to inoculation. Note that this medium

lacks the amino acids glutamine and asparagine. *S. epidermidis* growth curves utilized a modified CDM (CDM_{mod}) where Met was removed, and sulfates were also taken out by replacing $MgSO_4$ with MgCl and $(NH_4)_2SO_4$ with NH_4Cl. The CSSC stock was dissolved in 1N HCl while all other sulfur sources (and glucose) were dissolved in deionized water before filter sterilization. CDM agar plates were made by mixing a 1:1 ratio of 2x CDM and 2x Select Agar before plating in 20 mL aliquots. All plates were supplemented with 25 mM of CSSC as the sulfur source and lacked glutamine unless otherwise noted.

96-well plate growth curves. Overnight cultures were centrifuged at 4°C, 4000 rpm, washed in 5 mL phosphate buffered saline (PBS), and then normalized to an optical density at 600 nm (OD_{600}) equal to 1. From there the cells were sub-cultured 1:100 into the desired growth medium (i.e., starting OD_{600} is 0.01). The OD_{600} was monitored every hour for 24 h in a 96-well round bottom plate in an Epoc2 Biotek microplate spectrophotometer at 37°C, with continuous linear shaking. To remove background, blank measurements were subtracted from growth measurements. For each strain the growth condition was conducted in technical triplicate, which were blanked and then averaged. Averaged triplicates were considered as one biological replicate. All growth curves were conducted three independent times.

End point OD_{600} measurements of Cystic Fibrosis *S. aureus* isolates. Cells were prepared and 96-well round bottom plates containing CDM harboring no viable sulfur source or 25 mM CysGly were set up as described in the previous section. Inoculated plates were then incubated at 37°C, static, for 24 h. Wells were then gently resuspended before taking an endpoint OD_{600} using an Epoc2 Biotek microplate spectrophotometer. Averages of technical triplicates were acquired after being blanked. Percent growth of the

averaged value was then achieved by applying the endpoint OD_{600} to the following equation: $\frac{(CysGly-no\ sulfur)}{no\ sulfur}$. This experiment was performed four independent times for each strain.

Identification of DtpT homologs across bacteria. The USA300_FPR3757 (NC_007793.1) *S. aureus* DtpT protein sequence (SAUSA300_RS03825) was used as the query for homolog evaluation using Blastp (214), using refseq database, an e-value of 1e-05, and allowing 10,000 hits. Proteins that demonstrated at least 50% coverage and 40% identity were selected for downstream analysis. Protein sequences were then retrieved from NCBI and aligned using ClustalW2 (215). A phylogenetic tree was constructed using IQ-TREE (216) selecting LG+F+I+G4 as the substitution model. Tree visualization was conducted using Iroki (217). The computational analyses were provided by the Institute for Cyber Enabled Research at Michigan State University.

Murine model of systemic infection. TSB overnights of WT and *dtpT*::Tn were sub-cultured 1:100 into 5 mL TSB and grown for 3 h. Cultures were centrifuged at 4°C, 4000 rpm, before being washed into 12 mL of Dulbecco's Phosphate Buffered Saline (DPBS; no $CaCl_2$ or $MgCl_2$) and normalized to an OD_{600} = 0.4. Eight-week-old Balb/cJ female mice (Jackson Laboratories) were then anesthetized with avertin before being retro-orbitally infected with 10^7 CFU of either WT or the *dtpT*::Tn. After 96 hpi, mice were euthanized via CO_2 inhalation and the heart, liver, and kidneys were harvested. The heart and kidneys were homogenized in 500 µL DPBS using an Air-cooling Bullet Blender Storm 24 (Next Advance, Inc.) using Navy, 1.5 mL RINO lysis beads (Next Advance, Inc.). Once homogenized, 500 µL DPBS was added to bring the total volume to 1 mL DPBS for the heart and kidneys. Livers, once harvested, were placed into a Whirl-Pak (Nasco) and

had 1 mL DBPS added before being homogenized by rolling a 1 L glass Pyrex bottle over the organ 20 times. Liver homogenate was then transferred to a 1.5 mL Eppendorf tube. Bacterial burden in each tissue was enumerated through serial dilution onto TSA plates. Infections were performed at Michigan State University under the principles and guidelines described in the *Guide for the Care and Use of Laboratory Animals* (218). Executed animal work followed the protocol approved by Michigan State University Institutional Animal Care and Use Committee (IACUC): PROTO202200474.

Bialaphos Kirby Bauer assays. Overnight *Staphylococcus* cultures were centrifuged at 4°C (4000 rpm), washed once with an equal volume of PBS, and normalized to an OD_{600} of 1. For *S. aureus*, cells were then swabbed onto appropriate CDM agar plates or tryptic soy agar (TSA). *S. epidermidis* strains had 100 µL of normalized cells added to 1.5x CDM agar plates before being spread plated to ensure consistent growth on this medium. Sterilized, 6 mm Whatman disks were placed into an empty petri dish and had 10 µL of 10 mM bialaphos applied. Herbicide-soaked disks were applied to the center of the TSA or CDM agar plates. CDM agar plates had either 0 µM, 500 µM, or 2 mM Gln added with or without TMP. Only strains containing a pKK22-based plasmid were plated onto CDM agar plates harboring TMP to ensure maintenance of the pKK22-*dtpT* vector in the presence of bialaphos. Plates were then put at 37°C for 24 h before quantifying the zone of inhibition (ZOI) and resistant colonies (RC). For each condition, three technical replicates were averaged for ZOI and RC with the average being considered a biological replicate. Three biological replicates were conducted for each condition. Pictures were taken with an iPhone XR, using the same distance from lens and lens zoom.

Isolation of Genomic DNA and whole genome sequencing. Nine RC from the WT bialaphos Kirby Bauer assays were picked and struck for isolation onto TSA. Five mL TSB was inoculated and cultured at 37°C, 225 rpm, overnight. The cell wall was digested by resuspending the overnight in 485 μL water buffered with TSM (50 mM Tris, 500 mM sucrose, and 21 mM $MgCl_2$; pH 7.5) and 15 μL of 2 mg mL^{-1} lysostaphin (ABMI; Lawrence, NY) before incubation at 37°C for 30 min. Afterwards, the protoplast was obtained by spinning at 9000 rpm for 5 min and decanting the supernatant. Genomes were isolated using a Promega kit (Madison, WI) following manufacturer's instructions. Briefly, protoplast was resuspended in 600 μL nuclei lysis buffer and heated at 80°C for 10 min. After cooling to room temp, 10 μL of RNase was added to lysate and incubated at 37°C for 45 min. Then, 200 μL protein precipitation solution was added, and tubes were incubated on ice for 10 min before being centrifuged at top speed for 10 min. The DNA-containing fraction was then added to 600 μL isopropanol and gently rocked until the DNA precipitated. After pelleting the DNA (top speed, 5 min), the pellet was first washed with 600 μL of ice-cold 70% ethanol and then 90% ethanol. After completely drying, the pellet was resuspended in HPLC grade water. Following Qbit quantification, genomes were sent to SeqCoast Genomics (Newington, New Hampshire) for Illumina short-read whole genome sequencing using 150 bp paired end reads. For whole genome sequencing analysis, reads for both strands were uploaded into Geneious Prime 2022.0.2 (Dotmanics, Boston, MA). Adaptors and low-quality reads were trimmed using BBDuk default settings. Trimmed sequences were mapped to the *S. aureus* USA300_FRP3757 (NC_007793.1) or *S. epidermidis* 1457 (CP020463.1) reference genome. Variants were then called in the mapped genomes using a 0.9 minimum variant frequency. Mutations

not found in the WT strain and located within open reading frames (ORF) were then identified. The abovementioned reference genomes were also used to extract protein sequences of DtpT (*S. aureus*) and B4U56_10070 (*S. epidermidis*) for NCBI Blastp studies.

Data visualization. Growth curves and bar graphs were generated using GraphPad Prism software version 10.0.0 (153). All finalized figures were generated using the open source Inkscape 1.2.2 (b0a8486, 2022-12-01). Available at: https://inkscape.org.

TABLES

Table 3.1. *S. aureus* bialaphos resistant colony mutations.

Genome	Locus	Gene	Product	Nucleotide change	Amino acid change
RC01	SAUSA300_RS03825	*dtpT*	peptide MFS transporter	AACAAAAC C	Deletion
RC02				C -> A	G -> V
RC03				C -> T	G -> D
RC04				TATTAG	A -> ANT
RC04				CAA -> TCT	VV -> EI
RC05				A -> T	Transversion
RC06				G -> T	A -> D
RC07				G -> A	P -> L
RC08				G -> T	Q -> K
RC09				C -> T	G -> D
RC03	SAUSA300_RS04175	*emp*	extracellular matrix protein-binding adhesin Emp	A -> C	Transversion
RC07 RC08 RC09	SAUSA300_RS10835	*int3*	site-specific integrase	T -> A	L -> I
RC06	SAUSA300_RS13025	*tcyA*	transporter substrate-binding domain-containing protein	A -> T	Transversion
RC04 RC05 RC06	SAUSA300_RS13270	*pnbA*	carboxylesterase/lipase family protein	C -> T	Transition

Table 3.2. *S. epidermidis* bialaphos resistant colony mutations.

Genome	Locus	Product	Nucleotide change	Amino acid change
RC7	B4U56_01010	ABC transporter substrate-binding protein	C -> G	A -> G
RC1	B4U56_04105	RNA polymerase sigma factor SigB	G -> T	Transversion
RC3	B4U56_09585	methionine import ATP-binding protein MetN 1	G -> A	A -> V
RC1	B4U56_10070	MFS transporter	T -> A	Truncation
RC2			C -> A	S -> R
RC3			C -> G	N -> K
RC4			G -> A	G -> D
RC5				Deletion
RC6			C -> A	T -> N
RC7			T -> A	S -> R
RC8			G -> A	D -> N
RC9			C -> G	Truncation
RC6	B4U56_11050	DNA-directed RNA polymerase subunit β	C -> G	R -> T
RC5	B4U56_11965	hypothetical protein	G -> T	L -> F
RC5			G -> A	M -> I

Table 3.3. Strains used in this study.

Strain	Description	Reference
***Staphylococcus aureus* strains**		
S. aureus WT	JE2, derivative of USA300 LAC	(164, 166)
Δ*gisABCD-ggt*	Clean deletion of SAUSA300_0200-0404 genetic region	(89)
Δ*dtpT*	Clean deletion of *dtpT* (SAUSA300_0712); *sae* sequenced & α hemolysin positive	This study
dtpT::Tn	*B. aurealis* Tn insertion at genome position 2156268	This study
Δ*gisABCD-ggt* Δ*dtpT*	Clean deletion of the *dtpT* locus in the Δ*gisABCD-ggt* background strain; *sae* sequenced and α hemolysin positive	This study
HL1427	Resistant colony 1 (RC1) isolated from a bialaphos Kirby Bauer using WT *S. aureus*	This study
HL1419	RC2; Same as HL1427	This study
HL1420	RC3; Same as HL1427	This study
HL1421	RC4; Same as HL1427	This study
HL1422	RC5; Same as HL1427	This study
HL1423	RC6; Same as HL1427	This study
HL1424	RC7; Same as HL1427	This study
HL1425	RC8; Same as HL1427	This study
HL1426	RC9; Same as HL1427	This study
***Staphylococcus epidermidis* strains**		
S. epidermidis 1457 WT	Isolated from central venous catheter infection	(219)
HL1406	Resistant colony 1 (RC1) isolated from a bialaphos Kirby Bauer using WT *S. epidermis* 1457	This study
HL1407	RC2; Same as HL1406	This study
HL1408	RC3; Same as HL1406	This study
HL1409	RC4; Same as HL1406	This study
HL1010	RC5; Same as HL1406	This study
HL1411	RC6; Same as HL1406	This study
HL1412	RC7; Same as HL1406	This study
HL1413	RC8; Same as HL1406	This study
HL1414	RC9; Same as HL1406	This study

Table 3.4. Plasmids used in this study.

Plasmid	Description	Reference
pKK22	Derivative of the naturally occurring *S. aureus* plasmid LAC-p01. Maintains stability in *S. aureus* without antibiotics. Linearized for Gibson assembly using primers PK85 & PK86.	(153)
pKK22-*dtpT*	pKK22 expressing the WT *S. aureus dtpT* allele under native promoter conditions. Plasmid generated using primers PK27 and PK28.	This study
pKOR1	Temperature sensitive vector for generating clean deletions in *S. aureus*.	(213)
pKOR1-Δ*dtpT*	pKOR1 harboring 1 Kb upstream & 1 Kb downstream of *dtpT* to generate a clean deletion.	This study

Table 3.5. Primers used in this study.

Primer	Description	Sequence (5' → 3')
NE Martn-ermR*	Used to confirm Tn insertions on plus strand	CTCGATTCTATTAACAAGGG
NE Buster*	Used to confirm Tn insertions on minus strand	GCTTTTTCTAAATGTTTTTTAAGTAAATCAAGTAC
HL267	Used to confirm Tn insertion in *dtpT* (SAUSA300_RS03825)	CAACACTTCCGATAATAAGACC
PK126	Confirming *gisABCD-ggt* deletion	TCAAAGCTGGCGATGATGG
PK125	Confirming *gisABCD-ggt* deletion	TCAGTTGTTGGATCAGATGAGC
PK85	pKK22 amplification for Gibson assembly	GCGGCCGCTAGCCTAGGAGC
PK86	pKK22 amplification for Gibson assembly	ATCGCCTGTCACTTTGCTTGATATATGA
PK27	Amplification of *dtpT* from JE2 for Gibson assembly with pKK22	CAAGCAAAGTGACAGGCGATTTTTCCTAACTTATTGGTGTG
PK28	Amplification of *dtpT* from JE2 for Gibson assembly with pKK22	GCTCCTAGGCTAGCGGCCGCTTAACGTATACCTTTCATCG
PK102	To amplify 1kb upstream of *dtpT* to generate pKOR1-Δ*dtpT* using NotI restriction cut site. Pair with PK105 to PCR sew	GCGGCCGCTTTTCACAGCAATACTTGG
PK103	To amplify 1kb upstream of *dtpT* to generate pJET1.2-Δ*dtpT*. Has homology with PK104 for PCR sewing before putting into pJET1.2	GCCAACAATAGTATACATCCCATCCTTTC
PK104	To amplify 1kb downstream of *dtpT* to generate pJET1.2-Δ*dtpT* using KpnI restriction cut site. Has homology with PK103 for PCR sewing before cloning into pJET1	GGATGTATACTATTGTTGGCCTAATTCAAAAAAC

Table 3.5 (cont'd)

PK105	To amplify 1kb downstream of *dtpT* to generate pJET1.2-Δ*dtpT* using KpnI restriction cut site. Pair with PK102 for PCR sewing.	GGTACCTCCAATTCATGCTATCACG
PK116	To amplify the deleted *dtpT* region for PCR sequence confirmation	CACATTATATTGAAGTCTGG
PK117	To amplify the deleted *dtpT* region for PCR sequence confirmation	AACACCGTTTATAAGTTCG
TB96	*saeS* amplification	GCTTTACAACATATACCATCACAACTG
TB97	*saeS* amplification	AGCCCTCATTAATGGGAGCTTC

FIGURES

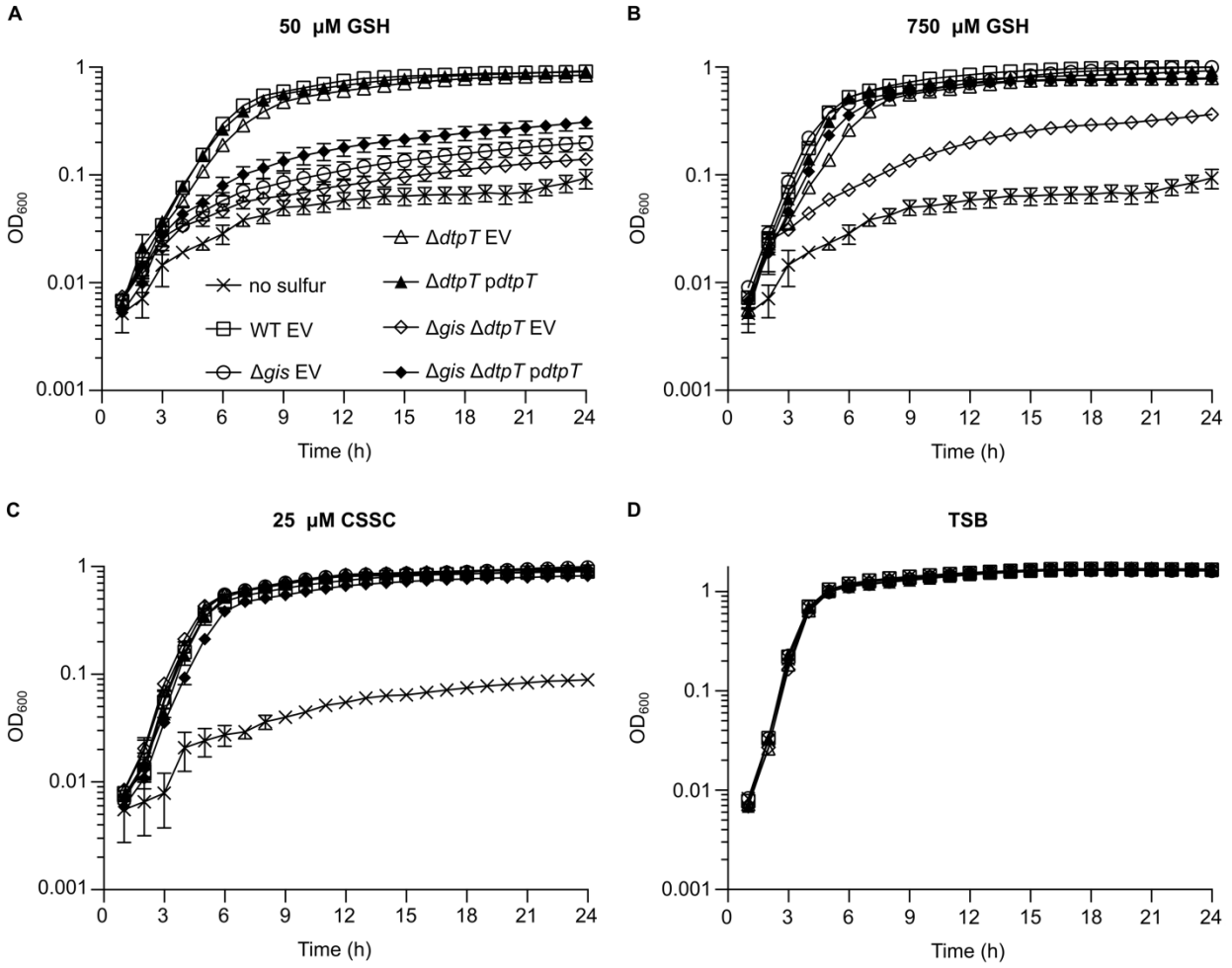

Figure 3.1. The di-tripeptide transporter, DtpT, supports *Staphylococcus aureus* growth on GSH as a source of nutrient sulfur. WT, Δ*gisABCD-ggt* (Δ*gis*), Δ*dtpT*, Δ*gisABCD-ggt* Δ*dtpT*, and their respective *dtpT* complements were cultured in chemically defined medium (CDM) supplemented with either 50 µM or 750 µM GSH (**A** and **B**, respectively), 25 µM cystine (CSSC; **C**), or tryptic soy broth (TSB; **D**). WT *S. aureus* maintaining an empty pKK22 vector (EV) cultured in CDM lacking a viable sulfur source denotes the no sulfur control. Each complementation strains express, under native promoter conditions, the WT *dtpT* allele from the pKK22 vector (p*dtpT*). The mean and ± 1 standard error of three biological replicates is depicted.

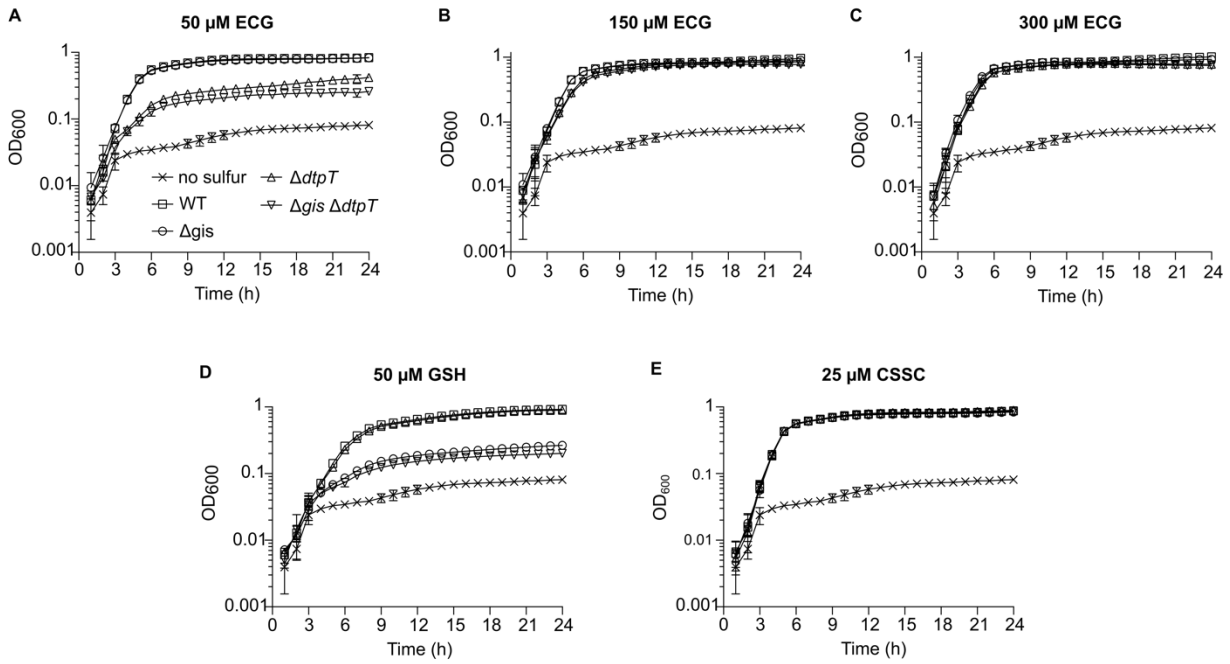

Figure 3.2. The γ-peptide confers specificity for GisABCD-supported growth on GSH. Growth assessments in CDM of WT, Δ*gisABCD-ggt*, Δ*dtpT* and the Δ*gisABCD-ggt*, Δ*dtpT* double transport mutant on glutamate-cysteine-glycine (ECG) tripeptide as the provided sulfur source. This GSH analog harbors and α-peptide bond between Glu and Cys rather than the γ-peptide found in GSH. Strains were cultured in a chemically defined medium supplemented with either 25 µM CSSC (**A**), 50 µM GSH (**B**), 50 µM, 150 µM, or 300 µM ECG (**C**, **D**, **E**, respectively). WT cultured in CDM lacking a sulfur source acts as the no sulfur control. Curves are the mean of three biological replicates with error bars denoting the ± 1 standard error.

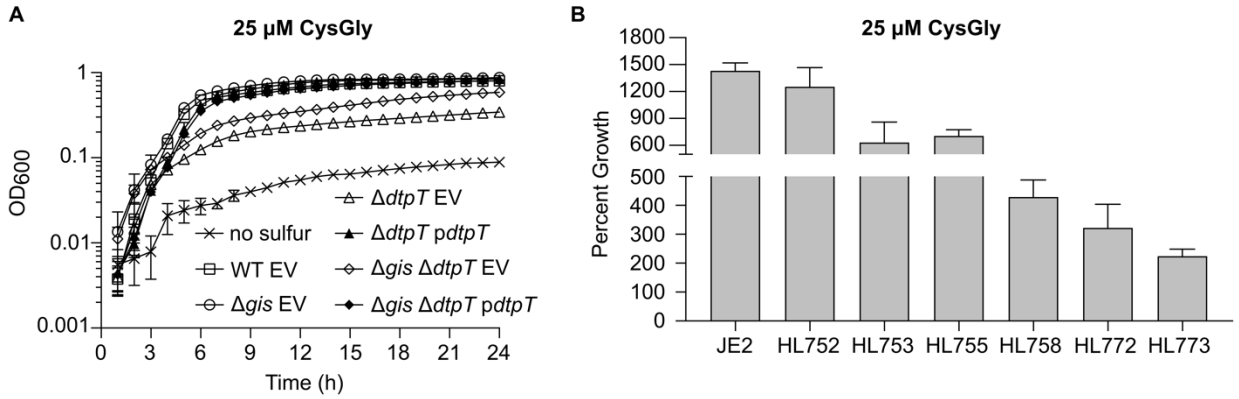

Figure 3.3. Cysteinyl-glycine (CysGly) is a viable sulfur source for *Staphylococcus aureus* in a DtpT-mediated fashion. A) growth kinetics of WT, Δ*gisABCD-ggt* (Δ*gis*), Δ*dtpT*, Δ*gisABCD-ggt* Δ*dtpT*, and the *dtpT* complement strains in CDM supplemented with 25 µM CysGly. pKK22 is the empty vector (EV) and pKK22-*dtpT*, expressing WT *dtpT* allele under native promoter conditions, is denoted as p*dtpT*. Each curve represents the means of three biological replicates with error bars indicating the standard error. WT EV cultured in CDM lacking a viable sulfur source designates the no sulfur control. **B**) Percent growth using endpoint OD_{600} values of clinical CF isolates grown in CDM supplemented with 25 µM CysGly. The average of four biological replicates are represented with error bars representing ± 1 standard error of the mean.

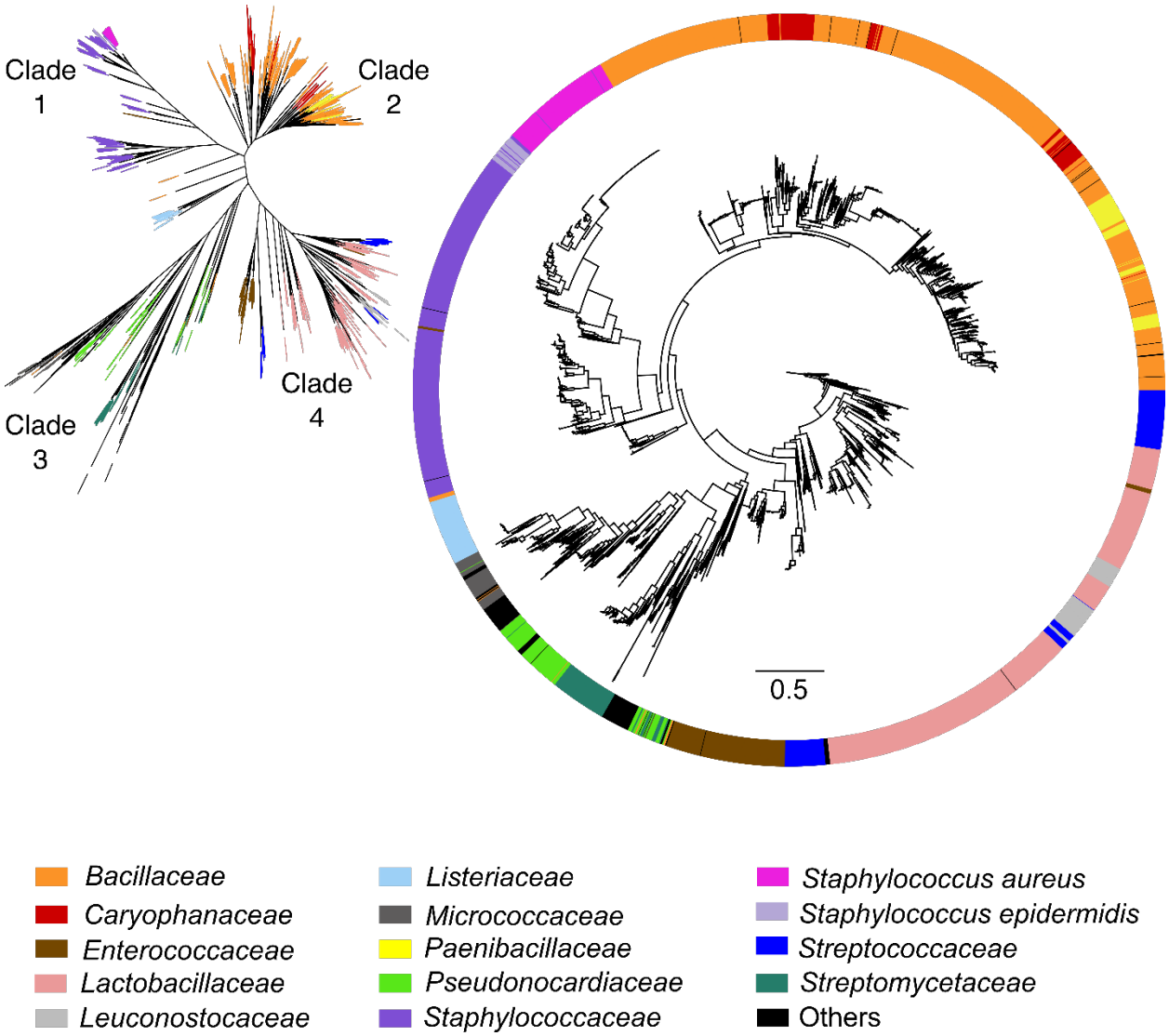

Figure 3.4. Distribution of DtpT homologs across Gram-positive bacteria. Phylogenetic reconstruction of DtpT homologs (*n*=3,649). Homologs are defined as those proteins sharing ≥50% coverage and ≥40% when aligned against *S. aureus* DtpT. Host species are grouped into families with each family containing ≥50 representatives. Each family is designated with its own unique color depicted within the circular tree as follows: *Bacillaceae* (orange), *Caryophanaceae* (red), *Enterococcaceae* (brown), *Lactobacillaceae* (salmon), *Leuconostocaceae* (light grey), *Listeriaceae* (light blue), *Micrococcaceae* (dark grey), *Paenibacillaceae* (yellow), *Pseudonocardiaceae* (light green), *Streptococcaceae* (royal blue), *Streptomycetaceae* (dark green). Families with <50 representatives were grouped together into one category: Others (black). The *Staphylococcaceae* family (purple) had *Staphylococcus aureus* (pink) and *Staphylococcus epidermidis* (lavender) split out as their own sub-families for emphasis. Clades were identified by displaying the DtpT homologs (*n*=3,649) as a radial tree (upper left).

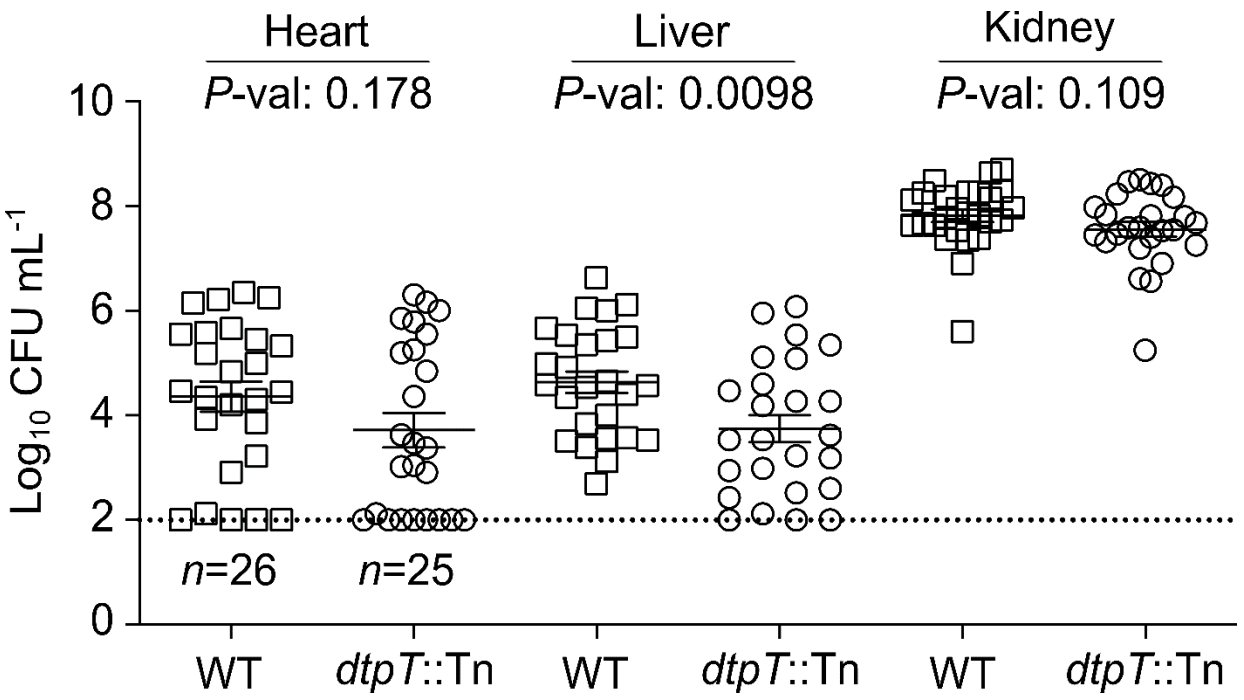

Figure 3.5. DtpT contributes to *Staphylococcus aureus* fitness during murine systemic infection. Bacterial burdens in the heart, liver, and kidneys of 8-week-old Balb/cJ female mice inoculated WT or *dtpT*::Tn. The limit of detection is 100 CFU and is represented with a dotted, horizontal line. Statistical significance within each organ was determined as follows: first the presence or absence of normal distribution was assessed with the Shaprio-Wilk test which returned the following *P*-values: WT_{heart} = 0.02415, $dtpT_{heart}$ = 0.001623, WT_{liver} = 0.6531, $dtpT_{liver}$ = 0.1715, WT_{kidney} = 0.002334, $dtpT_{kidney}$ = 0.01517. From this it was determined that the WT and *dtpT*::Tn liver Tables were normally distributed and thus an unpaired t-test with Welch's correction was conducted (see figure for *P*-value). All other Tables were determined as not normally distributed and the Mann-Whitney t-test was employed (see figure for *P*-values). Solid, horizontal lines represent the mean with error bars being ± 1 standard error of the mean.

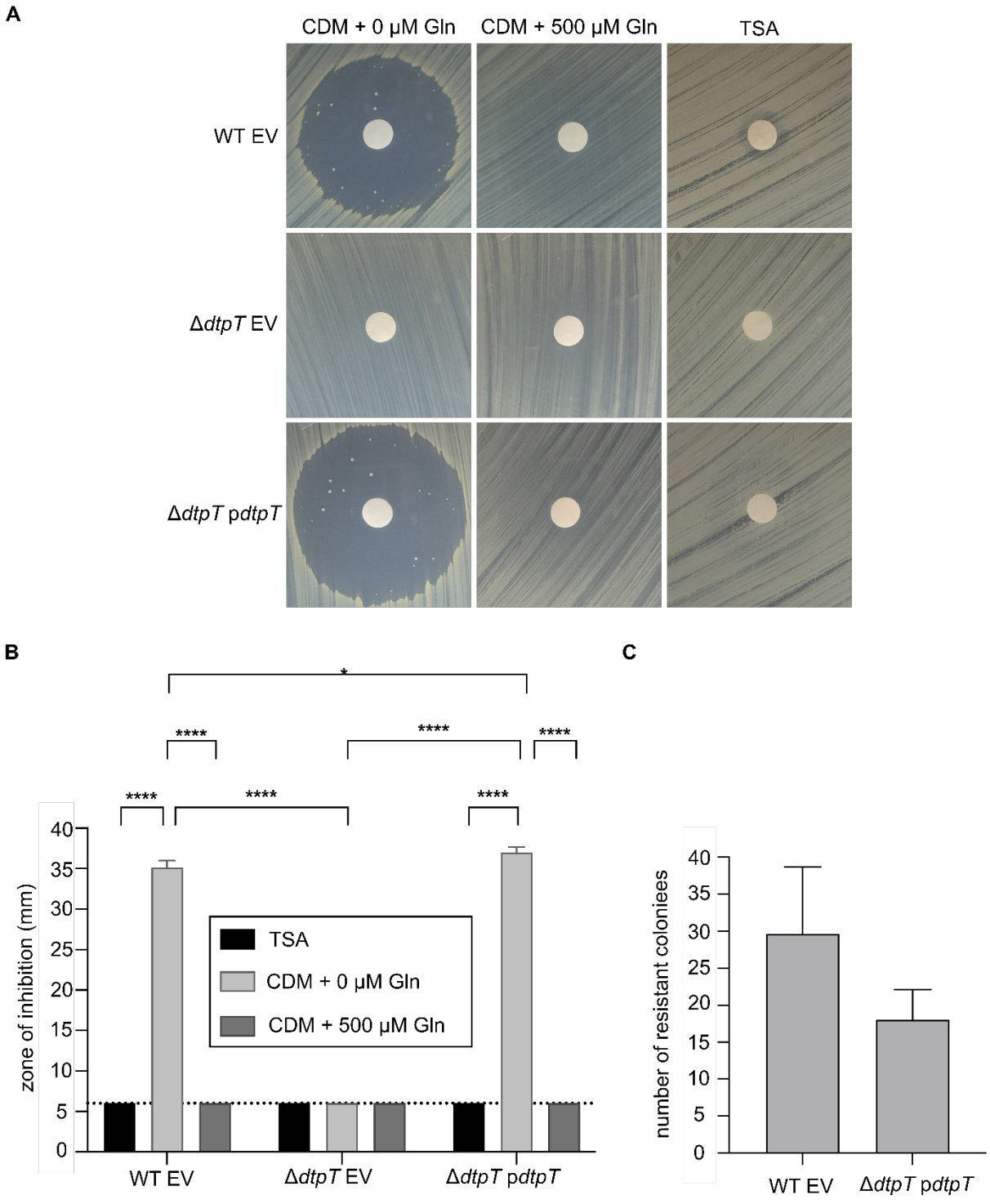

Figure 3.6. *Staphylococcus aureus* sensitivity to the tripeptide antibiotic, bialaphos, is glutamine- and DtpT dependent. The Kirby Bauer assay was preformed utilizing JE2 WT and the Δ*dtpT* mutant. WT harbors the empty pKK22 vector (EV) while Δ*dtpT* contains either EV or the p*dtpT* complement in which *dtpT* is expressed under native promoter conditions. **A**) Representative photo of each bialaphos Kirby Bauer assay

Figure 3.6 (cont'd)

using cells plated on CDM-trimethoprim agar plates (CDM-TMP) containing either 0 μM (left) or 500 μM Gln as well as tryptic soy agar (TSA). **B**) Quantification of the Kirby Bauer zone on inhibition. The limit of detection (6 mm) is defined by a horizontal, dashed line. Statistical analysis was conducted using a 2-way ANOVA using Tukey's multiple comparison test. *P*-values are represented as follows: * = 0.0409, **** = <0.0001. **C**) Enumeration of the Kirby Bauer resistant colonies. An unpaired t-test returned a non-significant *P*-value of 0.3061. **B** and **C** present the mean of three biological replicates ± 1 standard error of the mean.

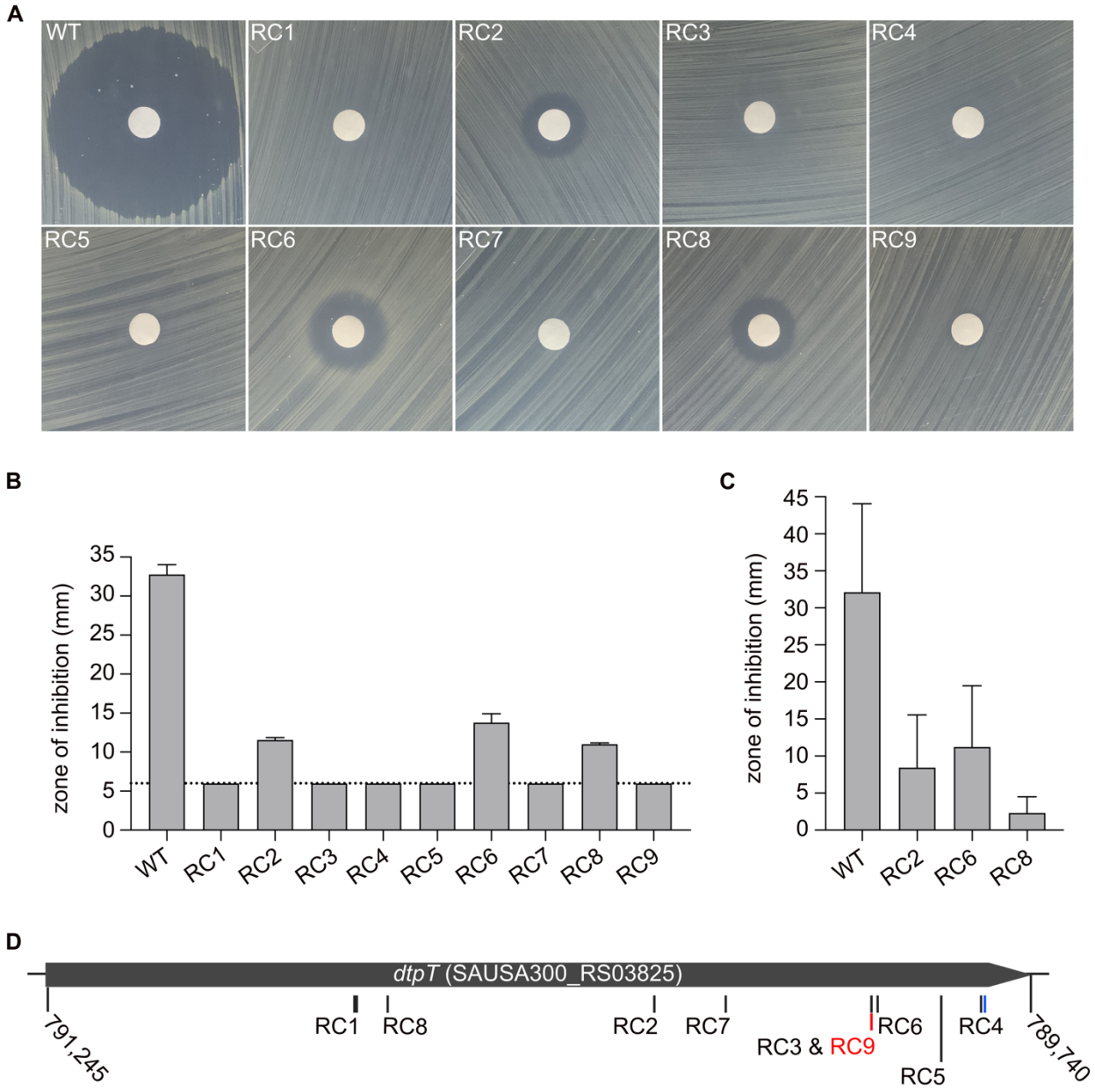

Figure 3.7. *Staphylococcus aureus* develops varying resistance to bialaphos due to *dtpT* mutation. A) Pictural representation of *S. aureus* WT and the nine bialaphos resistant colonies (RC1-9) when challenged against bialaphos in a Kriby Bauer assay. **B**) Quantification of the Kirby Bauer zone of inhibition. The limit of detection (6 mm) is denoted with a horizontal, dashed line. **C**) Enumeration of resistant colonies in the Kirby Bauer assays. For **B** and **C,** the mean of three biological replicates ± 1 standard error of the mean is shown. **D**) To-sale depiction of *dtpT* mutations in the bialaphos RCs as defined by whole genome sequencing. Red is to denote that RC9 has the same mutation as RC3. The blue line indicates a second mutation in *dtpT* for RC4. Please see Table 3.1 for specific information regarding mutations. Image created with BioRender.com.

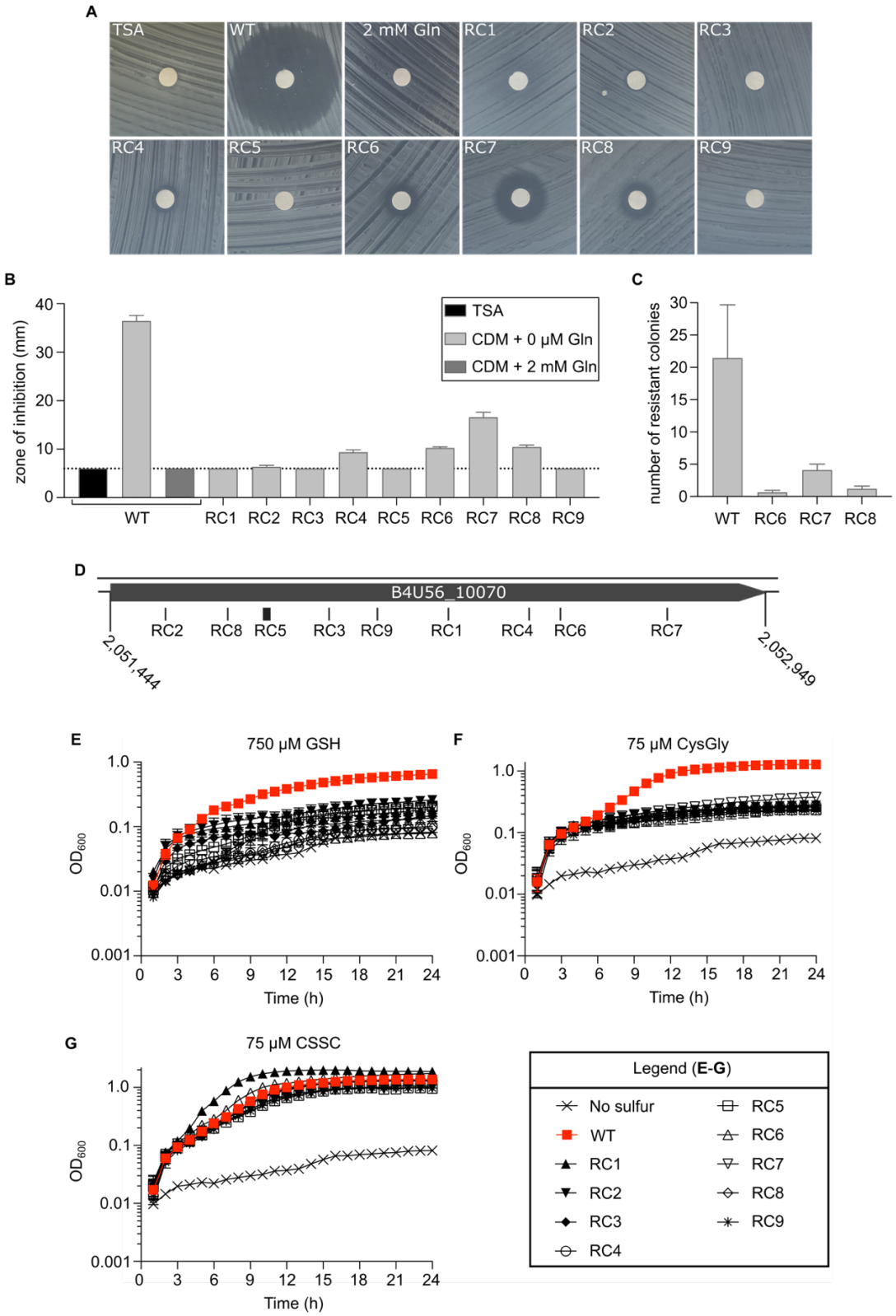

Figure 3.8. *Staphylococcus epidermidis* 1457 harbors a *dtpT* homolog, B4U56_10070, that supports growth on both GSH and the newly identified sulfur

Figure 3.8 (cont'd)

source, CysGly. A) Representative pictures of bialaphos Kirby Bauer on TSA (specified) and CDM with 2 mM Gln (specified) or no Gln (all other pictures, not specified). In the top row, the first three pictures (starting from the left) are WT *S. epidermidis* 1457. Bialaphos resistant colonies (RC) 1-9 are indicated in the appropriate picture. Bialaphos Kirby Bauer zones of inhibition (ZOI; **B**) and RCs that arose in the ZOI (**C**) were quantified. The limit of detection (6 mm) is defined by a horizontal, dashed line (**B**). **D**) Position specific location of the mutations in B4U56_10070 in each RC as defined by whole genome sequencing. Refer to Table 3.2 for mutation information. Image created with BioRender.com. **E-G**) Growth kinetics of *S. epidermidis* 1457 WT and RC1-9 on CDM_{mod} supplemented with either 75 μM CSSC (**C**), 75 μM CysGly (**D**), or 750 μM GSH (**E**). Both the Kirby Bauer and growth curve assays (**B**, **C**, **E**-**F**) were performed in biological triplicate with the mean and ± 1 standard error of the mean being presented.

CHAPTER 4: Employing MALDI-IMS to visualize the host-pathogen nutritional sulfur interface during *Staphylococcus aureus* systemic infection

ABSTRACT

The opportunistic pathogen *Staphylococcus aureus* persistently colonizes 20% of the population and is a leading cause of infections such as bacteremia and infective endocarditis. Successful proliferation of *S. aureus* throughout numerous host tissue depends on an ability to develop antibiotic resistance and procure essential nutrients from diverse metabolite forms within the local environment. With increasing knowledge regarding *S. aureus* host-sulfur acquisition, confirming the *in vivo* relevance of these pathways is important. This pioneering study examines the host-pathogen nutritional sulfur interface using Matrix-assisted laser desorption/ionization imaging mass spectrometry (MALDI-IMS) on systemically infected murine kidneys. In doing so, we have confirmed that three *S. aureus* sulfur sources—reduced and oxidized glutathione as well as cysteinyl-glycine—are present in this organ during infection. Additionally, the capacity of MALDI-IMS to identify biologically relevant sulfur sources is demonstrated with the mixed cysteine-glutathione disulfide, a metabolite particularly abundant within healthy or *S. aureus* colonized kidneys. Growth of *S. aureus* on cysteine-glutathione disulfide *in vitro* is supported by the cysteine/cystine transporters TcyABC and TcyP as well as the GisABCD-Ggt reduced/oxidized glutathione import and catabolism system. Lastly, the ability of GisABCD-Ggt to support *S. aureus* proliferation on GSH derivatives *S*-nitrosoglutathione and *S*-lactoylglutathione is established. In total, this investigation harnesses the unique capabilities of MALDI-IMS to better comprehend how this formidable pathogen impacts host sulfur metabolism during infection.

INTRODUCTION

Methicillin Resistant *Staphylococcus aureus* (MRSA) is an opportunistic pathogen and leading cause of hospital acquired infections in the United States (86, 87). This is due to the propensity of *S. aureus* to colonize numerous host organs and rapidly develop antibiotic resistance. Successful proliferation within tissue requires *S. aureus* acquisition of essential nutrients such as sulfur that are found within host metabolites (134). Though our understanding of *S. aureus* host-sulfur procurement is increasing, we lack insight regarding the distribution and abundance of these sulfur containing compounds during infection. Targeted metabolomics using mass spectrometry (MS) is a powerful tool commonly used to detect and quantify metabolites within a sample (e.g., tissue) (220). For assessing host-pathogen interfaces, though, MS alone is limiting when both quantity and distribution of a metabolite is also desired.

With recent advances in technology, descriptive spatial localization and relative quantification of a compound is possible with matrix-assisted laser desorption/ionization imaging mass spectrometry (MALDI-IMS) (221). Using this technique, spectra are obtained at discrete locations across a sample. From these spectra an image is generated using the intensity signal of a metabolite. In *S. aureus*, MALDI-IMS has provided invaluable data regarding host redistribution of nutrients such as calcium, manganese, and zinc during systemic infection (185). Additionally, MALDI-IMS can assess the abundance of either host (e.g., calprotectin) or *S. aureus* (e.g., siderophores) proteins, reinforcing the notion that this tool is well equipped for examining both sides of a host-pathogen interaction (185, 222).

Here, MALDI-IMS was utilized to gain preliminary insights on host sulfur distribution during *S. aureus* systemic infection of the murine kidney. We discover that several sulfur sources identified for this pathogen *in vitro* are present within healthy tissue and experience an increased relative abundance and/or redistribution upon infection. Furthermore, the efficacy of MALDI-IMS is exemplified by its discovery of a novel sulfur source in *S. aureus*, known as cysteine-glutathione mixed disulfide (CSSG). Growth of *S. aureus* on CSSG requires the collective presence of the GSH importer and γ-glutamyl transpeptidase (GisABCD-Ggt) machinery (89) as well as the cysteine (Cys)/cystine (CSSC) transporters, TcyABC and TcyP (90). Lastly, we demonstrate that two other GSH derivatives, *S*-nitrosoglutathione (GSNO) and *S*-lactoylglutathione (SLG) support the *S. aureus* nutritional sulfur requirement in a GisABCD-Ggt mediated fashion. Collectively, this body of work broadens our knowledge regarding the levels of redundancy employed by *S. aureus*—from the acquisition of structurally similar compounds to the use of multiple transporters for a single metabolite—to ensure that the nutritional sulfur status is maintained.

RESULTS

Matrix assisted laser desorption/ionization imaging mass spectrometry reveals the presence of known and putative *S. aureus* sulfur sources in the systemically infected murine kidney. Prior studies have revealed several host-derived sulfur sources reinforcing the *S. aureus* nutritional sulfur requirement *in vitro* (88–90). Our work has additionally observed several sulfur associated importers sustaining maximal propagation of *S. aureus* JE2 in the heart and/or liver (TcyP (89) and DtpT, see Chapter 3) during murine systemic infection. Nevertheless, the distribution of sulfur metabolites associated

with *S. aureus* within healthy and infected host tissue remains unknown. To begin addressing this, matrix assisted laser desorption/ionization imaging mass spectrometry (MALDI-IMS) was conducted on both mock infected mice and those inoculated with the WT USA300 LAC derivative, JE2 (Fig. 4.1). Kidney samples were used for downstream analysis given that WT colonization in this environment consistently results in abscess formation, a hallmark of *S. aureus* infection; this allows for easy discernment between mock and infected tissues using hematoxylin and eosin (H&E) staining (Fig. 4.1A). MALDI-IMS on kidney samples assessed the distribution of three known sulfur sources: reduced and oxidized glutathione (GSH and GSSG, respectively) (88, 89) as well as its breakdown product, cysteinyl-glycine (CysGly) (see Chapter 3). In a healthy kidney, both GSH and GSSG are present—here each metabolite has the highest abundance in the medulla but shows moderate levels throughout the tissue during *S. aureus* infection (Fig. 4.1B and 4.1C, respectively). However, during systemic infection the kidney experiences an increase in abundance throughout the kidney (Fig. 4.1B and 4.1C, respectively). Interestingly, the presence of a mixed GSH disulfide species, cysteine-glutathione disulfide (CSSG), displayed high abundance in the renal cortex (Fig. 4.1D). During *S. aureus* infection, CSSG increased its presence by spreading throughout the tissue sample (Fig. 4.1D). Ionization of CysGly, which is a breakdown product of GSH in the γ-glutamyl cycle, exhibited improved results when a different matrix was used compared to the one employed for GSH, GSSG, and CSSG (details in Materials and Methods). Consequently, distinct tissue samples from both mock and infected kidneys were used for H&E staining (Fig. 4.1E) and for the MALDI-IMS visualization of this metabolite. In the mock-infected murine kidney, CysGly is observed within the renal cortex with a slight

redistribution occurring towards the center during *S. aureus* infection (Fig. 4.1F). Collectively, these data indicate that sulfur sources identified *in vitro* for this pathogen can be found in at least one tissue environment during systemic infection.

***S. aureus* GisABCD, TcyABC, and TcyP support the use of CSSG as a source of nutritional sulfur.** Given that all GSH derivates tested thus far (i.e., GSSG and CysGly) are *S. aureus* sulfur sources, we predicted that CSSG would also support nutritional demands for this pathogen. Indeed, supplementation of a chemically defined medium (CDM) with 12.5 μM CSSG as the only viable sulfur source promotes robust growth of WT (Fig. 4.2A); we next ascertained the *S. aureus* machinery supporting this phenotype. Due to the mixed disulfide nature of CSSG, we hypothesized that several transporters are involved with growth on this nutrient. We first investigated the *gisABCD-ggt* genetic region, where *gisABCD* encodes a GSH/GSSG ABC transporter and *ggt* produces a γ-glutamyl transpeptidase cleaves the γ-peptide bond of these metabolites (89). Proliferation of a *gisABCD-ggt* clean deletion mutant (denoted as Δ*gis*) on CSSG is not impaired, potentially implying the presence of redundant systems that support growth on this nutrient (Fig. 4.2A). Considering the Cys residue of CSSG, the Cys/CSSC transporters TcyABC and TcyP (90) were next assessed. Transposon (Tn) inactivating mutations in either transporter (*tcyA*::Tn or *tcyP*::Tn) fails to impact *S. aureus* propagation on CSSG (Fig. 4.2A).

Given that the single transporter mutants all displayed WT-like growth, we investigated the growth kinetics of strains deficient for two of the three importers. A Δ*gis tcyA*::Tn mutant displayed in a modest growth defect compared to WT while the Δ*gis tcyP*::Tn strain did not (Fig. 4.2A). Interestingly, the *tcyA*::Tn *tcyP*::Tn mutant exhibited the growth

greatest impairment of all the double mutants tested (Fig. 4.2A). These observations indicate that all three transporters support, at different levels, *S. aureus* growth on CSSG. This is further indicated by the fact that a Δ*gis* Δ*tcyA tcyP*::Tn triple transport mutant fails to proliferate in CSSG (Fig. 4.2A). Furthermore, all phenotypes are sulfur specific as each mutant strain proliferates to WT-like levels when cultured in CDM harboring sodium thiosulfate (sTS) as the sulfur source (Fig. 4.2B).

***S. aureus* GisABCD drives the use of GSH-derived species to sustain the nutritional sulfur requirement *in vitro*.** Host GSH derivatives are not limited to GSSG, CysGly, and CSSG. *S*-nitrosogluathione (GSNO) forms when GSH indirectly reacts with nitric oxide (NO) (223). GSNO acts as a signaling molecule by transferring the NO to target proteins, effectively altering their function, and is found in the high picomole to low nanomole range human plasma (224, 225). Consistent with other GSH related metabolites evaluated, supplementation of CDM with 75 μM GSNO promotes WT proliferation if a functional *gisABCD-ggt* system is present (Fig. 4.3A). *S*-lactoylglutathione (SLG) is also found within the host environment as an intermediate in the methylglyoxyl detoxification pathway and is present at low micromolar concentrations (~12-16 μM) in human blood (226). As expected, SLG supports growth of *S. aureus* when provided at low micromolar concentrations (i.e., 50 μM) in CDM; use of this nutritional sulfur source largely depends on the GisABCD-Ggt system (Fig. 4.3B). Collectively, GSNO and SLG provide further evidence supporting the notion that GSH derivatives can be targeted as nutritional sulfur sources for *S. aureus* during infection.

DISCUSSION

This study of MALDI-IMS on the host-pathogen nutritional interface visualizes the distribution and relative abundance of three established sulfur sources (GSH, GSSG, and CysGly) during systemic *S. aureus* infection. Interestingly, both GSH and GSSG increased in relative abundance during infection (Figure 4.1B and C). This could result from the host immune response to *S. aureus*. Neutrophils combat *S. aureus* by delivering reactive oxygen species (ROS) to the site of infection and resulting have high intracellular levels of GSH to modulate internal ROS (227). As these neutrophils die, this GSH pool is likely released to the extracellular environment, becoming accessible to *S. aureus*. One might predict that this relative abundance of GSH and GSSG in the kidney might increase even more in mice infected with the Δ*gis* mutant; this would suggest that *S*. *aureus* is importing and catabolizing these nutrients during infection. From the GSH and GSSG MALDI-IMS data alone, it is also tempting to speculate on the state of the host sulfur pool in environments where *S. aureus* sulfur associated transporters contribute to maximal proliferation (e.g., heart (90) and liver; Chapter 3). Will MALDI-IMS reveal depletion of the metabolites associated with TcyP (i.e., Cys/CSSC) or DtpT (GSH, CysGly)? As discussed previously, would inactivating these transporters replenish the respective sulfur pools during systemic infection? Overall, MALDI-IMS has provided further support for the comprehensive characterization of sulfur acquisition systems in *S. aureus* in order to establish a clear understanding of the host-pathogen nutritional sulfur interface.

This investigation additionally highlights the robust utility of MALDI-IMS as a tool for unveiling novel sulfur sources for pathogens. Indeed, CSSG is highly abundant in both the mock and systemically infected kidney. Very little is known about the contributions of

CSSG to mammalian physiology, but it is ubiquitous within cells and can protect mice against acetaminophen-induced hepatotoxicity (228). Here CSSG is given a new function as a potent source of nutrient sulfur for *S. aureus*, as particularly low micromolar concentrations of this disulfide elicits robust proliferation of the bacterium. This could be related to the fact that, once reduced, Cys—the crux of sulfur distribution within cells—is immediately accessible to donate its sulfur atom to other biological processes (e.g., Fe-S cluster assembly). Interestingly, two distinct types of sulfur transporters are associated with *S. aureus* proliferation on CSSG as a nutritional sulfur source: GSH/GSSG (GisABCD) and Cys/CSSC (TcyABC and TcyP). Except for CSSG, all substrates implicated in the GisABCD system (GSH/GSSG, GSNO, SLG) share common tripeptide and γ-peptide bond features, as discussed in Chapter 3. CSSG deviates from this pattern as it involves an amino acid, Cys, forming a disulfide bond with GSH. This suggests that the substrate binding protein (SBP), GisA, may possess an active site primarily recognizing a single molecule of GSH, with limited or no involvement in recognizing the molecule disulfide-bonded to GSH. A similar concept could be applicable to TcyA, the substrate binding protein (SBP) of the TcyABC complex, and TcyP—here recognition of Cys in CSSG takes precedence, with GSH playing a minimal or negligible role in substrate recognition. This inference is drawn from the understanding that sulfur sources related to both TcyABC and TcyP primarily involve Cys and its close derivatives (such as CSSC, *N*-acetylcysteine, and homocystine) (90).

The above scenario only applies to CSSG if this metabolite is transported into the cell as a disulfide, implying that the reductase is intracellular (Fig. 4.4A). Supporting this model is the knowledge that Ggt, a cytoplasmic protein, can cleave the γ-peptide bond of

GSSG, suggesting that GSSG is reduced in this space (89). Indeed, most reductases are found within the cytoplasm, helping to drive the cytoplasmic redox status of the cell (229). However, in Gram-negative bacteria the Dsb system functions to introduce (DsbA, DsbB) and correct (DsbC, DsbD) protein disulfide bonds in the periplasm; *S. aureus* only encodes DsbA, a protein whose ability to regain the oxidative state is predicated to rely upon extracellular oxidants (230). One might wonder whether CSSG is involved in that process. With such a model, reduction of CSSG would occur before transportation through GisABCD, TcyABC, and TcyP (Fig. 4.4B). Promoting this model is the notion that neither TcyABC nor TcyP are associated with tripeptide import in bacteria, including *S. aureus* (90, 93, 231). There is one study in *Streptococcus mutans* where a GSH SBP (GhsT) acts in concert with the TcyBC component to import the metabolite into the cell (232). It is noteworthy to point out that, in the current study, the TcyBC components are intact in the Δ*gis* Δ*tcyA tcyP*::Tn mutant, suggesting that there is not an additional SBP that binds CSSG for import through the TcyBC complex. Future studies looking at the growth of a *dsbA* mutant on CSSG as the only sulfur source will shed light on whether *S. aureus* utilizes an extracytoplasmic protein to reduce sulfur sources before transportation into the cytoplasm.

Lastly, the implication of CSSG as a GisABCD substrate led us to hypothesize that other GSH derivatives are viable *S. aureus* sulfur sources. GSNO and SLG reinforce this notion as both can be utilized by *S. aureus* to meet the nutritional sulfur requirement. Importantly, growth is supported by the GisABCD-Ggt system when either metabolite is provided at a concentration above values reported for human blood (224–226). Determining whether GSNO and SLG are immediate Ggt substrates or if the respective

NO and D-lactate groups need to be removed before Ggt catalysis represents areas of future investigation. Overall, this pioneering work provides insight into the host's sulfur status during systemic infection and emphasizes the valuable role of MALDI-IMS in expanding our understanding of the sulfur metabolism strategies employed by this formidable pathogen.

ACKNOWLEDGMENTS

We sincerely thank Boone Prentice and Justin Ellenburg for conducting the MALDI-IMS and for their thoughtful insights on this work. Each transposon mutant was obtained from the Network on Antimicrobial Resistance in *Staphylococcus aureus* (NARSA) for distribution by BEI Resources, NIAID, NIH, and the Nebraska Transposon Mutant Library (NTML) Screening Array NR-48501. Funding for this work was provided by the National Institutes of Health R01 AI139074 and R21 AI142517.

MATERIALS AND METHODS

Strains, media, and growth conditions. All strains, plasmids, and primers used throughout the course of this study can be found in **Tables 4.1**, **4.2** and **4.3**, respectively. JE2, a derivative of community acquired USA300 LAC, is the WT *S. aureus* strain for this body of work (164). Correct Tn location and deletions were determined using PCR. Plasmids were generated via Gibson assembly in the *Escherichia coli* DH5a strain before being transferred to *S. aureus* RN4220 to obtain appropriate vector methylation patterns that would permit transformation into the appropriate JE2 background strain. Note that all plasmids were confirmed using Plasmidsaurus whole plasmid sequencing. Deletion of the *tcyA* gene was performed following a well-defined allelic exchange protocol using the pKOR1-mcs plasmid donated from the laboratory of Taeok Bae (213). Each strain was

cultured in 5 mL tryptic soy broth (TSB) overnight at 37°C, 225 rpm. The base chemically defined medium (CDM) was prepared as previously described with slight modifications (149, 150). For the full recipe, please refer to Chapter 2 Materials and Methods. CDM harboring 5 mg mL^{-1} of freshly prepared glucose was supplemented with either no sulfur source, 12.5 mM cysteine-glutathione disulfide (CSSG), 50 mM sodium thiosulfate (sTS), 75 mM *S*-nitrosoglutathione (GSNO), or 50 mM *S*-lactoylglutathione (SLG). For the stock sulfur sources CSSG, sTS, GSNO, SLG, and glucose were dissolved in deionized water before filter sterilization.

Murine model of systemic infection. A WT TSB overnight was sub-cultured 1:100 into 5 mL TSB and grown for an additional 3 h. The culture was pelleted at 4°C, 4000 rpm, before being washed into 12 mL of Dulbecco's Phosphate Buffered Saline (DPBS; no $CaCl_2$ or $MgCl_2$) and normalized to an OD_{600} = 0.4. Eight-week-old Balb/cJ female mice (Jackson Laboratories) were then anesthetized with avertin before being retro-orbitally infected with 10^7 CFU. After 96 hpi, mice were euthanized via CO_2 inhalation. The heart, liver, and kidneys were snap-frozen on dry ice and sent to the Prentice laboratory at University of Florida for imaging. Infections were performed at Michigan State University under the principles and guidelines described in the *Guide for the Care and Use of Laboratory Animals* (218). All animal work followed the protocol approved by Michigan State University Institutional Animal Care and Use Committee (IACUC): PROTO202200474.

Matrix-assisted laser desorption/ionization imaging mass spectrometry (MALDI-IMS). Frozen tissue samples were sectioned at 10 μm using a Leica CM3050S Cryostat. One section of PBS inoculated mouse kidney (control) and one section of *S. aureus* WT-

infected kidney were then thaw mounted onto an indium-tin oxide (ITO) coated slide. A matrix was then applied depending on the desired molecules to be ionized: 9-aminoacridine (9AA; prepared using 90% methanol) was used for GSH, GSSG, and CSSG tissue samples while those used for CysGly observation used dihydroxybenzoic acid (DHB). The designated matrix was applied using an M5 robotic sprayer (HTX Technologies) at 85°C with a 0.11 mL/min flow rate. Nozzle velocity was set to 700 mm/min with a 2 mm track spacing and crisscross pattern with the nitrogen pressure being set at 10 psi (2 L/min flow rate). IMS was conducted using a 7T solariX FT-ICR mass spectrometer (Bruker Daltonics) in negative ion mode. Continuous Accumulation of Selected Ions (CASI) was employed to improve ion signal over the mass window of *m/z* 280-620. All IMS experiments were performed at 150 μm spatial resolution. Mass resolution at *m/z* 400 is 67,000 measured by FWHM. Image processing was done utilizing flexImaging and SCiLS software (Buker Daltonics).

Tissue staining with Hematoxylin and eosin (H&E). After MALDI-IMS, the matrix was removed using a continuous flow of 100% ethanol (20 sec). Samples were then exposed to 95% ethanol (30 sec), 70% ethanol (30 sec), and then washed in Mili-Q water (30 sec) before hematoxylin solution was applied for 2 min. From there the tissues were washed in Milli-Q water (20 sec), 70% ethanol (30 sec), 95% ethanol (30 sec), and then eosin solution was administered (1 min). Additional applications of 95% ethanol (30 sec) and 100% ethanol (30 sec) preceded Xylene application (2-2.5 min). Once completed, a cover slip was added, and the tissue were imaged using an Azio imager M2 optical microscope (Zeiss).

96-well plate growth curves. Overnights were spun at 4°C, 4000 rpm, washed in 5 mL phosphate buffered saline (PBS), and then normalized to an optical density at 600 nm (OD_{600}) equal to 1. Normalized cells were sub-cultured at a 1:100 ratio into each growth condition. Using an Epoc2 Biotek microplate spectrophotometer (37°C, continuous shaking), the OD_{600} was observed every hour for 18 h in a 96-well round bottom plate. For each condition, a strain was inoculated into three wells (i.e., technical triplicate). After being blanked the technical triplicates were averaged, with the average representing a single biological replicate. All growth curves were performed independently three times.

Data visualization. Growth curves were generated using GraphPad Prism software version 10.0.0 (153). All finalized figures were generated using the open source Inkscape 1.2.2 (b0a8486, 2022-12-01). Available at: https://inkscape.org.

TABLES

Table 4.1. Strains used in this study.

Strain	Description	Reference
***Staphylococcus aureus* strains**		
S. aureus WT	JE2, derivative of USA300 LAC	(164, 166)
Δ*gisABCD-ggt*	Clean deletion of SAUSA300_0200-0404 genetic region	(89)
tcyA::Tn	*B. aurealis* Tn insertion at genome position	(90)
tcyP::Tn	*B. aurealis* Tn insertion at genome position	(90)
Δ*gisABCD-ggt tcyA*::Tn	*B. aurealis* Tn insertion at genome position in the Δ*gisABCD-ggt* background strain	This study
Δ*gisABCD-ggt tcyP*::Tn	*B. aurealis* Tn insertion at genome position in the Δ*gisABCD-ggt* background strain	This study
Δ*gisABCD-ggt* Δ*tcyA tcyP*::Tn	Clean deletion of the *tcyA* locus in the Δ*gisABCD-ggt* background strain; *sae* sequenced and α hemolysin positive	This study

Table 4.2. Plasmids used in this study.

Plasmid	Description	Reference
pKOR1	Temperature sensitive vector for generating clean deletions in *S. aureus*.	(213)
pKOR1-Δ*tcyA*	pKOR1 harboring 1 Kb upstream & 1 Kb downstream of *tcyA* to generate a clean deletion.	This study

Table 4.3. Primers used in this study.

Primer	Description	Sequence (5' → 3')
NE Martn-ermR*	Used to confirm Tn insertions on plus strand	CTCGATTCTATTAACAAGGG
NE Buster*	Used to confirm Tn insertions on minus strand	GCTTTTTCTAAATGTTTTTTAAGTAAATCAAGTAC
PK126	Confirming *gisABCD-ggt* deletion	TCAAAGCTGGCGATGATGG
PK125	Confirming *gisABCD-ggt* deletion	TCAGTTGTTGGATCAGATGAGC
HL130	Confirming the Tn insertion in *tcyA*	CGTCAATAAATATAAGTTGCTAGC
HL211	Confirming the Tn insertion in *tcyP*	CGAAGCAAATATCACGACAGC
JLD15	Amplifying 1kb downstream of *tcyA* for Gibson assembly into pKOR1	CATATGATGAGTTCACAAAAAAAGAAAATTAGT
JL16	Amplifying 1kb downstream of *tcyA* for Gibson assembly into pKOR1	ATAAAAATTAGATACGATGTTGCATGGTTATC
JLD25	Amplifying 1kb upstream of *tcyA* for Gibson assembly into pKOR1	TTCTATTTGAAGAATATATCTCCTTATTCTTATTATTCTAATC
JLD26	Amplifying 1kb upstream of *tcyA* for Gibson assembly into pKOR1	CGGAACCGGTACCAATGGATAACTACAATTAAAGTACCTATTGATTTTATTTC
JLD32	To amplify the deleted *tcyA* region for PCR sequence confirmation	ATGACCATTGTCATGCCTTCATT
JLD33	To amplify the deleted *tcyA* region for PCR sequence confirmation	TCTTAGGTAATTACTCGGCGG
TB96	*saeS* amplification	GCTTTACAACATATACCATCACAACTG
TB97	*saeS* amplification	AGCCCTCATTAATGGGAGCTTC

FIGURES

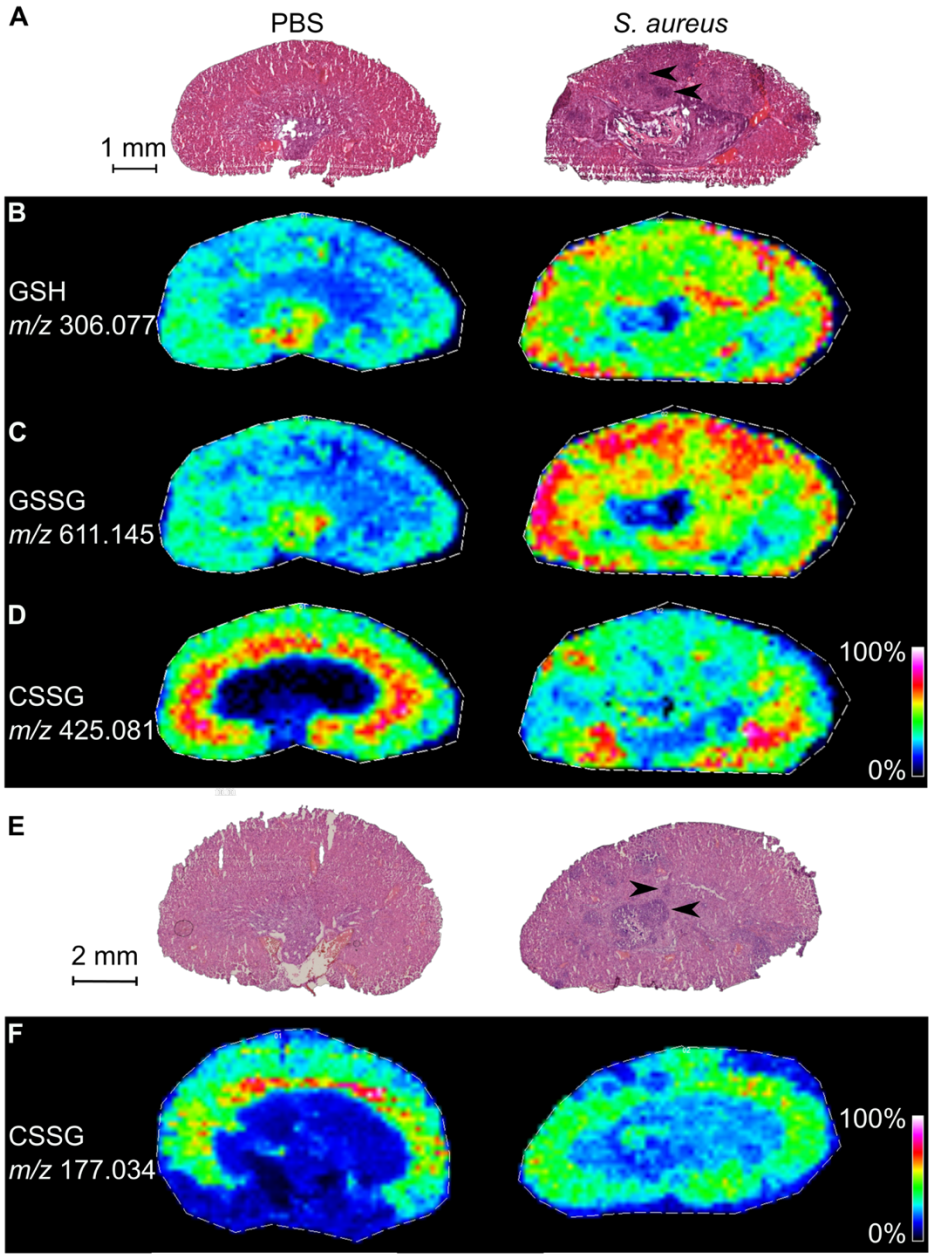

Figure 4.1. MALDI-IMS of the systemically infected kidney reveals a potential nutrient sulfur source for *Staphylococcus aureus*, cysteine-glutathione mixed disulfide (CSSG). A) Hematoxylin and eosin (H&E) stain of PBS (mock) inoculated kidney (left) and *S. aureus* WT-infected (right) murine kidney. Sections from these kidney samples were used for identification of metabolites that harbor glutathione (GSH). MALDI-IMS for GSH (B), oxidized glutathione (GSSG; C), and CSSG (D) are depicted. E) H&E stain of mock-infected (left) and WT-infected (right) kidney—sections from these kidneys were used to assess cysteinyl-glycine relative abundance and distribution (CysGly; F).

Figure 4.1 (cont'd)

For the H&E stains (A and E), representative *S. aureus* abscesses are denoted with black arrowheads. These images were produced in collaboration with the Prentice laboratory at the University of Florida.

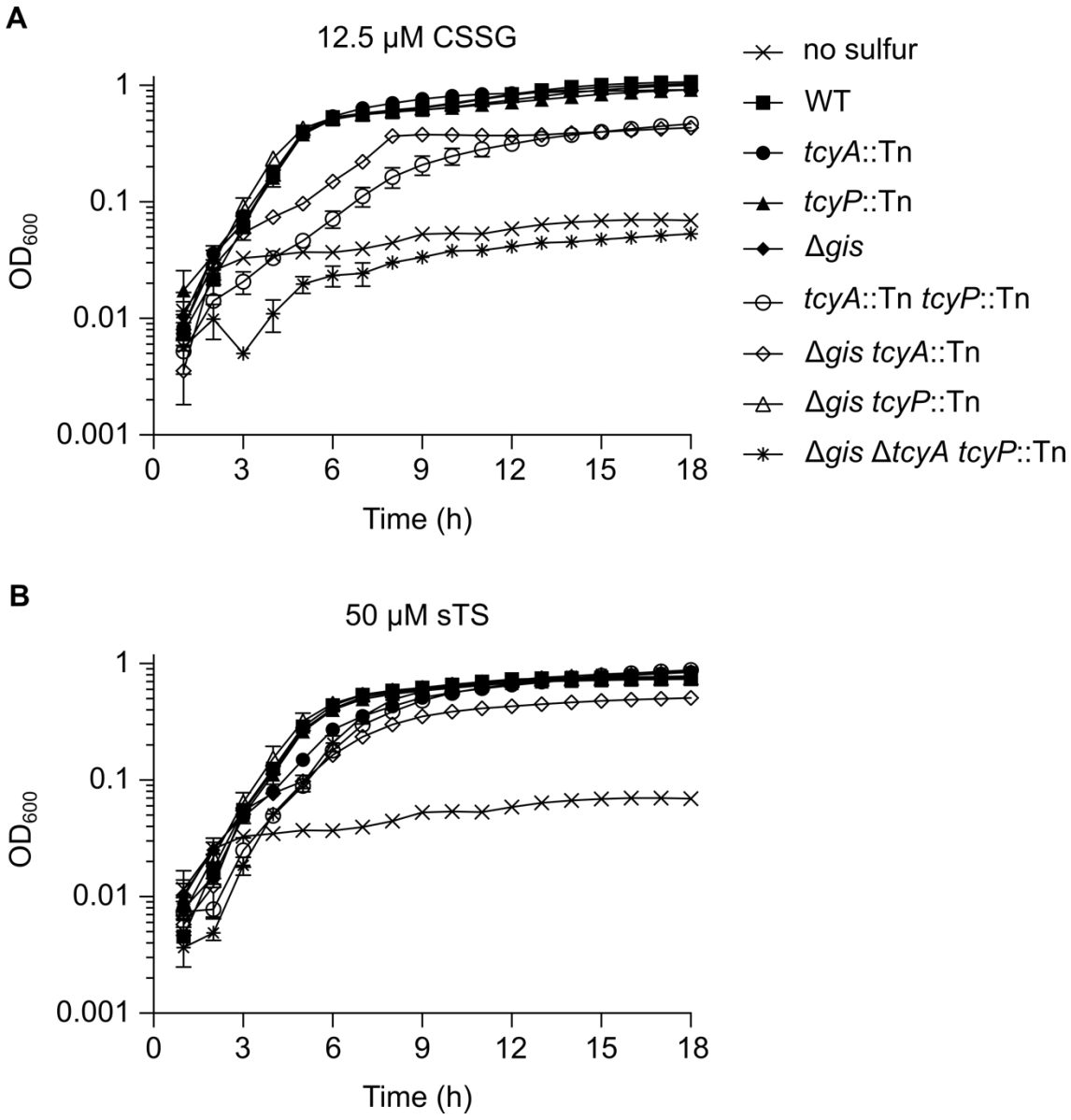

Figure 4.2. Cysteine-glutathione disulfide is a sulfur source for *Staphylococcus aureus*. Strains were cultured in chemically defined medium (CDM) supplemented with either 12.5 μM cysteine-glutathione disulfide (CSSG) (A) or 50 μM sodium thiosulfate (sTS) (B) as the sulfur source. WT *S. aureus* cultured in CDM lacking a viable sulfur source represents the no sulfur control. Each line represents the mean of three independent trials while the vertical bars depict ±1 standard error of the mean.

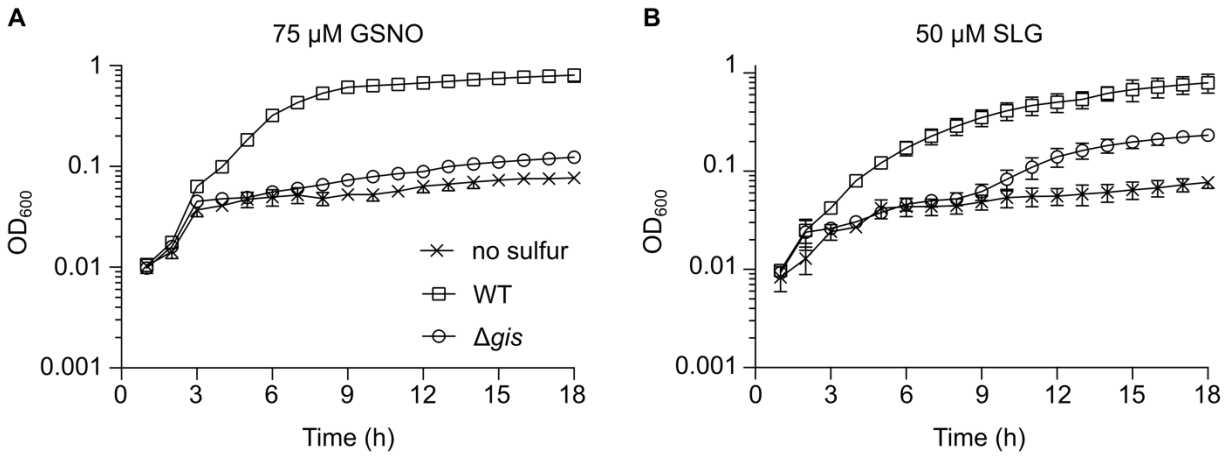

Figure 4.3. *Staphylococcus aureus* can meet the nutritional sulfur requirement using *S*-nitrosoglutathione and *S*-lactoylglutathione as sources of nutritional sulfur. *S. aureus* WT and the Δ*gisABCD-ggt* mutant (denoted Δ*gis*) were propagated in CDM harboring 75 μM *S*-nitrosoglutathione (GSNO) (A) or 50 μM *S*-lactoylglutathione (SLG) (B). Each line depicts the mean of three biological replicates ±1 standard error of the mean. SLG data courtesy of Joelis Lama Díaz.

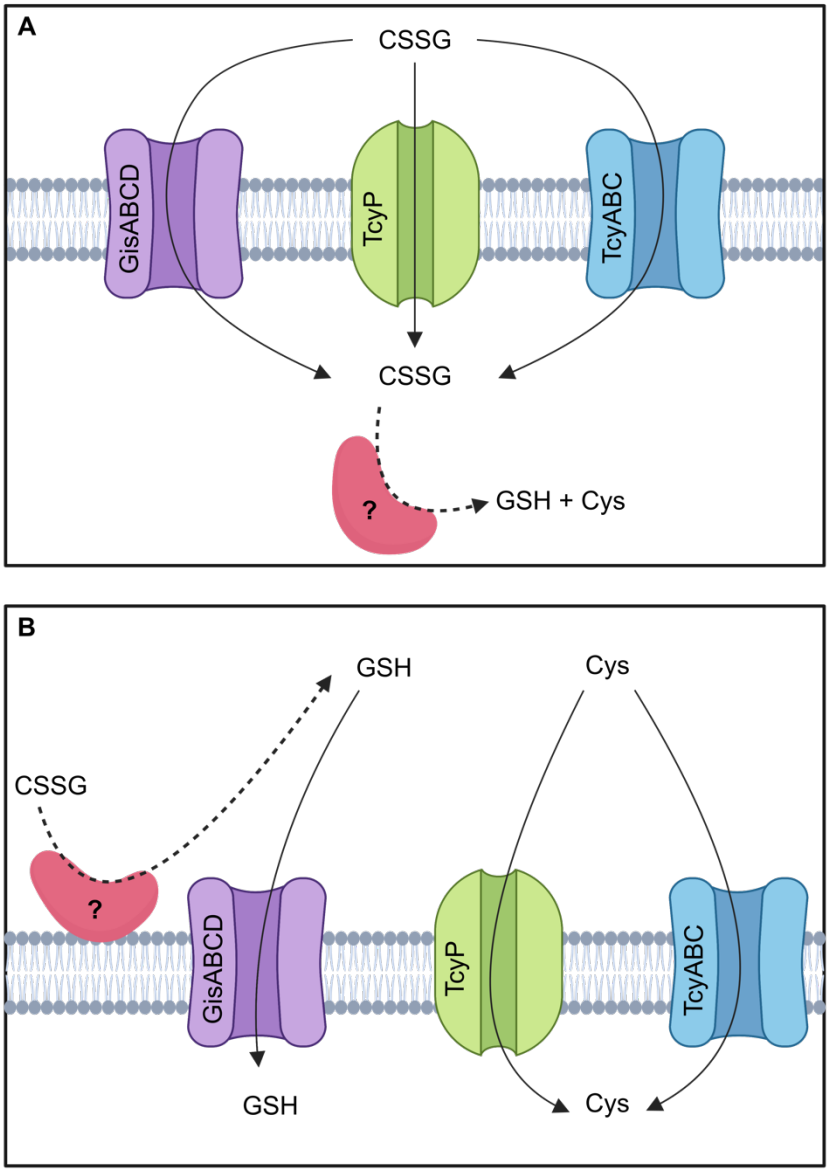

Figure 4.4. Potential mechanisms of cysteine-glutathione disulfide transportation. GisABCD is a reduced and oxidized glutathione (GSH/GSSG) importer (89) while TcyP and TcyABC have been associated with cysteine and cystine transportation (Cys/CSSC) (90). This study now implicates all three transporters with *S. aureus* growth on cysteine-glutathione disulfide (CSSG). However, it is unknown whether CSSG is imported as a disulfide and reduced in the cytoplasm (A) or if an extracytoplasmic enzyme acts on CSSG, allowing reduced GSH and free Cys to be imported through their respective transporters (B). Image created with BioRender.com.

CHAPTER 5: Summary and Future Directions

SUMMARY

In Chapter 1, we discuss the host sulfur pool, its influence on host well-being through sulfur metabolism, and the mechanisms employed by pathogens to acquire sulfur-containing metabolites. Cysteine (Cys) plays a pivotal role in the distribution of sulfur within cells, serving as the building block for numerous organic and inorganic compounds. These compounds collectively form the mammalian sulfur reservoir (134). The machinery responsible for synthesizing and breaking down these metabolites is present across various tissue types, each subject to intricate regulatory processes that govern metabolite levels and distribution (134). Consequently, one can view each tissue type as its own distinct sulfur pool. An illustrative example of this phenomenon is the γ-glutamyl cycle, characterized by its layered regulation that promotes the heightened expression of glutathione (GSH) synthesis enzymes in the liver, while GSH catabolism enzymes are less prevalent in this specific environment (134). Notably, imbalances in the γ-glutamyl cycle can lead to various health issues, such as an increased risk of cardiovascular diseases (related to γ-glutamyl transpeptidase and glutamate-cysteine ligase) or the development of hemolytic anemia (linked to GSH synthase) (134). Furthermore, pathogens like *S. aureus* have evolved mechanisms to import GSH into their cytoplasm (14, 89, 134, 232, 233). In fact, *S. aureus* possesses a characterized glutathione import system, GisABCD, as well as a γ-glutamyl transpeptidase (Ggt) system that transports GSH and initiates its breakdown for use as a sulfur source (89). Given the potential for altering sulfur metabolism to result in adverse outcomes within a normally healthy host, it becomes imperative to gain a comprehensive understanding of when, where, and how *S. aureus* impacts the host sulfur pool during infection.

As *S. aureus* encounters diverse sulfur environments during infection, Chapter 2 delves into how *S. aureus* physiology is altered when exposed to varying states of sulfur supplementation. Using RNAseq, we characterize the *S. aureus* transcriptional profile during sulfur starvation, a process predominantly governed by CymR-dependent genes, although a CymR-independent response is also observed. Strikingly, iron metabolism and oxidative stress genes were differentially expressed during sulfur starvation, prompting an investigation into the relationship between sulfur and these two pathways. In doing so, an additional role for GSH in *S. aureus* was discovered, where the free thiol of GSH provides protection against inhibitory concentrations of heme and hydrogen peroxide (H_2O_2) stress. Furthermore, we explore the *S. aureus* transcriptional response when comparing growth on various sulfur sources—such as organic Cys, GSH, oxidized GSH (GSSG), or inorganic thiosulfate (TS)—to cystine (CSSC). We demonstrate that two genes upregulated in the presence of TS, *tsuA* and *tsuB*, play a role in the ability of *S. aureus* to utilize TS as a source of nutritional sulfur, confirming that sulfur associated genes with altered expression under these conditions are indeed involved in sulfur metabolism.

Chapter 3 explores the machinery responsible for ensuring sulfur acquisition in *S. aureus*, building upon our improved understanding of how *S. aureus* responds to extracellular sulfur. DtpT is a di- and tripeptide transporter that is controlled by the stationary phase regulatory protein CodY (91). A direct mutagenesis approach unveiled the significance of the DtpT in utilizing not only physiologically relevant concentrations of GSH but also a newly identified sulfur source, cysteinyl-glycine (CysGly). Moreover, our studies demonstrate that this transporter plays a role in maximizing the fitness of *S.*

aureus within the systemically infected murine liver. These findings position DtpT as an ideal model protein for investigating how sulfur transporters can be hijacked to inhibit staphylococcal proliferation. To this end, we observed that the toxic peptide antibiotic, bialaphos, is delivered into *S. aureus* through DtpT, a mechanism also noted in another clinically relevant species, *Staphylococcus epidermidis*. Further investigations revealed the contributions of the *S. epidermidis* DtpT homolog to the proliferation of this organism when utilizing GSH and CysGly as nutrient sulfur sources, providing additional evidence that these two metabolites are substrates of DtpT. We also investigated conservation of DtpT and found broad conservation among Gram-positive bacteria, including cysteinyl-glycine 3-methyl-3-sulfanylhexanol (S-CysGly-3M3SH) transporters like PepT found in *Staphylococcus hominis* (103). These findings highlight the complexity surrounding *S. aureus* sulfur metabolism wherein broadly conserved, promiscuous proteins can reinforce the nutritional status of a cell.

Having investigated the properties surrounding acquisition of GSH and its derivative CysGly, Chapter 4 extends this narrative by delving into the host sulfur status during infection. MALDI-IMS emerged as an invaluable tool, shedding light on the presence of GSH, GSSG, and CysGly in both healthy and *S. aureus*-infected murine kidneys. Additionally, this technique unveils the substantial existence of a previously unrecognized sulfur source, cysteine-glutathione disulfide (CSSG), in the kidney. The growth of *S. aureus* on CSSG *in vitro* is intricately tied to the presence of GisABCD-Ggt, TcyABC, and TcyP. Lastly, this chapter drives home the importance of *S. aureus* GSH acquisition through the GisABCD system by identifying two other GSH derivatives that

support the *S. aureus* nutritional sulfur requirement: *S*-nitrosoglutathione (GSNO) and *S*-lactoylglutathione (SLG).

FUTURE DIRECTIONS

Chapters 2, 3, and 4 collectively represent significant progress in our understanding of *S. aureus* sulfur metabolism. These chapters also underscore the need for future experiments to comprehensively evaluate the impact of *S. aureus* redundancy during infection. Although the complete set of sulfur sources for *S. aureus* remains to be fully determined, we have gained substantial insights into the core sulfur transportation systems. This knowledge sets the stage for a more detailed examination of their roles during host colonization. Indeed, previous studies on TcyABC, TcyP, and GisABCD-Ggt (89, 90) have highlighted the challenges in elucidating the contributions of sulfur associated transporters to *S. aureus* colonization during systemic infection studies. In cases like TcyABC and TcyP, it required competition experiments against the wild type (WT) strain to reveal significant impairments, while the Δ*gisABCD-ggt* mutant exhibited no difference in bacterial burden compared to WT during mono-infection. Furthermore, even though DtpT impacts the ability of methicillin resistant *S. aureus* to achieve maximum proliferation within the liver during mono-infection, whether this is attributed to decreased import of GSH and/or CysGly rather than other di- and tripeptides remains to be determined.

From these infection studies one might question the actual impact sulfur transporters have on *S. aureus* proliferation *in vivo*. However, it is essential to bear in mind that the host sulfur pool is highly diverse, as discussed in Chapter 1. Additionally, *S. aureus* employs multiple transporters to acquire various metabolites, as highlighted in

previous studies (89, 90) along with Chapters 3 and 4. In some instances, this pathogen even possesses redundant systems dedicated to obtaining just one of these sulfur sources. This evolutionary strategy essentially safeguards *S. aureus* by compensating for the loss of one transporter or sulfur source with the ability to access a range of other sulfur-containing compounds. Consequently, when bacterial burdens are evaluated (i.e., at 96 hours post-infection), any defects observed in a sulfur transportation mutant might be concealed by the activity of alternative acquisition routes. Therefore, it would be valuable to conduct studies where systemic infections are terminated at earlier time points, such as 24 hpi or 48 hpi, to assess whether sulfur transporters like TycABC, TcyP, or GisABCD impact the initial colonization of the host.

Another avenue for investigation is to understand the collective impact of sulfur transporters during *S. aureus* systemic infection. Building on the findings from published work and Chapter 3, it would be intriguing to create a quadruple transport mutant (i.e., Δ*gisABCD-ggt* Δ*dtpT* Δ*tcyA* Δ*tcyP*) and evaluate the colonization abilities of this strain during a mono-systemic infection. We know from previous research that a *tcyP*::Tn mutant shows a competitive disadvantage compared to wild type (WT) JE2 in heart colonization (90). Therefore, any increased severity in the heart defect using the Δ*gisABCD-ggt* Δ*dtpT* Δ*tcyA* Δ*tcyP* would strongly implicate the importance of the TcyABC, GisABCD-Ggt, and DtpT systems for effective propagation in this organ. Increased severity in this context would likely manifest as a colonization defect during mono-infection. Similar outcomes would be anticipated in the liver, as the deletion of *dtpT* alone has been shown to impair growth in this environment. However, although a *dtpT* mutant results in significantly decreased colonization, the distribution of bacterial burdens

within individual mice is variable. For the anticipated decreased colonization in the Δ*gisABCD-ggt* Δ*dtpT* Δ*tcyA* Δ*tcyP* mutant, a narrower range of bacterial burdens is expected. This would suggest a more pronounced colonization defect due to the contributions of GisABCD-Ggt, TcyABC, and TcyP. Furthermore, we predict significantly reduced bacterial burdens in the kidneys. This expectation arises from the loss of all known transporters contributing to the acquisition of GSH, GSSG, CSSG, and CysGly, all of which are abundant during *S. aureus* infection in this organ.

Conversely, if we observe WT-like colonization of the kidneys with the quadruple transport mutant during both mono-infection and competition against WT, it may suggest the utilization of inorganic sulfur within this environment. Indeed, thiosulfate production in the kidney can result from the actions of Cysteinesulfinate Decarboxylase (Figure 1.1 and Table 1.1). Thus, it would be of interest to investigate the impact of deleting both inorganic sulfur transporters—the known thiosulfate transporter, *tsuA*, and the predicted sulfonate importer *ssuABC*—in the Δ*gisABCD-ggt* Δ*dtpT* Δ*tcyA* Δ*tcyP* background. This particular strain is likely to exhibit unique growth profiles *in vitro* due to the loss of so many sulfur importers. However, it is worth noting that growth can still be supported by the unknown di- and tripeptide transporter identified in Chapter 3. Therefore, supplementing the culture medium with higher concentrations (e.g., >100 μM) of ECG, GSH, or CysGly as the nutritional sulfur source should stimulate the proliferation of the Δ*gisABCD-ggt* Δ*dtpT* Δ*tcyA* Δ*tcyP* Δ*tsuA* Δ*ssuABC* strain *in vitro*. During systemic infection, we speculate that this sextuple transport mutant may result in bacterial burdens that are close to, if not below, the limit of detection in the heart and liver. At the very least, we expect significantly reduced colonization in the kidneys. These experiments would help confirm the key

players in *S. aureus* sulfur acquisition during systemic infection and contribute to identifying a hierarchy of contributors. In essence, by characterizing the colonization profiles of strains deficient in one to six transporters, we aim to elucidate which systems have a more substantial impact on *S. aureus* propagation in a host environment.

As described in Chapters 3 and 4, the redundancy of *S. aureus* sulfur transporters serves as an evolutionary strategy to ensure the acquisition of various related metabolites derived from the host. With such a nuanced system, it is vital to describe the nutritional sulfur interface from the host perspective as well. How does the host response to infection impact the sulfur composition at the infection site? Do tissues infected with a sulfur transportation mutant (e.g., a Δ*gisABCD-ggt* Δ*dtpT* Δ*tcyA* Δ*tcyP* strain) exhibit differences in sulfur distribution, abundance, or composition compared to tissues infected with WT *S. aureus*? These questions can be addressed through the continued use of MALDI-IMS, especially once we establish a baseline for how WT *S. aureus* influences the host sulfur pool during systemic infection. Indeed, examining the infection site from this perspective will undoubtedly yield a more comprehensive understanding of our systemic infection data. For instance, in Chapter 4, we illustrate the presence of at least four known sulfur sources (i.e., GSH, GSSG, CysGly, and CSSG) in the *S. aureus*-infected kidney, and we identify four transporters associated with the import of these metabolites (i.e., GisABCD-Ggt, DtpT, TcyABC, and TcyP). These insights help explain why kidney defects have never been observed in strains with single or double mutations in sulfur transporters of interest due to the presence of multiple viable sulfur sources and transporters to access them. Using the host perspective, MALDI-IMS has provided a rational basis for utilizing strains deficient in quadruple or even sextuple transporters during systemic infection.

To further expand our understanding of how the host responds to *S. aureus* infection from an elemental sulfur standpoint, MALDI-IMS can also be employed to look at the distribution of host sulfur metabolism proteins throughout infection as well. This line of investigation would be advantageous considering that there are several proteins such as GGT, CSB or CSE that inflict host disease when not abundance in regular concentrations (please see Chapter 1 for more information). Thus, a full picture of *S. aureus* infection would include an understanding of how acquisition of sulfur sources impacts the abundance and function of host enzymes whose downstream repercussions contribute to the clinical manifestations of *S. aureus* infection.

Chapter 2 also highlights the ability of *S. aureus* to utilize the tripeptide GSH, not for meeting its nutritional sulfur requirement, but as a resource to counter heme- and H_2O_2-induced oxidative stress. It is somewhat unsurprising that a metabolite with diverse functions within the host (as discussed in Chapter 1) also serves multiple roles within *S. aureus*. Consequently, future investigations into GSH in this organism are likely to unveil additional, unrecognized contributions. Akin to sulfur, the preference of compounds contributing to the nutritional nitrogen requirement in *S. aureus* remains underexplored compared to other bacteria such as *E. coli* or *Bacillus subtilis* (234, 235). In terms of nitrogen flux within a cell, imported nitrogen sources are assimilated to glutamate (Glu) and glutamine (Gln) which serve as the internal nitrogen donors for various biological processes (235). For *E. coli*, ammonium is the preferred nitrogen source although several other compounds such as Glu, Gln, and Glu precursors (e.g., proline, arginine, or glycine) can also drive proliferation when provided as nutritional nitrogen (235). Though ammonium also supports the *B. subtilis* nitrogen requirements, Gln is considered the preferred

nitrogen source. (234).

The nitrogen sources for *S. aureus* have been studied to some extent. For instance, researchers have investigated the ability of *S. aureus* to utilize ammonium (NH4), glutamine (Gln), or glutamate (Glu) as nutritional nitrogen sources (236). In this study, CDM devoid of Gln, Glu, and NH4 (denoted $CDM_{-Glu/Gln,-NH4}$) was used. The supplementation of $CDM_{-Glu/Gln,-NH4}$ with NH4 or Gln stimulated the growth of *S. aureus* strain LAC, while Glu did not have the same effect. As a result, the study concluded that NH4 and Gln are preferred nitrogen sources over Glu in *S. aureus* (236). However, it's important to note that only one concentration was tested for each potential nitrogen source—a crucial consideration given that Glu is the sole precursor to Gln. In the tested conditions, Glu was required both as a nitrogen source and as a source of Gln. Therefore, it remains undetermined whether Glu truly cannot meet the nitrogen requirement or if it requires higher concentrations due to the experimental design. To explore this, the experimental setup used one used by Zeden *et al*. (236) can be employed to assess the growth of *S. aureus* on $CDM_{-Glu/Gln,-NH4}$ with increasing Glu concentrations. It is predicted that higher concentrations of this amino acid will fulfill the nitrogen requirement in this organism. Once an environment is established where Glu is vital for robust growth, the $CDM_{-Glu/Gln,-NH4}$ can be supplemented with GSH to assess whether this tripeptide can act as a source of Glu. This is of particular interest given previous research indicating that tripeptides can serve as a source of Glu in *S. aureus* (192). It is predicted that *S. aureus* will proliferate in this medium when sufficient GSH is provided. This, in conjunction with the oxidative stress assays in Chapter 2, would underscore the necessity for researchers in this field to consider how *S. aureus* sulfur sources contribute to bacterial physiology

beyond meeting the nutritional sulfur requirement.

CONCLUDING REMARKS

My thesis has played a significant role in establishing the groundwork for understanding how *S. aureus* acquires sulfur sources from the host, offering both regulatory and mechanistic insights. Additionally, the application of MALDI-IMS has provided initial glimpses into the organization of host sulfur metabolism during *S. aureus* infection. It is my hope that this body of work serves as an inspiration for future experiments, guiding the next generation of researchers to delve deeper into characterizing the host-pathogen nutritional sulfur interface.

REFERENCES

1. Hood MI, Skaar EP. 2012. Nutritional immunity: Transition metals at the pathogen-host interface. Nat Rev Microbiol 10:525–537.

2. Tanaka KJ, Song S, Mason K, Pinkett HW. 2018. Selective substrate uptake: The role of ATP-binding cassette (ABC) importers in pathogenesis. Biochim Biophys Acta Biomembr 1860:868–877.

3. Vitko NP, Grosser MR, Khatri D, Lance TR, Richardson AR. 2016. Expanded glucose import capability affords *Staphylococcus aureus* optimized glycolytic flux during infection. mBio 7:1–11.

4. Poole LB. 2015. The basics of thiols and cysteines in redox biology and chemistry. Free Radic Biol Med 80:148–157.

5. Collet J-F, Bardwll JCA. 2002. Oxidative protein folding in bacteria. Mol Microbiol 44:1–8.

6. Mashruwala AA, Pang YY, Rosario-Cruz Z, Chahal HK, Benson MA, Mike LA, Skaar EP, Torres VJ, Nauseef WM, Boyd JM. 2015. Nfu facilitates the maturation of iron-sulfur proteins and participates in virulence in *Staphylococcus aureus*. Mol Microbiol 95:383–409.

7. Pietrocola F, Galluzzi L, Bravo-San Pedro JM, Madeo F, Kroemer G. 2015. Acetyl coenzyme A: A central metabolite and second messenger. Cell Metab 21:805–821.

8. Johnson DC, Dean DR, Smith AD, Johnson MK. 2005. Structure, function, and formation of biological iron-sulfur clusters. Annu Rev Biochem 74:247–281.

9. Begley TP, Xi J, Kinsland C, Taylor S, McLafferty F. 1999. The enzymology of sulfur activation during thiamin and biotin biosynthesis. Curr Opin Chem Biol 3:623–629.

10. Bindu Paul CD, Solomon Snyder TH, Sbodio JI, Snyder SH, Paul BD. 2018. Regulators of the transsulfuration pathway. Br J Pharmacol 176:583–593.

11. Stipanuk MH. 2020. Metabolism of sulfur-containing amino acids: How the Body copes with excess methionine, cysteine, and sulfide. J Nutr 150:2494S-2505S.

12. Lu SC. 2009. Regulation of glutathione synthesis. Mol Aspects Med 30:42–59.

13. Kloor D, Hermes M, Fink K, Schmid H, Klingel K, Mack A, Grenz A, Osswald H. 2007. Expression and localization of *S*-Adneosylhomocysteine-hydrolase in the rat

kidney following carbon monoxide induced hypoxia. Cellular Physiology and Biochemistry 19:57–66.

14. Lensmire JM, Hammer ND. 2019. Nutrient sulfur acquisition strategies employed by bacterial pathogens. Curr Opin Microbiol 47:52–58.

15. Zuhra K, Augsburger F, Majtan T, Szabo C. 2020. Cystathionine-β-synthase: Molecular regulation and pharmacological inhibition. Biomolecules 10:1–82.

16. Kamoun P. 2004. Endogenous production of hydrogen sulfide in mammals. Amino Acids 26:243–254.

17. Zhao K, Li H, Li S, Yang G. 2014. Regulation of cystathionine gamma-lyase/H_2S system and its pathological implication. Frontiers in Bioscience 19:1355–1369.

18. Stipanuk MH, Ueki I. 2011. Dealing with methionine/homocysteine sulfur: Cysteine metabolism to taurine and inorganic sulfur. J Inherit Metab Dis 34:17–32.

19. Fu M, Zhang W, Wu L, Yang G, Li H, Wang R. 2012. Hydrogen sulfide (H_2S) metabolism in mitochondria and its regulatory role in energy production. Proc Natl Acad Sci U S A 109:2943–2948.

20. Pajares MA, Markham GD. 2011. Methionine adenosyltransferase (*S*-adenosylmethionine synthetase), p. 449. In Advances in enzymology and related areas of molecular biology.

21. Wishart DS, Feunang YD, Marcu A, Guo AC, Liang K, Vázquez-Fresno R, Sajed T, Johnson D, Li C, Karu N, Sayeeda Z, Lo E, Assempour N, Berjanskii M, Singhal S, Arndt D, Liang Y, Badran H, Grant J, Serra-Cayuela A, Liu Y, Mandal R, Neveu V, Pon A, Knox C, Wilson M, Manach C, Scalbert A. 2018. HMDB 4.0: The human metabolome database for 2018. Nucleic Acids Res 46:D608–D617.

22. Meister Alton, Anderson Mary E. 1983. Glutathione. Ann Rev Biochem 52:711–760.

23. Kumar A, Tikoo S, Maity S, Sengupta S, Sengupta S, Kaur A, Bachhawat AK. 2012. Mammalian proapoptotic factor ChaC1 and its homologues function as γ-glutamyl cyclotransferases acting specifically on glutathione. EMBO Rep 13:1095–1101.

24. Ookhtens M, Kaplowitz N. 1998. Role of the Liver in interorgan homeostasis of glutathione and cyst(e)ine. Semin Liver Dis 18:313–329.

25. Turner AJ. 2013. Aminopeptidase N, p. 397–403. In Handbook of proteolytic enzymes, 3rd ed.

26. Chen R, Jiang X, Sun D, Han G, Wang F, Ye M, Wang L, Zou H. 2009. Glycoproteomics analysis of human liver tissue by combination of multiple enzyme digestion and hydrazide chemistry. J Proteome Res 8:651–661.

27. West MB, Segu ZM, Feasley CL, Kang P, Klouckova I, Li C, Novotny M V., West CM, Mechref Y, Hanigan MH. 2010. Analysis of site-specific glycosylation of renal and hepatic γ-glutamyl transpeptidase from normal human tissue. Journal of Biological Chemistry 285:29511–29524.

28. Mansoor MA, Svardal AM, Ueland PM. 1991. Determination of the in *in vivo* redox status of cysteine, cysteinylglycine, homocysteine, and glutathione in human plasma. Anal Biochem 200:218–229.

29. Enoiu M, Aberkane H, Salazar J-F, Leroy P, Groffen J, Siest G, Wellman M. 2000. Evidence for the pro-oxidant effect of y-glutamyltranspeptidase-related enzyme. Free Radic Biol Med 29:825–833.

30. Bates CJ, Mansoor MA, Gregory J, Pentieva K, Prentice A. 2002. Correlates of plasma homocysteine, cysteine and cysteinyl-glycine in respondents in the British National Diet and Nutrition Survey of Young People Aged 4–18 Years, and a comparison with the Survey of People Aged 65 Years and Over. British Journal of Nutrition 87:71–79.

31. Chikhi NN, Holic N, Guellaen G, Laperche Y. 1999. Gamma-glutamyl transpeptidase gene organization and expression: a comparative analysis in rat, mouse, pig and human species. Comparative Biochemistry and Physiology Part B 122:367–380.

32. Visvikis A, Pawlak AÂ, Accaoui MJÂ, Ichino K, Leh HÂ, Guellaen G, Wellman M. 2001. Structure of the 5' sequences of the human γ-glutamyltransferase gene. Eur J Biochem 268:317–325.

33. Whitfield JB. 2001. Gamma glutamyl transferase. Crit Rev Clin Lab Sci 38:263–355.

34. Hanigan MH, Frierson HFJ. 1996. Immunohistochemical detection of γ-glutamyl transpeptidase in normal human tissue. The Journal of Histochemistry and Cytochemistry 44:1101–1108.

35. Lee DH, Silventoinen K, Hu G, Jacobs DR, Jousilahti P, Sundvall J, Tuomilehto J. 2006. Serum gamma-glutamyltransferase predicts non-fatal myocardial infarction and fatal coronary heart disease among 28,838 middle-aged men and women. Eur Heart J 27:2170–2176.

36. Strasak AM, Kelleher CC, Klenk J, Brant LJ, Ruttmann E, Rapp K, Concin H, Diem G, Pfeiffer KP, Ulmer H. 2008. Longitudinal change in serum gamma-glutamyltransferase and cardiovascular disease mortality: A prospective population-based study in 76,113 Austrian adults. Arterioscler Thromb Vasc Biol 28:1857–1865.

37. Lee DH, Buijsse B, Steffen L, Holtzman J, Luepker R, Jacobs DR. 2009. Association between serum gamma-glutamyltransferase and cardiovascular mortality varies by age: The Minnesota Heart Survey. Eur J Prev Cardiol 16:16–20.

38. Fraser A, Harris R, Sattar N, Ebrahim S, Smith GD, Lawlor DA. 2007. Gamma-glutamyltransferase is associated with incident vascular events independently of alcohol intake: Analysis of the British Women's Heart and Health study and meta-analysis. Arterioscler Thromb Vasc Biol 27:2729–2735.

39. Ghouri N, Preiss D, Sattar N. 2010. Liver enzymes, nonalcoholic fatty liver disease, and incident cardiovascular disease: A narrative review and clinical perspective of prospective data. Hepatology 52:1156–1161.

40. Whitfield JB, Pounder RE, Neale G, Moss DW. 1972. Serum γ-glytamyl transpeptidase activity in liver disease. Gut 13:702–708.

41. Tahan V, Canbakan B, Balci H, Dane F, Akin H, Can G, Hatemi I, Olgac V, Sonsuz A, Ozbay G, Yurdakul I, Senturk H. 2008. Serum gamma-glutamyltranspeptidase distinguishes non-alcoholic fatty liver disease at high risk. Hepatogastroenterology 55:1433—1438.

42. Lu SC. 2013. Glutathione synthesis. Biochim Biophys Acta Gen Subj 1830:3143–3153.

43. Longo A, Toro M Di, Galimberti C, Carenzi A. 1991. Determination of N-acetylcysteine in human plasma by gas chromatography-mass spectrometry. J Chromatogr 562:639–645.

44. Yang Y, Dieter MZ, Chen Y, Shertzer HG, Nebert DW, Dalton TP. 2002. Initial characterization of the glutamate-cysteine ligase modifier subunit *Gclm*(-/-) knockout mouse: Novel model system for a severely compromised oxidative stress response. Journal of Biological Chemistry 277:49446–49452.

45. Chen Y, Shertzer HG, Schneider SN, Nebert DW, Dalton TP. 2005. Glutamate cysteine ligase catalysis: Dependence on ATP and modifier subunit for regulation of tissue glutathione levels. Journal of Biological Chemistry 280:33766–33774.

46. Chao Yan C, Huxtable RJ. 1996. Effects of monocrotaline, a pyrrolizidine alkaloid, on glutathione metabolism in the rat. Biochem Pharmacol 51:375–379.

47. Cohen G, Hochstein P. 1963. Glutathione peroxidase: The primary agent for the elimination of hydrogen peroxide in erythrocytes*. Biochemistry 2:1420–1427.

48. Kaplowitz N, Aw Y, Ookhtens M. 1985. The regulation of hepatic glutathione. Ann Rev Pharmacol Toxicol 25:715–759.

49. Cooper AJL, Pinto JT, Callery PS. 2011. Reversible and irreversible protein glutathionylation: Biological and clinical aspects. Expert Opin Drug Metab Toxicol 7:891–910.

50. Ripps H, Shen W. 2012. Review: Taurine: A “very essential” amino acid. Mol Vis 18:2673–2686.

51. Guenter Schwarz C, Kohl JB, Mellis A-T, Schwarz G. 2019. Homeostatic impact of sulfite and hydrogen sulfide on cysteine catabolism. Br J Pharmacol 176:554.

52. Dominy JE, Hirschberger LL, Coloso RM, Stipanuk MH. 2006. Regulation of cysteine dioxygenase degradation is mediated by intracellular cysteine levels and the ubiquitin-26 S proteasome system in the living rat. Biochemical Journal 394:267–273.

53. Cechetto JD, Sadacharan SK, Berk PD, Gupta RS. 2002. Immunogold localization of mitochondrial aspartate aminotransferase in mitochondria and on the cell surface in normal rat tissues. Histol Histopathol 17:353–364.

54. Miyamoto R, Otsuguro KI, Yamaguchi S, Ito S. 2014. Contribution of cysteine aminotransferase and mercaptopyruvate sulfurtransferase to hydrogen sulfide production in peripheral neurons. J Neurochem 130:29–40.

55. Markovich D. 2001. Physiological roles and regulation of mammalian sulfate transporters. Physiological Reviews 81:1499–1533.

56. Stipanuk MH, Ueki I, Dominy JE, Simmons CR, Hirschberger LL. 2009. Cysteine dioxygenase: A robust system for regulation of cellular cysteine levels. Amino Acids 37:55–63.

57. Ueki I, Roman HB, Valli A, Fieselmann K, Lam J, Peters R, Hirschberger LL, Stipanuk MH. 2011. Knockout of the murine cysteine dioxygenase gene results in severe impairment in ability to synthesize taurine and an increased catabolism of cysteine to hydrogen sulfide. Am J Physiol Endocrinol Metab 301:668–684.

58. Shibuya N, Tanaka M, Yoshida M, Ogasawara Y, Togawa T, Ishii K, Kimura H. 2009. 3-Mercaptopyruvate sulfurtransferase produces hydrogen sulfide and bound sulfane sulfur in the brain. Antioxid Redox Signal 11:703–714.

59. Yadav PK, Yamada K, Chiku T, Koutmos M, Banerjee R. 2013. Structure and kinetic analysis of H_2S production by human mercaptopyruvate sulfurtransferase. Journal of Biological Chemistry 288:20002–20013.

60. Shibuya N, Koike S, Tanaka M, Ishigami-Yuasa M, Kimura Y, Ogasawara Y, Fukui K, Nagahara N, Kimura H. 2013. A novel pathway for the production of hydrogen sulfide from D-cysteine in mammalian cells. Nat Commun 4:1–7.

61. Cadenas E, Davies KJA, Powis G, Mustacich D, Coon A. 2000. The role of the redox protein thioredoxin in cell growth and cancer. Free Radic Biol Med 29:312–322.

62. Stipanuk MH, Witte Beck P. 1982. Characterization of the enzymic capacity for cysteine desulphhydration in liver and kidney of the rat. Biochem J 206:267–277.

63. Abe K, Kimura H. 1996. The possible role of hydrogen sulfide as an endogenous neuromodulator. The Journal of Neuroscience 76:1066–1071.

64. Zhao W, Wang R, Wang R. 2002. H_2S-induced vasorelaxation and underlying cellular and molecular mechanisms. Am J Physiol Heart Circ Physiol 283:474–480.

65. Yang G, Wu L, Jiang B, Yang W, Qi J, Cao K, Meng Q, Mustafa AK, Mu W, Zhang S, Snyder SH, Wang R. 2008. H_2S as a physiologic vasorelaxant: Hypertension in mice with deletion of cystathionine γ-lyase. Science (1979) 322:587–590.

66. Papapetropoulos A, Pyriochoua A, Altaanyb Z, Yangb G, Maraziotia A, Zhouc Z, Jeschked MG, Branskid LK, Herndond DN, Wangb R, Szabo C. 2009. Hydrogen sulfide is an endogenous stimulator of angiogenesis. PNAS 106:21972–21977.

67. Olson KR, Dombkowski RA, Russell MJ, Doellman MM, Head SK, Whitfield NL, Madden JA. 2006. Hydrogen sulfide as an oxygen sensor/transducer in vertebrate hypoxic vasoconstriction and hypoxic vasodilation. Journal of Experimental Biology 209:4011–4023.

68. Zanardo RCO, Brancaleone V, Distrutti E, Fiorucci S, Cirino G, Wallace JL, Zanardo RCO, Brancaleone V, Distrutti E, Fiorucci S, Cirino G, Wallace JL. 2006. Hydrogen sulfide is an endogenous modulator of leukocyte-mediated inflammation. The FASEB Journal 20:2118–2120.

69. Kimura H. 2011. Hydrogen sulfide: Its production, release and functions. Amino Acids 41:113–121.

70. Kimura Y, Kimura H. 2004. Hydrogen sulfide protects neurons from oxidative stress. The FASEB Journal 18:1165–1167.

71. Nicholls P, Marshall DC, Cooper CE, Wilson MT. 2013. Sulfide inhibition of and metabolism by cytochrome *c* oxidase. Biochem Soc Trans 41:1312–1316.

72. Olson KR, Straub KD. 2016. The role of hydrogen sulfide in evolution and the evolution of hydrogen sulfide in metabolism and signaling. Physiology 31:60–72.

73. Shahak Y., Hauska G. 2008. Sulfide oxidation from cyanobacteria to humans: Sulfide–quinone oxidoreductase (SQR), p. 319–335. In Hell R., Dahl C., Knaff D., Leustek T. (eds.), Sulfur metabolism in phototrophic organisms. Springer, Dordrecht.

74. Klein JM, Schwarz G. 2012. Cofactor-dependent maturation of mammalian sulfite oxidase links two mitochondrial import pathways. J Cell Sci 125:4876–4855.

75. Marutani E, Ichinose F. 2020. Emerging pharmacological tools to control hydrogen sulfide signaling in critical illness. Intensive Care Med Exp 8:1–14.

76. Olson KR, DeLeon ER, Gao Y, Hurley K, Sadauskas V, Batz C, Stoy GF, Olson KR. 2013. Thiosulfate: a readily accessible source of hydrogen sulfide in oxygen sensing. Am J Physiol Regul Integr Comp Physiol 305:592–603.

77. Mikami Y, Shibuya N, Kimura Y, Nagahara N, Ogasawara Y, Kimura H. 2011. Thioredoxin and dihydrolipoic acid are required for 3-mercaptopyruvate sulfurtransferase to produce hydrogen sulfide. Biochemical Journal 439:479–485.

78. Westley J. 1981. Thiosulfate:Cyanide Sulfertransferase (Rhodanese). Methods Enzymol 77:285–291.

79. Zhang X, Xin Y, Chen Z, Xia Y, Xun L, Liu H, Zhang X, Xin Y, Chen Z, Xia Y, Xun L, Liu H. 2021. Sulfide-quinone oxidoreductase is required for cysteine synthesis and indispensable to mitochondrial health. Redox Biol 47:102169.

80. Ackermann M, Kubitza M, Hauska G, Piña AL. 2014. The vertebrate homologue of sulfide-quinone reductase in mammalian mitochondria. Cell Tissue Res 358:779–792.

81. Budde MW, Roth MB. 2011. The response of *Caenorhabditis elegans* to hydrogen

sulfide and hydrogen cyanide. Genetics 189:521–532.

82. Eto K, Asada T, Arima K, Makifuchi T, Kimura H. 2002. Brain hydrogen sulfide is severely decreased in Alzheimer's disease. Biochem Biophys Res Commun 293:1485–1488.

83. Palmfeldt J, Vang S, Stenbroen V, Pavlou E, Baycheva M, Buchal G, Monavari AA, Augoustides-Savvopoulou P, Mandel H, Gregersen N. 2011. Proteomics reveals that redox regulation is disrupted in patients with ethylmalonic encephalopathy. J Proteome Res 10:2389–2396.

84. Jin HS, Kim J, Park S, Park E, Kim BY, Choi VN, Yoo YH, Kim BT, Jeong SY. 2015. Association of the I264T variant in the sulfide quinone reductase-like (SQRDL) gene with osteoporosis in Korean postmenopausal women. PLoS One 10:1–17.

85. Cai X, Yi X, Zhang Y, Zhang D, Zhi L, Liu H. 2018. Genetic susceptibility of postmenopausal osteoporosis on sulfide quinone reductase-like gene. Osteoporosis International 29:2041–2047.

86. Lakhundi S, Zhang K. 2018. Methicillin-Resistant *Staphylococcus aureus*: Molecular Characterization, Evolution, and Epidemiology. Clin Microbiol Rev 31.

87. 2019. Antibiotic resistance threats in the United States, 2019. Atlanta, Georgia.

88. Lithgow JK, Hayhurst EJ, Cohen G, Aharonowitz Y, Foster SJ. 2004. Role of a Cysteine Synthase in *Staphylococcus aureus*. J Bacteriol 186:1579–1590.

89. Lensmire JM, Wischer MR, Kraemer-Zimpel C, Kies PJ, Sosinski L, Ensink E, Dodson JP, Shook JC, Delekta PC, Cooper CC, Havlichek DH, Mulks MH, Lunt SY, Ravi J, Hammer ND. 2023. The glutathione import system satisfies the *Staphylococcus aureus* nutrient sulfur requirement and promotes interspecies competition. PLoS Genet 19:e1010834.

90. Lensmire JM, Dodson JP, Hsueh BY, Wischer MR, Delekta PC, Shook JC, Ottosen EN, Kies PJ, Ravi J, Hammer ND. 2020. The *Staphylococcus aureus* cystine transporters TcyABC and TcyP facilitate nutrient sulfur acquisition during infection. Infect Immun 88:e00690-19.

91. Fuchs S, Mehlan H, Bernhardt J, Hennig A, Michalik S, Surmann K, Pané-Farré J, Giese A, Weiss S, Backert L, Herbig A, Nieselt K, Hecker M, Völker U, Mäder U. 2018. AureoWiki - The repository of the *Staphylococcus aureus* research and annotation community. International Journal of Medical Microbiology 308:558–568.

92. Saier MH. 2000. Families of transmembrane transporters selective for amino acids and their derivatives. Microbiology (N Y) 146:1775–1795.

93. Burguière P, Auger S, Hullo MF, Danchin A, Martin-Verstraete I. 2004. Three different systems participate in L-cystine uptake in *Bacillus subtilis*. J Bacteriol 186:4875–4884.

94. Sengupta S, Wehbe C, Majors AK, Ketterer ME, DiBello PM, Jacobsen DW. 2001. Relative roles of albumin and ceruloplasmin in the formation of homocystine, homocysteine-cysteine-mixed disulfide, and cystine in circulation. Journal of Biological Chemistry 276:46896–46904.

95. Turell L, Radi R, Alvarez B. 2013. The thiol pool in human plasma: The central contribution of albumin to redox processes. Free Radic Biol Med 65:244–253.

96. Refsum H, Ueland PM, Nygård O, Vollset SE. 1998. Homocysteine and cardiovascular disease. Annu Rev Medicine 49:31–62.

97. Kalra DK. 2004. Homocysteine and Cardiovascular Disease. Curr Atheroscler Rep 6:101–106.

98. Sen CK. 1997. Review Nutritional biochemistry of cellular glutathione. Nutritional Biochemistry 8:660–672.

99. Caitlin Pedati M, Jennifer House D, Jessica Hancock-Allen M, Leah Colton P, Katie Bryan M, Dustin Ortbahn, Lon Kightlinger P, Kiersten Kugeler P, Jeannine Petersen P, Paul Mead M, Tom Safranek MD, Bryan Buss DVM. 2015. Increase in human cases of tuleremia-Colorado, Nebraska, South Dakota, and Wyoming, January-September 2015. MMWR Morb and Mortal Wkly Rep 64:1317–1318.

100. Alkhuder K, Meibom KL, Dubail I, Dupuis M, Charbit A. 2009. Glutathione provides a source of cysteine essential for intracellular multiplication of *Francisella tularensis*. PLoS Pathog 5:1–11.

101. Ramsey KM, Ledvina HE, Tresko TM, Wandzilak JM, Tower CA, Tallo T, Schramm CE, Brook Peterson S, Skerrett SJ, Mougous JD, Dove SL. 2020. Tn-Seq reveals hidden complexity in the utilization of host-derived glutathione in *Francisella tularensis*. PLoS Pathog 16.

102. Szemraj M, Grazul M, Balcerczak E, Szewczyk EM. 2020. Staphylococcal species less frequently isolated from human clinical specimens - Are they a threat for hospital patients? BMC Infect Dis 20.

103. Minhas GS, Bawdon D, Herman R, Rudden M, Stone AP, Gordon James A, Thomas GH, Newstead S. 2018. Structural basis of malodour precursor transport in the human axilla. Elife 7:1–26.

104. Dickinson DA, Forman HJ. 2002. Glutathione in defense and signaling: lessons from a small thiol. Ann NY Acad Sci 973:488–504.

105. Wasilko NP, Larios-Valencia J, Steingard CH, Nunez BM, Verma SC, Miyashiro T. 2019. Sulfur availability for *Vibrio fischeri* growth during symbiosis establishment depends on biogeography within the squid light organ. Mol Microbiol 111:621–636.

106. Wasilko NP, Ceron JS, Baker ER, Cecere AG, Wollenberg MS, Miyashiro TI. 2021. *Vibrio fischeri* imports and assimilates sulfate during symbiosis with *Euprymna scolopes*. Mol Microbiol 116:926–942.

107. Pajor AM. 2006. Molecular properties of the SLC13 family of dicarboxylate and sulfate transporters. Pflugers Arch 451:597–605.

108. Park S, Imlay JA. 2003. High levels of intracellular cysteine promote oxidative DNA damage by driving the Fenton reaction. J Bacteriol 185:1942–1950.

109. Chonoles Imlay KR, Korshunov S, Imlay JA. 2015. Physiological roles and adverse effects of the two cystine importers of *Escherichia coli*. J Bacteriol 197:3629–3644.

110. Van Der Ploeg JR, Iwanicka-Nowicka R, Kertesz MA, Leisinger T, Hryniewicz MM. 1997. Involvement of CysB and Cbl regulatory proteins in expression of the *tauABCD* operon and other sulfate starvation-inducible genes in *Escherichia coli*. J Bacteriol 179:7671–7678.

111. Stec E, Witkowska-Zimny M, Hryniewicz MM, Neumann P, Wilkinson AJ, Brzozowski AM, Verma CS, Zaim J, Wysocki S, D. Bujacz G. 2006. Structural basis of the sulphate starvation response in *E. coli*: Crystal structure and mutational analysis of the cofactor-binding domain of the Cbl transcriptional regulator. J Mol Biol 364:309–322.

112. Epshtein V, Mironov AS, Nudler E. 2003. The riboswitch-mediated control of sulfur metabolism in bacteria. PNAS 29:5052–5056.

113. Jones-Mortimer MC, Wheldraket JF, Pasternak CA. 1968. The control of sulphate reduction in *Escherichia coli* by *O*-Acetyl-L-serine. Biochem J 107:51–53.

114. Kredich NM. 1971. Regulation of L-cysteine biosynthesis in *Salmonella typhimurium* I. Effects of growth on varying sulfur sources and *O*-Acetyl-L-Serine

on gene expression*. J Biol Chem 246:3474–3484.

115. Kredich NM, Tomkins GM. 1966. The enzymic synthesis of L-cysteine in *Escherichia coli* and *Salmonella typhimurium*. J Biol Chem 241:4955–4966.

116. Kredich NM, Becker MA, Tomkins GM. 1969. Purification and characterization of cysteine synthetase, a bifunctional protein complex, from *Salmonella typhimurium*. J Biol Chem 244:2428–2439.

117. Even S, Burguière P, Auger S, Soutourina O, Danchin A, Martin-Verstraete I. 2006. Global control of cysteine metabolism by CymR in *Bacillus subtilis*. J Bacteriol 188:2184–2197.

118. Soutourina O, Poupel O, Coppée JY, Danchin A, Msadek T, Martin-Verstraete I. 2009. CymR, the master regulator of cysteine metabolism in *Staphylococcus aureus*, controls host sulphur source utilization and plays a role in biofilm formation. Mol Microbiol 73:194–211.

119. Hullo MF, Auger S, Soutourina O, Barzu O, Yvon M, Danchin A, Martin-Verstraete I. 2007. Conversion of methionine to cysteine in *Bacillus subtilis* and its regulation. J Bacteriol 189:187–197.

120. Tanous C, Soutourina O, Raynal B, Hullo MF, Mervelet P, Gilles AM, Noirot P, Danchin A, England P, Martin-Verstraete I. 2008. The CymR regulator in complex with the enzyme CysK controls cysteine metabolism in *Bacillus subtilis*. Journal of Biological Chemistry 283:35551–35560.

121. Ji Q, Zhang L, Sun F, Deng X, Liang H, Bae T, He C. 2012. *Staphylococcus aureus* CymR is a new thiol-based oxidation-sensing regulator of stress resistance and oxidative response. Journal of Biological Chemistry 287:21102–21109.

122. Soutourina O, Dubrac S, Poupel O, Msadek T, Martin-Verstraete I. 2010. The pleiotropic CymR regulator of *Staphylococcus aureus* plays an important role in virulence and stress response. PLoS Pathog 6:1–13.

123. Gebhardt MJ, Czyz DM, Singh S, Zurawski D V, Becker L, Shuman HA. 2021. GigC, a LysR family transcription regulator, is required for cysteine metabolism and virulence in *Acinetobacter baumannii*. Infect Immun 89:1–13.

124. Gebhardt MJ, Gallagher LA, Jacobson RK, Usacheva EA, Peterson LR, Zurawski D V., Shuman HA. 2015. Joint transcriptional control of virulence and resistance to antibiotic and environmental stress in *Acinetobacter baumannii*. mBio 6:1–12.

125. Klevens RM, Morrison MA, Nadle J, Petit S, Gershman K, Ray S, Harrison LH, Lynfield R, Dumyati G, Townes JM, Craig AS, Zell ER, Fosheim GE, Mcdougal LK, Carey RB, Fridkin SK. 2007. Invasive methicillin-resistant *Staphylococcus aureus* infections in the United States. JAMA 298:1763–1771.

126. Price EE, Boyd JM. 2020. Genetic Regulation of metal ion homeostasis in *Staphylococcus aureus*. Trends Microbiol 28:821–831.

127. Imlay JA. 2003. Pathways of Oxidative Damage. Annu Rev Microbiol 57:395–418.

128. Cotruvo JA, Stubbe J. 2012. Metallation and mismetallation of iron and manganese proteins *in vitro* and *in vivo*: The class I ribonucleotide reductases as a case study. Metallomics 4:1020–1036.

129. Park S, Klotzsche M, Wilson DJ, Boshoff HI, Eoh H, Manjunatha U, Blumenthal A, Rhee K, Barry CE, Aldrich CC, Ehrt S, Schnappinger D. 2011. Evaluating the sensitivity of *Mycobacterium tuberculosis* to biotin deprivation using regulated gene expression. PLoS Pathog 7.

130. Feng Y, Napier BA, Manandhar M, Henke SK, Weiss DS, Cronan JE. 2014. A Francisella virulence factor catalyses an essential reaction of biotin synthesis. Mol Microbiol 91:300–314.

131. Poole LB, Nelson KJ. 2008. Discovering mechanisms of signaling-mediated cysteine oxidation. Curr Opin Chem Biol 12:18–24.

132. Nagy P, Becker JD, Mallo RC, Ashby MT. 2007. The Jekyll and Hyde roles of cysteine derivatives during oxidative stress, p. 193–212. In Zhu, PC (ed.), New Biocides Development, 967th ed. American Chemical Society.

133. Fontenot CR, Tasnim H, Valdes KA, Popescu C v., Ding H. 2020. Ferric uptake regulator (Fur) reversibly binds a [2Fe-2S] cluster to sense intracellular iron homeostasis in *Escherichia coli*. Journal of Biological Chemistry 295:15454–15463.

134. Kies PJ, Hammer ND. 2022. A resourceful race: bacterial scavenging of host sulfur metabolism during colonization. Infect Immun 90:e00579-21.

135. Morigasaki S, Umeyama A, Kawano Y, Aizawa Y, Ohtsu I. 2020. Defect of RNA pyrophosphohydrolase Rpph enhances fermentative production of L-cysteine in *Escherichia coli*. Journal of General and Applied Microbiology 66:307–314.

136. Verstraete MM, Daniela Morales L, Kobylarz MJ, Loutet SA, Laakso HA, Pinter TB, Stillman MJ, Heinrichs DE, Murphy MEP. 2019. The heme-sensitive regulator SbnI

has a bifunctional role in staphyloferrin B production by *Staphylococcus aureus*. Journal of Biological Chemistry 294:11622–11636.

137. Loi V Van, Busche T, Tedin K, Bernhardt J, Wollenhaupt J, Huyen NTT, Weise C, Kalinowski J, Wahl MC, Fulde M, Antelmann H. 2018. Redox-sensing under hypochlorite stress and infection conditions by the Rrf2-family repressor HypR in *Staphylococcus aureus*. Antioxid Redox Signal 29:615–636.

138. Manna A, Cheung AL. 2001. Characterization of *sarR*, a modulator of *sar* expression in *Staphylococcus aureus*. Infect Immun 69:885–896.

139. Hobman JL. 2007. MerR family transcription activators: Similar designs, different specificities. Mol Microbiol 63:1275–1278.

140. Mazmanian SK, Skaar EP, Gaspar AH, Humayun M, Gornicki P, Jelenska J, Joachmiak A, Missiakas DM, Scheewind O. 2003. Passage of heme-iron across the envelope of *Staphylococcus aureus*. Science (1979) 299:906–909.

141. Choby JE, Mike LA, Mashruwala AA, Dutter BF, Dunman PM, Sulikowski GA, Boyd JM, Skaar EP. 2016. A small-molecule inhibitor of iron-sulfur cluster assembly uncovers a link between virulence regulation and metabolism in *Staphylococcus aureus*. Cell Chem Biol 23:1351–1361.

142. Shepard EM, Boyd ES, Broderick JB, Peters JW. 2011. Biosynthesis of complex iron-sulfur enzymes. Curr Opin Chem Biol 15:319–327.

143. Stewart LJ, Ong C-LY, Zhang MM, Brouwer S, Mcintyre L, Davies MR, Walker MJ, Mcewan AG, Waldron KJ, Djoko KY. 2020. Role of glutathione in buffering excess intracellular copper in *Streptococcus pyogenes*. Molecular Biology and Physiology 11:e02804-20.

144. Potter AJ, Trappetti C, Paton JC. 2012. *Streptococcus pneumoniae* uses glutathione to defend against oxidative stress and metal ion toxicity. J Bacteriol 194:6248–6254.

145. Aich A, Freundlich M, Vekilov PG. 2015. The free heme concentration in healthy human erythrocytes. Blood Cells Mol Dis 55:402–409.

146. Georgiou-Siafis SK, Samiotaki MK, Demopoulos VJ, Panayotou G, Tsiftsoglou AS. 2022. Glutathione–hemin/hematin adduct formation to disintegrate cytotoxic oxidant hemin/hematin in human K562 cells and red blood cells' hemolysates: impact of glutathione on the hemolytic disorders and homeostasis. Antioxidants 11.

147. Torres VJ, Stauff DL, Pishchany G, Bezbradica JS, Gordy LE, Iturregui J, Anderson KLL, Dunman PM, Joyce S, Skaar EP. 2007. A *Staphylococcus aureus* regulatory system that responds to host heme and modulates virulence. Cell Host Microbe 1:109–119.

148. Stauff DL, Bagaley D, Torres VJ, Joyce R, Anderson KL, Kuechenmeister L, Dunman PM, Skaar EP. 2008. *Staphylococcus aureus* HrtA Is an ATPase required for protection against heme toxicity and prevention of a transcriptional heme stress response. J Bacteriol 190:3588–3596.

149. Pattee PA, Neveln DS. 1975. Transformation analysis of three linkage groups in *Staphylococcus aureus*. J Bacteriol 124:201–211.

150. Vitko NP, Richardson AR. 2013. Laboratory maintenance of methicillin-resistant *Staphylococcus aureus* (MRSA), p. 9C–2. *In* Current Protocols in Microbiology.

151. Luebke JL, Shen J, Bruce KE, Kehl-Fie TE, Peng H, Skaar EP, Giedroc DP. 2014. The CsoR-like sulfurtransferase repressor (CstR) is a persulfide sensor in *Staphylococcus aureus*. Mol Microbiol 94:1343–1360.

152. Tanaka Y, Yoshikaie K, Takeuchi A, Ichikawa M, Mori T, Uchino S, Sugano Y, Hakoshima T, Takagi H, Nonaka G, Tsukazaki T. 2020. Crystal structure of a YeeE/YedE family protein engaged in thiosulfate uptake. Sci Adv 6:1–10.

153. Krute CN, Krausz KL, Markiewicz MA, Joyner JA, Pokhrel S, Hall PR, Bose JL. 2016. Generation of a stable plasmid for *in vitro* and *in vivo* studies of Staphylococcus species. Appl Environ Microbiol 82:6859–6869.

154. Nikolic P, Mudgil P. 2023. The cell wall, cell membrane and virulence factors of *Staphylococcus aureus* and their role in antibiotic resistance. Microorganisms 11:1–20.

155. Nikolic P, Mudgil P, Harman DG, Whitehall J. 2022. Untargeted lipidomic differences between clinical strains of methicillin-sensitive and methicillin-resistant *Staphylococcus aureus*. Infect Dis 54:497–507.

156. Imperi F, Tiburzi F, Fimia GM, Visca P. 2010. Transcriptional control of the *pvdS* iron starvation sigma factor gene by the master regulator of sulfur metabolism CysB in *Pseudomonas aeruginosa*. Environ Microbiol 12:1630–1642.

157. Shviro Y, Swaklai N. 1987. Glutathione as a scavenger of free hemin. Biochem Pharmacol 36:3801–3807.

158. Atamna H, Ginsburg H. 1995. Heme degradation in the presence of glutathione. Journal of Biological Chemistry 270:24876–24883.

159. Van 'T Erve TJ, Wagner BA, Ryckman KK, Raife TJ, Buettner GR. 2013. The concentration of glutathione in human erythrocytes is a heritable trait. Free Radic Biol Med 65:742–749.

160. Yoshida T, Prudent M, D'Alessandro A. 2019. Red blood cell storage lesion: Causes and potential clinical consequences. Blood Transfusion 17:27–52.

161. Sirko A, Hryniewicz M, Hulanicka D, Bock2 A. 1990. Sulfate and thiosulfate transport in *Escherichia coli* K-12: Nucleotide sequence and expression of the *cysTWAM* gene cluster. J Bacteriol 172:3351–3357.

162. Sirko A, Zatyka M, Sadowy E, Hulanicka D. 1995. Sulfate and thiosulfate transport in *Escherichia coli* K-12: Evidence for a functional overlapping of sulfate-and thiosulfate-binding proteins. J Bacteriol 177:4134–4136.

163. Hryniewicz M, Sirko A, Palucha A, Bock A, Hulanicka D. 1990. Sulfate and thiosulfate transport in *Escherichia coli* K-12: Identification of a gene encoding a novel protein involved in thiosulfate binding. J Bacteriol 172:3358–3366.

164. Fey PD, Endres JL, Yajjala VK, Widhelm TJ, Boissy RJ, Bose JL, Bayles KW. 2013. A genetic resource for rapid and comprehensive phenotype screening of nonessential *Staphylococcus aureus* genes. mBio 4:e00537-12.

165. Novick R. 1967. Properties of a cryptic high-frequency transducing phage in *Staphylococcus aureus*. Virology 33:155–166.

166. Bae T, Glass EM, Schneewind O, Missiakas D. 2008. Generating a collection of insertion mutations in the *Staphylococcus aureus* genome using *Bursa aurealis*, p. 103–116. In Osterman, AL, Gerdes, SY (eds.), Methods in Molecular Biology: Microbial Gene Essentiality. Humana Press.

167. Love MI, Huber W, Anders S. 2014. Moderated estimation of fold change and dispersion for RNA-seq data with DESeq2. Genome Biol 15.

168. Huerta-Cepas J, Szklarczyk D, Heller D, Hernández-Plaza A, Forslund SK, Cook H, Mende DR, Letunic I, Rattei T, Jensen LJ, Von Mering C, Bork P. 2019. EggNOG 5.0: A hierarchical, functionally and phylogenetically annotated orthology resource based on 5090 organisms and 2502 viruses. Nucleic Acids Res 47:D309–D314.

169. Cantalapiedra CP, Herņandez-Plaza A, Letunic I, Bork P, Huerta-Cepas J. 2021.

eggNOG-mapper v2: Functional annotation, orthology assignments, and domain prediction at the metagenomic scale. Mol Biol Evol 38:5825–5829.

170. Hernández-Plaza A, Szklarczyk D, Botas J, Cantalapiedra CP, Giner-Lamia J, Mende DR, Kirsch R, Rattei T, Letunic I, Jensen LJ, Bork P, von Mering C, Huerta-Cepas J. 2023. eggNOG 6.0: enabling comparative genomics across 12 535 organisms. Nucleic Acids Res 51:D389–D394.

171. Austin CM, Garabaglu S, Krute CN, Ridder MJ, Seawell NA, Markiewicz MA, Boyd JM, Bose JL. 2019. Contribution of YjbIH to virulence factor expression and host colonization in *Staphylococcus aureus*. Infect Immun 87:1–21.

172. Galperin MY, Makarova KS, Wolf YI, Koonin E V. 2015. Expanded Microbial genome coverage and improved protein family annotation in the COG database. Nucleic Acids Res 43:D261–D269.

173. Tatusov RL, Koonin E V, Lipman DJ. 1997. A Genomic Perspective on Protein Families. Science (1979) 278:631–637.

174. Elston DM. 2007. Community-acquired methicillin-resistant *Staphylococcus aureus*. J Am Acad Dermatol 56:1–16.

175. Dantes R, Mu Y, Belflower R, Aragon D, Dumyati G, Harrison LH, Lessa FC, Lynfield R, Nadle J, Petit S, Ray SM, Schaffner W, Townes J, Fridkin S. 2013. National burden of invasive methicillin-resistant *Staphylococcus aureus* infections, United States, 2011. JAMA Intern Med 173:1970–1979.

176. Kallen AJ, Mu Y, Bulens S, Reingold A, Petit S, Gershman K, Ray SM, Harrison LH, Lynfield R, Dumyati G, Townes JM, Schaffner W, Patel PR, Fridkin SK. 2010. Health Care-Associated Invasive MRSA Infections, 2005-2008JAMA.

177. Holden MTG, Feil EJ, Lindsay JA, Peacock SJ, Day NPJ, Enright MC, Foster TJ, Moore CE, Hurst L, Atkin R, Barron A, Bason N, Bentley SD, Chillingworth C, Chillingworth T, Churcher C, Clark L, Corton C, Cronin A, Doggett J, Dowd L, Feltwell T, Hance Z, Harris B, Hauser H, Holroyd S, Jagels K, James KD, Lennard N, Line A, Mayes R, Moule S, Mungall K, Ormond D, Quail MA, Rabbinowitsch E, Rutherford K, Sanders M, Sharp S, Simmonds M, Stevens K, Whitehead S, Barrell BG, Spratt BG, Parkhill J. 2004. Complete genomes of two clinical *Staphylococcus aureus* strains: Evidence for the rapid evolution of virulence and drug resistance. Proceedings of the National Academy of Sciences 101:9786–9791.

178. Mwangi MM, Wu SW, Zhou Y, Sieradzki K, de Lencastre H, Richardson P, Bruce D, Rubin E, Myers E, Siggia ED, Tomasz A. 2007. Tracking the *in vivo* evolution of multidrug resistance in *Staphylococcus aureus* by whole-genome sequencing.

Proceedings of the National Academy of Sciences 104:9451–9456.

179. Jakob HG, Borneff-Lipp M, Bach A, Von Pu Èckler S, Èrgen Windeler J, Sonntag H-GÈ, Hagl S. 2000. The endogenous pathway is a major route for deep sternal wound infection. European Journal of Cario-thoracis Surgery 17:154–160.

180. Kluytmans JAJA, Mouton JW, Ijzerman EPF, Vandenbroucke-Grauls CMJE, Maat AWPM, Wagenvoort JHT, Verbrugh HA. 1995. Nasal carriage of *Staphylococcus aureus* as a major risk factor for wound infections after cardiac surgery. Journal of Infectious Diseases 171:216–219.

181. Han SM, Sorabella RA, Vasan S, Grbic M, Lambert D, Prasad R, Wang C, Kurlansky P, Borger MA, Gordon R, George I. 2017. Influence of *Staphylococcus aureus* on outcomes after valvular surgery for infective endocarditis. J Cardiothorac Surg 12.

182. Halsey CR, Lei S, Wax JK, Lehman MK, Nuxoll AS, Steinke L, Sadykov M, Powers R, Fey PD. 2017. Amino acid catabolism in *Staphylococcus aureus* and the function of carbon catabolite repression. mBio 8.

183. Skaar EP, Humayun M, Bae T, Debord KL, Schneewind O. 2004. Iron-source preference of *Staphylococcus aureus* infections. Science (1979) 305:1626–1628.

184. Hammer ND, Skaar EP. 2011. Molecular mechanisms of *Staphylococcus aureus* iron acquisition. Annu Rev Microbiol 65:129–147.

185. Kehl-Fie TE, Zhang Y, Moore JL, Farrand AJ, Hood MI, Rathi S, Chazin WJ, Caprioli RM, Skaar EP. 2013. MntABC and MntH contribute to systemic *Staphylococcus aureus* infection by competing with calprotectin for nutrient manganese. Infect Immun 81:3395–3405.

186. Murdoch CC, Skaar EP. 2022. Nutritional immunity: the battle for nutrient metals at the host–pathogen interface. Nat Rev Microbiol https://doi.org/10.1038/s41579-022-00745-6.

187. Nagy P, Winterbourn CC. 2010. Redox chemistry of biological thiols. Advances in Molecular Toxicology 4:183–222.

188. Ganguli D, Kumar C, Bachhawat AK. 2007. The alternative pathway of glutathione degradation is mediated by a novel protein complex involving three new genes in *Saccharomyces cerevisiae*. Genetics 175:1137–1151.

189. Kaur H, Ganguli D, Bachhawat AK. 2012. Glutathione degradation by the alternative

pathway (DUG pathway) in *Saccharomyces cerevisiae* is initiated by (Dug2p-Dug3p)2 complex, a novel glutamine amidotransferase (GATase) enzyme acting on glutathione. Journal of Biological Chemistry 287:8920–8931.

190. Sherrill C, Fahey RC. 1998. Import and metabolism of glutathione by *Streptococcus mutans*. J Bacteriol 180:1454–1459.

191. Vergauwen B, Pauwels F, Vaneechoutte M, Van Beeumen JJ. 2003. Exogenous glutathione completes the defense against oxidative stress in *Haemophilus influenzae*. J Bacteriol 185:1572–1581.

192. Hiron A, Borezée-Durant E, Piard JC, Juillard V. 2007. Only one of four oligopeptide transport systems mediates nitrogen nutrition in *Staphylococcus aureus*. J Bacteriol 189:5119–5129.

193. Lehman MK, Nuxoll AS, Yamada KJ, Kielian T, Carson SD, Fey PD. 2019. Protease-mediated growth of *Staphylococcus aureus* on host proteins is *opp3* dependent. mBio 10:1–17.

194. Coulter SN, Schwan WR, Ng EYW, Langhorne MH, Ritchie HD, Westbrock-Wadman S, Hufnagle WO, Folger KR, Bayer AS, Stover CK. 1998. *Staphylococcus aureus* genetic loci impacting growth and survival in multiple infection environments. Mol Microbiol 30:393–404.

195. Bæk KT, Frees D, Renzoni A, Barras C, Rodriguez N, Manzano C, Kelley WL. 2013. Genetic variation in the *Staphylococcus aureus* 8325 strain lineage revealed by whole-genome sequencing. PLoS One 8:1–16.

196. Bayer E, Gugel KH, Hagele K, Hagenmaier H, Jessipow' S, Konig WA, Zahner H. 1972. Stoffwechselprodukte von Mikroorganismen. 98. Mitteilung. Phosphinothricin und phosphinothricyl-alanyl-alanin. Helv Chim Acta 55:244–239.

197. Peck SC, Gao J, Van Der Donk WA. 2012. Discovery and biosynthesis of phosphonate and phosphinate natural products, p. 101–123. In Methods in Enzymology. Academic Press Inc.

198. Diddens H, Zähner H, Kraas E, Göhring W, Jung G. 1976. On the Transport of Tripeptide Antibiotics in Bacteria. Eur J Biochem 66:11–23.

199. Perego M, Higgins CF, Pearce SR, Gallagher MP, Hoch JA. 1991. The oligopeptide transport system of *Bacillus subtilis* plays a role in the initiation of sporulation. Mol Microbiol 5:173–185.

200. Solomon J, Su L, Shyn S, Grossman AD. 2003. Isolation and characterization of mutants of the *Bacillus subtilis* oligopeptide permease with altered specificity of oligopeptide transport. J Bacteriol 185:6425–6433.

201. Abouhamad WN, Manson M, Gibson MM, Higgins CF. 1991. Peptide transport and chemotaxis in *Escherichia coli* and *Salmonella typhimurium*: Characterization of the dipeptide permease (Dpp) and the dipeptide-binding protein. Mol Microbiol 5:1035–1047.

202. Borezee E, Pellegrini E, Berche P. 2000. OppA of *Listeria monocytogenes*, an oligopeptide-binding protein required for bacterial growth at low temperature and involved in intracellular survival. Infect Immun 68:7069–7077.

203. Nguyen TH, Park MD, Otto M. 2017. Host response to *Staphylococcus epidermidis* colonization and infections. Front Cell Infect Microbiol 7:1–7.

204. Götz F. 2002. Staphylococcus and biofilms. Mol Microbiol 43:1367–1378.

205. Paysan-Lafosse T, Blum M, Chuguransky S, Grego T, Pinto BL, Salazar GA, Bileschi ML, Bork P, Bridge A, Colwell L, Gough J, Haft DH, Letunić I, Marchler-Bauer A, Mi H, Natale DA, Orengo CA, Pandurangan AP, Rivoire C, Sigrist CJA, Sillitoe I, Thanki N, Thomas PD, Tosatto SCE, Wu CH, Bateman A. 2022. InterPro in 2022. Nucleic Acids Res https://doi.org/10.1093/nar/gkac993.

206. Solcan N, Kwok J, Fowler PW, Cameron AD, Drew D, Iwata S, Newstead S. 2012. Alternating access mechanism in the POT family of oligopeptide transporters. EMBO Journal 31:3411–3421.

207. Newstead S. 2017. Recent advances in understanding proton coupled peptide transport via the POT family. Curr Opin Struct Biol 45:17–24.

208. Samsudin F, Parker JL, Sansom MSP, Newstead S, Fowler PW. 2016. Accurate prediction of ligand affinities for a proton-dependent oligopeptide transporter. Cell Chem Biol 23:299–309.

209. Vorwerk H, Mohr J, Huber C, Wensel O, Schmidt-Hohagen K, Gripp E, Josenhans C, Schomburg D, Eisenreich W, Hofreuter D. 2014. Utilization of host-derived cysteine-containing peptides overcomes the restricted sulphur metabolism of *Campylobacter jejuni*. Mol Microbiol 93:1224–1245.

210. Spyrakis F, Singh R, Cozzini P, Campanini B, Salsi E, Felici P, Raboni S, Benedetti P, Cruciani G, Kellogg GE, Cook PF, Mozzarelli A. 2013. Isozyme-specific ligands for *O*-acetylserine sulfhydrylase, a novel antibiotic target. PLoS One 8:1-13.

211. Salsi E, Bayden AS, Spyrakis F, Amadasi A, Campanini B, Bettati S, Dodatko T, Cozzini P, Kellogg GE, Cook PF, Roderick SL, Mozzarelli A. 2010. Design of *O*-acetylserine sulfhydrylase inhibitors by mimicking nature. J Med Chem 53:345–356.

212. Nagpal I, Raj I, Subbarao N, Gourinath S. 2012. Virtual screening, identification and in vitro testing of novel inhibitors of *O*-acetyl-L-serine sulfhydrylase of *Entamoeba histolytica*. PLoS One 7.

213. Bae T, Schneewind O. 2006. Allelic replacement in *Staphylococcus aureus* with inducible counter-selection. Plasmid 55:58–63.

214. Camacho C, Coulouris G, Avagyan V, Ma N, Papadopoulos J, Bealer K, Madden TL. 2009. BLAST+: Architecture and applications. BMC Bioinformatics 10:1–9.

215. Sievers F, Higgins DG. 2018. Clustal Omega for making accurate alignments of many protein sequences. Protein Science 27:135–145.

216. Nguyen LT, Schmidt HA, Von Haeseler A, Minh BQ. 2015. IQ-TREE: A fast and effective stochastic algorithm for estimating maximum-likelihood phylogenies. Mol Biol Evol 32:268–274.

217. Moore RM, Harrison AO, McAllister SM, Polson SW, Eric Wommack K. 2020. Iroki: Automatic customization and visualization of phylogenetic trees. PeerJ 8:1–22.

218. National Research Council (U.S.). Committee for the Update of the Guide for the Care and Use of Laboratory Animals., Institute for Laboratory Animal Research (U.S.). 2011. Guide for the care and use of laboratory animals. National Academies Press.

219. Mack D, Siemssen N, Laufs R. 1992. Parallel induction by glucose of adherence and a polysaccharide antigen specific for plastic-adherent *Staphylococcus epidermidis*: Evidence for functional relation to intercellular adhesion. Infect Immun 60:2048–2057.

220. Anwardeen NR, Diboun I, Mokrab Y, Althani AA, Elrayess MA. 2023. Statistical methods and resources for biomarker discovery using metabolomics. BMC Bioinformatics 24.

221. Spraggins JM, Rizzo DG, Moore JL, Noto MJ, Skaar EP, Caprioli RM. 2016. Next-generation technologies for spatial proteomics: Integrating ultra-high speed MALDI-TOF and high mass resolution MALDI FTICR imaging mass spectrometry for protein analysis. Proteomics 16:1678–1689.

222. Perry WJ, Spraggins JM, Sheldon JR, Grunenwald CM, Heinrichs DE, Cassat JE, Skaar EP, Caprioli RM. 2019. *Staphylococcus aureus* exhibits heterogeneous siderophore production within the vertebrate host. PNAS 116:21980–21982.

223. Broniowska KA, Diers AR, Hogg N. 2013. *S*-Nitrosoglutathione. Biochim Biophys Acta Gen Subj 1830:3173–3181.

224. Jourd'heuil D, Hallén K, Feelisch M, Grisham MB. 2000. Dynamic state of *S*-Nitrosothiols in human plasma and whole blood. Free Radical Biologiy & Medicine 28:409–417.

225. Tsikas D, Schmidt M, Böhmer A, Zoerner AA, Gutzki FM, Jordan J. 2013. UPLC-MS/MS measurement of *S*-nitrosoglutathione (GSNO) in human plasma solves the *S*-nitrosothiol concentration enigma. J Chromatogr B Analyt Technol Biomed Life Sci 927:147–157.

226. Kalapos MP, Antognelli C, Bari L de. 2022. Metabolic Shades of S-D-Lactoylglutathione. Antioxidants 11.

227. Bilzer M, Lauterburg BH. 1991. Glutathione metabolism in activated human neutrophils: stimulation of glutathione synthesis and consumption of glutathione by reactive oxygen species. Eur J Clin Invest 21:316–322.

228. Berkeley LI, Cohen JF, Crankshaw DL, Shirota FN, Nagasawa HT. 2003. Hepatoprotection by L-cysteine-glutathione mixed disulfide, a sulfhydryl-modified prodrug of glutathione. J Biochem Mol Toxicol 17:95–97.

229. De Crouy-Chanel A, Richarme G. 2001. Amount and redox state of cytoplasmic, membrane and periplasmic proteins in *Escherichia coli* redox mutants. Res. Microbiol 152:663-669.

230. Heras B, Kurz M, Jarrott R, Shouldice SR, Frei P, Robin G, Čemažar M, Thöny-Meyer L, Glockshuber R, Martin JL. 2008. *Staphylococcus aureus* DsbA does not have a destabilizing disulfide: A new paradigm for bacterial oxidative folding. Journal of Biological Chemistry 283:4261–4271.

231. Kim J, Senadheera DB, Lévesque CM, Cvitkovitch DG. 2012. TcyR regulates L-cystine uptake via the TcyABC transporter in *Streptococcus mutans*. FEMS Microbiol Lett 328:114–121.

232. Vergauwen B, Verstraete K, Senadheera DB, Dansercoer A, Cvitkovitch DG, Guédon E, Savvides SN. 2013. Molecular and structural basis of glutathione import in Gram-positive bacteria via GshT and the cystine ABC importer TcyBC of

Streptococcus mutans. Mol Microbiol 89:288–303.

233. Vergauwen B, Elegheert J, Dansercoer A, Devreese B, Savvides SN, Zambryski PC. 2010. Glutathione import in Haemophilus influenzae Rd is primed by the periplasmic heme-binding protein HbpA. PNAS 107(30):13270-13275.

234. Fisher SH. 1999. Regulation of nitrogen metabolism in *Bacillus subtilis*: Vive la diffèrence! Mol Microbiol 32:223–232.

235. Reitzer L. 2003. Nitrogen assimilation and global regulation in *Escherichia coli*. Annu Rev Microbiol 57:155–176.

236. Zeden MS, Kviatkovski I, Schuster CF, Thomas VC, Fey PD, Gründling A. 2020. Identification of the main glutamine and glutamate transporters in *Staphylococcus aureus* and their impact on c-di-AMP production. Mol Microbiol 113:1085–1100.

APPENDIX A: Chapter 2 sulfur starvation Tables

Table A-1. WT sulfur starvation.

Genes upregulated in WT sulfur starvation when compared to WT cystine (CSSC)

Shared with *cymR*::Tn -S (Table 3)	COG	Locus	Old locus	Gene	Product	TPM.1 Starv	TPM.2 Starv	TPM.1 CSSC	TPM.2 CSSC	DE Log_2 FC	DE Adj. *P*-value
Yes	O	SAUSA300_RS10980	SAUSA300_1997		sulfurtransferase TusA family protein	719.68	710.69	2.67	2.08	6.52450659 6	1.56827E-48
Yes	S	SAUSA300_RS10985	SAUSA300_1998		YeeE/YedE family protein	170.77	130.2	0.74	0.43	6.33919187 4	1.13221E-52
Yes	P	SAUSA300_RS11525	SAUSA300_2092		Dps family protein	24049	29749.5	209.59	66.25	6.10401684 8	4.15346E-38
Yes	I	SAUSA300_RS00930	SAUSA300_0177		acyl-CoA/acyl-ACP dehydrogenase	547.15	115.03	2.77	1.16	5.54308137 9	1.58552E-27
No	S	SAUSA300_RS00910	SAUSA300_0173		DUF4242 domain-containing protein	694.9	626.57	4.54	4.88	5.39613928 7	6.36763E-33
Yes	P	SAUSA300_RS02335	SAUSA300_0436		methionine ABC transporter permease	638.33	220.44	2.72	2.91	5.33935652 2	4.85064E-30
Yes	S	SAUSA300_RS04570	SAUSA300_0846		Na+/H+ antiporter family protein	171.08	76	1.42	0.65	5.23716145 8	1.95686E-36

Table A-1 (cont'd)

Yes	P	SAUSA300_RS02340	SAUSA300_0437	*gmpC*	dipeptide ABC transporter glycylmethionine-binding lipoprotein	1906.11	1201.65	10.16	14.16	5.13808140 8	1.41043E-27
Yes	no homolog found	SAUSA300_RS16040		*hisF*	imidazole glycerol phosphate synthase subunit HisF	43.09	28.36	0.34	0.37	4.88966808 4	7.38696E-27
Yes	P	SAUSA300_RS10250	SAUSA300_1874	*ftnA*	H-type ferritin FtnA	6482.34	4756.04	77.14	50.27	4.85896820 4	8.35149E-36
Yes	P	SAUSA300_RS01055	SAUSA300_0200		ABC transporter ATP-binding protein	182.95	207.45	1.44	2.45	4.81528742 7	1.63682E-19
Yes	P	SAUSA300_RS02330	SAUSA300_0435		methionine ABC transporter ATP-binding protein	343.69	145.18	2.36	2.49	4.81508731 4	9.67075E-27
Yes	S	SAUSA300_RS14570	SAUSA300_2622		rhodanese-related sulfurtransferase	371.08	274.76	5.35	2.72	4.76875260 4	1.24925E-33
No	P	SAUSA300_RS00925	SAUSA300_0176		ABC transporter permease	118.62	84.08	1.5	0.99	4.71241826 9	1.46665E-30
No	P	SAUSA300_RS00915	SAUSA300_0174		ABC transporter ATP-binding protein	125.49	72.45	2.15	0.58	4.63614025	5.56276E-24
Yes	E	SAUSA300_RS14090	SAUSA300_2539		aspartate aminotransferase family protein	118.75	123	1.2	2.18	4.32946737 9	7.90882E-16

Table A-1 (cont'd)

Yes	no homolog found	SAUSA300_RS07125			hypothetical protein	2859.37	3129.02	89.03	22.95	4.31647520 8	1.89065E-18
No	J	SAUSA300_RS01820	SAUSA300_0343		GNAT family protein	160.39	159.38	3.32	2.77	4.10308227 7	5.37253E-20
Yes	S	SAUSA300_RS12540	SAUSA300_2268		bile acid:sodium symporter family protein	63.15	76.14	1.59	1.16	4.08691557 2	2.21742E-18
Yes	F	SAUSA300_RS00725	SAUSA300_0138	*deoD*	purine-nucleoside phosphorylase	32.2	29.05	0.56	0.58	4.06106887 4	3.42094E-17
No	no homolog found	SAUSA300_RS15260	SAUSA300_0937		hypothetical protein	1230.36	1900.55	43.62	23.66	4.06078001 2	6.51546E-17
Yes	no homolog found	SAUSA300_RS10255			hypothetical protein	139.24	87.37	3.88	1.33	3.83481737 4	9.77567E-15
Yes	C	SAUSA300_RS07500	SAUSA300_1373		ferredoxin	3199.55	2852.95	98.5	51.47	3.82958655 8	1.03868E-20
No	E	SAUSA300_RS09195	SAUSA300_1683		bifunctional 3-deoxy-7-phosphoheptulonate synthase/chorismate mutase	1457.39	1317.56	52.47	23.75	3.71063807 9	6.54452E-19

Table A-1 (cont'd)

Yes	E	SAUSA300_RS02320	SAUSA300_0433	*mccA*	cysteine synthase family protein	28.3	17.42	0.52	0.56	3.663963457	6.02326E-15
Yes	P	SAUSA300_RS12340	SAUSA300_2235		ABC transporter substrate-binding protein	289.03	81.16	6.61	2.65	3.639705478	3.63552E-14
No	no homolog found	SAUSA300_RS05130			hypothetical protein	28.16	66.88	1.65	0.97	3.601051422	4.09584E-08
Yes	NOU	SAUSA300_RS08765	SAUSA300_1609		A24 family peptidase	15.85	22.63	0.83	0.33	3.579029533	2.1629E-11
Yes	C	SAUSA300_RS05570	SAUSA300_1035	*isdG*	staphylobilin-forming heme oxygenase IsdG	43.52	46.29	1.76	0.88	3.569199321	2.57049E-13
No	P	SAUSA300_RS00920	SAUSA300_0175		ABC transporter substrate-binding protein	75.98	41.15	2.57	0.88	3.557110479	5.03363E-16
Yes	S	SAUSA300_RS03075	SAUSA300_0575		DUF1450 domain-containing protein	333.15	267.12	9.41	7.44	3.552414542	4.47957E-17
No	S	SAUSA300_RS09315	SAUSA300_1706		TIGR01212 family radical SAM protein	87.53	59.39	2.18	1.85	3.542615228	5.94219E-17
Yes	K	SAUSA300_RS14655	SAUSA300_2639		cold-shock protein	22322.8	27330.69	1319.58	382.56	3.484235408	2.28916E-12

Table A-1 (cont'd)

Yes	S	SAUSA300_RS14550	SAUSA300_2618		ECF-type riboflavin transporter substrate-binding protein	41.15	45.27	1.11	1.36	3.441470198	2.17006E-11
Yes	H	SAUSA300_RS03735	SAUSA300_0696	*queD*	6-carboxytetrahydropterin synthase QueD	74.16	31.83	1.57	1.37	3.424769445	1.98647E-13
No	S	SAUSA300_RS05050	SAUSA300_0940		DoxX family protein	191.37	208.37	10.54	3.61	3.404615948	6.41637E-13
Yes	E	SAUSA300_RS01075	SAUSA300_0204	*ggt*	γ-glutamyltransferase	119.21	118.08	2.76	4.15	3.365084711	7.15816E-11
Yes	S	SAUSA300_RS00890	SAUSA300_0169		YbaN family protein	72.45	46.03	3.25	0.88	3.347788833	2.28916E-12
Yes	C	SAUSA300_RS04255	SAUSA300_0788		nitroreductase	671.49	488.31	27.67	14.18	3.278612523	1.88799E-16
No	M	SAUSA300_RS04310	SAUSA300_0798		MetQ/NlpA family ABC transporter substrate-binding protein	217.58	157.33	10.05	4.1	3.247845107	5.8223E-15
No	S	SAUSA300_RS01875	SAUSA300_0354		low temperature requirement protein A	45.08	29.37	1.85	1.02	3.144511613	1.97162E-14

Table A-1 (cont'd)

No	E	SAUSA300_RS02855	SAUSA300_0534		M20 family metallopeptidase	82.32	42.25	3.57	1.5	3.07904484 9	2.31118E-13
Yes	H	SAUSA300_RS03730	SAUSA300_0695	*queE*	7-carboxy-7-deazaguanine synthase QueE	107.12	33.76	1.97	2.64	3.03759705	8.16854E-09
Yes	S	SAUSA300_RS10920	SAUSA300_1986		nitroreductase family protein	37.79	40.11	1.78	1.44	3.03597010 7	1.55384E-10
Yes	C	SAUSA300_RS06395	SAUSA300_1183		2-oxoacid:ferredoxin oxidoreductase subunit β	201.36	129.74	8.87	4.97	3.03533978 7	1.97314E-14
No	S	SAUSA300_RS13940	SAUSA300_2511		DUF896 domain-containing protein	186.18	230.01	11.9	6.79	3.00953177 6	1.63466E-10
No	S	SAUSA300_RS01485	SAUSA300_0277		CHAP domain-containing protein	18.43	20.75	1.18	0.62	2.96924929 1	6.33613E-10
Yes	S	SAUSA300_RS07495	SAUSA300_1372		helix-turn-helix domain-containing protein	96.9	111.15	6.3	3.4	2.96327268 1	6.6658E-11
Yes	K	SAUSA300_RS14555	SAUSA300_2619		S-adenosyl-l-methionine hydroxide adenosyltransferase family protein	19.02	14.91	0.83	0.62	2.95893782 9	1.02343E-10

Table A-1 (cont'd)

Yes	D	SAUSA300_RS07900	SAUSA300_1447	*xerD*	site-specific tyrosine recombinase XerD	254.37	128.39	11.84	5.09	2.95797855	9.17936E-13
Yes	H	SAUSA300_RS00040	SAUSA300_0007		NAD(P)H-hydrate dehydratase	148.89	134.1	7.95	4.96	2.94173211 8	3.37304E-12
No	not classified	SAUSA300_RS06580	SAUSA300_1213		hypothetical protein	12.05	17.92	1.29	0.14	2.92301785	2.60438E-05
No	Q	SAUSA300_RS04575	SAUSA300_0847		PaaI family thioesterase	515.21	437.99	29.12	15.76	2.91756117 6	1.82618E-12
No	E	SAUSA300_RS02325	SAUSA300_0434	*mccB*	bifunctional cystathionine γ-lyase/homocysteine desulfhydrase	46.14	33.39	1.09	1.95	2.90685451 7	5.07223E-08
No	E	SAUSA300_RS05115	SAUSA300_0952		aminotransferase class I/II-fold pyridoxal phosphate-dependent enzyme	208.94	179.38	12.99	5.91	2.90252660 7	5.4386E-12
Yes	O	SAUSA300_RS02020	SAUSA300_0379	*ahpF*	alkyl hydroperoxide reductase subunit F	2994.44	1970.33	103.4	106.2	2.88993674 4	6.57898E-11

Table A-1 (cont'd)

Yes	F	SAUSA300_RS03850	SAUSA300_0717	*nrdF*	class 1b ribonucleoside-diphosphate reductase subunit β	1920.34	866.82	94.33	35.28	2.88801193	2.41988E-11
No	E	SAUSA300_RS00055	SAUSA300_0010		AzlC family ABC transporter permease	48.26	38.96	1.96	1.87	2.882358415	2.9833E-10
Yes	O	SAUSA300_RS02025	SAUSA300_0380	*ahpC*	alkyl hydroperoxide reductase subunit C	3967.13	3243.81	215.86	133.72	2.84685053	2.87044E-12
Yes	HP	SAUSA300_RS03395	SAUSA300_0633		ABC transporter ATP-binding protein	144.2	58.29	7.25	2.39	2.8421453	7.90995E-10
Yes	C	SAUSA300_RS02385	SAUSA300_0446		glutamate synthase subunit β	483.98	241.21	25.93	10.25	2.80106218	2.90306E-11
Yes	K	SAUSA300_RS00650	SAUSA300_0126	*sbnI*	bifunctional transcriptional regulator/O-phospho-L-serine synthase SbnI	43.44	26.75	2.35	1.17	2.78662502	4.36095E-11
No	K	SAUSA300_RS04190	SAUSA300_0777		cold-shock protein	7723.34	10264.53	757.17	261.19	2.78015390	2.15934E-08
Yes	E	SAUSA300_RS13265	SAUSA300_2395		APC family permease	42.04	29.12	2.34	1.36	2.73506481	2.13842E-11

Table A-1 (cont'd)

No	D	SAUSA300_RS09440	SAUSA300_1726		CrcB family protein	30.4	32.26	1.79	1.43	2.730502552	4.39193E-08
Yes	C	SAUSA300_RS01085	SAUSA300_0206		FMN-dependent NADH-azoreductase	48.05	65.73	2.77	2.98	2.720025604	2.23804E-07
No	K	SAUSA300_RS04840	SAUSA300_0898	*spxA*	transcriptional regulator SpxA	55513.94	65522.85	4499.83	2337.74	2.709965145	2.55331E-09
Yes	C	SAUSA300_RS00885	SAUSA300_0168	*isdI*	staphylobilin-forming heme oxygenase IsdI	193.94	172	15.34	5.57	2.707974015	1.95023E-09
No	C	SAUSA300_RS01170	SAUSA300_0222		glycerophosphoryl diester phosphodiesterase membrane domain-containing protein	18.07	10.31	0.96	0.52	2.701692580	1.67174E-10
No	O	SAUSA300_RS04535	SAUSA300_0839		NifU family protein	4814.96	5336.37	417.58	174.05	2.695715368	3.6312E-09
No	F	SAUSA300_RS03845	SAUSA300_0716	*nrdE*	class 1b ribonucleoside-diphosphate reductase subunit α	1116.49	521.77	57.24	28.15	2.694654306	4.45016E-11
Yes	P	SAUSA300_RS07905	SAUSA300_1448		Fur family transcriptional regulator	935.77	709.56	64.75	27.78	2.691939219	9.20153E-11

Table A-1 (cont'd)

No	U	SAUSA300_RS02035	SAUSA300_0382		L-cystine transporter	1423.29	1354.04	45.72	82.63	2.67855695	1.02379E-06
No	K	SAUSA300_RS09185	SAUSA300_1682	*ccpA*	catabolite control protein A	373.68	401.82	28.23	16.05	2.667456163	1.62138E-09
No	G	SAUSA300_RS01135	SAUSA300_0216	*uhpT*	hexose-6-phosphate:phosphate antiporter	14.3	20.83	0.63	1.08	2.666430007	5.56809E-06
No	S	SAUSA300_RS00060	SAUSA300_0011		AzlD domain-containing protein	94.05	74.4	5.7	3.55	2.656315627	6.27563E-10
No	T	SAUSA300_RS03705	SAUSA300_0690	*saeS*	two-component system sensor histidine kinase SaeS	2407.99	1402.87	159.5	60.93	2.627225308	3.87829E-10
Yes	E	SAUSA300_RS14085	SAUSA300_2538		amino acid permease	358.57	405.99	17.23	22.37	2.623200085	3.81764E-07
No	S	SAUSA300_RS12610	SAUSA300_2282	*sdpC*	CPBP family intramembrane glutamic endopeptidase SdpC	160.72	96.58	10.9	4.13	2.618371103	6.33613E-10
Yes	E	SAUSA300_RS11075	SAUSA300_2014	*ilvA*	threonine ammonia-lyase IlvA	131.77	80	7.82	4.12	2.618185608	6.0662E-11
No	S	SAUSA300_RS01480	SAUSA300_0276		DUF5080 family protein	20.16	22.76	2.11	0.6	2.605738989	7.7373E-07

Table A-1 (cont'd)

Yes	F	SAUSA300_RS03840	SAUSA300_0715	*nrdI*	class Ib ribonucleoside-diphosphate reductase assembly flavoprotein NrdI	194.35	97.21	10.72	5.56	2.59478534 1	3.76957E-10
Yes	F	SAUSA300_RS05655	SAUSA300_1050		XTP/dITP diphosphatase	174.07	62.9	9.64	3.72	2.56523973 3	2.95742E-08
No	S	SAUSA300_RS06575	SAUSA300_1212		polymorphic toxin type 50 domain-containing protein	26.85	47.17	3.59	1.33	2.54068494	6.61255E-06
No	no homolog found	SAUSA300_RS09505	SAUSA300_1738		DUF4909 domain-containing protein	25.49	35.7	3.5	0.82	2.49777330 6	1.11106E-05
No	S	SAUSA300_RS05145	SAUSA300_0957		osmotic stress response protein	511.21	609.69	56.93	20.16	2.49528233 5	2.59117E-07
Yes	P	SAUSA300_RS03880	SAUSA300_0721		siderophore ABC transporter substrate-binding protein	63.71	27.31	3.76	1.68	2.49417382 5	1.21652E-08
No	S	SAUSA300_RS04485	SAUSA300_0831		DUF3055 domain-containing protein	123.17	176.13	17.41	4.1	2.49008913 2	7.88104E-06

Table A-1 (cont'd)

No	EP	SAUSA300_RS01060	SAUSA300_0201		ABC transporter permease	27.04	25.9	0.74	1.91	2.489752563	4.23608E-05
No	K	SAUSA300_RS05125	SAUSA300_0954		MarR family transcriptional regulator	28.82	51.17	3.79	1.69	2.487859148	6.48821E-06
Yes	CH	SAUSA300_RS13660	SAUSA300_2463		D-lactate dehydrogenase	184.4	176.07	10.9	10.55	2.480584775	9.5205E-08
No	not classified	SAUSA300_RS09430			hypothetical protein	77.65	107.67	9.87	3.23	2.474508355	2.39113E-06
Yes	C	SAUSA300_RS12320	SAUSA300_2231	*fdhD*	formate dehydrogenase accessory sulfurtransferase FdhD	64.6	50.42	5.64	2.1	2.459944656	2.90229E-08
No	no homolog found	SAUSA300_RS10520			hypothetical protein	340.84	332.33	29.83	15.37	2.444650672	2.38578E-08
No	no homolog found	SAUSA300_RS15420			hypothetical protein	37.28	43.88	4.18	1.49	2.439609614	4.11583E-06
Yes	L	SAUSA300_RS03790	SAUSA300_0705	*recQ*	DNA helicase RecQ	86.19	30.45	4.75	2.28	2.438996846	6.03946E-08

Table A-1 (cont'd)

No	G	SAUSA300_RS08910	SAUSA300_1633	*gap*	type I glyceraldehyde-3-phosphate dehydrogenase	24.26	13.46	1.4	0.92	2.43111499	2.11678E-08
No	C	SAUSA300_RS14025	SAUSA300_2528		epoxyqueuosine reductase QueH	54.83	46.16	4.7	2.2	2.41530322	2.77985E-08
No	V	SAUSA300_RS00290	SAUSA300_0056		DUF1643 domain-containing protein	11	12.13	0.82	0.65	2.41036544	7.04598E-06
No	P	SAUSA300_RS05410	SAUSA300_1005		Nramp family divalent metal transporter	107.94	89.1	8.57	4.75	2.40174594	7.86521E-09
No	P	SAUSA300_RS03400	SAUSA300_0634		iron ABC transporter permease	70.71	40.61	4.21	2.82	2.40077713	6.00437E-09
No	O	SAUSA300_RS14575	SAUSA300_2623	*pcp*	pyroglutamyl-peptidase I	38.31	36.65	2.78	2.14	2.39500032	2.17187E-07
No	P	SAUSA300_RS10870	SAUSA300_1979		TrkH family potassium uptake protein	39.46	43.09	3.98	1.93	2.37760245	2.2641E-07
Yes	S	SAUSA300_RS10695	SAUSA300_1949		dUTP pyrophosphatase	68.32	40.19	2.35	3.76	2.36517681	6.96158E-06
Yes	E	SAUSA300_RS11055	SAUSA300_2010		2-isopropylmalate synthase	58.74	40.37	3.86	2.67	2.36463665	1.08191E-08

Table A-1 (cont'd)

No	NOT	SAUSA300_RS04845	SAUSA300_0899	*mecA*	adaptor protein MecA	1349.11	1117.69	136.01	46.21	2.35584619	1.72318E-07
No	EG	SAUSA300_RS03830	SAUSA300_0713	*queF*	preQ(1) synthase	132.18	207.44	15.06	9.52	2.35284193	3.89942E-06
No	K	SAUSA300_RS08020	SAUSA300_1469	*argR*	transcriptional regulator ArgR	131.1	122.41	13.47	5.25	2.34822851	2.2641E-07
Yes	no homolog found	SAUSA300_RS10730	SAUSA300_1956		hypothetical protein	43.12	18.05	1.65	1.84	2.34533538	1.20209E-05
No	not classified	SAUSA300_RS06570	SAUSA300_1211		hypothetical protein	84.09	108.96	9.19	4.88	2.34442779	2.54566E-06
Yes	E	SAUSA300_RS01070	SAUSA300_0203		ABC transporter substrate-binding protein	23.3	13.38	0.75	1.32	2.33716317	1.52935E-05
No	not classified	SAUSA300_RS12240	SAUSA300_2218	*sarV*	HTH-type transcriptional regulator SarV	84.74	118.46	11.66	4.28	2.31862304	6.72502E-06
Yes	L	SAUSA300_RS10735	SAUSA300_1957		DnaD domain-containing protein	54.9	24.35	1.64	2.78	2.31629998	1.92809E-05
No	S	SAUSA300_RS03810	SAUSA300_0709		5'-3'-deoxyribonucleotidase	208.27	198.59	15	12.92	2.30837631	4.15228E-07
No	O	SAUSA300_RS05300	SAUSA300_0985	*nrdH*	glutaredoxin-like protein NrdH	130.8	136.87	12.78	7.02	2.30384259	4.97166E-07

Table A-1 (cont'd)

No	L	SAUSA300_RS10260	SAUSA300_1875		3'-5' exonuclease	180.6	131.52	17.95	5.77	2.30003317	4.38169E-07
Yes	U	SAUSA300_RS11755	SAUSA300_2135		iron ABC transporter permease	50.33	30.96	3.9	1.93	2.28754227	3.617E-08
No	O	SAUSA300_RS06825	SAUSA300_1256	*msrA*	peptide-methionine (S)-S-oxide reductase MsrA	292.88	266.37	27.9	14.22	2.27986174	1.07796E-07
No	S	SAUSA300_RS01615	SAUSA300_0303		DUF4467 domain-containing protein	19.94	10.29	1.79	0.43	2.27681024	3.50029E-05
Yes	EGP	SAUSA300_RS11720	SAUSA300_2128	*sdrM*	multidrug efflux MFS transporter SdrM	88.69	42.39	5.65	3.47	2.24982656	6.37222E-08
No	D	SAUSA300_RS05870	SAUSA300_1083		cell division protein SepF	453.74	262.4	35.79	17.19	2.24490419	3.29004E-08
No	K	SAUSA300_RS03710	SAUSA300_0691	*saeR*	response regulator transcription factor SaeR	1658.72	546.84	114.68	41.91	2.24078712	2.56322E-06
No	S	SAUSA300_RS04480	SAUSA300_0830		YutD family protein	124.89	116.87	13.56	5.71	2.23249280	7.32722E-07
Yes	E	SAUSA300_RS11070	SAUSA300_2013	*leuD*	3-isopropylmalate dehydratase small subunit	54.54	20.11	3.65	1.65	2.22042757	2.30785E-06

Table A-1 (cont'd)

Yes	L	SAUSA300_RS08280	SAUSA300_1517	deoxyribonuclease IV	132.64	76.96	11.13	4.85	2.21693093	1.04643E-07
No	no homolog found	SAUSA300_RS04145	SAUSA300_0769	DUF5067 domain-containing protein	14.1	11.83	1.7	0.43	2.21525171	2.63925E-05
No	M	SAUSA300_RS02875	SAUSA300_0538	NAD-dependent epimerase/dehydratase family protein	167.98	52.98	7.28	6.75	2.21132300	6.54146E-06
No	O	SAUSA300_RS13000	SAUSA300_2354	DsbA family protein	149.21	78.06	13.23	4.45	2.20510484	9.65563E-07
No	S	SAUSA300_RS10715	SAUSA300_1953	phi PVL orf 51-like protein	32.41	10.52	1.59	1.17	2.20212062	7.28484E-05
No	H	SAUSA300_RS13380	SAUSA300_2417	AbgT family transporter	93.95	70.54	7.87	4.7	2.20107237	8.47296E-08
No	no homolog found	SAUSA300_RS13590		hypothetical protein	43.71	58.72	6.27	2.28	2.19481224	0.00013026
Yes	no homolog found	SAUSA300_RS10765	SAUSA300_1963	DUF2482 family protein	98.21	49.58	5.1	4.94	2.19414883	2.86225E-06

Table A-1 (cont'd)

No	E	SAUSA300_RS07075	SAUSA300_1300	*brnQ*	branched-chain amino acid transport system II carrier protein	40.33	33.11	4.13	1.79	2.19412238 7	4.78111E-07
No	S	SAUSA300_RS13585	SAUSA300_2450		DedA family protein	64.71	60.55	7.02	3.26	2.17480999 7	1.15701E-06
Yes	P	SAUSA300_RS06680	SAUSA300_1232		catalase	539.85	377.22	43.86	27.02	2.17019843 7	7.71006E-08
No	E	SAUSA300_RS13700	SAUSA300_2469	*sdaAA*	L-serine ammonia-lyase, iron-sulfur-dependent, subunit α	43.54	41.45	3.34	3.04	2.16932606 5	3.91126E-06
No	S	SAUSA300_RS05660	SAUSA300_1051		metallophosphoesterase	235.47	162.52	23.34	9.38	2.15353223 6	4.61705E-07
No	S	SAUSA300_RS10770			DUF1270 domain-containing protein	182.23	135.63	11.69	11.67	2.14116198 2	4.42701E-06
No	CH	SAUSA300_RS12455	SAUSA300_2255		FAD-dependent monooxygenase	65.93	43.69	5.69	3.16	2.11840739 6	2.44262E-07
No	S	SAUSA300_RS00935	SAUSA300_0178		DUF2294 domain-containing protein	1908.25	1196.98	184.75	75.82	2.10840937 1	4.82712E-07

Table A-1 (cont'd)

No	K	SAUSA300_RS11435	SAUSA300_2077		helix-turn-helix domain-containing protein	667.12	625.41	66.68	41.15	2.105100838	1.14479E-06
Yes	C	SAUSA300_RS14195	SAUSA300_2554		assimilatory sulfite reductase (NADPH) flavoprotein subunit	38.99	12.76	2.52	1.35	2.103699815	6.84236E-06
No	S	SAUSA300_RS04235	SAUSA300_0784		LysE/ArgO family amino acid transporter	377.98	376.58	45.08	20.84	2.101665577	2.37372E-06
Yes	L	SAUSA300_RS10740	SAUSA300_1958	*ssb*	single-stranded DNA-binding protein	56.97	25.12	2.3	3.24	2.093198139	6.78953E-05
Yes	no homolog found	SAUSA300_RS15665	SAUSA300_2604		hypothetical protein	143.32	151.57	21.54	5.79	2.092301467	5.31546E-05
No	ET	SAUSA300_RS13025	SAUSA300_2359		transporter substrate-binding domain-containing protein	182.01	61.38	11.72	6.67	2.082761385	5.37996E-06
No	no homolog found	SAUSA300_RS10745	SAUSA300_1959		MBL fold metallo-hydrolase	41.42	27.47	1.95	2.93	2.080390075	7.4325E-05
Yes	EP	SAUSA300_RS01065	SAUSA300_0202		ABC transporter permease	35.16	28.03	1.1	3.06	2.078408830	0.00082141

Table A-1 (cont'd)

No	S	SAUSA300_RS05875	SAUSA300_1084		YggT family protein	483.89	615.57	60.84	36.34	2.06734911 2	1.4633E-05
No	E	SAUSA300_RS13015	SAUSA300_2357		amino acid ABC transporter ATP-binding protein	696.03	354.07	37.73	39.69	2.06262947 2	7.41113E-06
Yes	C	SAUSA300_RS06390	SAUSA300_1182		2-oxoacid:acceptor oxidoreductase subunit α	28.17	10.25	1.6	1.25	2.05982620 4	1.12055E-05
No	S	SAUSA300_RS03640	SAUSA300_0678		DUF1361 domain-containing protein	91.9	44.78	8.99	2.81	2.05386324 5	1.16133E-05
Yes	M	SAUSA300_RS14270	SAUSA300_2565	*clfB*	MSCRAMM family adhesin clumping factor ClfB	50.07	27.8	4.24	2.28	2.04584785 8	5.33369E-07
No	S	SAUSA300_RS09900	SAUSA300_1809		PTS transporter subunit IIC	60.73	49.38	6.38	3.33	2.03741538 8	1.63132E-06
Yes	no homolog found	SAUSA300_RS14185			hypothetical protein	286.09	209.65	26.66	15.83	2.03142813	2.30027E-06
No	S	SAUSA300_RS10775	SAUSA300_1964		DUF771 domain-containing protein	194.1	153.02	12.37	14.71	2.02663681 9	3.24239E-05
Yes	U	SAUSA300_RS04915	SAUSA300_0914		alanine/glycine:cation symporter family protein	65.79	68.24	6.08	5.26	2.02587756 7	1.59505E-05

Table A-1 (cont'd)

No	C	SAUSA300_RS14205	SAUSA300_2555		glutathione peroxidase	18.74	12.72	1.87	0.85	2.02505763 1	1.96932E-05
No	J	SAUSA300_RS03975	SAUSA300_0738	*prfB*	peptide chain release factor 2	159.54	115.56	14.02	9.4	2.02267811 7	1.02379E-06
No	P	SAUSA300_RS13185	SAUSA300_2384		sodium:proton antiporter	52.71	25.91	4.39	2.25	2.01828401 9	1.36616E-06
No	E	SAUSA300_RS09890	SAUSA300_1807		amino acid ABC transporter ATP-binding protein	18.92	10.72	1.66	0.86	2.01508411 1	9.03649E-06
Yes	M	SAUSA300_RS13530	SAUSA300_2441	*fnbA*	fibronectin-binding protein FnbA	46.33	20.75	3.52	2.03	2.00975835 7	1.99491E-06
No	no homolog found	SAUSA300_RS15465			IS5/IS1182 family transposase	36.02	24.35	3.73	1.59	2.00941557 9	4.40003E-05
No	K	SAUSA300_RS13930	SAUSA300_2509		TetR/AcrR family transcriptional regulator	27.57	19.52	2.89	1.32	2.00893044 7	8.28441E-06
No	S	SAUSA300_RS10725	SAUSA300_1955		RusA family crossover junction endodeoxyribonuclease	21.45	11.32	0.84	1.47	2.00820549 5	0.00052331 6
No	Q	SAUSA300_RS10395	SAUSA300_1899		isochorismatase family cysteine hydrolase	146.37	80.05	13.36	6.34	2.00794065 1	1.52524E-06

Table A-1 (cont'd)

No	L	SAUSA300_RS07325	SAUSA300_1343	*nth*	endonuclease III	44.97	19.52	4.35	1.33	2.00179183 2	4.17484E-05
No	K	SAUSA300_RS03330	SAUSA300_0621		metal-dependent transcriptional regulator	211.55	167	25.36	10.03	1.99815442 9	4.80413E-06
No	S	SAUSA300_RS01850	SAUSA300_0349		DUF1398 family protein	20.26	13.22	1.74	1.09	1.99726080 4	3.39129E-05
No	G	SAUSA300_RS01655	SAUSA300_0310		PTS sugar transporter subunit IIC	199.8	211.88	18.38	16.98	1.99385926 9	2.98069E-05
No	F	SAUSA300_RS08440	SAUSA300_1548		ComE operon protein 2	230.34	236.89	32.44	12.64	1.99284589 6	1.8413E-05
No	U	SAUSA300_RS01840	SAUSA300_0347	*tatC*	twin-arginine translocase subunit TatC	61.7	80.23	7.46	5.44	1.98803162 2	5.55484E-05
No	F	SAUSA300_RS04970	SAUSA300_0925		bifunctional UDP-sugar hydrolase/5'-nucleotidase	70.4	56.56	7.76	3.92	1.98304419	2.60656E-06
No	C	SAUSA300_RS10400	SAUSA300_1900		manganese-dependent inorganic pyrophosphatase	854.14	452.11	66.92	43.79	1.98124896 3	1.27114E-06
No	M	SAUSA300_RS09320	SAUSA300_1707		class I SAM-dependent methyltransferase	51.74	21.28	3.4	2.51	1.96669127 6	1.96223E-05

Table A-1 (cont'd)

No	not classified	SAUSA300_RS07840			hypothetical protein	72.01	53.27	8.65	3.28	1.95939362	1.45055E-05
No	K	SAUSA300_RS12705	SAUSA300_2300		TetR/AcrR family transcriptional regulator	50.55	52.78	7.6	2.72	1.95372136 1	5.72942E-05
No	no homolog found	SAUSA300_RS10510			hypothetical protein	306.82	241.94	34.91	17.01	1.9456827	5.37206E-06
No	E	SAUSA300_RS03805	SAUSA300_0708	*hisC*	histidinol-phosphate transaminase	26.35	26.04	2.54	2.17	1.93737263 9	4.40003E-05
No	K	SAUSA300_RS10810	SAUSA300_1969		XRE family transcriptional regulator	87.88	65.87	8.1	5.72	1.93713986 5	5.50702E-06
No	S	SAUSA300_RS10720	SAUSA300_1954		SA1788 family PVL leukocidin-associated protein	30.01	14.97	1.56	1.94	1.93612980 5	0.00023856 8
No	not classified	SAUSA300_RS03655	SAUSA300_0681		hypothetical protein	59.26	52.14	9.23	2.23	1.93325251	0.00020353 1
No	not classified	SAUSA300_RS10790	SAUSA300_1967		hypothetical protein	162.06	89.91	8.02	11.61	1.92750194	0.00019246 9
No	S	SAUSA300_RS09830	SAUSA300_1796		DUF445 domain-containing protein	50.05	35.16	6.33	2.14	1.90947471 3	2.70534E-05

Table A-1 (cont'd)

No	C	SAUSA300_RS13655	SAUSA300_2462		NAD(P)H-dependent oxidoreductase	59.66	47.8	5.09	4.51	1.90898717	2.77905E-05
No	K	SAUSA300_RS13640	SAUSA300_2459		MarR family transcriptional regulator	54.31	68.16	6.7	5	1.90846815	0.00012736
No	no homolog found	SAUSA300_RS10690			hypothetical protein	27.4	11.26	1.36	1.64	1.89976769	0.00081940
No	no homolog found	SAUSA300_RS04435			chorismate mutase	16.94	14.48	2.25	0.78	1.89064755	0.00238163
No	S	SAUSA300_RS12415	SAUSA300_2249		CHAP domain-containing protein	278.53	305.02	40.58	19.23	1.88681090	4.0952E-05
No	K	SAUSA300_RS12490	SAUSA300_2261		YafY family protein	183.26	148.19	22.38	10.7	1.88031699	9.83299E-06
Yes	EH	SAUSA300_RS11940	SAUSA300_2166	*alsS*	acetolactate synthase AlsS	15.3	12.12	1.39	1.14	1.88018716	3.39129E-05
No	S	SAUSA300_RS11480	SAUSA300_2085		DUF2750 domain-containing protein	188.89	109.31	21.61	7.96	1.87505992	1.85888E-05
No	no homolog found	SAUSA300_RS15825			transposase	21.6	19.82	2.97	1.22	1.87495478	0.00018818

Table A-1 (cont'd)

No	S	SAUSA300_RS03180	SAUSA300_0592		HD domain-containing protein	87.98	34.06	7.72	3.52	1.87209845	3.08519E-05
No	P	SAUSA300_RS12660	SAUSA300_2291	*gltS*	sodium/glutamate symporter	13.27	14.67	1.4	1.25	1.86267898	0.00020641
No	no homolog found	SAUSA300_RS13775			hypothetical protein	241.28	321.89	39.21	19.85	1.86251965	0.00019993
No	S	SAUSA300_RS12535	SAUSA300_2267		HAD family hydrolase	74.01	62.21	6.97	5.85	1.85344532	4.18114E-05
No	S	SAUSA300_RS02940	SAUSA300_0551	*folE2*	GTP cyclohydrolase FolE2	188.03	166.43	26.63	10.78	1.84228825	3.59856E-05
Yes	I	SAUSA300_RS02535	SAUSA300_0472	*ispE*	4-(cytidine 5'-diphospho)-2-C-methyl-D-erythritol kinase	72.98	23.43	6.6	2.45	1.83943461	0.00020557
No	no homolog found	SAUSA300_RS15405			transposase	11.47	10.09	1.97	0.27	1.83480243	0.00834528
No	M	SAUSA300_RS03450	SAUSA300_0643		GNAT family N-acetyltransferase	146.82	184.16	24.03	11.53	1.83451461	0.00015266
No	no homolog found	SAUSA300_RS05725			hypothetical protein	12.01	23.82	2.28	1.46	1.81410521	0.00663641

Table A-1 (cont'd)

Yes	S	SAUSA300_RS02775	SAUSA300_0518		NYN domain-containing protein	94.09	45.85	7.92	5.27	1.81107936	2.63534E-05
Yes	L	SAUSA300_RS02485	SAUSA300_0463	*yabA*	DNA replication initiation control protein YabA	67.87	30.67	6.61	3.03	1.80870223	7.18461E-05
Yes	S	SAUSA300_RS10760	SAUSA300_1962		DUF1108 family protein	84.77	40.92	5	5.87	1.80493507	0.00034324
Yes	P	SAUSA300_RS11750	SAUSA300_2134		iron chelate uptake ABC transporter family permease subunit	70.34	52.01	7.99	4.49	1.80470979	1.63142E-05
No	U	SAUSA300_RS04110	SAUSA300_0762	*secG*	preprotein translocase subunit SecG	1586.21	2144.2	307.22	117.39	1.80140828	0.00037516
No	not classified	SAUSA300_RS03445	SAUSA300_0642		hypothetical protein	91.32	111.61	14.26	7.69	1.79994223	0.00019357
No	S	SAUSA300_RS09490	SAUSA300_1736	*yidD*	membrane protein insertion efficiency factor YidD	380.37	535.45	59.17	38.66	1.79811070	0.00033496
No	K	SAUSA300_RS00590	SAUSA300_0114	*sarS*	HTH-type transcriptional regulator SarS	195.79	230.61	28.5	16.99	1.79779920	0.00013022
No	J	SAUSA300_RS08660	SAUSA300_1589	*dtd*	D-aminoacyl-tRNA deacylase	289.09	115.86	30.19	10.56	1.79491439	0.00013212

Table A-1 (cont'd)

No	not classified	SAUSA300_RS05730		hypothetical protein	28.78	53.13	6.28	3.01	1.78487629	0.00212483
No	not classified	SAUSA300_RS02080	SAUSA300_0390	hypothetical protein	29.79	23.44	3.52	1.99	1.78421963	7.18371E-05
No	no homolog found	SAUSA300_RS09565		hypothetical protein	18.04	13.46	2.79	0.53	1.77864316	0.01112162
No	J	SAUSA300_RS05325	SAUSA300_0989	ribonuclease J	663.64	360.39	72.69	33.59	1.76703865	2.03189E-05
No	not classified	SAUSA300_RS15095	SAUSA300_0428	hypothetical protein	14.83	29.95	3.6	1.61	1.76358423	0.00312662
No	P	SAUSA300_RS08160	SAUSA300_1495	rhodanese-like domain-containing protein	427.18	610.36	90.88	32.37	1.75862165	0.00076924
No	EGP	SAUSA300_RS13160	SAUSA300_2379	multidrug effflux MFS transporter	156.44	203.53	24.91	14.93	1.75802937	0.0002983
No	S	SAUSA300_RS02905	SAUSA300_0544	Cof-type HAD-IIB family hydrolase	48.43	31.25	5.62	2.78	1.75643502	3.30869E-05
No	not classified	SAUSA300_RS06935	SAUSA300_1277	hypothetical protein	67.91	81.45	10.89	5.74	1.75615137	0.00031422

Table A-1 (cont'd)

Yes	H	SAUSA300_RS14190	SAUSA300_2553		NAD(P)-binding protein	203.83	96.11	18.93	11	1.75313600 4	3.25669E-05
No	no homolog found	SAUSA300_RS15500			hypothetical protein	55.39	32.86	3	4.8	1.74317271 4	0.00158401 6
No	S	SAUSA300_RS03715	SAUSA300_0692		DoxX family protein	1484.7	458.67	124.72	63.56	1.74307573 6	0.00023661 5
No	S	SAUSA300_RS10750	SAUSA300_1960		recombinase RecT	66.81	40.57	4.92	5.27	1.73720398 3	0.00022483 7
No	no homolog found	SAUSA300_RS16000			minor capsid protein	17.86	28.08	3.59	1.78	1.72709674 7	0.00145406 5
No	S	SAUSA300_RS10675	SAUSA300_1946		transcriptional activator RinB	62.75	25.43	3.59	4.26	1.71952293 7	0.00179340 4
No	not classified	SAUSA300_RS10755	SAUSA300_1961		AAA family ATPase	48.5	27.36	3.34	3.81	1.71937548 4	0.00033738 4
No	E	SAUSA300_RS00985	SAUSA300_0188	*brnQ*	branched-chain amino acid transport system II carrier protein	97.47	106.11	13.61	8.9	1.71926991 3	0.00019993 9
No	X	SAUSA300_RS09695	SAUSA300_1771		DUF1828 domain-containing protein	48.56	53.25	8.13	3.69	1.71646918 3	0.00029813 1

Table A-1 (cont'd)

Yes	JKL	SAUSA300_RS08285	SAUSA300_1518		DEAD/DEAH box helicase	39.64	11.31	3.57	1.51	1.71413596	0.00073575
No	U	SAUSA300_RS01845	SAUSA300_0348		twin-arginine translocase TatA/TatE family subunit	61.35	67.04	7.49	6.3	1.70474902	0.00068447
No	P	SAUSA300_RS13050	SAUSA300_2363		cation diffusion facilitator family transporter	43.89	25.19	4.28	2.9	1.69930836	7.18461E-05
No	S	SAUSA300_RS13005	SAUSA300_2355		DUF4467 domain-containing protein	46.01	18.06	5.14	1.73	1.69673033	0.00083523
No	no homolog found	SAUSA300_RS15635	SAUSA300_2510		hypothetical protein	101.3	126.94	15.17	10.59	1.69439063	0.00055602
Yes	J	SAUSA300_RS06190	SAUSA300_1144	*trmFO*	methylenetetrahydrofolate--tRNA-(uracil(54)- C(5))-methyltransferase (FADH(2)-oxidizing) TrmFO	172.3	69.25	15.26	9.33	1.68727586	0.00012027
No	not classified	SAUSA300_RS06490			hypothetical protein	47.73	33.75	7.87	1.84	1.68468911	0.00193069
No	P	SAUSA300_RS11760	SAUSA300_2136		Fe(3+) dicitrate ABC transporter substrate-binding protein	188.92	91.93	24.06	7.65	1.68342459	0.00031422

Table A-1 (cont'd)

No	P	SAUSA300_RS13020	SAUSA300_2358		amino acid ABC transporter permease	220.04	59.36	11.75	13.04	1.681138635	0.00193244 6
No	I	SAUSA300_RS12345	SAUSA300_2236		acyl-CoA dehydrogenase family protein	97.08	73.56	5.7	10.29	1.676211053	0.00272435 4
No	S	SAUSA300_RS11025	SAUSA300_2005	*tsaE*	tRNA (adenosine(37)-N6)-threonylcarbamoyltransferase complex ATPase subunit type 1 TsaE	20.13	12.47	2.89	0.87	1.669732628	0.00109692 4
No	not classified	SAUSA300_RS11740	SAUSA300_2132		hypothetical protein	150.93	368.82	38.3	25.11	1.664578512	0.00555708 9
No	not classified	SAUSA300_RS15975	SAUSA300_0768		hypothetical protein	39.53	26.78	5.21	2.27	1.662988147	0.00111993 6
No	no homolog found	SAUSA300_RS15905			hypothetical protein	96.84	155.02	20.88	10.19	1.660536919	0.00227024 5
No	not classified	SAUSA300_RS06930			hypothetical protein	74.61	86.51	12.43	6.67	1.657178493	0.00080940 9
No	C	SAUSA300_RS12870	SAUSA300_2329		cation:dicarboxylase symporter family transporter	292.5	208.56	35.5	20.85	1.656153848	5.82762E-05

Table A-1 (cont'd)

No	S	SAUSA300_RS05405	SAUSA300_1004		DUF4064 domain-containing protein	194.91	240.49	38.37	15.77	1.655269727	0.000806909
No	S	SAUSA300_RS11450	SAUSA300_2080		DUF2529 domain-containing protein	57.9	48.55	9.91	3.17	1.64893889 6	0.000645819
No	no homolog found	SAUSA300_RS13480		*scrA*	SaeRS system activator ScrA	34.34	33.12	6.55	1.89	1.647152432	0.001974267
No	E	SAUSA300_RS13195	SAUSA300_2385		APC family permease	67.76	60.73	10.37	5.01	1.639351855	0.000195078
No	not classified	SAUSA300_RS10680	SAUSA300_1947		hypothetical protein	40.26	14.33	1.6	3.16	1.632325486	0.007859125
No	no homolog found	SAUSA300_RS12995			hypothetical protein	32.75	11.74	2.79	1.63	1.632135188	0.009310501
No	T	SAUSA300_RS09390	SAUSA300_1719	*arsC*	arsenate reductase (thioredoxin)	33.91	24.06	3.97	2.54	1.631256399	0.000335618
No	K	SAUSA300_RS09835	SAUSA300_1797		helix-turn-helix transcriptional regulator	111.03	110.62	24.08	5.11	1.627429772	0.003237722
No	S	SAUSA300_RS03940	SAUSA300_0732		YigZ family protein	60.53	52.27	9.99	3.9	1.626131423	0.000409 56

Table A-1 (cont'd)

Yes	I	SAUSA300_RS08990	SAUSA300_1647	*accD*	acetyl-CoA carboxylase, carboxyltransferase subunit β	73.89	17.53	6.93	2.7	1.623180772	0.00277458 9
No	T	SAUSA300_RS11395	SAUSA300_2069		low molecular weight protein arginine phosphatase	58.8	37.2	7.65	3.56	1.619684593	0.00022134 3
No	S	SAUSA300_RS03185	SAUSA300_0593		YwhD family protein	270.65	186.92	38.43	16.36	1.619222156	0.00015636 6
Yes	C	SAUSA300_RS00940	SAUSA300_0179		NAD-dependent formate dehydrogenase	25.32	13.8	1.88	2.09	1.616894033	0.00101738 8
No	EG	SAUSA300_RS13720	SAUSA300_2472		DMT family transporter	28.16	27.58	3.54	2.84	1.610332368	0.00069870 3
No	L	SAUSA300_RS11145	SAUSA300_2026		type II toxin-antitoxin system PemK/MazF family toxin	303.07	267.28	49.84	21.14	1.603507244	0.00034227 3
No	no homolog found	SAUSA300_RS05670	SAUSA300_1052	*ecb*	complement convertase inhibitor Ecb	624.16	640.92	114.79	46.23	1.603235623	0.00062243 9
No	not classified	SAUSA300_RS03725	SAUSA300_0694		hypothetical protein	53.58	55.47	8.89	4.56	1.601717115	0.00059348 8
No	S	SAUSA300_RS14600	SAUSA300_2628	*rarD*	EamA family transporter RarD	14.96	16.43	2.48	1.38	1.595719717	0.00111013 6

Table A-1 (cont'd)

No	Znot classified	SAUSA300_RS07320	SAUSA300_1342		hypothetical protein	72.6	56.24	12.22	4.04	1.59394347	0.00084922
No	O	SAUSA300_RS04430	SAUSA300_0822	*sufB*	Fe-S cluster assembly protein SufB	488.44	407.95	58.61	44.74	1.59229723	0.00028978
No	Znot classified	SAUSA300_RS06715			DNA damage-induced cell division inhibitor SosA	24.94	36.32	6.61	1.74	1.58958277	0.00785912
No	Znot classified	SAUSA300_RS05685	SAUSA300_1054		hypothetical protein	61.87	109.79	15.22	7.48	1.57969408	0.00418745
No	S	SAUSA300_RS05000	SAUSA300_0931		YkvS family protein	412.01	333.02	75.98	21.64	1.57245449	0.00141517
Yes	J	SAUSA300_RS08600	SAUSA300_1578	*mnmA*	tRNA 2-thiouridine(34) synthase MnmA	108.1	45.93	12.87	5.2	1.57114724	0.00053436
No	S	SAUSA300_RS02480	SAUSA300_0462		stage 0 sporulation family protein	40.16	15.18	4.94	1.62	1.56143048	0.00191110
No	S	SAUSA300_RS10670	SAUSA300_1945		DUF1514 family protein	77.39	22.66	4.25	5.4	1.54910709	0.00755492
No	E	SAUSA300_RS12515	SAUSA300_2265		amino acid permease	177.98	165.92	26.76	16.09	1.54863797	0.00044467

Table A-1 (cont'd)

No	S	SAUSA300_RS09795	SAUSA300_1789		DUF3267 domain-containing protein	10.34	15.83	3	0.73	1.54451003 6	0.01168031 6
No	J	SAUSA300_RS04835	SAUSA300_0897	*trpS*	tryptophan--tRNA ligase	176.94	72.64	18.67	10.16	1.53692679 2	0.00047404 1
No	S	SAUSA300_RS09125	SAUSA300_1671		HAD family hydrolase	181.18	51.06	17.44	8.69	1.52279607 8	0.0022461
Yes	I	SAUSA300_RS08985	SAUSA300_1646		acetyl-CoA carboxylase carboxyltransferase subunit α	161.64	40.81	12.76	8.77	1.52033318 9	0.00343958 9
No	S	SAUSA300_RS10420	SAUSA300_1903		YolD-like family protein	23.55	16.87	2.47	2.22	1.51751130 6	0.00211311 7
No	K	SAUSA300_RS12900	SAUSA300_2336		MerR family transcriptional regulator	16.05	19.11	3.28	1.46	1.51576496 1	0.00301818 5
Yes	E	SAUSA300_RS11035	SAUSA300_2006	*ilvD*	dihydroxy-acid dehydratase	77.99	73.24	6.57	10.21	1.50812546 9	0.00630868 1
No	G	SAUSA300_RS01790	SAUSA300_0337	*glpT*	glycerol-3-phosphate transporter	19.07	18.53	2.83	1.92	1.50748102 1	0.00121541

Table A-1 (cont'd)

No	K	SAUSA300_RS12510	SAUSA300_2264		MurR/RpiR family transcriptional regulator	189.99	121.53	26.15	13.14	1.50609563	0.00029813
No	KT	SAUSA300_RS08665	SAUSA300_1590		bifunctional (p)ppGpp synthetase/guanosine-3',5'-bis(diphosphate) 3'-pyrophosphohydrolase	78.57	29.84	8.98	4.03	1.50334361	0.00105211
Yes	S	SAUSA300_RS03690	SAUSA300_0687		hemolysin family protein	264.2	76.41	25.64	13.21	1.50265353	0.00227024
No	E	SAUSA300_RS10305	SAUSA300_1883	*putP*	sodium/proline symporter PutP	94.24	79.08	13	8.77	1.49832046	0.00058324
No	M	SAUSA300_RS08655	SAUSA300_1588		N-acetylmuramoyl-L-alanine amidase	186.42	93.69	26.29	9.52	1.49789991	0.00093835
No	no homolog found	SAUSA300_RS05040	SAUSA300_0938		hypothetical protein	24.21	13.03	4.33	0.65	1.49691738	0.01616133

Table A-1 (cont'd)

No	M	SAUSA300_RS03340	SAUSA300_0623		N-acetylglucosaminyldiphosphoundecaprenol N-acetyl-β-D-mannosaminyltransferase TarA	51.13	36.6	8.93	2.93	1.49017036	0.001615193
No	M	SAUSA300_RS05045	SAUSA300_0939		glycosyltransferase	47.35	29.22	7.63	2.56	1.48518234 2	0.001287735
Yes	S	SAUSA300_RS13755	SAUSA300_2479	*cidA*	holin-like murein hydrolase modulator CidA	13.21	14.08	2.19	1.36	1.48383005 5	0.005137741
No	not classified	SAUSA300_RS03635			hypothetical protein	181.71	149.03	36.03	10.23	1.48321901 8	0.002886031
No	S	SAUSA300_RS06050	SAUSA300_1118		Asp23/Gls24 family envelope stress response protein	161.02	67.71	24.19	5.77	1.48178445 7	0.005286269
No	K	SAUSA300_RS01375	SAUSA300_0258		GntR family transcriptional regulator	103.76	66.51	15.49	6.75	1.48053195 4	0.000590547
No	S	SAUSA300_RS10665	SAUSA300_1944		hypothetical protein	135.26	80.61	12.3	12.55	1.47637346 9	0.001746908
Yes	S	SAUSA300_RS00020	SAUSA300_0003	*yaaA*	S4 domain-containing protein YaaA	449.75	303.91	65.56	32.56	1.47216923	0.000467088

Table A-1 (cont'd)

No	no homolog found	SAUSA300_RS05780			hypothetical protein	23.86	11.79	3.42	1.14	1.4708668898	0.00984594 2
No	K	SAUSA300_RS08625	SAUSA300_1583		Rrf2 family transcriptional regulator	182.36	158.87	34.91	12.67	1.4662710 28	0.00174379 6
No	S	SAUSA300_RS13610	SAUSA300_2454		ABC transporter permease	136.9	240.33	33.92	19.38	1.4614452 06	0.00755863 4
No	E	SAUSA300_RS09110	SAUSA300_1669		alanine--glyoxylate aminotransferase family protein	61.48	47.37	8.48	5.52	1.4583752 86	0.00071171 6
No	DZ	SAUSA300_RS10915	SAUSA300_1985		SdrH family protein	71.79	43.47	10.37	4.75	1.4561889 72	0.00062267 1
No	J	SAUSA300_RS08250	SAUSA300_1511	*rpmG*	50S ribosomal protein L33	2136.37	2911.45	611.49	156.7	1.4543599 43	0.00963741 5
Yes	L	SAUSA300_RS07130	SAUSA300_1309	*tnpA*	IS200/IS605 family transposase	149.18	117.55	18.98	14.74	1.4500266 57	0.00112153 7
No	S	SAUSA300_RS10785	SAUSA300_1966		phage antirepressor KilAC domain-containing protein	93.28	54.55	7.6	9.22	1.4499373 81	0.00361269 5

Table A-1 (cont'd)

Yes	H	SAUSA300_RS11040	SAUSA300_2007	*ilvB*	biosynthetic-type acetolactate synthase large subunit	32	28.37	3.48	3.85	1.44732409	0.00380994
No	no homolog found	SAUSA300_RS16075	SAUSA300_1325		hypothetical protein	58.59	74.56	11.9	6.59	1.4448954	0.00636126
No	S	SAUSA300_RS13650	SAUSA300_2461		VOC family protein	37.41	45.32	6.17	4.81	1.44303479	0.00414988
No	not classified	SAUSA300_RS04200	SAUSA300_0779		hypothetical protein	35.52	18.55	4.6	2.3	1.44099013	0.00258444
No	J	SAUSA300_RS06460	SAUSA300_1196	*hfq*	RNA chaperone Hfq	173.2	145.91	27.04	15.61	1.4408706	0.00110529
No	S	SAUSA300_RS04405	SAUSA300_0817		DUF368 domain-containing protein	68.46	74	11.14	7.88	1.43957636	0.00247351
No	not classified	SAUSA300_RS06510	SAUSA300_1204		hypothetical protein	13.37	15.09	2.66	1.27	1.4369496	0.01668044
No	no homolog found	SAUSA300_RS13785			hypothetical protein	68.92	92.59	18.19	6	1.4358146	0.00835562
No	G	SAUSA300_RS14335	SAUSA300_2577	*manA*	mannose-6-phosphate isomerase, class I	36.49	42.77	6.4	4.35	1.4347801	0.00340078

Table A-1 (cont'd)

No	K	SAUSA300_RS08905	SAUSA300_1632	*nrdR*	transcriptional regulator NrdR	121.18	54.72	15.69	6.99	1.43159773	0.00142500 6
No	J	SAUSA300_RS00420	SAUSA300_0082		tRNA-dihydrouridine synthase	36.49	14.62	3.37	2.66	1.42455196 8	0.00386172 9
No	H	SAUSA300_RS14050	SAUSA300_2532		aspartate 1-decarboxylase	55.14	49.81	9.29	5.09	1.42353577	0.00196699 3
Yes	C	SAUSA300_RS00280	SAUSA300_0055		zinc-dependent alcohol dehydrogenase family protein	129.55	78.69	8.73	14.51	1.41652421 7	0.01012381 3
Yes	E	SAUSA300_RS02755	SAUSA300_0514	*cysE*	serine O-acetyltransferase	43.79	18.54	5.02	2.82	1.41436425 8	0.00203345 8
No	G	SAUSA300_RS14330	SAUSA300_2576		PTS fructose transporter subunit IIABC	96.44	137.23	16.91	14.84	1.40624172 8	0.00799770 6
No	S	SAUSA300_RS12620	SAUSA300_2284		MOSC domain-containing protein	28.14	19.23	4.05	2.32	1.39918894 2	0.00167506 2
No	S	SAUSA300_RS11745	SAUSA300_2133		YjiH family protein	43.93	48.18	7.17	5.41	1.39603756 1	0.00384165 3
No	not classified	SAUSA300_RS12530			hypothetical protein	245.37	316.22	40.84	35.72	1.38884351 3	0.00756597 2
No	M	SAUSA300_RS02345	SAUSA300_0438	*aaa*	autolysin/adhesin Aaa	171.67	92.28	23.93	11.67	1.38759625 6	0.00105315

Table A-1 (cont'd)

No	S	SAUSA300_RS05005	SAUSA300_0932		CPBP family glutamic-type intramembrane protease	285.94	286	70.5	18.18	1.38510093	0.00877972
No	S	SAUSA300_RS12650	SAUSA300_2289		DUF805 domain-containing protein	42.42	44.88	7.92	4.54	1.38311275 1	0.00362052 2
No	no homolog found	SAUSA300_RS09120			hypothetical protein	213.73	78.28	26.86	11.41	1.37549677	0.00573130 2
No	P	SAUSA300_RS06475	SAUSA300_1199		aminotransferase class I/II-fold pyridoxal phosphate-dependent enzyme	24.91	20.2	3.62	2.52	1.37023067 8	0.00229806 1
No	M	SAUSA300_RS09260	SAUSA300_1695		phosphotransferase family protein	284.6	127.69	42.69	14.61	1.36990349 4	0.00365029 5
No	S	SAUSA300_RS10150	SAUSA300_1858	*yfkAB*	radical SAM/CxCxxxxC motif protein YfkAB	35.64	15.8	4.29	2.44	1.36522991 8	0.00227024 5
No	S	SAUSA300_RS12735	SAUSA300_2304		YdcF family protein	404.74	329.84	78.14	30.52	1.36443482 4	0.00254971 5
No	K	SAUSA300_RS06710	SAUSA300_1237	*lexA*	transcriptional repressor LexA	471.54	387.51	73.52	46.5	1.35965185	0.00170079 1

Table A-1 (cont'd)

No	J	SAUSA300_RS10095	SAUSA300_1848		DUF402 domain-containing protein	141.98	105.94	24.03	11.53	1.35810847	0.00171715
No	P	SAUSA300_RS05250	SAUSA300_0977		energy-coupling factor transporter transmembrane protein EcfT	13.13	12.19	2.24	1.35	1.3541714	0.00516210
No	M	SAUSA300_RS06755	SAUSA300_1244	*mscL*	large conductance mechanosensitive channel protein MscL	1290.88	1343.27	288.63	114.56	1.35085586	0.00480331
No	S	SAUSA300_RS11535	SAUSA300_2094		EVE domain-containing protein	87.56	60.64	14.48	6.79	1.35040686	0.00161872
Yes	G	SAUSA300_RS11545	SAUSA300_2096		class I mannose-6-phosphate isomerase	49.11	21.43	6.21	3.22	1.34811544	0.00267915
No	S	SAUSA300_RS12440	SAUSA300_2253		CHAP domain-containing protein	160.5	164.41	35.71	14.09	1.34651571	0.00513774
Yes	E	SAUSA300_RS02380	SAUSA300_0445	*gltB*	glutamate synthase large subunit	78.5	37.18	8.79	6.24	1.34566566	0.00201178
No	EGP	SAUSA300_RS13275	SAUSA300_2397		MFS transporter	30.51	24.01	3.1	3.82	1.34295767	0.00919007
No	F	SAUSA300_RS08670	SAUSA300_1591		adenine phosphoribosyltransferase	129.76	56.52	17.86	7.75	1.3417588	0.00321031

Table A-1 (cont'd)

No	H	SAUSA300_RS13220	SAUSA300_2388		2-dehydropantoate 2-reductase	37.75	19.42	4.78	2.92	1.339121204	0.002241516
Yes	J	SAUSA300_RS02770	SAUSA300_0517	*rlmB*	23S rRNA (guanosine(2251)-2'-O)-methyltransferase RlmB	35.86	12.43	3.87	2.32	1.338191718	0.006297465
No	M	SAUSA300_RS11485	SAUSA300_2086		hypothetical protein	31.57	17.72	4.62	2.29	1.335272429	0.002131744
Yes	V	SAUSA300_RS09580	SAUSA300_1751		restriction endonuclease subunit S	23.34	11.7	3.67	1.37	1.323031408	0.004931537
No	J	SAUSA300_RS01950	SAUSA300_0368	*rpsR*	30S ribosomal protein S18	1193.48	1377.16	211.7	160.76	1.320528403	0.006936416
No	G	SAUSA300_RS09395	SAUSA300_1720		N-acetylglucosaminidase	230.74	155.28	44.78	14.16	1.319494047	0.005285517
No	not classified	SAUSA300_RS10230	SAUSA300_1871		hypothetical protein	11.21	17.89	3.44	1.26	1.317955911	0.027988599
No	not classified	SAUSA300_RS04135	SAUSA300_0767		hypothetical protein	21.31	28.68	5.26	2.52	1.316636742	0.016108155
No	K	SAUSA300_RS12325	SAUSA300_2232		GNAT family N-acetyltransferase	24.73	12.98	3.13	2	1.312803711	0.003773251

Table A-1 (cont'd)

No	F	SAUSA300_RS05970	SAUSA300_1102	*gmk*	guanylate kinase	204.42	96.8	33.1	11.1	1.30589543 2	0.00587962 2
No	no homolog found	SAUSA300_RS11885			hypothetical protein	26.46	27.79	5.32	2.82	1.30440647 1	0.01655111 3
No	P	SAUSA300_RS04300	SAUSA300_0796		methionine ABC transporter ATP-binding protein	38.65	25.81	4.9	3.94	1.30035872 9	0.00386172 9
No	L	SAUSA300_RS08430	SAUSA300_1546	*holA*	DNA polymerase III subunit delta	19.83	15.23	4.28	1.24	1.29889407 5	0.01057318
No	L	SAUSA300_RS05345	SAUSA300_0992		YkyA family protein	196.76	166.27	45.06	13.18	1.29723529 3	0.00934947 6
No	P	SAUSA300_RS04955	SAUSA300_0922		TerC family protein	173.37	172.35	34.48	18.67	1.28411193 6	0.00516210 3
No	F	SAUSA300_RS08550	SAUSA300_1568	*udk*	uridine kinase	149.76	58.64	23.67	7.14	1.27660253 4	0.01190017
No	S	SAUSA300_RS11735	SAUSA300_2131		metal-dependent hydrolase	79.04	54.84	13.23	6.8	1.27326640 5	0.00336443 1
No	G	SAUSA300_RS10415	SAUSA300_1902		beta-propeller fold lactonase family protein	152.96	54.17	16.85	10.86	1.27269841 4	0.00686438 2

Table A-1 (cont'd)

Yes	E	SAUSA300_RS11065	SAUSA300_2012	*leuC*	3-isopropylmalate dehydratase large subunit	20.69	10.39	2.56	1.75	1.27200293	0.00475079
No	F	SAUSA300_RS02075	SAUSA300_0389	*guaA*	glutamine-hydrolyzing GMP synthase	683.85	496.37	131.34	52.41	1.271320228	0.00419132
No	J	SAUSA300_RS06455	SAUSA300_1195	*miaA*	tRNA (adenosine(37)-N6)-dimethylallyltransferaseMiaA	50.03	41.51	10.21	4.29	1.25800725	0.00603220
No	S	SAUSA300_RS05865	SAUSA300_1082		YggS family pyridoxal phosphate-dependent enzyme	90.45	18.25	10.67	4.05	1.25707792	0.03228346
No	S	SAUSA300_RS07195	SAUSA300_1321		bacilliredoxin BrxA	158.7	182.24	33.62	19.98	1.25426703	0.00959696
No	S	SAUSA300_RS03545	SAUSA300_0660		DUF456 domain-containing protein	63.61	94.19	15.26	9.91	1.24973368	0.01893260
No	S	SAUSA300_RS01810	SAUSA300_0341		YeiH family protein	21.29	24.82	4.46	2.77	1.24874336	0.01210829
No	A	SAUSA300_RS02045	SAUSA300_0383		hypothetical protein	158.2	100.1	29.15	11.23	1.24777189	0.00528551

Table A-1 (cont'd)

No	S	SAUSA300_RS03610	SAUSA300_0673		GTP-binding protein	71.89	81.92	14.82	9.38	1.240629169	0.010466966
No	S	SAUSA300_RS13395	SAUSA300_2420		DUF1433 domain-containing protein	12.45	10.01	2.93	0.79	1.233584658	0.029958322
No	F	SAUSA300_RS08180	SAUSA300_1499		shikimate kinase	84.65	84.64	16.47	10.07	1.232984508	0.008390269
No	G	SAUSA300_RS06435	SAUSA300_1191		MIP/aquaporin family protein	61.75	77.99	15.24	7.79	1.229988934	0.014537716
No	S	SAUSA300_RS05690	SAUSA300_1055	*efb*	complement convertase inhibitor Efb	157.64	51.02	21.7	8.61	1.229128562	0.014774272
No	O	SAUSA300_RS06465	SAUSA300_1197		glutathione peroxidase	257.37	246.94	51.13	28.85	1.227608328	0.007125036
No	K	SAUSA300_RS03605	SAUSA300_0672	*mgrA*	HTH-type transcriptional regulator MgrA	10215.53	6639.23	2075.02	663.12	1.226514155	0.009413098
No	no homolog found	SAUSA300_RS10805			transcriptional regulator	51.87	51.53	7.93	7.37	1.224012267	0.019717755
No	not classified	SAUSA300_RS03240	SAUSA300_0603		hypothetical protein	79.8	57.29	13.22	7.76	1.224009055	0.004623973

Table A-1 (cont'd)

Yes	L	SAUSA300_RS08900	SAUSA300_1631		replication initiation and membrane attachment family protein	38.67	10.3	4.78	2.11	1.22085193	0.02188066
No	H	SAUSA300_RS12260	SAUSA300_2219	*moaA*	GTP 3',8-cyclase MoaA	39.26	17.5	5.65	2.78	1.21572261	0.00755863
No	V	SAUSA300_RS13605	SAUSA300_2453		ATP-binding cassette domain-containing protein	58.55	53.07	13.06	5.48	1.20461912	0.01041708
No	S	SAUSA300_RS03525	SAUSA300_0657		DUF402 domain-containing protein	52.73	29.16	8.59	4.1	1.19855853	0.00687217
Yes	H	SAUSA300_RS11050	SAUSA300_2009	*ilvC*	ketol-acid reductoisomerase	20.65	13.93	3.04	2.17	1.19636089	0.00842999
No	no homolog found	SAUSA300_RS08890			hypothetical protein	904.28	1279.89	302.92	93.32	1.19340428	0.03261905
No	K	SAUSA300_RS10800			helix-turn-helix transcriptional regulator	67.8	50.72	8.01	9.05	1.17865765	0.02229163
No	S	SAUSA300_RS05695	SAUSA300_1056	*scb*	complement inhibitor SCIN-B	191.45	101.47	33.86	13.22	1.17521708	0.00995154

Table A-1 (cont'd)

No	no homolog found	SAUSA300_RS07845			hypothetical protein	246.16	171.27	42.45	24.01	1.16813638 2	0.00757869
No	H	SAUSA300_RS09465	SAUSA300_1730	*metK*	methionine adenosyltransferase	222.55	164.99	40.92	21.89	1.16711073 5	0.00659009 3
No	not classified	SAUSA300_RS04215			hypothetical protein	50.22	48.82	12.3	4.8	1.16437255 2	0.02089623
Yes	E	SAUSA300_RS06640	SAUSA300_1225		aspartate kinase	36.67	21.13	6.66	2.77	1.15905377 4	0.00989382 8
No	S	SAUSA300_RS03995			CsbA family protein	23.37	25.11	6.84	1.88	1.15873752 3	0.04602923 6
No	S	SAUSA300_RS13320	SAUSA300_2405		CPBP family lipoprotein N-acylation protein LnsB	33.91	42.42	9.76	3.9	1.15489972 7	0.02767165 6
No	S	SAUSA300_RS07045	SAUSA300_1296	*msaA*	regulatory protein MsaA	75.87	58.62	12.87	8.55	1.15377095 3	0.01111118 1
No	S	SAUSA300_RS02910	SAUSA300_0545		NADPH-dependent FMN reductase	152.82	129.63	31.42	15.85	1.15372675 8	0.00995980 9
No	G	SAUSA300_RS12460	SAUSA300_2256		N-acetylglucosaminidase	48.97	24.28	8.33	3.5	1.14208471 7	0.01278423 7

Table A-1 (cont'd)

No	J	SAUSA300_RS10300	SAUSA300_1882	*gatC*	Asp-tRNA(Asn)/Glu-tRNA(Gln) amidotransferase subunit GatC	31.63	21.33	7.42	1.88	1.13743769	0.03887032
No	K	SAUSA300_RS10060	SAUSA300_1842	*perR*	peroxide-responsive transcriptional repressor PerR	1089.67	1425.44	309.67	142.52	1.13366594	0.02712680
No	L	SAUSA300_RS08675	SAUSA300_1592	*recJ*	single-stranded-DNA-specific exonuclease RecJ	40.63	12.69	6.23	2.16	1.13289978	0.03154264
No	K	SAUSA300_RS14275	SAUSA300_2566		Crp/Fnr family transcriptional regulator	18.07	16.91	3.88	2.07	1.13104366	0.01959857
No	S	SAUSA300_RS00960	SAUSA300_0183		YagU family protein	669.07	851.03	107.16	130.92	1.12645836	0.04575790
No	S	SAUSA300_RS13310	SAUSA300_2403		DUF1307 domain-containing protein	328.56	390.16	88.57	40.57	1.12200643	0.02443578
No	S	SAUSA300_RS10795			DUF2829 domain-containing protein	125.16	72.27	12.11	15.99	1.11872981	0.03635245
No	T	SAUSA300_RS09085	SAUSA300_1665		GAF domain-containing protein	96.91	75.87	17.75	10.9	1.11569292	0.01201021

Table A-1 (cont'd)

No	K	SAUSA300_RS12805	SAUSA300_2318		GNAT family N-acetyltransferase	29.12	13.13	4.4	2.3	1.10893827	0.02372204
No	S	SAUSA300_RS03785	SAUSA300_0704		ABC-F family ATP-binding cassette domain-containing protein	24.76	10.19	4.31	1.49	1.10368294	0.02650557
No	not classified	SAUSA300_RS04195	SAUSA300_0778		hypothetical protein	49.17	23.9	7.52	4.14	1.10088045	0.02349894
No	no homolog found	SAUSA300_RS05705			hypothetical protein	99.57	68.67	18.39	9.88	1.10008968	0.01517820
No	F	SAUSA300_RS02070	SAUSA300_0388	*guaB*	IMP dehydrogenase	170.9	95.65	29.65	14.65	1.09977313	0.01046696
No	S	SAUSA300_RS13170	SAUSA300_2381		C39 family peptidase	53.1	56.51	11.8	7.28	1.09442907	0.02398781
No	S	SAUSA300_RS05400	SAUSA300_1003		DUF4064 domain-containing protein	817.4	399.26	125.95	70.47	1.09371469	0.01134414
No	EGP	SAUSA300_RS12235	SAUSA300_2217		MFS transporter	15.16	15.95	2.92	2.3	1.09329894	0.03063703
No	H	SAUSA300_RS14065	SAUSA300_2535		oxidoreductase	62.47	66.33	12.81	9.17	1.09234415	0.02500889

Table A-1 (cont'd)

No	M	SAUSA300_RS04935	SAUSA300_0918		diglucosyl diacylglycerol synthase	34.8	14.53	5.05	2.79	1.090026894	0.018530833
No	S	SAUSA300_RS11150		*mazE*	type II toxin-antitoxin system antitoxin MazE	333.34	355.51	89.76	37.35	1.084169038	0.028347204
No	O	SAUSA300_RS08835	SAUSA300_1621	*clpX*	ATP-dependent Clp protease ATP-binding subunit ClpX	247.41	76.03	33.69	16.79	1.082928586	0.03063703
No	U	SAUSA300_RS11265	SAUSA300_2046	*yidC*	membrane protein insertase YidC	346.25	176	61.76	26.6	1.081719129	0.01504576
No	S	SAUSA300_RS02370	SAUSA300_0443		YibE/F family protein	21.74	21.15	5.18	2.52	1.079125106	0.024601686
No	P	SAUSA300_RS03405	SAUSA300_0635		iron ABC transporter permease	148.02	109.39	25.24	17.57	1.078861474	0.014255404
No	J	SAUSA300_RS09255	SAUSA300_1694	*trmB*	tRNA (guanosine(46)-N7)-methyltransferase TrmB	192.66	112.86	41.54	13.17	1.073044375	0.026482251
No	E	SAUSA300_RS06675	SAUSA300_1231		amino acid permease	92.52	65.14	14.47	11.31	1.070536522	0.016926355
No	P	SAUSA300_RS08270	SAUSA300_1515		metal ABC transporter permease	29.89	18.53	4.3	3.46	1.068113848	0.021342355

Table A-1 (cont'd)

No	H	SAUSA300_RS08815	SAUSA300_1617	*hemC*	hydroxymethylbilane synthase	69.66	38.64	10.69	7	1.06752749	0.01465515
No	H	SAUSA300_RS04475	SAUSA300_0829	*lipA*	lipoyl synthase	609.92	403.17	94.8	72.1	1.05554954	0.01668044
No	S	SAUSA300_RS02950	SAUSA300_0553		YojF family protein	69.63	55.93	15.25	7.4	1.04538281	0.02336741
No	S	SAUSA300_RS10240	SAUSA300_1872		type 1 glutamine amidotransferase	84.42	34.78	13.93	6.27	1.03475426	0.02823519
No	E	SAUSA300_RS07930	SAUSA300_1452	*proC*	pyrroline-5-carboxylate reductase	70.76	53.81	12.44	8.94	1.03301388	0.02228597
No	K	SAUSA300_RS12730	SAUSA300_2303		MarR family transcriptional regulator	1378.09	1057.11	334.34	122.64	1.03220521	0.02767165
No	S	SAUSA300_RS02530	SAUSA300_0471		Veg family protein	1717.12	2224.68	498	260.61	1.01474517	0.04795060
No	S	SAUSA300_RS08290	SAUSA300_1519		Nif3-like dinuclear metal center hexameric protein	58.94	29.78	10.56	5.04	1.00720848	0.02443578
No	L	SAUSA300_RS10815	SAUSA300_1970		exonuclease domain-containing protein	39.35	29.05	9.36	3.58	1.0056324	0.03343446

Table A-1 (cont'd)

Genes downregulated in WT sulfur starvation when compared to WT CSSC

Shared with *cymR*::Tn -S (Table 3)	COG	Locus	Old locus	Gene	Product	TPM.1 Starv	TPM.2 Starv	TPM.1 CSSC	TPM.2 CSSC	DE Log_2 FC	DE Adj. *P*-value
No	F	SAUSA300_RS05215	SAUSA300_0970	*purQ*	phosphoribosylformylglycinamidine synthase I	0.86	0.22	40.41	23.03	-7.11186249	4.62044E-51
No	F	SAUSA300_RS05230	SAUSA300_0973	*purM*	phosphoribosylformylglycinamidine cyclo-ligase	0.77	0.13	29.22	21.31	-7.09625442	3.32562E-44
No	F	SAUSA300_RS05220	SAUSA300_0971	*purL*	phosphoribosylformylglycinamidine synthase subunit PurL	0.89	0.41	36.43	30.92	-7.03678370	1.5917E-61
Yes	F	SAUSA300_RS05210	SAUSA300_0969	*purS*	phosphoribosylformylglycinamidine synthase subunit PurS	1.35	0.49	72.1	33.02	-6.95103635	4.96882E-48
No	F	SAUSA300_RS05235	SAUSA300_0974	*purN*	phosphoribosylglycinamide formyltransferase	0.85	0.19	31.59	19.8	-6.89135605	1.59232E-44

Table A-1 (cont'd)

No	F	SAUSA300_RS05225	SAUSA300_0972	*purF*	amidophosphoribosyltransferase	1.31	0.57	38.02	34.89	-6.65596430 1	5.45843E-52
No	F	SAUSA300_RS05200	SAUSA300_0967	*purK*	5-(carboxyamino)imidazole ribonucleotide synthase	0.74	0.25	28.8	13.9	-6.65459084 2	8.32301E-50
No	F	SAUSA300_RS05240	SAUSA300_0975	*purH*	bifunctional phosphoribosylaminoimidazolecarboxamide formyltransferase /IMP cyclohydrolase	1.56	0.53	46.45	29.42	-6.51550422 8	1.99821E-51
No	F	SAUSA300_RS05205	SAUSA300_0968	*purC*	phosphoribosylaminoimidazolesuccinocarboxamide synthase	1	0.83	38.29	15.25	-5.98158317 1	1.23956E-41
Yes	F	SAUSA300_RS05245	SAUSA300_0976	*purD*	phosphoribosylamine--glycine ligase	16.71	11.24	317.59	233.79	-5.64400475 5	3.70564E-47
Yes	S	SAUSA300_RS04760	SAUSA300_0883		MAP domain-containing protein	41.55	17.26	414.14	432.32	-5.30289579 8	1.58378E-32

Table A-1 (cont'd)

No	no homolog found	SAUSA300_RS11930	SAUSA300_2164		MAP domain-containing protein	32.26	11.96	158.3	288.11	-4.847769742	1.23411E-19
Yes	S	SAUSA300_RS03005			C1q-binding complement inhibitor VraX	25631.12	16475.97	18299 6.97	23280 9.5	-4.736802525	7.23362E-25
No	S	SAUSA300_RS13975	SAUSA300_2518		alpha/beta hydrolase	9.82	6.47	43.36	106.54	-4.645387926	2.06063E-16
Yes	not classified	SAUSA300_RS03000			hypothetical protein	637.53	308.74	4243.07	3649.74	-4.509440129	1.58552E-27
No	S	SAUSA300_RS13280	SAUSA300_2398		iron export ABC transporter permease subunit FetB	19.01	15.86	78.94	208.88	-4.455029685	1.80183E-14
No	no homolog found	SAUSA300_RS15545	SAUSA300_2141		IS1182 family transposase	5.88	2.45	28.69	30	-4.307278293	2.89563E-21
No	S	SAUSA300_RS11805	SAUSA300_2142	*asp23*	Asp23/Gls24 family envelope stress response protein	594.68	188.28	2619.07	2540.32	-4.231069998	2.44386E-19

Table A-1 (cont'd)

No	GM	SAUSA300_RS11550	SAUSA300_2097		SDR family oxidoreductase	10.23	6	46.7	59.05	-4.16936178 3	6.34611E-19
No	G	SAUSA300_RS01005	SAUSA300_0191	*ptsG*	glucose-specific PTS transporter subunit IIBC	6.6	4.59	36.3	35.28	-4.09207745 2	2.1623E-21
Yes	F	SAUSA300_RS05195	SAUSA300_0966	*purE*	5-(carboxyamino)imidazole ribonucleotide mutase	1.66	2.67	19.08	13.89	-4.08978647 1	7.69067E-16
Yes	S	SAUSA300_RS13155	SAUSA300_2378		membrane protein	52.31	22.37	212.38	198.04	-3.94896652 1	1.91046E-19
Yes	O	SAUSA300_RS09140	SAUSA300_1674		trypsin-like peptidase domain-containing protein	41.35	23.5	184.67	173.58	-3.92111562 2	2.10326E-20
Yes	no homolog found	SAUSA300_RS09670	SAUSA300_1767	epiA	gallidermin/nisin family lantibiotic	5.99	11.07	61.45	44.39	-3.77482775 1	1.14084E-12
No	Q	SAUSA300_RS00950	SAUSA300_0181		non-ribosomal peptide synthetase	11.5	4.61	39.43	35.55	-3.72075236 1	3.13434E-17

Table A-1 (cont'd)

Yes	no homolog found	SAUSA300_RS15740			phenol-soluble modulin PSM-alpha-1	24086.72	14456.95	80513.32	90835.34	-3.629966141	6.55375E-16
Yes	no homolog found	SAUSA300_RS15735			phenol-soluble modulin PSM-alpha-2	32964.12	19614	100663.79	128039.36	-3.612456006	1.13777E-14
Yes	G	SAUSA300_RS02960	SAUSA300_0555		3-hexulose-6-phosphate synthase	12.15	4.89	29.42	40.12	-3.575866782	1.01985E-12
No	M	SAUSA300_RS01750	SAUSA300_0329		aldehyde reductase	11.47	5.05	20.74	45.12	-3.563956953	2.42518E-10
No	no homolog found	SAUSA300_RS06215			hypothetical protein	30.93	27.32	128.66	128.85	-3.524484833	3.07167E-14
No	F	SAUSA300_RS14175	SAUSA300_2551	*nrdD*	anaerobic ribonucleoside-triphosphate reductase	16.57	6.48	28.93	55.94	-3.467182511	2.93264E-10
No	G	SAUSA300_RS13740	SAUSA300_2476	*ptsG*	glucose-specific PTS transporter subunit IIBC	4.83	2.17	11.81	14.77	-3.457841722	7.11611E-13

Table A-1 (cont'd)

No	I	SAUSA300_RS13270	SAUSA300_2396	*pnbA*	carboxylesterase/lipase family protein	19.06	8.99	38.39	66.14	-3.45453656 3	4.36095E-11
No	M	SAUSA300_RS13750	SAUSA300_2478	*cidB*	LrgB family protein	18.38	13.8	44.89	79.26	-3.42731880 8	8.01927E-11
No	F	SAUSA300_RS09165	SAUSA300_1678	*fhs*	formate--tetrahydrofolate ligase	60.98	26.29	177.73	153.63	-3.42373895 5	2.1717E-15
No	H	SAUSA300_RS00955	SAUSA300_0182		4'-phosphopantetheinyl transferase superfamily protein	26.78	24.44	117.58	96.52	-3.42176003 8	3.03873E-15
Yes	no homolog found	SAUSA300_RS15090			phenol-soluble modulin PSM-alpha-3	36859.41	23267.68	98132.17	125806.27	-3.38787570 3	6.41637E-13
No	C	SAUSA300_RS11360	SAUSA300_2063	*atpE*	F0F1 ATP synthase subunit C	32.97	17.66	90.41	96.99	-3.37919918 1	1.17799E-13
No	I	SAUSA300_RS00355	SAUSA300_0070		alpha/beta hydrolase	18.61	12.36	54.45	61.27	-3.36805660 6	1.50626E-13

Table A-1 (cont'd)

No	not classified	SAUSA300_RS02995	SAUSA300_0561		protein VraC	6.12	2.31	14.5	14.94	-3.31634688	1.58193E-11
Yes	M	SAUSA300_RS02965	SAUSA300_0556		6-phospho-3-hexuloisomerase	30.97	21.99	68.49	115.78	-3.293196014	2.37257E-10
Yes	J	SAUSA300_RS02850	SAUSA300_0533	*tuf*	elongation factor Tu	1122.7	991.56	3207.41	4132.39	-3.226531685	3.21503E-11
Yes	H	SAUSA300_RS04995	SAUSA300_0930		lipoate--protein ligase	7.75	5.74	33.94	16.76	-3.224479773	2.55879E-15
No	S	SAUSA300_RS12470	SAUSA300_2257		DUF1641 domain-containing protein	13.01	7.36	32.33	35.22	-3.219981614	2.30572E-12
No	S	SAUSA300_RS11810	SAUSA300_2143		DUF2273 domain-containing protein	234.92	76.71	547.93	459.11	-3.219377471	3.21076E-12
No	M	SAUSA300_RS07485	SAUSA300_1370	*ebpS*	elastin-binding protein EbpS	78.5	57.76	222	241.36	-3.216091479	1.08808E-12
No	O	SAUSA300_RS04245	SAUSA300_0786		organic hydroperoxide resistance protein	37.67	28.21	92.19	128.05	-3.212643788	6.57898E-11

Table A-1 (cont'd)

No	I	SAUSA300_RS03070	SAUSA300_0574		phosphomevalonate kinase	5.16	2.82	10.06	15.37	-3.202019673	3.82896E-10
No	K	SAUSA300_RS06210	SAUSA300_1148	*codY*	GTP-sensing pleiotropic transcriptional regulator CodY	67.53	37.35	156.14	178.68	-3.18282773 3	3.37304E-12
No	P	SAUSA300_RS00900	SAUSA300_0171		cation diffusion facilitator family transporter	8.63	4.65	17.97	23.15	-3.15136336 7	6.6658E-11
No	G	SAUSA300_RS14010	SAUSA300_2525		fructosamine kinase family protein	14.48	11.97	27.03	55.83	-3.13304462 5	2.07198E-08
No	S	SAUSA300_RS10180	SAUSA300_1864		YihY/virulence factor BrkB family protein	20.06	12.9	37.38	57.47	-3.04209501 8	1.71195E-09
Yes	no homolog found	SAUSA300_RS15730			phenol-soluble modulin PSM-alpha-4	28076.72	19700.69	67198.08	73350.18	-3.02394534 4	2.17006E-11
No	IQ	SAUSA300_RS12575	SAUSA300_2275		SDR family oxidoreductase	32.61	21.9	52.95	99.17	-3.00762496 4	2.19604E-08

Table A-1 (cont'd)

No	G	SAUSA300_RS04090	SAUSA300_0758	*tpiA*	triose-phosphate isomerase	15.05	5.81	21.08	34.31	-3.00565227 3	1.94875E-08
No	D	SAUSA300_RS01705	SAUSA300_0320		YSIRK domain-containing triacylglycerol lipase Lip2/Geh	140.97	59.25	207.49	325.49	-3.00079235 3	6.98697E-09
No	O	SAUSA300_RS14170	SAUSA300_2550	*nrdG*	anaerobic ribonucleoside-triphosphate reductase activating protein	18.17	13.98	23.29	64.75	-2.97452011 3	8.51614E-07
No	G	SAUSA300_RS04495	SAUSA300_0833		TIGR01457 family HAD-type hydrolase	9.43	3.31	16.45	16.48	-2.92197974 6	1.45098E-09
No	G	SAUSA300_RS14100	SAUSA300_2540		fructose bisphosphate aldolase	199.82	89.39	418.88	342.23	-2.89928851 4	1.13291E-11
Yes	E	SAUSA300_RS04565	SAUSA300_0845	*ampA*	M17 family metallopeptidase	22.02	15.65	63.44	42.71	-2.89004652 9	7.30874E-13
No	F	SAUSA300_RS04085	SAUSA300_0757	*pgk*	phosphoglycerate kinase	35.94	20.82	53.97	89.46	-2.8873278	2.54518E-08

Table A-1 (cont'd)

No	no homolog found	SAUSA300_RS12420			hypothetical protein	319.15	307.09	1125.37	722.8	-2.883800105	1.40191E-11
No	H	SAUSA300_RS10075	SAUSA300_1845	*hemL*	glutamate-1-semialdehyde 2,1-aminomutase	10.28	6.22	23.73	20.27	-2.877796016	1.19583E-11
No	Q	SAUSA300_RS00990	SAUSA300_0189	*entB*	isochorismatase family protein	4.71	5.33	15.04	13.73	-2.858098288	4.36957E-09
No	S	SAUSA300_RS09455	SAUSA300_1728		aldo/keto reductase	20.21	12.56	38.57	43.51	-2.822570804	8.70681E-10
Yes	H	SAUSA300_RS01160	SAUSA300_0221	*pflA*	pyruvate formate-lyase-activating protein	9.12	6.73	10.15	27.96	-2.803287417	3.78005E-06
No	C	SAUSA300_RS05170	SAUSA300_0962	*qoxB*	cytochrome aa3 quinol oxidase subunit I	69.9	32.65	87.12	148.15	-2.789086363	1.30522E-07
No	G	SAUSA300_RS03675	SAUSA300_0685	*fruA*	fructose-specific PTS transporter subunit EIIC	16.67	15.01	19.71	57.27	-2.787508093	5.88931E-06

Table A-1 (cont'd)

No	F	SAUSA300_RS05190	SAUSA300_0965	*folD*	bifunctional methylenetetrahydrofolate dehydrogenase/ methenyltetrahydrofolate cyclohydrolase FolD	71.94	31.74	114.24	122.83	-2.74303919 7	3.23624E-09
Yes	S	SAUSA300_RS13645	SAUSA300_2460		GNAT family N-acetyltransferase	24.61	28.86	99.44	51.19	-2.73165759 2	2.96638E-09
No	C	SAUSA300_RS06765	SAUSA300_1246	*acnA*	aconitate hydratase AcnA	51.23	22.95	65.18	95.79	-2.70464100 5	1.04643E-07
No	H	SAUSA300_RS01405	SAUSA300_0262	*rbsK*	ribokinase	6.74	6.85	13.94	18.15	-2.66207194 7	2.19334E-07
No	not classified	SAUSA300_RS09275	SAUSA300_1698		YtxH domain-containing protein	58.85	39.14	125.7	101.93	-2.66154169 7	2.0399E-10
No	C	SAUSA300_RS05355	SAUSA300_0994	*pdhB*	transketolase C-terminal domain-containing protein	28.65	13.24	52.12	40.31	-2.63828701 9	5.04402E-10

Table A-1 (cont'd)

No	S	SAUSA300_RS05995	SAUSA300_1107		TM2 domain-containing protein	1035.35	1191.02	2439.26	2604.9	-2.557126156	2.2641E-07
No	C	SAUSA300_RS11365	SAUSA300_2064	*atpB*	F0F1 ATP synthase subunit A	28.1	13	42.65	39.51	-2.527327063	1.56447E-08
No	C	SAUSA300_RS01155	SAUSA300_0220	*pflB*	formate C-acetyltransferase	39.54	24.31	38.44	84.3	-2.523759754	8.49484E-06
Yes	G	SAUSA300_RS04670	SAUSA300_0865	*pgi*	glucose-6-phosphate isomerase	91.76	46.06	156.97	120.85	-2.501360287	1.95023E-09
No	S	SAUSA300_RS08360	SAUSA300_1533		flotillin-like protein FloA	123.59	67.69	180.49	194.35	-2.498332432	4.01657E-08
No	not classified	SAUSA300_RS08355	SAUSA300_1532		hypothetical protein	121.68	52.38	174.58	163.11	-2.498179723	2.77985E-08
No	C	SAUSA300_RS03190	SAUSA300_0594	*adh*	alcohol dehydrogenase AdhP	159.25	78.73	184.05	250.8	-2.445448141	7.98498E-07

Table A-1 (cont'd)

No	not classified	SAUSA300_RS04225	SAUSA300_0781		hypothetical protein	132.88	103.79	248.99	225.57	-2.44293389	2.89806E-08
No	S	SAUSA300_RS14620	SAUSA300_2632		HdeD family acid-resistance protein	51.71	37.15	64.51	102.99	-2.44267941	2.78567E-06
No	I	SAUSA300_RS13795	SAUSA300_2484		hydroxymethylglutaryl-CoA synthase	84.76	62.34	164.89	131.17	-2.44014220	6.51191E-09
No	K	SAUSA300_RS03665	SAUSA300_0683		DeoR/GlpR family DNA-binding transcription regulator	108.22	53.2	152.77	145.06	-2.41271013	5.29521E-08
No	KOT	SAUSA300_RS10935	SAUSA300_1989	*agrB*	accessory gene regulator AgrB	926.34	501.35	1575.92	1121.46	-2.38648572	4.64379E-09
No	P	SAUSA300_RS04605	SAUSA300_0853	*mnhC*	Na+/H+ antiporter Mnh1 subunit C	34.2	17.04	54.14	41.16	-2.38338307	2.39295E-08
No	S	SAUSA300_RS04220	SAUSA300_0782		sterile α motif-like domain-containing protein	248.01	192.61	383.73	439.2	-2.37810837	4.78111E-07

Table A-1 (cont'd)

No	C	SAUSA300_RS05360	SAUSA300_0995		dihydrolipoamide acetyltransferase family protein	26.25	11.84	32.46	34.41	-2.36985281 6	3.81764E-07
Yes	J	SAUSA300_RS03960	SAUSA300_0736	*yfiA*	ribosome-associated translation inhibitor RaiA	1334.07	1434.27	3386.21	2297.34	-2.36278535 7	1.38771E-07
No	G	SAUSA300_RS06725	SAUSA300_1239	*tkt*	transketolase	83.27	51.86	117.51	123.98	-2.34632222 5	2.20895E-07
No	E	SAUSA300_RS03030	SAUSA300_0566		amino acid permease	30.32	20.78	39.1	50.82	-2.33423180 4	1.68595E-06
Yes	not classified	SAUSA300_RS13040	SAUSA300_2361		putative metal homeostasis protein	749.1	1675.86	1920.36	3051.79	-2.33327593 4	0.000189715
No	P	SAUSA300_RS00595	SAUSA300_0115	*sirC*	staphyloferrin B ABC transporter permease subunit SirC	29.97	24.63	44.59	53.55	-2.31975872 4	1.63674E-06
Yes	J	SAUSA300_RS02575	SAUSA300_0479		50S ribosomal protein L25/general stress proteinCtc	698.21	446.92	1187.14	887.42	-2.30826470 7	1.89693E-08

Table A-1 (cont'd)

No	S	SAUSA300_RS11815	SAUSA300_2144		alkaline shock response membrane anchor protein AmaP	329	156.74	463.15	377.18	-2.30396945	7.38859E-08
No	K	SAUSA300_RS03250	SAUSA300_0605	*sarA*	global transcriptional regulator SarA	550.54	628.5	1240	1037.55	-2.30081455	1.06132E-06
No	O	SAUSA300_RS10900	SAUSA300_1982	*groEL*	chaperonin GroEL	74.38	38.88	95.38	86.68	-2.2047383 85	4.6807E-07
No	T	SAUSA300_RS09015	SAUSA300_1652		universal stress protein	315.7	260.73	601.59	401.91	-2.18455110 2	1.89501E-07
No	not classified	SAUSA300_RS12160	SAUSA300_2206		hypothetical protein	95.1	78.95	192.53	113.24	-2.17223099 1	2.05121E-07
No	no homolog found	SAUSA300_RS08615	SAUSA300_1581		SAS049 family protein	549.05	509.88	1111.67	745.8	-2.17193099 9	5.07968E-07
Yes	no homolog found	SAUSA300_RS08745			hypothetical protein	144.25	117.94	318.89	146.68	-2.14116857	5.30006E-07

Table A-1 (cont'd)

No	C	SAUSA300_RS11335	SAUSA300_2058	*atpD*	F0F1 ATP synthase subunit beta	47.87	24.09	63.18	48.62	-2.135689036	4.39788E-07
No	G	SAUSA300_RS04080	SAUSA300_0756	*gap*	type I glyceraldehyde-3-phosphate dehydrogenase	1310.2	855.86	881	2226.45	-2.124844296	0.00037335 4
Yes	S	SAUSA300_RS09825	SAUSA300_1795		YlbF/YmcA family competence regulator	388.16	375.77	977.95	392.66	-2.094666041	3.34279E-06
No	G	SAUSA300_RS05420	SAUSA300_1007		inositol monophosphatase	198.74	144.31	276.3	247.69	-2.075756972	2.12178E-06
No	G	SAUSA300_RS00740	SAUSA300_0141	*deoB*	phosphopentomutase	54.96	32.81	52.9	69.29	-2.034365177	3.50149E-05
No	no homolog found	SAUSA300_RS10940	SAUSA300_1990	agrD	cyclic lactone autoinducer peptide	923.01	345.81	1059.02	737.23	-2.026643283	5.16629E-06
Yes	S	SAUSA300_RS07160	SAUSA300_1314		YozE family protein	272.86	134.55	352.33	236.94	-2.014720783	1.26339E-06
No	M	SAUSA300_RS07315	SAUSA300_1341	*pbp2*	transglycosylase domain-containing protein	67.46	48.33	91.11	78.4	-2.012426433	3.34279E-06

Table A-1 (cont'd)

No	S	SAUSA300_RS12165	SAUSA300_2207		NCS2 family permease	90.94	73.55	138.33	109.02	-2.01231831	3.11505E-06
Yes	no homolog found	SAUSA300_RS15985			hypothetical protein	1448.5	2256.86	2477.47	3277.31	-2.00338213 9	0.0004034 76
No	G	SAUSA300_RS11445	SAUSA300_2079	*fba*	fructose-bisphosphate aldolase	1472.76	839.2	1540.16	1574.67	-1.96291082 5	1.48111E-05
Yes	no homolog found	SAUSA300_RS13850	SAUSA300_2493		cell wall inhibition responsive protein CwrA	290.15	271.08	514.48	325.63	-1.93812754 9	8.18239E-06
No	T	SAUSA300_RS00340	SAUSA300_0067		universal stress protein	291.2	304.97	352.79	478.64	-1.93770956 5	0.0002288 25
Yes	C	SAUSA300_RS14075	SAUSA300_2537		L-lactate dehydrogenase	43.61	41.66	69.96	54.33	-1.93280898 3	1.7014E-05
No	M	SAUSA300_RS09205	SAUSA300_1684		membrane protein	68.77	30.08	93.4	43.63	-1.90190508	9.18074E-06
Yes	S	SAUSA300_RS13765	SAUSA300_2481		sterile α motif-like domain-containing protein	4957.16	6293.84	8840.81	7590.77	-1.89472036 4	0.0001302 26

Table A-1 (cont'd)

No	S	SAUSA300_RS01990	SAUSA300_0374		GlsB/YeaQ/YmgE family stress response membrane protein	1269.32	1302.36	1739.99	1802.05	-1.88660073	0.000109907
No	G	SAUSA300_RS04230	SAUSA300_0783		histidine phosphatase family protein	48.94	40.27	64.72	56.33	-1.881093558	2.72916E-05
No	S	SAUSA300_RS02055	SAUSA300_0385		general stress protein	282.45	309.05	401.34	416.98	-1.880197199	0.000150692
No	K	SAUSA300_RS13560	SAUSA300_2445		MerR family transcriptional regulator	44.52	36.46	55.51	52.21	-1.866869954	4.34783E-05
No	S	SAUSA300_RS12400	SAUSA300_2246		PH domain-containing protein	81.81	60.2	106.81	80.57	-1.839012131	1.65575E-05
Yes	G	SAUSA300_RS07165	SAUSA300_1315	*crr*	PTS glucose transporter subunit IIA	306.25	144.11	347.84	219.6	-1.817023682	1.38301E-05
No	S	SAUSA300_RS08620	SAUSA300_1582		CsbD family protein	668.9	555.41	868.96	717.19	-1.806682431	4.24847E-05

Table A-1 (cont'd)

No	F	SAUSA300_RS08975	SAUSA300_1644	*pyk*	pyruvate kinase	329.3	123.81	273.98	249.21	-1.78819782	0.00014408
No	S	SAUSA300_RS13385	SAUSA300_2418		carboxymuconolactone decarboxylase family protein	75.26	62.59	97.35	75.63	-1.75096406	6.82537E-05
Yes	J	SAUSA300_RS06310	SAUSA300_1166	*rpsO*	30S ribosomal protein S15	515.94	553.33	962.48	482.16	-1.72218715	0.00016530
No	G	SAUSA300_RS04100	SAUSA300_0760	*eno*	surface-displayed α-enolase	368.42	166.6	238.85	325.77	-1.69915174	0.00094837
No	D	SAUSA300_RS02550	SAUSA300_0475		septation regulator SpoVG	611.84	344.53	528.79	535.02	-1.69568955	0.00021307
No	P	SAUSA300_RS07060	SAUSA300_1299		toxic anion resistance protein	99.85	40.68	79.45	73.06	-1.69309711	0.00028290
No	S	SAUSA300_RS05960	SAUSA300_1100		VOC family protein	135.48	94.36	158.58	112.66	-1.68259702	6.16704E-05
No	S	SAUSA300_RS01545	SAUSA300_0289		TIGR01741 family protein	60.83	50.32	85.5	50.93	-1.67270061	8.87108E-05

Table A-1 (cont'd)

No	O	SAUSA300_RS05460	SAUSA300_1015	*ctaA*	heme A synthase	52.3	38.18	43.04	51.9	-1.595463743	0.001217768
No	not classified	SAUSA300_RS11230	SAUSA300_2041		Lmo0850 family protein	564.44	834.15	615.27	857.41	-1.488720266	0.010598817
Yes	C	SAUSA300_RS03045	SAUSA300_0569		heme-dependent peroxidase	174.23	122.96	200.16	110.88	-1.465510251	0.00042298
No	no homolog found	SAUSA300_RS10555			hypothetical protein	315.09	400.4	376.61	351.22	-1.407068848	0.006812525
Yes	no homolog found	SAUSA300_RS04395	SAUSA300_0815	*ear*	DUF4888 domain-containing protein	273.4	262.32	451.33	144.39	-1.385160382	0.004946248
No	L	SAUSA300_RS07430	SAUSA300_1362	*hup*	HU family DNA-binding protein	27446.33	29697.55	33446.33	23578.56	-1.362588253	0.003873353
No	S	SAUSA300_RS12820	SAUSA300_2320		DUF2871 domain-containing protein	76.41	81.38	63.99	72.04	-1.242294554	0.018181659

Table A-1 (cont'd)

No	no homolog found	SAUSA300_RS15795		type I toxin-antitoxin system Fst family toxin PepA1	567.95	857.84	707.22	620.21	-1.24163196	0.02328664
No	D	SAUSA300_RS07290	SAUSA300_1337	cell division regulator GpsB	150.52	42	94.14	49.94	-1.11877976	0.03034066

Table A-2. CymR regulon.

Genes upregulated in *cymR*::Tn CSSC when compared to WT CSSC

COG	Locus	Old locus	Gene	Product	TPM. 1 *cymR*	TPM. 2 *cymR*	TPM. 1 WT	TPM. 2 WT	DE Log_2 FC	DE Adj. *P*-value
S	SAUSA300_RS10985	SAUSA300_1998		YeeE/YedE family protein	14.91	45.03	0.74	0.43	3.435179048	5.131E-07
S	SAUSA300_RS00910	SAUSA300_0173		DUF4242 domain-containing protein	112.93	431.81	4.54	4.88	3.430292895	0.000001335
O	SAUSA300_RS10980	SAUSA300_1997		sulfurtransferase TusA family protein	61.56	165.78	2.67	2.08	3.324841314	9.084E-07
P	SAUSA300_RS00925	SAUSA300_0176		ABC transporter permease	27.65	65.91	1.5	0.99	3.109131580	0.000002476
I	SAUSA300_RS00930	SAUSA300_0177		acyl-CoA/acyl-ACP dehydrogenase	50.29	74.56	2.77	1.16	3.059228719	5.169E-07
M	SAUSA300_RS13915	SAUSA300_2506	*isaA*	lytic transglycosylase IsaA	11584.71	594.81	189.31	89.28	2.806840145	0.001255
U	SAUSA300_RS02035	SAUSA300_0382		L-cystine transporter	1520.78	2546.04	45.72	82.63	2.699312658	0.0001428
S	SAUSA300_RS05050	SAUSA300_0940		DoxX family protein	89.95	169.47	10.54	3.61	2.368999526	0.0006815
A	SAUSA300_RS02045	SAUSA300_0383		hypothetical protein	404.49	285.21	29.15	11.23	2.290278175	0.0002041

Table A-2 (cont'd)

P	SAUSA300_RS01055	SAUSA300_0200		ABC transporter ATP-binding protein	28.76	56.72	1.44	2.45	2.26561963	0.003735
P	SAUSA300_RS02340	SAUSA300_0437	*gmpC*	dipeptide ABC transporter glycylmethionine-binding lipoprotein	123.34	372.09	10.16	14.16	2.19365352	0.006966
S	SAUSA300_RS12610	SAUSA300_2282	*sdpC*	CPBP family intramembrane glutamic endopeptidaseSdpC	86.59	133.02	10.9	4.13	2.10425690	0.00228
P	SAUSA300_RS00915	SAUSA300_0174		ABC transporter ATP-binding protein	8.87	33.74	2.15	0.58	2.05318192	0.01266
L	SAUSA300_RS05345	SAUSA300_0992		YkyA family protein	205.89	639.29	45.06	13.18	2.04837860	0.01382
E	SAUSA300_RS02635	SAUSA300_0491	*cysK*	cysteine synthase A	7140.91	3976.77	143.08	389.91	2.03504764	0.01199
not classified	SAUSA300_RS09430			hypothetical protein	49.89	138.24	9.87	3.23	2.02010295	0.01388
E	SAUSA300_RS02325	SAUSA300_0434		bifunctional cystathionine γ-lyase/homocysteine desulfhydrase	44.68	14.89	1.09	1.95	1.98823317	0.0225
P	SAUSA300_RS02335	SAUSA300_0436		methionine ABC transporter permease	18.51	76.09	2.72	2.91	1.97659445	0.02036
D	SAUSA300_RS09440	SAUSA300_1726		CrcB family protein	11.73	38.91	1.79	1.43	1.97602321	0.009513

Table A-2 (cont'd)

S	SAUSA300_RS01875	SAUSA300_0354	low temperature requirement protein A	12.65	27.98	1.85	1.02	1.93338716 3	0.01404
V	SAUSA300_RS13605	SAUSA300_2453	ATP-binding cassette domain-containing protein	67.04	179.73	13.06	5.48	1.90619927	0.01654
P	SAUSA300_RS00920	SAUSA300_0175	ABC transporter substrate-binding protein	13.13	31.1	2.57	0.88	1.90444637 4	0.02249
P	SAUSA300_RS02330	SAUSA300_0435	methionine ABC transporter ATP-binding protein	18.79	54.32	2.36	2.49	1.90414439 5	0.01135
I	SAUSA300_RS12685	SAUSA300_2296	alpha/beta hydrolase	126.11	251.35	21.03	8.72	1.87824894 3	0.03211
EP	SAUSA300_RS01060	SAUSA300_0201	ABC transporter permease	16.22	29.78	0.74	1.91	1.83429987 2	0.03649
S	SAUSA300_RS13940	SAUSA300_2511	DUF896 domain-containing protein	46.83	202.17	11.9	6.79	1.82478807 2	0.04623
S	SAUSA300_RS04485	SAUSA300_0831	DUF3055 domain-containing protein	47.5	218.25	17.41	4.1	1.82208257	0.01364
E	SAUSA300_RS02855	SAUSA300_0534	M20 family metallopeptidase	22.75	37.22	3.57	1.5	1.78498265	0.0225
no homolog found	SAUSA300_RS07460	SAUSA300_1366	hypothetical protein	70.61	48.87	8.01	2.2	1.72474927 6	0.02352
ET	SAUSA300_RS13025	SAUSA300_2359	transporter substrate-binding domain-containing protein	70.83	138.45	11.72	6.67	1.69326231 4	0.02663

Table A-2 (cont'd)

S	SAUSA300_RS13320	SAUSA300_2405		CPBP family lipoprotein N-acylation protein LnsB	52.3	92.92	9.76	3.9	1.65357398 7	0.03853
not classified	SAUSA300_RS10230	SAUSA300_1871		hypothetical protein	17.61	31.65	3.44	1.26	1.64639224 1	0.03008
M	SAUSA300_RS05540	SAUSA300_1029	*isdA*	LPXTG-anchored heme-scavenging protein IsdA	148.9	229.49	28	9.65	1.64610995 7	0.03382
K	SAUSA300_RS12705	SAUSA300_2300		TetR/AcrR family transcriptional regulator	39.08	65.85	7.6	2.72	1.62036634 8	0.04532
S	SAUSA300_RS11450	SAUSA300_2080		DUF2529 domain-containing protein	43.3	86.72	9.91	3.17	1.61841672 3	0.02554
P	SAUSA300_RS00605	SAUSA300_0117	*sirA*	staphyloferrin B ABC transporter substrate-binding protein SirA	23.01	28.48	3.46	1.62	1.60809829 1	0.02782
S	SAUSA300_RS12440	SAUSA300_2253		CHAP domain-containing protein	332.01	177.41	35.71	14.09	1.58754982 5	0.03896
M	SAUSA300_RS03340	SAUSA300_0623		N-acetylglucosaminyldiphosphoundecaprenol N-acetyl-β-D-mannosaminyltransferase TarA	45.52	68.2	8.93	2.93	1.53181557 1	0.03008
F	SAUSA300_RS07465	SAUSA300_1367	*cmk*	(d)CMP kinase	87.02	69.66	11.29	5.19	1.52986373 1	0.02784

Table A-2 (cont'd)

OU	SAUSA300_RS04060	SAUSA300_0752	*clpP*	ATP-dependent Clp endopeptidase proteolytic subunit ClpP	1027.25	715.24	109.04	67.12	1.52499860 2	0.04532
E	SAUSA300_RS00985	SAUSA300_0188	*brnQ1*	branched-chain amino acid transport system II carrier protein	81.89	139.01	13.61	8.9	1.50277736 8	0.04983
not classified	SAUSA300_RS04205	SAUSA300_0780		lipoprotein N-acylation protein LnsA	16.59	12.18	2.19	0.86	1.49823469 3	0.03766
E	SAUSA300_RS07075	SAUSA300_1300	*brnQ3*	branched-chain amino acid transport system II carrier protein	31.17	23.58	4.13	1.79	1.46859987 3	0.04532
no homolog found	SAUSA300_RS15260	SAUSA300_0937		hypothetical protein	262.33	350.44	43.62	23.66	1.45437516 2	0.04532
S	SAUSA300_RS09900	SAUSA300_1809		PTS transporter subunit IIC	40.1	47.08	6.38	3.33	-1.454	0.04532

Genes downregulated in *cymR*::Tn CSSC when compared to WT CSSC

COG	Locus	Old locus	Gene	Product	TPM. 1 *cymR*	TPM. 2 *cymR*	TPM. 1 WT	TPM. 2 WT	DE Log_2 FC	DE Adj. *P*-value
Q	SAUSA300_RS00950	SAUSA300_0181		non-ribosomal peptide synthetase	8.18	7.12	39.43	35.55	-3.45924731 5	1.966E-09
H	SAUSA300_RS00955	SAUSA300_0182		4'-phosphopantetheinyl transferase superfamily protein	32.46	19.17	117.58	96.52	-3.24507261 2	3.242E-08

Table A-2 (cont'd)

C	SAUSA300_RS00800	SAUSA300_0151	*adhE*	bifunctional acetaldehyde-CoA/alcohol dehydrogenase	3.63	2.35	10.06	12.51	-3.132786825	5.131E-07
C	SAUSA300_RS03190	SAUSA300_0594	*adhP*	alcohol dehydrogenase AdhP	80.52	51.88	184.05	250.8	-2.963093541	0.000002476
F	SAUSA300_RS14175	SAUSA300_2551	*nrdD*	anaerobic ribonucleoside-triphosphate reductase	17.5	10.03	28.93	55.94	-2.862058643	0.00003716
no homolog found	SAUSA300_RS15730			phenol-soluble modulin PSM-alpha-4	9480.7	29491.47	67198.08	73350.18	-2.833246222	0.00009013
no homolog found	SAUSA300_RS15735			phenol-soluble modulin PSM-alpha-2	15900.9	49372.47	100663.79	128039.36	-2.804712203	0.0001313
no homolog found	SAUSA300_RS15090			phenol-soluble modulin PSM-alpha-3	15050.63	48596.27	98132.17	125806.27	-2.800294206	0.0001415
no homolog found	SAUSA300_RS15740			phenol-soluble modulin PSM-alpha-1	12580.61	37405.9	80513.32	90835.34	-2.785891745	0.0001135

Table A-2 (cont'd)

no homolog found	SAUSA300_RS11930	SAUSA300_2164		MAP domain-containing protein	112.67	54.61	158.3	288.11	-2.688556285	0.0001321
no homolog found	SAUSA300_RS16065			hypothetical protein	5.51	2.81	10.91	10.1	-2.507917201	0.0004496
F	SAUSA300_RS05225	SAUSA300_0972	*purF*	amidophosphoribosyltransferase	28.41	4.72	38.02	34.89	-2.319549281	0.00413
no homolog found	SAUSA300_RS15985			hypothetical protein	1916.24	1268.31	2477.47	3277.31	-2.224683415	0.001255
F	SAUSA300_RS04085	SAUSA300_0757		phosphoglycerate kinase	35.37	43.12	53.97	89.46	-2.196429109	0.003047
G	SAUSA300_RS04080	SAUSA300_0756	*gap*	type I glyceraldehyde-3-phosphate dehydrogenase	1063.41	916.25	881	2226.45	-2.032929124	0.01337
E	SAUSA300_RS06650	SAUSA300_1227	*thrC*	threonine synthase	14.77	13.7	26.55	12.51	-1.73992651	0.01083
M	SAUSA300_RS00400	SAUSA300_0079		YdhK family protein	531.33	177.06	555.41	355.03	-1.71013977	0.02577

Table A-2 (cont'd)

no homolog found	SAUSA300_RS16085	SAUSA300_1988		delta-lysin family phenol-soluble modulin	139687.59	115668.38	171845.71	141512.48	-1.69854326	0.01364
KOT	SAUSA300_RS10935	SAUSA300_1989	*agrB*	accessory gene regulator AgrB	1532.17	771.5	1575.92	1121.46	-1.628804813	0.02389
O	SAUSA300_RS04245	SAUSA300_0786		organic hydroperoxide resistance protein	113.51	84.07	92.19	128.05	-1.623959073	0.03649
no homolog found	SAUSA300_RS09675			gallidermin/nisin family lantibiotic	14.87	9.96	13.46	14.32	-1.580812946	0.04532
K	SAUSA300_RS10950	SAUSA300_1992		LytTR family DNA-binding domain-containing protein	886.04	496.31	978.24	525.34	-1.490740497	0.03783

Table A-3. *cymR*::Tn sulfur starvation.

Genes upregulated in *cymR*::Tn sulfur starvation when compared to *cymR*::Tn CSSC

Shared with WT -S (Table 1)	COG	Locus	Old locus	Gene	Product	TPM. 1 Starv	TPM. 2 Starv	TPM. 1 CSSC	TPM. 2 CSSC	DE Log_2 FC	DE Adj. *P*-value
No	K	SAUSA300_RS03085	SAUSA300_0577		redox-sensitive transcriptional regulator HypR	129.22	208.29	2.85	2.38	4.45532441	9.67E-19
Yes	no homolog found	SAUSA300_RS16040			imidazole glycerol phosphate synthase subunit HisF	62.91	69.67	1.25	1.08	4.33557811	1.43E-19
Yes	H	SAUSA300_RS03730	SAUSA300_0695		7-carboxy-7-deazaguanine synthase QueE	158.38	170.61	5.52	3.19	3.79084639	1.08E-13
Yes	E	SAUSA300_RS11070	SAUSA300_2013	*leuD*	3-isopropylmalate dehydratase small subunit	46.54	87.07	2.11	1.25	3.75867167	1.6E-11
Yes	H	SAUSA300_RS03735	SAUSA300_0696		6-carboxytetrahydropterin synthase QueD	123.22	128.87	4.38	2.46	3.73484001	8.85E-13
Yes	no homolog found	SAUSA300_RS07125			hypothetical protein	7557.16	5803.42	126.23	213.09	3.72755005	1.15E-10
No	E	SAUSA300_RS14510	SAUSA300_2610	*hisC*	histidinol-phosphate transaminase	12.41	21.95	0.36	0.56	3.58475176	3.14E-09

Table A-3 (cont'd)

No	J	SAUSA300_RS02765	SAUSA300_0516		Mini-ribonuclease 3	74.72	204.03	3.31	4.49	3.490208849	2.98E-08
Yes	E	SAUSA300_RS11055	SAUSA300_2010	*leuA*	2-isopropylmalate synthase	74.75	96.74	3.34	2.36	3.486006304	8.57E-13
Yes	E	SAUSA300_RS14090	SAUSA300_2539		aspartate aminotransferase family protein	127.32	101.53	4.15	3.82	3.415574162	1.6E-11
Yes	C	SAUSA300_RS02385	SAUSA300_0446	*gltD*	glutamate synthase subunit β	844.68	835.11	30.82	30.48	3.362788134	2.28E-12
Yes	J	SAUSA300_RS02770	SAUSA300_0517		23S rRNA (guanosine(2251)-2'-O)-methyltransferase RlmB	97.82	237.26	6.14	6.25	3.205913056	3.62E-08
Yes	E	SAUSA300_RS11075	SAUSA300_2014	*ilvA*	threonine ammonia-lyase IlvA	131.96	156.38	7.44	4.71	3.17146442	1.47E-10
No	E	SAUSA300_RS14505	SAUSA300_2609	*hisB*	imidazoleglycerol-phosphate dehydratase HisB	10.94	17.9	0.28	0.71	3.16153044	0.00000581
Yes	S	SAUSA300_RS02775	SAUSA300_0518		NYN domain-containing protein	197.07	407.75	13.49	12.5	3.054291712	2.56E-08
No	K	SAUSA300_RS02780	SAUSA300_0519		RNA polymerase sigma factor	52.53	171.88	4.57	4.36	3.03108725	0.00000314
Yes	H	SAUSA300_RS11050	SAUSA300_2009	*ilvC*	ketol-acid reductoisomerase	35.82	71.09	1.99	2.61	3.006183716	0.000000208

Table A-3 (cont'd)

No	E	SAUSA300_RS11770	SAUSA300_2137		staphyloferrin A biosynthesis protein SfaC	161.89	189.07	10.54	6.29	2.99380187	3.4E-09
No	EGP	SAUSA300_RS11780	SAUSA300_2139		staphyloferrin A export MFS transporter	19.37	36.64	0.73	1.54	2.9936046	0.00000405
No	E	SAUSA300_RS11045	SAUSA300_2008	*ilvN*	ACT domain-containing protein	40.75	71.61	1.7	3	2.98788901	0.00000223
Yes	P	SAUSA300_RS10250	SAUSA300_1874		H-type ferritin FtnA	4155.65	3220.95	239.97	120.68	2.95371107	0.000000164
Yes	P	SAUSA300_RS11525	SAUSA300_2092	*dps*	Dps family protein	14143.25	8173.12	657.63	425.59	2.94865299	0.000000361
Yes	O	SAUSA300_RS02020	SAUSA300_0379	*ahpF*	alkyl hydroperoxide reductase subunit F	3971.04	3699.54	254.37	126.65	2.9390326	7.14E-08
Yes	H	SAUSA300_RS11040	SAUSA300_2007	*ilvB*	biosynthetic-type acetolactate synthase large subunit	53.7	75.39	3.36	3.01	2.93686154	2.48E-09
Yes	K	SAUSA300_RS00650	SAUSA300_0126		bifunctional transcriptional regulator/O-phospho-L-serine synthase SbnI	89.65	70.75	5.35	2.49	2.9345896	0.000000443
No	EGP	SAUSA300_RS00625	SAUSA300_0121		staphyloferrin B export MFS transporter	11.22	11.03	0.49	0.58	2.92152969	0.000000211

Table A-3 (cont'd)

No	E	SAUSA300_RS14495	SAUSA300_2607	*hisA*	1-(5-phosphoribosyl)-5-((5-phosphoribosylamino)methylideneamino)imidazole-4- carboxamide isomerase	12.66	18.8	0.61	0.82	2.914910078	0.00000937
No	P	SAUSA300_RS04800	SAUSA300_0890	*oppF*	ATP-binding cassette domain-containing protein	103.25	184.9	3.44	8.95	2.887785934	0.00000196
Yes	S	SAUSA300_RS14550	SAUSA300_2618		ECF-type riboflavin transporter substrate-binding protein	59.48	61.13	1.84	3.77	2.878379506	0.00000367
Yes	P	SAUSA300_RS12340	SAUSA300_2235		ABC transporter substrate-binding protein	539.01	417.54	22.65	26.15	2.876611631	7.62E-08
Yes	O	SAUSA300_RS02025	SAUSA300_0380	*ahpC*	alkyl hydroperoxide reductase subunit C	7815.91	7102.56	433.15	381.58	2.824062328	8.5E-09
No	P	SAUSA300_RS05560	SAUSA300_1033		hemin ABC transporter permease protein IsdF	35.02	25.1	1.07	1.91	2.816188073	0.00000694
Yes	S	SAUSA300_RS04570	SAUSA300_0846		Na+/H+ antiporter family protein	178.14	170.77	7.69	10.87	2.792917631	0.00000269

Table A-3 (cont'd)

Yes	E	SAUSA300_RS01070	SAUSA300_0203		ABC transporter substrate-binding protein	63.79	125.82	4.39	5.53	2.76549278 9	0.00000108
Yes	E	SAUSA300_RS11065	SAUSA300_2012	*leuC*	3-isopropylmalate dehydratase large subunit	24.04	59.93	2.65	1.78	2.74784485 1	0.00000601
No	Q	SAUSA300_RS11775	SAUSA300_2138		staphyloferrin A synthetase SfaB	31.11	50.58	2.13	2.41	2.72796356 7	0.00000029 7
No	P	SAUSA300_RS14545	SAUSA300_2617		ABC transporter ATP-binding protein	23.41	40.7	1.18	2.18	2.71045101 7	0.0000119
Yes	F	SAUSA300_RS00725	SAUSA300_0138	*deoD*	purine-nucleoside phosphorylase	45.01	45.75	3.84	1.42	2.67976217 1	0.0000144
No	P	SAUSA300_RS03875	SAUSA300_0720		ABC transporter ATP-binding protein	15.44	26.79	1.18	1.2	2.67860090 9	0.00000299
Yes	E	SAUSA300_RS01075	SAUSA300_0204	*ggt*	γ-glutamyltransferase	281.57	322.87	20.97	15.89	2.67815357 4	2.66E-08
No	S	SAUSA300_RS05565	SAUSA300_1034	*srtB*	class B sortase	40.4	24.82	1.21	2.41	2.63814982 9	0.0000906
No	F	SAUSA300_RS03740	SAUSA300_0697		7-cyano-7-deazaguanine synthase QueC	29.94	31.62	2.54	1.2	2.63510957 2	0.00000581
Yes	C	SAUSA300_RS07500	SAUSA300_1373		ferredoxin	4511.53	4046.46	373.45	160.17	2.61942294	0.00000702

Table A-3 (cont'd)

No	J	SAUSA300_RS14535	SAUSA300_2615		GNAT family protein	20.23	28.74	1.13	1.78	2.576869264	0.0000221
Yes	S	SAUSA300_RS10920	SAUSA300_1986		nitroreductase family protein	83.95	156.78	6.44	8.15	2.576741171	0.00000606
No	G	SAUSA300_RS14530	SAUSA300_2614		polysaccharide deacetylase family protein	20.11	28.81	1.39	1.73	2.537721202	0.00000405
Yes	no homolog found	SAUSA300_RS10765	SAUSA300_1963		DUF2482 family protein	20.32	109.16	0.63	4.63	2.529315636	0.01058
Yes	M	SAUSA300_RS14270	SAUSA300_2565	*clfB*	MSCRAMM family adhesin clumping factor ClfB	139.02	176	10.8	10.81	2.493377017	0.000000361
No	E	SAUSA300_RS14525	SAUSA300_2613	*hisZ*	ATP phosphoribosyltransferase regulatory subunit	14.33	17.64	0.78	1.3	2.469308117	0.00006 03
No	E	SAUSA300_RS14515	SAUSA300_2611	*hisD*	histidinol dehydrogenase	17.69	21.44	0.47	1.77	2.467 9434	0.001 37
Yes	NOU	SAUSA300_RS08765	SAUSA300_1609		A24 family peptidase	21.53	21.48	1.11	1.78	2.443256805	0.00005 78
Yes	H	SAUSA300_RS14190	SAUSA300_2553		NAD(P)-binding protein	581.78	450.41	46.1	28.47	2.441969265	0.00000746

Table A-3 (cont'd)

Yes	O	SAUSA300_RS10980	SAUSA300_1997		sulfurtransferase TusA family protein	1885.83	1726.83	61.56	165.78	2.43544524 7	0.0004639
Yes	C	SAUSA300_RS06395	SAUSA300_1183		2-oxoacid:ferredoxin oxidoreductase subunit β	290.52	386.86	27.28	22.34	2.41391365 4	0.00000802
Yes	no homolog found	SAUSA300_RS14185			hypothetical protein	898.38	767.62	76.27	46.76	2.41090450 4	0.00000751
Yes	C	SAUSA300_RS04255	SAUSA300_0788		nitroreductase	1218.82	1274.44	88.01	94.12	2.41006426 9	0.00000141
Yes	EH	SAUSA300_RS11940	SAUSA300_2166	*alsS*	acetolactate synthase AlsS	16.19	19.64	1.05	1.48	2.39452469 7	0.00002 07
No	M	SAUSA300_RS13525	SAUSA300_2440	*fnbB*	fibronectin-binding protein FnbB	27.16	22.5	1.99	1.75	2.3760687	0.00000603
Yes	S	SAUSA300_RS10760	SAUSA300_1962		DUF1108 family protein	17.32	116.32	1.16	5.34	2.37473191 1	0.01538
Yes	S	SAUSA300_RS14570	SAUSA300_2622		rhodanese-related sulfurtransferase	402.46	389.28	43.22	16.55	2.35350110 8	0.0001274
Yes	P	SAUSA300_RS02335	SAUSA300_0436		methionine ABC transporter permease	748.05	768.96	18.51	76.09	2.35290244 7	0.002996

Table A-3 (cont'd)

Yes	HP	SAUSA300_RS03395	SAUSA300_0633	*fhuA*	ABC transporter ATP-binding protein	300.62	326.41	25.45	22.91	2.350574393	0.00000145
Yes	L	SAUSA300_RS10740	SAUSA300_1958		single-stranded DNA-binding protein	10.8	61.75	0.59	3.13	2.32223030 7	0.01864
Yes	M	SAUSA300_RS13530	SAUSA300_2441	*fnbA*	fibronectin-binding protein FnbA	121.61	104.32	7.1	10.32	2.29023314 5	0.0000635
Yes	E	SAUSA300_RS02380	SAUSA300_0445	*gltB*	glutamate synthase large subunit	137.76	206.56	5.99	17.77	2.27272553 8	0.001912
Yes	I	SAUSA300_RS08990	SAUSA300_1647	*accD*	acetyl-CoA carboxylase, carboxyltransferase subunit β	109.66	144.67	12.09	8.74	2.26316651 7	0.00000694
No	P	SAUSA300_RS14540	SAUSA300_2616		energy-coupling factor transporter transmembranecomponent T	22.09	36.34	1.43	2.86	2.25106912 5	0.0007266
No	P	SAUSA300_RS05555	SAUSA300_1032		heme ABC transporter substrate-binding protein IsdE	34.67	29.27	1.15	3.41	2.24932260 1	0.002651
No	CE	SAUSA300_RS11060	SAUSA300_2011	*leuB*	3-isopropylmalate dehydrogenase	22.09	55.34	3.91	2.03	2.24574867 9	0.00006683
No	E	SAUSA300_RS04805	SAUSA300_0891	*oppA*	peptide ABC transporter substrate-binding protein	405.96	587.84	25.82	49.53	2.24165553 1	0.00003603

Table A-3 (cont'd)

No	C	SAUSA300_RS03080	SAUSA300_0576		hypothiocyanous acid reductase MerA	71.74	127.86	8.91	7.22	2.24152742	0.0000298
Yes	L	SAUSA300_RS10735	SAUSA300_1957		DnaD domain-containing protein	10.42	64.94	0.69	3.46	2.23788533	0.02457
Yes	C	SAUSA300_RS05570	SAUSA300_1035		staphylobilin-forming heme oxygenase IsdG	233.89	109	5.78	18.34	2.23162571	0.006752
Yes	S	SAUSA300_RS03690	SAUSA300_0687		hemolysin family protein	647.85	721.8	70.53	47.41	2.21029214	0.0000105
Yes	P	SAUSA300_RS07905	SAUSA300_1448		Fur family transcriptional regulator	1799.9	1559.7	187.21	105.66	2.19156570	0.0000697
Yes	no homolog found	SAUSA300_RS10730	SAUSA300_1956		hypothetical protein	11.05	56.14	0.67	3.32	2.16705141	0.03123
No	J	SAUSA300_RS02760	SAUSA300_0515	*cysS*	cysteine--tRNA ligase	100.51	218.8	17.01	9.95	2.15679562	0.000384
Yes	P	SAUSA300_RS01055	SAUSA300_0200		ABC transporter ATP-binding protein	560.59	480.76	28.76	56.72	2.15414874	0.0008821
Yes	D	SAUSA300_RS07900	SAUSA300_1447	*xerD*	site-specific tyrosine recombinase XerD	350.68	327.55	38.84	23.94	2.11307162	0.0000709

Table A-3 (cont'd)

Yes	P	SAUSA300_RS02340	SAUSA300_0437		dipeptide ABC transporter glycylmethionine-binding lipoprotein	2857.81	3414.82	123.34	372.09	2.11260531	0.004659
No	C	SAUSA300_RS04425	SAUSA300_0821		SUF system NifU family Fe-S cluster assembly protein	73.21	154.28	12.48	7.44	2.109192344	0.0005562
Yes	C	SAUSA300_RS06390	SAUSA300_1182		2-oxoacid:acceptor oxidoreductase subunit α	50	64.63	4.66	5.58	2.108932814	0.0000709
Yes	E	SAUSA300_RS02755	SAUSA300_0514	*cysE*	serine O-acetyltransferase	103.89	143.94	10.54	11.66	2.107872005	0.0000635
No	no homolog found	SAUSA300_RS05575			hypothetical protein	29.79	15.46	0.76	2.46	2.104844003	0.02746
Yes	S	SAUSA300_RS03075	SAUSA300_0575		DUF1450 domain-containing protein	287.35	198.41	26.21	18.61	2.104126932	0.0002521
No	O	SAUSA300_RS08555	SAUSA300_1569		U32 family peptidase	78.89	103.05	10.96	5.81	2.097466488	0.0001548
Yes	S	SAUSA300_RS10985	SAUSA300_1998		YeeE/YedE family protein	409.6	333.59	14.91	45.03	2.094939329	0.005985

Table A-3 (cont'd)

No	P	SAUSA300_RS03865	SAUSA300_0718		ABC transporter permease	10.81	14.08	1.2	1.04	2.089818408	0.0001951
No	P	SAUSA300_RS04795	SAUSA300_0889	*oppD*	ABC transporter ATP-binding protein	26.5	64.84	2.4	5.34	2.001735702	0.008266
Yes	S	SAUSA300_RS10695	SAUSA300_1949	*dut*	dUTP pyrophosphatase	12.62	67.03	0.87	4.58	2.000992404	0.0494
No	S	SAUSA300_RS04365	SAUSA300_0809		phage/plasmid primase, P4 family	38.21	23.66	3.89	2.31	1.988165711	0.001511
Yes	F	SAUSA300_RS03850	SAUSA300_0717	*nrdF*	class 1b ribonucleoside-diphosphate reductase subunit β	3385.68	4233.06	315.61	430.52	1.971420605	0.0004094
Yes	P	SAUSA300_RS03880	SAUSA300_0721		siderophore ABC transporter substrate-binding protein	135.83	190.99	18.67	14.4	1.970966015	0.0001214
Yes	K	SAUSA300_RS14555	SAUSA300_2619		S-adenosyl-L-methionine hydroxide adenosyltransferase family protein	27.21	28.52	2.62	2.99	1.958078283	0.0004355
No	K	SAUSA300_RS11905	SAUSA300_2160		MerR family transcriptional regulator	10.7	15.89	1.65	0.97	1.934529354	0.00395

Table A-3 (cont'd)

Yes	P	SAUSA300_RS02330	SAUSA300_0435		methionine ABC transporter ATP-binding protein	381.52	394.48	18.79	54.32	1.90102864 2	0.01246
No	T	SAUSA300_RS06020	SAUSA300_1112		protein-serine/threonine phosphatase Stp1	52.4	86.83	7.62	6.89	1.90020096 5	0.0005763
Yes	E	SAUSA300_RS11035	SAUSA300_2006	*ilvD*	dihydroxy-acid dehydratase	117.87	89.78	11.72	10.72	1.88874799 2	0.0007114
Yes	K	SAUSA300_RS14655	SAUSA300_2639		cold-shock protein	31165.95	38909.15	2344	4676.49	1.87881243 2	0.004656
No	F	SAUSA300_RS14520	SAUSA300_2612	*hisG*	ATP phosphoribosyltransferase	12.44	16.58	0.44	2.09	1.87807789 2	0.03823
No	no homolog found	SAUSA300_RS16065			hypothetical protein	32.67	47.74	5.51	2.81	1.8590956	0.008444
Yes	C	SAUSA300_RS14195	SAUSA300_2554		assimilatory sulfite reductase (NADPH) flavoprotein subunit	78.46	71.39	7.45	8.83	1.85893782 5	0.000838
Yes	EP	SAUSA300_RS01065	SAUSA300_0202		ABC transporter permease	100.24	118.03	10.39	13.38	1.83853411 3	0.001002
Yes	S	SAUSA300_RS00890	SAUSA300_0169		YbaN family protein	132.17	114.65	9.43	16.76	1.82943090 1	0.005769

Table A-3 (cont'd)

No	no homolog found	SAUSA300_RS04375	SAUSA300_0811		hypothetical protein	34.03	20.2	4.18	1.66	1.8197260336	0.02193
Yes	F	SAUSA300_RS03840	SAUSA300_0715	*nrdI*	class Ib ribonucleoside-diphosphate reductase assembly flavoprotein NrdI	430.27	617.2	17	82.06	1.7891168337	0.0477
Yes	CH	SAUSA300_RS13660	SAUSA300_2463	*ddh*	D-lactate dehydrogenase	392.33	291.12	59.74	18.72	1.7869759922	0.0158
Yes	C	SAUSA300_RS12320	SAUSA300_2231	*fdhD*	formate dehydrogenase accessory sulfurtransferase FdhD	144.13	150.35	20.34	14.5	1.7780256999	0.0007485
Yes	S	SAUSA300_RS07495	SAUSA300_1372		helix-turn-helix domain-containing protein	150.73	178.21	26.69	11.79	1.7762105222	0.00428
No	S	SAUSA300_RS05285	SAUSA300_0982		hypothetical protein	420.34	696.24	62.01	65.54	1.7680935881	0.001622
No	E	SAUSA300_RS12580	SAUSA300_2276		M20 peptidase aminoacylase family protein	22.11	25.47	1.99	3.31	1.76726895	0.006011
Yes	no homolog found	SAUSA300_RS10255			hypothetical protein	86.18	69.13	13.79	3.7	1.7546638339	0.0321

Table A-3 (cont'd)

No	P	SAUSA300_RS13240	SAUSA300_2392	*opuCb*	ABC transporter permease	32.79	44.43	5.52	3.65	1.74940789 2	0.002075
No	F	SAUSA300_RS06655	SAUSA300_1228	*thrB*	homoserine kinase	40.14	69.39	6.45	6.29	1.74186855 1	0.002579
No	M	SAUSA300_RS13235	SAUSA300_2391	*opuCc*	osmoprotectant ABC transporter substrate-bindingprotein	77.03	99.33	12.26	9.11	1.73226185 3	0.001069
No	-	SAUSA300_RS04355	SAUSA300_0807		hypothetical protein	32.42	19.37	3.7	2.51	1.72492731 3	0.01387
Yes	L	SAUSA300_RS08900	SAUSA300_1631		replication initiation and membrane attachment family protein	85.06	154.12	9.57	17.22	1.71586395 5	0.01269
No	S	SAUSA300_RS04360	SAUSA300_0808		DUF1474 family protein	44	26.88	4.5	4.02	1.70682078 1	0.01423
No	V	SAUSA300_RS05030	SAUSA300_0936		ABC transporter ATP-binding protein	21.87	15.19	1.6	2.71	1.70045988 2	0.01988
Yes	U	SAUSA300_RS11755	SAUSA300_2135		iron ABC transporter permease	108.5	124.48	15.58	13.37	1.70018686 2	0.001069
Yes	E	SAUSA300_RS14085	SAUSA300_2538		amino acid permease	731.16	576.5	62.48	93.99	1.69946733 6	0.007759

Table A-3 (cont'd)

Yes	S	SAUSA300_RS12540	SAUSA300_2268		bile acid:sodium symporter family protein	79.33	62.56	4.15	11.71	1.6910455845	0.03554
No	not classified	SAUSA300_RS15215			hypothetical protein	63.8	39.7	9.06	3.56	1.6810705478	0.03059
No	J	SAUSA300_RS06015	SAUSA300_1111		23S rRNA (adenine(2503)-C(2))-methyltransferase RlmN	40.29	74.21	8.63	5.48	1.6737961478	0.006054
No	O	SAUSA300_RS04410	SAUSA300_0818	*sufC*	Fe-S cluster assembly ATPase SufC	210.98	289.56	30.02	32.6	1.6609524773	0.002513
Yes	E	SAUSA300_RS02320	SAUSA300_0433	*cysM*	cysteine synthase family protein	50.07	39.27	6.04	5.48	1.6485674166	0.005019
No	not classified	SAUSA300_RS04345	SAUSA300_0805		helix-turn-helix domain-containing protein	81.86	44.92	11.97	4.21	1.6339050076	0.04207
Yes	I	SAUSA300_RS08985	SAUSA300_1646	*accA*	acetyl-CoA carboxylase carboxyltransferase subunit α	288.96	304.7	51.18	27.08	1.6299141311	0.005878
Yes	U	SAUSA300_RS04915	SAUSA300_0914		alanine/glycine:cation symporter family protein	84.57	75.06	11.04	10.02	1.6211638114	0.00335
Yes	C	SAUSA300_RS01085	SAUSA300_0206		FMN-dependent NADH-azoreductase	169.98	178.97	25.6	21.21	1.6018221555	0.002651

Table A-3 (cont'd)

Yes	E	SAUSA300_RS13265	SAUSA300_2395		APC family permease	39.16	45.52	3.75	6.86	1.599917453	0.01833
No	E	SAUSA300_RS06650	SAUSA300_1227	*thrC*	threonine synthase	82.97	133.36	14.77	13.7	1.589696012	0.005027
No	E	SAUSA300_RS04420	SAUSA300_0820	*sufS*	cysteine desulfurase	85.92	166.65	19.61	13.63	1.581474562	0.01014
No	no homolog found	SAUSA300_RS13715			hypothetical protein	180.02	305.25	36.61	27.93	1.577368951	0.007251
Yes	C	SAUSA300_RS00885	SAUSA300_0168		staphylobilin-forming heme oxygenase IsdI	526.12	366.61	37.96	75.76	1.574732171	0.03466
Yes	I	SAUSA300_RS00930	SAUSA300_0177		acyl-CoA/acyl-ACP dehydrogenase	456.28	496.21	50.29	74.56	1.574632793	0.01062
Yes	I	SAUSA300_RS02535	SAUSA300_0472	*ipk*	4-(cytidine 5'-diphospho)-2-C-methyl-D-erythritol kinase	108	182.76	15.31	22.22	1.564847353	0.01549
Yes	S	SAUSA300_RS13755	SAUSA300_2479	*cidA*	holin-like murein hydrolase modulator CidA	35.32	33.97	4.33	5.01	1.55870114	0.01209
Yes	H	SAUSA300_RS01160	SAUSA300_0221	*pflA*	pyruvate formate-lyase-activating protein	23.14	67.26	7.33	4.26	1.557733927	0.0398

Table A-3 (cont'd)

No	O	SAUSA300_RS04415	SAUSA300_0819	*sufD*	Fe-S cluster assembly protein SufD	84.79	163.66	16.42	16.94	1.53359869	0.01325
No	C	SAUSA300_RS12475	SAUSA300_2258		formate dehydrogenase subunit α	30.3	67.91	7.26	5.91	1.53048046	0.01884
Yes	P	SAUSA300_RS11750	SAUSA300_2134		iron chelate uptake ABC transporter family permease subunit	178.16	175.29	30.27	20.31	1.522591774	0.006752
Yes	L	SAUSA300_RS08280	SAUSA300_1517		deoxyribonuclease IV	198.68	214.14	38.88	21	1.500511213	0.01254
Yes	E	SAUSA300_RS06640	SAUSA300_1225		aspartate kinase	45.43	52.12	4.69	8.7	1.477243402	0.03452
Yes	L	SAUSA300_RS07130	SAUSA300_1309		IS200/IS605 family transposase	289.43	227.22	50.14	27.04	1.465628033	0.02368
Yes	no homolog found	SAUSA300_RS15665	SAUSA300_2604		hypothetical protein	203.06	247.71	34.59	31.87	1.456725418	0.009251
No	L	SAUSA300_RS06155	SAUSA300_1137	*rnhB*	ribonuclease HII	13.27	21.65	2.93	2.14	1.449170368	0.02342
Yes	C	SAUSA300_RS00940	SAUSA300_0179		NAD-dependent formate dehydrogenase	36.3	41.91	5.91	5.82	1.431737941	0.01168

Table A-3 (cont'd)

Yes	F	SAUSA300_RS05655	SAUSA300_1050		XTP/dITP diphosphatase	291.5	295.17	33.89	51.69	1.42982128 7	0.02799
No	not classified	SAUSA300_RS04370	SAUSA300_0810		hypothetical protein	49.06	33.44	7.63	4.9	1.42856537 8	0.03895
No	M	SAUSA300_RS05650	SAUSA300_1049	*murI*	glutamate racemase	137.05	140.32	14.61	25.67	1.41622281 6	0.0406
Yes	H	SAUSA300_RS00040	SAUSA300_0007		NAD(P)H-hydrate dehydratase	152.04	111.48	16.95	23.56	1.37445170 1	0.04415
No	P	SAUSA300_RS05255	SAUSA300_0978		ABC transporter ATP-binding protein	25.48	24.9	4.49	3.51	1.37174870 6	0.01877
Yes	P	SAUSA300_RS06680	SAUSA300_1232		catalase	606.82	615.49	93.79	98.44	1.37129191 7	0.01609
No	no homolog found	SAUSA300_RS01180	SAUSA300_0224	*coa*	staphylocoagulase	12.09	14.67	1.96	2.21	1.36308916 7	0.02499
No	BQ	SAUSA300_RS09180	SAUSA300_1681	*acuC*	acetoin utilization protein AcuC	25.27	25.74	4.67	3.48	1.36043943 1	0.02085
Yes	J	SAUSA300_RS06190	SAUSA300_1144	*gid*	methylenetetrahydrofolate--tRNA-(uracil(54)- C(5))-methyltransferase (FADH(2)-oxidizing) TrmFO	260.2	365.22	61.61	38.45	1.35426774 6	0.0232

Table A-3 (cont'd)

Yes	L	SAUSA300_RS03790	SAUSA300_0705	*recQ*	DNA helicase RecQ	153.97	141.14	17.71	28.07	1.34565723	0.04775
Yes	JKL	SAUSA300_RS08285	SAUSA300_1518		DEAD/DEAH box helicase	64.94	83.11	12.31	11.62	1.32944090	0.01919
Yes	S	SAUSA300_RS00020	SAUSA300_0003		S4 domain-containing protein YaaA	763.57	867.3	102.04	155.98	1.31666309	0.04702
No	L	SAUSA300_RS00025	SAUSA300_0004	*recF*	DNA replication/repair protein RecF	284.39	343.66	49.13	53.42	1.30892491	0.02435
Yes	L	SAUSA300_RS02485	SAUSA300_0463		DNA replication initiation control protein YabA	174.12	216.6	38.02	27.16	1.30156573	0.02499
Yes	EGP	SAUSA300_RS11720	SAUSA300_2128		multidrug efflux MFS transporter SdrM	78.96	93.2	18.13	10.78	1.29900995	0.0323
Yes	C	SAUSA300_RS00280	SAUSA300_0055		zinc-dependent alcohol dehydrogenase family protein	95.33	87.76	19.62	11.34	1.29875954	0.03933
No	F	SAUSA300_RS03815	SAUSA300_0711		diacylglycerol kinase family lipid kinase	163.7	260.55	33.34	36.19	1.28261428	0.03762
Yes	V	SAUSA300_RS09580	SAUSA300_1751	*hsdS*	restriction endonuclease subunit S	42.79	41.67	7.33	7.15	1.25722753	0.03504
Yes	G	SAUSA300_RS11545	SAUSA300_2096	*manA*	class I mannose-6-phosphate isomerase	107	94.53	20.09	15.44	1.23701318	0.0406

Table A-3 (cont'd)

No	V	SAUSA300_RS01645	SAUSA300_0308		FtsX-like permease family protein	27.83	39.43	5.35	6.07	1.23601849	0.0494
No	E	SAUSA300_RS07385	SAUSA300_1355	*aroA*	3-phosphoshikimate 1-carboxyvinyltransferase	32.35	50.24	7.72	6.76	1.20727057	0.04936
Yes	J	SAUSA300_RS08600	SAUSA300_1578	*mnmA*	tRNA 2-thiouridine(34) synthase MnmA	197.31	212.32	40.31	34.26	1.18478652	0.04032

Genes downregulated in *cymR*::Tn sulfur starvation when compared to *cymR*::Tn CSSC

Shared with WT -S (Table 1)	COG	Locus	Old locus	Gene	Product	TPM. 1 Starv	TPM. 2 Starv	TPM. 1 CSSC	TPM. 2 CSSC	DE Log_2 FC	DE Adj. *P*-value
Yes	F	SAUSA300_RS05210	SAUSA300_0969	*purS*	phosphoribosylformylglycinamidine synthase subunit PurS	2.47	3.94	71.99	13.69	-4.149577267	1.81E-08
Yes	O	SAUSA300_RS09140	SAUSA300_1674		trypsin-like peptidase domain-containing protein	85.06	85.76	1357.31	388.28	-4.0295346118	1.47E-10
Yes	F	SAUSA300_RS05245	SAUSA300_0976	*purD*	phosphoribosylamine--glycine ligase	19.9	25.17	550.46	48.93	-3.95756855 2	0.00000131

Table A-3 (cont'd)

No	S	SAUSA300_RS01635	SAUSA300_0307	5'-nucleotidase, lipoprotein e(P4) family	18.71	13.8	108.69	134.9	-3.80758815	1.36E-12
No	not classified	SAUSA300_RS15375		hypothetical protein	121.8	164.6	571	1344.17	-3.61437204	0.00000008
Yes	not classified	SAUSA300_RS03000		hypothetical protein	791.77	650.78	5797.02	3465.16	-3.58974782	3.42E-12
Yes	S	SAUSA300_RS03005		C1q-binding complement inhibitor VraX	38489.16	31696.59	223911.13	205445.74	-3.57143228	7.47E-13
Yes	no homolog found	SAUSA300_RS15740		phenol-soluble modulin PSM-alpha-1	4289.85	3326.41	12580.61	37405.9	-3.49537831	0.00000312
Yes	no homolog found	SAUSA300_RS15735		phenol-soluble modulin PSM-alpha-2	5730.32	4555.63	15900.9	49372.47	-3.44653104	0.00000589
Yes	no homolog found	SAUSA300_RS15090		phenol-soluble modulin PSM-alpha-3	6345.06	5161.13	15050.63	48596.27	-3.26740945	0.00000328

Table A-3 (cont'd)

No	M	SAUSA300_RS09800	SAUSA300_1790	*prsA*	peptidylprolyl isomerase	421.53	472.95	2316.62	1527.7	-3.10276006	1.47E-10
Yes	F	SAUSA300_RS05195	SAUSA300_0966	*purE*	5-(carboxyamino)imidazole ribonucleotide mutase	3.99	5.78	34.58	12.45	-3.09627570	0.00000084
Yes	E	SAUSA300_RS04565	SAUSA300_0845	*ampA*	M17 family metallopeptidase	36.03	30.19	174.09	110.97	-3.06439436	3.2E-09
Yes	no homolog found	SAUSA300_RS15730			phenol-soluble modulin PSM-alpha-4	4781.15	3722.92	9480.7	29491.47	-3.03154555	0.00000163
Yes	S	SAUSA300_RS04760	SAUSA300_0883		MAP domain-containing protein	124.67	114.66	461.46	414.03	-2.89012139	3.65E-09
Yes	no homolog found	SAUSA300_RS08745			hypothetical protein	197.34	199.97	814	614.86	-2.86549480	3.65E-09
No	E	SAUSA300_RS06940	SAUSA300_1278	*pepF*	oligoendopeptidase F	75.95	58.57	300.94	192.94	-2.83784688	9.86E-08

Table A-3 (cont'd)

No	GH	SAUSA300_RS00995	SAUSA300_0190	*ipdC*	alpha-keto acid decarboxylase family protein	10.1	6.08	45.98	18.64	-2.821409821	0.0000101
No	J	SAUSA300_RS10275	SAUSA300_1878	*rumA*	23S rRNA (uracil(1939)-C(5))-methyltransferase RlmD	32.74	30.2	110.13	106.33	-2.80767328	1.45E-08
Yes	no homolog found	SAUSA300_RS09670	SAUSA300_1767	*epiA*	gallidermin/nisin family lantibiotic	14.79	14.8	62.42	43.05	-2.802094714	0.0000001912
Yes	no homolog found	SAUSA300_RS13850	SAUSA300_2493		cell wall inhibition responsive protein CwrA	494.41	405.76	1253.62	1809.15	-2.76138450 9	0.0000008225
Yes	no homolog found	SAUSA300_RS04395	SAUSA300_0815	*ear*	DUF4888 domain-containing protein	285.78	247.57	514.54	1337.86	-2.72108987 5	0.000056
No	S	SAUSA300_RS04990	SAUSA300_0929		IDEAL domain-containing protein	546.22	445.01	1192.94	2058.93	-2.69453938 8	0.0000061 7
Yes	H	SAUSA300_RS04995	SAUSA300_0930		lipoate--protein ligase	21.94	21.55	83.77	52.52	-2.65177849 5	0.0000002 24

Table A-3 (cont'd)

Yes	J	SAUSA300_RS02850	SAUSA300_0533	*tuf*	elongation factor Tu	2098.2	1576.56	9598.42	2950.33	-2.59900773	0.0000999
No	M	SAUSA300_RS10340	SAUSA300_1890		cysteine protease staphopain A	23.86	17.48	90.7	41.01	-2.580730205	0.0000165
No	S	SAUSA300_RS08750	SAUSA300_1606		DUF4930 family protein	115.45	102.37	381.64	263.35	-2.57756366	0.0000041 6
No	C	SAUSA300_RS00705	SAUSA300_0135		superoxide dismutase	327.14	159.59	813.05	687.41	-2.53840489 9	0.0000398
No	no homolog found	SAUSA300_RS10505	SAUSA300_1918		phospholipase	231.88	358.24	247.86	1370.52	-2.33174297 4	0.00675249
No	S	SAUSA300_RS03335	SAUSA300_0622		M50 family metallopeptidase	33.18	27.28	90.42	59.45	-2.31937854 2	0.0000144
No	no homolog found	SAUSA300_RS12715			hypothetical protein	29.21	27.54	62.52	74.48	-2.30803231 2	0.0000341
No	K	SAUSA300_RS12480	SAUSA300_2259		LCP family protein	71.48	67.66	173.82	151.62	-2.28443859 2	0.0000482

Table A-3 (cont'd)

No	H	SAUSA300_RS09355	SAUSA300_1712	*ribH*	6,7-dimethyl-8-ribityllumazine synthase	125.94	114.01	276.51	281.84	-2.276222481	0.00000889
No	not classified	SAUSA300_RS10455	SAUSA300_1910		phenol-soluble modulin export ABC transporter permease subunit PmtD	95.33	102.77	117.43	363.08	-2.253531766	0.00232582 1
Yes	J	SAUSA300_RS06310	SAUSA300_1166	*rpsO*	30S ribosomal protein S15	1299.07	1092.22	5369.18	1160	-2.251184274	0.00327264 7
Yes	G	SAUSA300_RS04670	SAUSA300_0865	*pgi*	glucose-6-phosphate isomerase	173.21	188.57	531.08	307.54	-2.244104162	0.0000186
No	I	SAUSA300_RS12685	SAUSA300_2296		alpha/beta hydrolase	74.21	90.01	126.11	251.35	-2.243174137	0.00038308 8
No	V	SAUSA300_RS03590	SAUSA300_0669		undecaprenyl-diphosphate phosphatase	95.13	92.82	380.4	100.77	-2.22261993	0.00184399 7
No	S	SAUSA300_RS10345			staphostatin A	59.61	55.49	168.82	96.37	-2.216196221	0.0000495

Table A-3 (cont'd)

No	K	SAUSA300_RS10185	SAUSA300_1865	*vraR*	two-component system response regulator VraR	124.08	133.13	359.45	217.24	-2.20343570 3	0.0000221
No	S	SAUSA300_RS12500	SAUSA300_2262		CPBP family intramembrane glutamic endopeptidaseSdpB	63.68	66.42	223.47	84.83	-2.19661617	0.0004387 36
Yes	S	SAUSA300_RS13155	SAUSA300_2378		membrane protein	114.14	105.74	368.7	143.9	-2.17079242 5	0.0005211 9
No	S	SAUSA300_RS06705	SAUSA300_1236		CAP domain-containing protein	46.6	56.85	133.65	88.75	-2.16530558 6	0.0000196
No	not classified	SAUSA300_RS11565	SAUSA300_2100		lytic regulatory protein	211.95	349.99	728.49	464.11	-2.14536723 7	0.0000709
Yes	J	SAUSA300_RS02575	SAUSA300_0479		50S ribosomal protein L25/general stress proteinCtc	1009.33	776.59	3437.61	870.14	-2.11603300 3	0.0048453 34
No	O	SAUSA300_RS04625	SAUSA300_0857		peptidylprolyl isomerase	143.49	218.35	532.07	240.14	-2.10318800 8	0.0004387 36

Table A-3 (cont'd)

No	S	SAUSA300_RS12865	SAUSA300_2328		DUF4889 domain-containing protein	146.95	178.13	295.08	348.69	-2.07952448	0.00007099
No	not classified	SAUSA300_RS10200	SAUSA300_1868		hypothetical protein	33.4	42.96	69.49	79.98	-2.06292856	0.000099
Yes	M	SAUSA300_RS02965	SAUSA300_0556		6-phospho-3-hexuloisomerase	63.36	91.24	204.55	108.49	-2.05730151	0.00026039
No	C	SAUSA300_RS00155	SAUSA300_0030		glycerophosphoryl diester phosphodiesterase	27.56	42.18	64.24	68.28	-2.02599487	0.00014352
No	S	SAUSA300_RS04765	SAUSA300_0884		YjzD family protein	396.44	436.44	787.7	775.42	-2.00229876	0.00006975
No	EJ	SAUSA300_RS07470	SAUSA300_1368	*ansA*	asparaginase	27.49	29.51	68.76	41.19	-1.99735650	0.00019452
No	OU	SAUSA300_RS04060	SAUSA300_0752	*clpP*	ATP-dependent Clp endopeptidase proteolytic subunit ClpP	440.64	477.36	1027.25	715.24	-1.99596247	0.00008221

Table A-3 (cont'd)

No	S	SAUSA300_RS05185	SAUSA300_0964	DUF5011 domain-containing protein	1334.4	993.77	1790.96	2632.43	-1.97172832	0.00136213
No	K	SAUSA300_RS12390	SAUSA300_2245	HTH-type transcriptional regulator SarR	1604.75	1808.51	2792.06	3279.78	-1.93171892	0.00026039
No	no homolog found	SAUSA300_RS07815	SAUSA300_1432	hypothetical protein	230.19	344.16	486.16	523.1	-1.92280399	0.00032817
Yes	S	SAUSA300_RS09825	SAUSA300_1795	YlbF/YmcA family competence regulator	1580.86	1536.39	3185.12	2401.33	-1.91619496	0.00018578
No	no homolog found	SAUSA300_RS07460	SAUSA300_1366	hypothetical protein	36.42	28.53	70.61	48.87	-1.90330707	0.00140393
No	no homolog found	SAUSA300_RS06620	SAUSA300_1221	hypothetical protein	45.16	89.89	130.31	106.45	-1.89675278	0.00123968
Yes	C	SAUSA300_RS14075	SAUSA300_2537	L-lactate dehydrogenase	95.89	87.56	172.62	150.26	-1.89415454	0.00026964
No	no homolog found	SAUSA300_RS16085	SAUSA300_1988	delta-lysin family phenol-soluble modulin	77389.75	67469.88	139687.59	115668.38	-1.88906454	0.00032817

Table A-3 (cont'd)

No	not classified	SAUSA300_RS08150	SAUSA300_1493		SA1362 family protein	73.65	114.33	171.75	149.82	-1.87727516	0.00043873
No	K	SAUSA300_RS07035	SAUSA300_1295		cold shock protein CspA	6674.63	7960.83	8195.49	17190.01	-1.86859809	0.00578183
Yes	G	SAUSA300_RS02960	SAUSA300_0555		3-hexulose-6-phosphate synthase	31.5	53.55	80.68	63.24	-1.85573885	0.00076234
No	S	SAUSA300_RS10195	SAUSA300_1867		cell wall-active antibiotics response protein LiaF	51.05	51.63	83.33	82.76	-1.79203336	0.00066746
No	O	SAUSA300_RS09055	SAUSA300_1659	*tpx*	thiol peroxidase	541.7	543.17	1042.42	725.7	-1.78258335	0.00072659
No	E	SAUSA300_RS02635	SAUSA300_0491	*cysK*	cysteine synthase A	3633.25	2980.47	7140.91	3976.77	-1.77897610	0.00260445
Yes	not classified	SAUSA300_RS13040	SAUSA300_2361		putative metal homeostasis protein	1679.47	1321.49	3210.33	1826.03	-1.77418544	0.00287907

Table A-3 (cont'd)

Yes	C	SAUSA300_RS03045	SAUSA300_0569		heme-dependent peroxidase	363.72	351.6	698.13	442.77	-1.74031010 8	0.00150938 5
Yes	S	SAUSA300_RS13645	SAUSA300_2460		GNAT family N-acetyltransferase	65.19	95.56	123.23	120.22	-1.71748581 2	0.00159011 4
No	T	SAUSA300_RS10190	SAUSA300_1866	*vraS*	sensor histidine kinase	48.93	50.75	86.62	63.01	-1.67641484 4	0.00161703 9
Yes	S	SAUSA300_RS07160	SAUSA300_1314		YozE family protein	436.41	557.28	824.27	630.16	-1.65836285 2	0.00158791 1
No	S	SAUSA300_RS10910	SAUSA300_1984		CPBP family intramembrane glutamic endopeptidaseMroQ	111.71	104.09	126.21	189.52	-1.64590080 7	0.00832515 7
No	K	SAUSA300_RS05805	SAUSA300_1070		N-acetyltransferase	267.34	256.59	400.9	353.67	-1.62709675 1	0.00238303 3
Yes	J	SAUSA300_RS03960	SAUSA300_0736	*yfiA*	ribosome-associated translation inhibitor RaiA	5021.99	4039.9	5701.51	6755.99	-1.55314604 1	0.00995202 1

Table A-3 (cont'd)

No	S	SAUSA300_RS12720	SAUSA300_2302	*tcaA*	glycopeptide resistance protein TcaA	72.33	66.7	100.73	88.6	-1.54715648	0.00490233 6
Yes	G	SAUSA300_RS07165	SAUSA300_1315	*crr*	PTS glucose transporter subunit IIA	503.1	567.8	752.04	659.13	-1.51842218 5	0.00431367 4
No	H	SAUSA300_RS09425	SAUSA300_1725		transaldolase	380.74	299.7	509.03	398.74	-1.49584226 9	0.01058877 8
Yes	no homolog found	SAUSA300_RS15985			hypothetical protein	1270.74	1137.97	1916.24	1268.31	-1.48295495 6	0.01058877 8
No	F	SAUSA300_RS02705	SAUSA300_0505		pyridoxal 5'-phosphate synthase glutaminase subunit PdxT	152.55	146.59	154.76	231.17	-1.48055009 1	0.02100904 7
No	not classified	SAUSA300_RS06630	SAUSA300_1223		hypothetical protein	98.31	107.22	156.93	107.31	-1.46407273 7	0.00844839 6
Yes	S	SAUSA300_RS13765	SAUSA300_2481		sterile α motif-like domain-containing protein	5481.61	5785.93	6156.04	8057.18	-1.46091964 1	0.01481135 7

Table A-3 (cont'd)

No	no homolog found	SAUSA300_RS15910			hypothetical protein	467.29	484.78	547.11	613.57	-1.412598823	0.014597145
No	J	SAUSA300_RS08135	SAUSA300_1490	*efp*	elongation factor P	536.87	635.14	581.37	712.16	-1.287341467	0.033784
No	no homolog found	SAUSA300_RS15830			hypothetical protein	95.61	104.44	114.85	103.42	-1.248380442	0.040106722

APPENDIX B: Chapter 2 sulfur source Tables

Table B-1. Cysteine (Cys) differentially expressed genes.

Genes upregulated in Cys when compared to cystine (CSSC)

Locus	Old locus	Gene	Product	TPM.1 Cys	TPM.2 Cys	TPM.1 CSSC	TPM.2 CSSC	DE Log_2 FC	DE Adj. *P*-value
SAUSA300_RS15735			phenol-soluble modulin PSM-alpha-2	6414.07	22311.29	1675.5	4447.18	1.198345086	7.64841E-05
SAUSA300_RS15740			phenol-soluble modulin PSM-alpha-1	5005.57	17730.55	1294.02	3576.07	1.193139353	8.3552E-05
SAUSA300_RS15090			phenol-soluble modulin PSM-alpha-3	6602.59	24391.96	1880.69	4471.81	1.190219679	8.90957E-05
SAUSA300_RS15730			phenol-soluble modulin PSM-alpha-4	4712.08	16717.7	1439.61	3355.4	1.130860907	0.000192115

Genes downregulated in Cys when compared to CSSC

Locus	Old locus	Gene	Product	TPM.1 Cys	TPM.2 Cys	TPM.1 CSSC	TPM.2 CSSC	DE Log_2 FC	DE Adj. *P*-value
SAUSA300_RS04580	SAUSA300_0848		FAD/NAD(P)-binding protein	9.93	10.43	29.4	171.15	-1.769049937	4.77602E-09
SAUSA300_RS06690	SAUSA300_1234	*rpsN*	30S ribosomal protein S14	554.57	552.48	991.64	2246.49	-1.060341408	0.000256525

Table B-2. Oxidized glutathione (GSSG) differentially expressed genes.

Genes upregulated in GSSG when compared to CSSC

Locus	Old locus	Gene	Product	TPM.1 GSSG	TPM.2 GSSG	TPM.1 CSSC	TPM.2 CSSC	DE Log_2 FC	DE Adj. *P*-value
SAUSA300_RS00930	SAUSA300_0177		acyl-CoA/acyl-ACP dehydrogenase	115.41	240.12	2.69	9.11	4.157543995	3.04382E-22
SAUSA300_RS02185	SAUSA300_0407		superantigen-like protein SSL11	60.15	76.27	2.18	5.91	3.439076082	5.42187E-17
SAUSA300_RS00925	SAUSA300_0176		ABC transporter permease	78.28	96.38	4.22	2.74	3.303313167	9.01551E-10
SAUSA300_RS00915	SAUSA300_0174		ABC transporter ATP-binding protein	14.09	28.88	1.31	1.85	2.830762445	9.05749E-09
SAUSA300_RS02340	SAUSA300_0437	*gmpC*	dipeptide ABC transporter glycylmethionine-binding lipoprotein	667.4	817.5	30.16	144.44	2.654314417	9.05749E-09
SAUSA300_RS03085	SAUSA300_0577		redox-sensitive transcriptional regulator HypR	79.95	217.72	12.24	7.56	2.550101035	1.54999E-05
SAUSA300_RS13745	SAUSA300_2477		pyruvate oxidase	176.31	224.87	16.24	30.98	2.459729837	9.05749E-09
SAUSA300_RS02325	SAUSA300_0434		bifunctional cystathionine γ-lyase/homocysteine desulfhydrase	66.24	118.57	6.96	15.5	2.424127828	2.57027E-08
SAUSA300_RS00920	SAUSA300_0175		ABC transporter substrate-binding protein	20.65	35.29	2.69	2.58	2.408938291	4.67518E-06
SAUSA300_RS00910	SAUSA300_0173		DUF4242 domain-containing protein	174.59	290.64	14.98	49.04	2.371131373	6.13964E-08
SAUSA300_RS13525	SAUSA300_2440	*fnbB*	fibronectin-binding protein FnbB	60.43	59.28	5.83	8.01	2.357341809	7.51319E-07

Table B-2 (cont'd)

SAUSA300_RS02035	SAUSA300_0382		L-cystine transporter	1284.59	1070.76	127.04	125.62	2.306320567	1.28398E-05
SAUSA300_RS02190	SAUSA300_0408		FKLRK protein	132.34	186.81	14.95	26.75	2.289237921	1.87629E-07
SAUSA300_RS10920	SAUSA300_1986		nitroreductase family protein	74.65	74.1	5.47	16.95	2.276437635	4.49694E-07
SAUSA300_RS13910	SAUSA300_2505		GNAT family N-acetyltransferase	18.59	30.85	0.55	7	2.224312445	0.000261289
SAUSA300_RS07500	SAUSA300_1373		ferredoxin	2280.42	2592.1	274.46	309.79	2.219360193	8.76536E-06
SAUSA300_RS10985	SAUSA300_1998		YeeE/YedE family protein	45.26	77.02	4.7	14.19	2.196473104	7.51319E-07
SAUSA300_RS04170	SAUSA300_0773	*vwb*	von Willebrand factor binding protein Vwb	22.43	39.39	2.02	8.27	2.139849726	7.0435E-06
SAUSA300_RS01055	SAUSA300_0200		ABC transporter ATP-binding protein	82.97	88.98	9.74	14.41	2.136824537	6.18049E-06
SAUSA300_RS02315	SAUSA300_0432		sodium-dependent transporter	160.87	163.73	16.69	35.07	2.108173714	2.0706E-06
SAUSA300_RS01185			hypothetical protein	61.49	77.54	6.01	16.16	2.102102385	1.90088E-05
SAUSA300_RS01180	SAUSA300_0224	*coa*	staphylocoagulase	37.03	72.45	4.59	14	2.056129945	7.69607E-06
SAUSA300_RS07495	SAUSA300_1372		helix-turn-helix domain-containing protein	153.75	146.57	17.77	29.53	2.039023845	1.48728E-05
SAUSA300_RS02335	SAUSA300_0436		methionine ABC transporter permease	58.66	85.25	4.85	23.05	1.986024342	5.44287E-05
SAUSA300_RS14570	SAUSA300_2622		rhodanese-related sulfurtransferase	169.47	471.86	25.72	85.02	1.983040622	9.43471E-05
SAUSA300_RS02330	SAUSA300_0435		methionine ABC transporter ATP-binding protein	45.39	68.57	6.07	13.82	1.982114069	7.69607E-06

Table B-2 (cont'd)

SAUSA300_RS10980	SAUSA300_1997		sulfurtransferase TusA family protein	270.78	321.08	39.77	54.14	1.939189828	7.77652E-05
SAUSA300_RS13025	SAUSA300_2359		transporter substrate-binding domain-containing protein	167.41	263.08	19.34	69.69	1.868432696	5.3321E-05
SAUSA300_RS01075	SAUSA300_0204	*ggt*	γ-glutamyltransferase	28.66	33.84	4.18	7.39	1.842347726	7.74037E-05
SAUSA300_RS05520	SAUSA300_1026		DUF177 domain-containing protein	1413.86	2722.12	153.02	729.17	1.839326382	0.000295 32
SAUSA300_RS01060	SAUSA300_0201		ABC transporter permease	20.73	22.11	3.3	3.88	1.815353512	0.000587 577
SAUSA300_RS02320	SAUSA300_0433		cysteine synthase family protein	15.84	16.98	2.64	2.54	1.806100258	0.001534 208
SAUSA300_RS16005			hypothetical protein	61.05	73.6	3.59	26.52	1.788917197	0.002760 437
SAUSA300_RS11935	SAUSA300_2165	*budA*	acetolactate decarboxylase	22.63	52.06	4.02	10.73	1.786263268	0.000363 127
SAUSA300_RS06225			hypothetical protein	466.01	690.17	71.03	167.17	1.777937733	7.77652E-05
SAUSA300_RS06500	SAUSA300_1203		hypothetical protein	23.75	20.62	1.84	7.85	1.764981 25	0.002486 839
SAUSA300_RS00935	SAUSA300_0178		DUF2294 domain-containing protein	598.61	688.18	92.52	169.33	1.737166884	0.000187 161
SAUSA300_RS01440	SAUSA300_0268		MFS transporter	19.46	21.64	2.57	6.44	1.732819023	0.000196 649
SAUSA300_RS06625	SAUSA300_1222		thermonuclease family protein	47.77	64.22	4.64	22.12	1.722156579	0.000769 904
SAUSA300_RS12110	SAUSA300_2196	*rpmC*	50S ribosomal protein L29	96.44	188.73	14.13	49.61	1.717032349	0.000561 759
SAUSA300_RS10510			hypothetical protein	474.99	538.81	47.79	197.93	1.712390344	0.000472 33

Table B-2 (cont'd)

SAUSA300_RS05670	SAUSA300_1052	*ecb*	complement convertase inhibitor Ecb	10430.33	8507.61	1011.3	3581.72	1.700447 58	0.000630005
SAUSA300_RS13755	SAUSA300_2479	*cidA*	holin-like murein hydrolase modulator CidA	83.68	81.85	10.97	26.05	1.698177302	0.000352912
SAUSA300_RS10255			hypothetical protein	22.66	36.96	3.61	8.17	1.695415345	0.005250193
SAUSA300_RS12415	SAUSA300_2249		CHAP domain-containing protein	1972.19	2369.74	375.46	388.13	1.695127202	0.001996199
SAUSA300_RS06695	SAUSA300_1235	*guaC*	GMP reductase	17.25	31.11	2.02	9.81	1.658868724	0.002041038
SAUSA300_RS09830	SAUSA300_1796		DUF445 domain-containing protein	115.14	89.24	7.76	47.79	1.619763721	0.005623452
SAUSA300_RS02805	SAUSA300_0524	*rplJ*	50S ribosomal protein L10	11616.08	13656.03	1888.15	3950.63	1.617289669	0.000415338
SAUSA300_RS08875	SAUSA300_1627	*infC*	translation initiation factor IF-3	430.38	791.62	69.57	229.93	1.611253418	0.000796613
SAUSA300_RS12105	SAUSA300_2195	*rpsQ*	30S ribosomal protein S17	113.03	200.29	20.36	53.63	1.604231927	0.000769904
SAUSA300_RS06705	SAUSA300_1236		CAP domain-containing protein	132.19	145.28	12.84	63.9	1.56883287	0.003192373
SAUSA300_RS13915	SAUSA300_2506	*isaA*	lytic transglycosylase IsaA	7884.88	8642.19	1471.51	2548.49	1.488456096	0.002608647
SAUSA300_RS10250	SAUSA300_1874	*ftnA*	H-type ferritin FtnA	492.8	949.36	122.59	214.34	1.483656263	0.003553971
SAUSA300_RS02845	SAUSA300_0532	*fusA*	elongation factor G	519.94	1145.37	121.77	295.86	1.476887914	0.003553971
SAUSA300_RS12090	SAUSA300_2192	*rplE*	50S ribosomal protein L5	154.45	292	35.53	75.61	1.469091457	0.002999274
SAUSA300_RS03735	SAUSA300_0696	*queD*	6-carboxytetrahydropterin synthase QueD	15.48	26.72	3.84	6.07	1.444043835	0.010359352

Table B-2 (cont'd)

SAUSA300_RS12085	SAUSA300_2191		type Z 30S ribosomal protein S14	249.57	376.99	58.41	92.01	1.441464039	0.005140203
SAUSA300_RS12075	SAUSA300_2189	*rplF*	50S ribosomal protein L6	193.04	286.33	43.19	76.27	1.436941322	0.003727587
SAUSA300_RS03880	SAUSA300_0721		siderophore ABC transporter substrate-binding protein	222.08	263.1	18	134.3	1.435417673	0.021157034
SAUSA300_RS04410	SAUSA300_0818	*sufC*	Fe-S cluster assembly ATPase SufC	71.9	125.91	9.8	48.93	1.431476197	0.010359352
SAUSA300_RS13020	SAUSA300_2358		amino acid ABC transporter permease	119.53	376.58	19.62	127.31	1.377126022	0.040614674
SAUSA300_RS02840	SAUSA300_0531	*rpsG*	30S ribosomal protein S7	642.56	1202.65	162.63	325.5	1.373234814	0.006761354
SAUSA300_RS08430	SAUSA300_1546	*holA*	DNA polymerase III subunit delta	34.2	35.18	4.79	16.68	1.366320996	0.008896376
SAUSA300_RS01435	SAUSA300_0267		IS1182 family transposase	12.61	16	2.04	6.4	1.345979451	0.021157034
SAUSA300_RS12080	SAUSA300_2190	*rpsH*	30S ribosomal protein S8	240.15	345.35	62.37	82.95	1.341118802	0.015622243
SAUSA300_RS03445	SAUSA300_0642		hypothetical protein	175.73	162.03	16.71	97.23	1.340310845	0.027666854
SAUSA300_RS02795	SAUSA300_0522	*rplK*	50S ribosomal protein L11	6887.07	8204.74	1597.14	2381.7	1.323476865	0.013419835
SAUSA300_RS11455	SAUSA300_2081		CTP synthase	112.31	246.97	25.14	82.44	1.322800643	0.014780092
SAUSA300_RS06220	SAUSA300_1149	*rpsB*	30S ribosomal protein S2	2338.33	3407.46	547.49	1071.67	1.315580016	0.008059084
SAUSA300_RS09505	SAUSA300_1738		DUF4909 domain-containing protein	16.8	14.12	3.24	5.12	1.313933411	0.031711545
SAUSA300_RS01470	SAUSA300_0274		hypothetical protein	76.11	61.94	8.81	37.54	1.312230047	0.022468518

Table B-2 (cont'd)

SAUSA300_RS01175	SAUSA300_0223		complement inhibitor SCIN family protein	1078.39	749.06	218.67	246.2	1.286669411	0.045188836
SAUSA300_RS03655	SAUSA300_0681		hypothetical protein	194	164.09	35.4	71.4	1.28398078	0.017977586
SAUSA300_RS12020	SAUSA300_2178		DNA-directed RNA polymerase subunit α	111.66	241.24	27.47	79.22	1.282624568	0.017455078
SAUSA300_RS05300	SAUSA300_0985	*nrdH*	glutaredoxin-like protein NrdH	152.35	101.25	23.84	53.83	1.282292065	0.028431659
SAUSA300_RS13015	SAUSA300_2357		amino acid ABC transporter ATP-binding protein	587.87	1126.44	153.55	347.3	1.279374623	0.013517702
SAUSA300_RS02800	SAUSA300_0523	*rplA*	50S ribosomal protein L1	2815.97	4907.22	649.39	1722.04	1.273765546	0.011596632
SAUSA300_RS05600	SAUSA300_1040	*zapA*	cell division protein ZapA	150.58	163.48	20.25	87.95	1.265909775	0.024410672
SAUSA300_RS05880	SAUSA300_1085		RNA-binding protein	134.09	132.96	16.44	77.46	1.261247318	0.02873826
SAUSA300_RS08870	SAUSA300_1626	*rpmI*	50S ribosomal protein L35	1426.77	2117.93	348.36	707.89	1.252620214	0.013387071
SAUSA300_RS02345	SAUSA300_0438	*aaa*	autolysin/adhesin Aaa	136.6	235.56	32.67	82.52	1.250136779	0.014232282
SAUSA300_RS09325	SAUSA300_1708		MarR family transcriptional regulator	1856.63	1352.39	372.38	532.57	1.242653826	0.040537541
SAUSA300_RS02835	SAUSA300_0530	*rpsL*	30S ribosomal protein S12	449.46	921.64	114.35	311.34	1.242140915	0.020375529
SAUSA300_RS06750	SAUSA300_1243		exonuclease subunit SbcC	24.78	25.9	4.61	11.82	1.238571117	0.015981333
SAUSA300_RS09395	SAUSA300_1720		N-acetylglucosaminidase	348.44	399.63	56.98	199.5	1.237168972	0.018201307
SAUSA300_RS12150	SAUSA300_2204	*rplC*	50S ribosomal protein L3	61.97	135.63	18.58	39.74	1.22708297	0.027466148

Table B-2 (cont'd)

SAUSA300_RS14655	SAUSA300_2639		cold-shock protein	85383.85	73729.38	15403.29	36858.2	1.212849751	0.023895526
SAUSA300_RS07285	SAUSA300_1336		class I SAM-dependent RNA methyltransferase	23.54	38.19	6.02	13.94	1.171757401	0.027320561
SAUSA300_RS04180	SAUSA300_0775		hypothetical protein	107.1	137.98	18.31	70.73	1.167447496	0.034250049
SAUSA300_RS05430	SAUSA300_1009	*typA*	translational GTPase TypA	43.52	66.53	10.76	25.73	1.1584696	0.025045599
SAUSA300_RS12115	SAUSA300_2197	*rplP*	50S ribosomal protein L16	100.6	225.21	34.63	62.4	1.157264551	0.049442479
SAUSA300_RS09090	SAUSA300_1666	*rpsD*	30S ribosomal protein S4	8545.8	10848.68	2335.75	3461.35	1.153968675	0.04070841
SAUSA300_RS11210	SAUSA300_2037		DEAD/DEAH box helicase	461.01	801.74	96.45	354	1.153909403	0.037063284
SAUSA300_RS11405	SAUSA300_2071	*prmC*	peptide chain release factor N(5)-glutamine methyltransferase	74.85	150.33	20.07	54.97	1.153509969	0.036318346
SAUSA300_RS12070	SAUSA300_2188	*rplR*	50S ribosomal protein L18	224.25	336.27	67.79	97.07	1.145681757	0.048416068
SAUSA300_RS11990	SAUSA300_2172	*rplM*	50S ribosomal protein L13	2485.64	3347.5	710.57	1079.1	1.123728432	0.048067748

Genes downregulated in GSSG when compared to CSSC

Locus	**Old locus**	**Gene**	**Product**	**TPM.1 GSSG**	**TPM.2 GSSG**	**TPM.1 CSSC**	**TPM.2 CSSC**	**DE Log_2 FC**	**DE Adj. *P*-value**
SAUSA300_RS05795	SAUSA300_1068			157.97	172.34	3464.54	3534.23	-4.304727876	1.5934E-20

Table B-2 (cont'd)

SAUSA300_RS05790	SAUSA300_1067		beta-class phenol-soluble modulin	231.76	231.64	4820.71	4917	-4.278890597	3.97915E-20
SAUSA300_RS04580	SAUSA300_0848		beta-class phenol-soluble modulin	3.18	4.13	29.4	171.15	-4.207916659	3.97915E-20
SAUSA300_RS13360	SAUSA300_2413	*cntL*	FAD/NAD(P)-binding protein	3.35	2.17	42.35	67.31	-4.063514424	1.42843E-18
SAUSA300_RS15090			D-histidine (S)-2-aminobutanoyltransferase CntL	152.59	251.82	1880.69	4471.81	-3.89758922	3.04382E-22
SAUSA300_RS15740			phenol-soluble modulin PSM-alpha-3	119.21	201.39	1294.02	3576.07	-3.807526925	4.6765E-21
SAUSA300_RS15735			phenol-soluble modulin PSM-alpha-1	153.88	267.81	1675.5	4447.18	-3.762671691	1.00147E-20
SAUSA300_RS15730			phenol-soluble modulin PSM-alpha-2	128.55	212.57	1439.61	3355.4	-3.754098002	1.00147E-20
SAUSA300_RS03005		*vraX*	phenol-soluble modulin PSM-alpha-4	14226.21	7060.01	130098.29	60616.24	-3.029380781	7.51319E-07
SAUSA300_RS13040	SAUSA300_2361		C1q-binding complement inhibitor VraX	7009.33	4703.8	51134.91	41439.61	-2.981950513	3.35575E-08
SAUSA300_RS03000			putative metal homeostasis protein	350	157.34	2775.63	1589.92	-2.971963 65	7.51319E-07

Table B-2 (cont'd)

SAUSA300_RS13355	SAUSA300_2412	*cntM*	hypothetical protein	4.26	2.14	16.89	38.39	-2.875251245	1.07614E-08
SAUSA300_RS13330	SAUSA300_2407		staphylopine dehydrogenase CntM	3.36	4.52	11.71	53.39	-2.792107182	2.8376E-09
SAUSA300_RS13340	SAUSA300_2409		ABC transporter ATP-binding protein	5.79	4.06	20.31	54.35	-2.763128 79	3.44703E-09
SAUSA300_RS06690	SAUSA300_1234	*rpsN*	ABC transporter permease	295.61	181.4	991.64	2246.49	-2.642568704	3.35575E-08
SAUSA300_RS10275	SAUSA300_1878	*rlmD*	30S ribosomal protein S14	12.68	16.55	86.77	64.72	-2.575287956	2.0706E-06
SAUSA300_RS08880	SAUSA300_1628		23S rRNA (uracil(1939)-C(5))-methyltransferase RlmD	32.89	39.93	113.06	312.07	-2.542314586	1.2333E-09
SAUSA300_RS07010	SAUSA300_1290	*dapD*	amino acid permease	108.46	111.7	455.49	710.32	-2.520651649	2.56794E-08
SAUSA300_RS13325	SAUSA300_2406		2,3,4,5-tetrahydropyridine-2,6-dicarboxylate N-acetyltransferase	93.2	55.58	310.49	534.53	-2.470429805	7.51319E-07
SAUSA300_RS07015	SAUSA300_1291		MFS transporter	15.12	19.69	63.58	90.07	-2.326963795	6.21097E-07
SAUSA300_RS16085	SAUSA300_1988		amidohydrolase	7032.08	5470.08	18503.83	35902.11	-2.171867176	4.12707E-06

Table B-2 (cont'd)

SAUSA300_RS14175	SAUSA300_2551	*nrdD*	delta-lysin family phenol-soluble modulin	6.42	13.29	34.12	39.52	-2.159393763	2.99305E-05
SAUSA300_RS14170	SAUSA300_2550	*nrdG*	anaerobic ribonucleoside-triphosphate reductase	15.87	30.72	89.47	81	-2.155609012	7.81136E-05
SAUSA300_RS09670	SAUSA300_1767		anaerobic ribonucleoside-triphosphate reductase activating protein	10.86	17.86	68.29	38.64	-2.150037555	0.000540373
SAUSA300_RS12890	SAUSA300_2333		gallidermin/nisin family lantibiotic	39.45	38.95	112.39	200.42	-2.122475632	3.60293E-06
SAUSA300_RS01625	SAUSA300_0305		nitrate/nitrite transporter	115.35	157.04	429.39	544.99	-2.081032901	1.90088E-05
SAUSA300_RS05195	SAUSA300_0966	*purE*	formate/nitrite transporter family protein	7.16	7.74	17.97	42.28	-2.066362184	7.22394E-06
SAUSA300_RS07025	SAUSA300_1293	*lysA*	5-(carboxyamino)imidazole ribonucleotide mutase	67.99	119.49	195.47	534.7	-2.039270385	4.12707E-06
SAUSA300_RS01635	SAUSA300_0307		diaminopimelate decarboxylase	49.76	43.86	160.97	150.13	-1.968653763	0.00036855
SAUSA300_RS07000	SAUSA300_1288	*dapA*	5'-nucleotidase, lipoprotein e(P4) family	10.77	19.16	33.36	64.28	-1.892834032	4.93298E-05
SAUSA300_RS10485			4-hydroxy-tetrahydrodipicolinate synthase	83.85	97.64	375.59	160.57	-1.892503751	0.00461996

Table B-2 (cont'd)

SAUSA300_RS06990	SAUSA300_1286		hypothetical protein	12.16	22.17	29.3	94.79	-1.887325956	4.93298E-05
SAUSA300_RS06995	SAUSA300_1287		aspartate kinase	12.53	22.2	36.57	76.45	-1.872870427	4.85665E-05
SAUSA300_RS07020	SAUSA300_1292		aspartate-semialdehyde dehydrogenase	7.21	12.84	19	45.97	-1.825669371	7.74037E-05
SAUSA300_RS12480	SAUSA300_2259		alanine racemase	40.79	50.98	113.18	157.63	-1.810349562	0.00022337
SAUSA300_RS13350	SAUSA300_2411	*cntA*	LCP family protein	32.03	26.97	38.2	205.11	-1.809368607	0.00074024
SAUSA300_RS13345	SAUSA300_2410		staphylopine-dependent metal ABC transporter substrate-binding protein CntA	40.11	30.46	59.12	204.03	-1.806048803	0.00029532
SAUSA300_RS13860	SAUSA300_2495	*copZ*	ABC transporter permease	3092.61	2654.74	10217.43	5935.91	-1.799606649	0.004998035
SAUSA300_RS05185	SAUSA300_0964		copper chaperone CopZ	1478.3	715.6	4004.37	2605.7	-1.780312978	0.008012672
SAUSA300_RS07005	SAUSA300_1289	*dapB*	DUF5011 domain-containing protein	23.2	44.89	54.26	165.98	-1.761777941	0.000196649
SAUSA300_RS10195	SAUSA300_1867	*liaF*	4-hydroxy-tetrahydrodipicolinate reductase	26.5	29.03	56.96	110.14	-1.750826039	0.000169321

Table B-2 (cont'd)

SAUSA300_RS10185	SAUSA300_1865	*vraR*	cell wall-active antibiotics response protein LiaF	96.99	137.47	277.59	350.5	-1.715320027	0.000792279
SAUSA300_RS04855	SAUSA300_0902	*pepF*	two-component system response regulator VraR	38.22	65.6	87.93	218.14	-1.702472242	0.000195422
SAUSA300_RS13045	SAUSA300_2362		oligoendopeptidase F	872.15	1164.6	1514.2	4828.17	-1.684102273	0.000212094
SAUSA300_RS12545	SAUSA300_2269		2,3-diphosphoglycerate-dependent phosphoglycerate mutase	252.38	174.56	573.51	583.69	-1.666865506	0.004942313
SAUSA300_RS15795		*pepA1*	hypothetical protein	786.73	766.47	2456.95	1290.29	-1.639394493	0.015438398
SAUSA300_RS04985	SAUSA300_0928		type I toxin-antitoxin system Fst family toxin PepA1	9.63	12.1	19.18	40.77	-1.620672046	0.000667423
SAUSA300_RS06940	SAUSA300_1278	*pepF*	competence protein ComK	95.77	95.44	207.72	271.22	-1.585420486	0.002808289
SAUSA300_RS10555			oligoendopeptidase F	657.54	372.43	1740.21	716.33	-1.561943065	0.038624179
SAUSA300_RS09355	SAUSA300_1712	*ribE*	hypothetical protein	111.62	124.06	240.59	334.73	-1.553846145	0.002773409
SAUSA300_RS00995	SAUSA300_0190		6,7-dimethyl-8-ribityllumazine synthase	13.28	10.78	25.77	34.11	-1.539930896	0.005623452

Table B-2 (cont'd)

SAUSA300_RS01265	SAUSA300_0237		alpha-keto acid decarboxylase family protein	21.17	25.76	50.02	59.68	-1.533685135	0.005005037
SAUSA300_RS12970			nucleoside hydrolase	35.76	27.36	81.4	67.56	-1.526447487	0.018992461
SAUSA300_RS03335	SAUSA300_0622		hypothetical protein	65.9	56.11	140.33	140.73	-1.499598783	0.012737296
SAUSA300_RS13725	SAUSA300_2473		M50 family metallopeptidase	102.73	95.64	212.77	237.78	-1.478666015	0.010359352
SAUSA300_RS04185	SAUSA300_0776		alpha/beta hydrolase	37.61	25.45	55.04	109.15	-1.477780793	0.006955209
SAUSA300_RS12780	SAUSA300_2313		thermonuclease family protein	330.15	656.83	887.06	1282.53	-1.455396328	0.007016909
SAUSA300_RS14075	SAUSA300_2537		L-lactate permease	130.81	164.88	241.49	410.57	-1.396183733	0.005316458
SAUSA300_RS05245	SAUSA300_0976	*purD*	L-lactate dehydrogenase	37.61	46.72	68	118.94	-1.393551826	0.005316458
SAUSA300_RS00400	SAUSA300_0079		phosphoribosylamine--glycine ligase	198.61	283.22	361.26	716.43	-1.389355943	0.004227754
SAUSA300_RS00215	SAUSA300_0040		YdhK family protein	7.35	7.29	16.36	14.43	-1.384991387	0.04070841

Table B-2 (cont'd)

SAUSA300_RS09140	SAUSA300_1674		hypothetical protein	148.65	184.75	242.45	500.75	-1.362142313	0.004998035
SAUSA300_RS12865	SAUSA300_2328		trypsin-like peptidase domain-containing protein	511.71	418.1	1025.36	853.36	-1.360750229	0.039399129
SAUSA300_RS09800	SAUSA300_1790		DUF4889 domain-containing protein	381.96	370.98	476.97	1357.86	-1.358439536	0.006449607
SAUSA300_RS01235	SAUSA300_0233		peptidylprolyl isomerase	19.82	38.78	48.66	69.56	-1.327572511	0.024225047
SAUSA300_RS01990	SAUSA300_0374		hypothetical protein	3030.82	4042.18	6286.49	7095.9	-1.288102453	0.028749116
SAUSA300_RS04565	SAUSA300_0845		GlsB/YeaQ/YmgE family stress response membrane protein	54.52	70.8	93.39	150.85	-1.249780323	0.019408834
SAUSA300_RS10935	SAUSA300_1989	*agrB*	M17 family metallopeptidase	561.54	883.99	1150.16	1544.07	-1.248530597	0.028033267
SAUSA300_RS00395	SAUSA300_0078		accessory gene regulator AgrB	39.14	77.35	66.5	171.55	-1.217530251	0.022101684
SAUSA300_RS10950	SAUSA300_1992		heavy metal translocating P-type ATPase	173.36	289.98	304.64	592.32	-1.216270388	0.020463346
SAUSA300_RS07160	SAUSA300_1314		LytTR family DNA-binding domain-containing protein	237.96	273.35	397.04	556.21	-1.210166496	0.033546539

Table B-2 (cont'd)

SAUSA300_RS13150	SAUSA300_2377	DUF4064 domain-containing protein	33.59	34.15	42.16	91.11	-1.160898774	0.028749116

Table B-3. Reduced glutathione (GSH) differentially expressed genes.

Genes upregulated in GSH when compared to CSSC

Locus	Old locus	Gene	Product	TPM. 1 GSH	TPM. 2 GSH	TPM. 1 CSSC	TPM. 2 CSSC	DE Log_2 FC	DE Adj. *P*-value
SAUSA300_RS00930	SAUSA300_0177		acyl-CoA/acyl-ACP dehydrogenase	121.53	319.76	2.69	9.11	4.046721405	8.67351E-15
SAUSA300_RS00925	SAUSA300_0176		ABC transporter permease	66.92	130.67	4.22	2.74	3.125833599	5.35039E-07
SAUSA300_RS02185	SAUSA300_0407		superantigen-like protein SSL11	34.84	122.95	2.18	5.91	3.083548435	1.13366E-07
SAUSA300_RS00915	SAUSA300_0174		ABC transporter ATP-binding protein	17.3	47.95	1.31	1.85	2.989014416	3.54407E-07
SAUSA300_RS02340	SAUSA300_0437	*gmpC*	dipeptide ABC transporter glycylmethionine-binding lipoprotein	579.84	889.89	30.16	144.44	2.315679543	4.10697E-05
SAUSA300_RS02330	SAUSA300_0435		methionine ABC transporter ATP-binding protein	68.43	117.68	6.07	13.82	2.290401543	1.35302E-05
SAUSA300_RS00920	SAUSA300_0175		ABC transporter substrate-binding protein	18.04	50.12	2.69	2.58	2.282409423	0.000547181
SAUSA300_RS11740	SAUSA300_2132		hypothetical protein	757.25	1059.95	76.55	120.09	2.173372354	8.53142E-05
SAUSA300_RS01185			hypothetical protein	90.86	88.68	6.01	16.16	2.150083564	0.000299038
SAUSA300_RS06580	SAUSA300_1213		hypothetical protein	44.88	53.03	0.47	12.46	2.111810188	0.006845352
SAUSA300_RS06505			hypothetical protein	18.79	21.99	0.61	4.2	2.108785522	0.004475634
SAUSA300_RS06500	SAUSA300_1203		hypothetical protein	32.66	40.54	1.84	7.85	2.106875855	0.000740514
SAUSA300_RS12110	SAUSA300_2196	*rpmC*	50S ribosomal protein L29	87.92	495.63	14.13	49.61	2.102650383	0.002677665

Table B-3 (cont'd)

SAUSA300_RS01180	SAUSA300_0224	*coa*	staphylocoagulase	38.28	115.67	4.59	14	2.100463489	0.000549967
SAUSA300_RS02190	SAUSA300_0408		FKLRK protein	141.8	206.04	14.95	26.75	2.087502758	0.000123001
SAUSA300_RS00910	SAUSA300_0173		DUF4242 domain-containing protein	217.47	240.98	14.98	49.04	2.081816612	0.000140982
SAUSA300_RS12105	SAUSA300_2195	*rpsQ*	30S ribosomal protein S17	104.23	549.36	20.36	53.63	2.018096815	0.003351341
SAUSA300_RS06575	SAUSA300_1212		polymorphic toxin type 50 domain-containing protein	92.16	106.2	2.68	27.94	2.014684719	0.003861321
SAUSA300_RS02845	SAUSA300_0532	*fusA*	elongation factor G	1772.98	1197.1	121.77	295.86	2.008587337	0.000773725
SAUSA300_RS02335	SAUSA300_0436		methionine ABC transporter permease	52.72	145.66	4.85	23.05	1.995195436	0.001769395
SAUSA300_RS04425	SAUSA300_0821		SUF system NifU family Fe-S cluster assembly protein	16.24	72.76	2.17	9.09	1.989773533	0.004149892
SAUSA300_RS10920	SAUSA300_1986		nitroreductase family protein	93.24	55.54	5.47	16.95	1.967346647	0.001769395
SAUSA300_RS02315	SAUSA300_0432		sodium-dependent transporter	221.14	143.42	16.69	35.07	1.950671187	0.001418977
SAUSA300_RS03730	SAUSA300_0695	*queE*	7-carboxy-7-deazaguanine synthase QueE	23.67	32.52	1.9	7.02	1.897046743	0.001191171
SAUSA300_RS10510			hypothetical protein	801.28	621.05	47.79	197.93	1.860210621	0.002530158
SAUSA300_RS02035	SAUSA300_0382		L-cystine transporter	1328.76	696.74	127.04	125.62	1.838262363	0.008980218
SAUSA300_RS08430	SAUSA300_1546	*holA*	DNA polymerase III subunit delta	48.34	81.67	4.79	16.68	1.831156883	0.001418977
SAUSA300_RS16005			hypothetical protein	56.24	127.08	3.59	26.52	1.825859258	0.009253583

Table B-3 (cont'd)

SAUSA300_RS06695	SAUSA300_1235	*guaC*	GMP reductase	21.38	49.87	2.02	9.81	1.817537523	0.004149892
SAUSA300_RS04170	SAUSA300_0773	*vwb*	von Willebrand factor binding protein Vwb	19.7	41.67	2.02	8.27	1.800915624	0.003061771
SAUSA300_RS13910	SAUSA300_2505		GNAT family N-acetyltransferase	12.17	33.32	0.55	7	1.797004954	0.01941728
SAUSA300_RS12090	SAUSA300_2192	*rplE*	50S ribosomal protein L5	165.46	642.53	35.53	75.61	1.791827537	0.006829885
SAUSA300_RS13525	SAUSA300_2440	*fnbB*	fibronectin-binding protein FnbB	41.09	55.47	5.83	8.01	1.765491147	0.003120213
SAUSA300_RS05520	SAUSA300_1026		DUF177 domain-containing protein	1746.21	3104.06	153.02	729.17	1.755979103	0.003781697
SAUSA300_RS13025	SAUSA300_2359		transporter substrate-binding domain-containing protein	174.47	335.89	19.34	69.69	1.753694235	0.002677665
SAUSA300_RS08875	SAUSA300_1627	*infC*	translation initiation factor IF-3	614.08	1101.33	69.57	229.93	1.748295789	0.002247546
SAUSA300_RS12150	SAUSA300_2204	*rplC*	50S ribosomal protein L3	120.94	250.51	18.58	39.74	1.747184815	0.002629918
SAUSA300_RS12045	SAUSA300_2183		adenylate kinase	64.45	331.5	17.28	36.57	1.746041028	0.013423043
SAUSA300_RS05375	SAUSA300_0998		XRE family transcriptional regulator	29.92	66.4	3.57	12.93	1.740230711	0.004368127
SAUSA300_RS06705	SAUSA300_1236		CAP domain-containing protein	176.98	225.94	12.84	63.9	1.737886173	0.004215597
SAUSA300_RS01440	SAUSA300_0268		MFS transporter	37.36	14.92	2.57	6.44	1.728656723	0.013484163
SAUSA300_RS01075	SAUSA300_0204	*ggt*	γ-glutamyltransferase	35.54	35.95	4.18	7.39	1.721707092	0.0032995
SAUSA300_RS01435	SAUSA300_0267		IS1182 family transposase	34.68	12.85	2.04	6.4	1.707867216	0.021031039

Table B-3 (cont'd)

SAUSA300_RS05535	SAUSA300_1028	*isdB*	heme uptake protein IsdB	17.83	21.34	1.43	6.1	1.702097085	0.004475634
SAUSA300_RS01055	SAUSA300_0200		ABC transporter ATP-binding protein	93.69	55.55	9.74	14.41	1.667394083	0.01218702
SAUSA300_RS04145	SAUSA300_0769		DUF5067 domain-containing protein	19.39	24.04	0.43	8.37	1.656659585	0.039557101
SAUSA300_RS06570	SAUSA300_1211		hypothetical protein	229.55	207.01	16.71	72.57	1.643349984	0.0087662
SAUSA300_RS15905			hypothetical protein	277.42	219.28	17.01	86.2	1.643349642	0.012312678
SAUSA300_RS12025	SAUSA300_2179	*rpsK*	30S ribosomal protein S11	62.73	394.55	20.99	45.01	1.638206467	0.028096832
SAUSA300_RS04410	SAUSA300_0818	*sufC*	Fe-S cluster assembly ATPase SufC	94.03	206.31	9.8	48.93	1.634455126	0.011020586
SAUSA300_RS09470	SAUSA300_1731	*pckA*	phosphoenolpyruvate carboxykinase (ATP)	31.12	45.89	4.33	9.46	1.630951725	0.003949272
SAUSA300_RS09830	SAUSA300_1796		DUF445 domain-containing protein	107.55	157.84	7.76	47.79	1.623346219	0.012533987
SAUSA300_RS12085	SAUSA300_2191		type Z 30S ribosomal protein S14	236.76	744.24	58.41	92.01	1.601495869	0.015633984
SAUSA300_RS00935	SAUSA300_0178		DUF2294 domain-containing protein	649.74	819.41	92.52	169.33	1.597830273	0.005440727
SAUSA300_RS12115	SAUSA300_2197	*rplP*	50S ribosomal protein L16	115.79	522.55	34.63	62.4	1.588833404	0.024819405
SAUSA300_RS16000			minor capsid protein	58.13	70.81	5.38	21.52	1.588269635	0.008734929
SAUSA300_RS12075	SAUSA300_2189	*rplF*	50S ribosomal protein L6	173.37	567.81	43.19	76.27	1.570311496	0.01764915
SAUSA300_RS04390	SAUSA300_0814		Abi family protein	582.4	670	29.73	254.5	1.563656708	0.027633932

Table B-3 (cont'd)

SAUSA300_RS02840	SAUSA300_0531	*rpsG*	30S ribosomal protein S7	1277.12	1284.06	162.63	325.5	1.557184282	0.007975117
SAUSA300_RS07030	SAUSA300_1294	*msaC*	sarA expression modulator MsaC	17.75	18.1	2.12	4.81	1.542714621	0.015456886
SAUSA300_RS02325	SAUSA300_0434		bifunctional cystathionine γ-lyase/homocysteine desulfhydrase	46.92	69.42	6.96	15.5	1.539307173	0.007415367
SAUSA300_RS12020	SAUSA300_2178		DNA-directed RNA polymerase subunit α	132.56	445.86	27.47	79.22	1.537620634	0.019443584
SAUSA300_RS05670	SAUSA300_1052	*ecb*	complement convertase inhibitor Ecb	8660.72	12958.51	1011.3	3581.72	1.5337034	0.0087662
SAUSA300_RS05600	SAUSA300_1040	*zapA*	cell division protein ZapA	247.98	234.51	20.25	87.95	1.529310202	0.014935747
SAUSA300_RS01060	SAUSA300_0201		ABC transporter permease	21.52	21.05	3.3	3.88	1.524008315	0.020157954
SAUSA300_RS03445	SAUSA300_0642		hypothetical protein	207.4	295.48	16.71	97.23	1.522128826	0.019432255
SAUSA300_RS12095	SAUSA300_2193	*rplX*	50S ribosomal protein L24	124.74	558.74	41.81	65.15	1.508505601	0.036752967
SAUSA300_RS08565	SAUSA300_1571		methyltransferase domain-containing protein	12.83	25.92	1.63	6.46	1.50193637	0.019694909
SAUSA300_RS09690	SAUSA300_1770		hypothetical protein	13.9	16.32	1.08	5.73	1.495006061	0.027633932
SAUSA300_RS12080	SAUSA300_2190	*rpsH*	30S ribosomal protein S8	230.67	663.44	62.37	82.95	1.487024905	0.028066756
SAUSA300_RS06625	SAUSA300_1222		thermonuclease family protein	65.51	47.86	4.64	22.12	1.479386077	0.028096832
SAUSA300_RS07500	SAUSA300_1373		ferredoxin	1852.46	1504.25	274.46	309.79	1.478478639	0.028096832
SAUSA300_RS06635	SAUSA300_1224		hypothetical protein	121.88	147.16	18.86	34.11	1.467923086	0.013302658

Table B-3 (cont'd)

SAUSA300_RS09695	SAUSA300_1771		DUF1828 domain-containing protein	129.99	153.43	9.95	58.37	1.462832805	0.027218672
SAUSA300_RS02815	SAUSA300_0526		class I SAM-dependent methyltransferase	57.03	117.76	6.44	33.14	1.460212935	0.027218672
SAUSA300_RS06390	SAUSA300_1182		2-oxoacid:acceptor oxidoreductase subunit α	12.95	25.82	1.98	6.27	1.458786422	0.016960367
SAUSA300_RS02835	SAUSA300_0530	*rpsL*	30S ribosomal protein S12	850.54	1081.74	114.35	311.34	1.44297068	0.01218702
SAUSA300_RS08295	SAUSA300_1520		tRNA (adenine(22)-N(1))-methyltransferase TrmK	13.6	43.2	1.83	10.5	1.442435919	0.046986359
SAUSA300_RS12145	SAUSA300_2203	*rplD*	50S ribosomal protein L4	274.46	210.01	36.9	61.43	1.424425489	0.027218672
SAUSA300_RS03735	SAUSA300_0696	*queD*	6-carboxytetrahydropterin synthase QueD	24.28	26.15	3.84	6.07	1.423536204	0.028004122
SAUSA300_RS08400	SAUSA300_1541	*grpE*	nucleotide exchange factor GrpE	34.77	97.47	4.95	24.8	1.415184437	0.040816815
SAUSA300_RS04255	SAUSA300_0788		nitroreductase	499.08	521.35	53.82	191.23	1.406648838	0.019694909
SAUSA300_RS13775			hypothetical protein	436.55	370.82	34.13	169.66	1.40162398	0.036577794
SAUSA300_RS08015	SAUSA300_1468	*recN*	DNA repair protein RecN	27.49	87.77	4.41	21.76	1.386790721	0.049099554
SAUSA300_RS00010	SAUSA300_0001	*dnaA*	chromosomal replication initiator protein DnaA	49.1	100.92	6.12	29.82	1.386662694	0.03551508
SAUSA300_RS04180	SAUSA300_0775		hypothetical protein	192.87	163.26	18.31	70.73	1.378876713	0.031094167
SAUSA300_RS08555	SAUSA300_1569		U32 family peptidase	19.76	55.56	3.9	12.58	1.37597343	0.036752967
SAUSA300_RS06750	SAUSA300_1243		exonuclease subunit SbcC	26.76	46.2	4.61	11.82	1.361881461	0.020732042

Table B-3 (cont'd)

SAUSA300_RS06225			hypothetical protein	359.14	729.79	71.03	167.17	1.350173181	0.027218672
SAUSA300_RS01470	SAUSA300_0274		hypothetical protein	76.55	106.04	8.81	37.54	1.342806873	0.031205807
SAUSA300_RS07495	SAUSA300_1372		helix-turn-helix domain-containing protein	114.17	105.28	17.77	29.53	1.340504493	0.034301114
SAUSA300_RS10985	SAUSA300_1998		YeeE/YedE family protein	33.44	42.54	4.7	14.19	1.304988845	0.030246065
SAUSA300_RS05880	SAUSA300_1085		RNA-binding protein	150.45	200.08	16.44	77.46	1.293837497	0.043970121
SAUSA300_RS14570	SAUSA300_2622		rhodanese-related sulfurtransferase	209.25	216.06	25.72	85.02	1.288210782	0.036054453
SAUSA300_RS03505	SAUSA300_0654	*sarX*	HTH-type transcriptional regulator SarX	25.49	38.97	4.17	12.09	1.243927166	0.049141271
SAUSA300_RS09570	SAUSA300_1749		DUF1433 domain-containing protein	48.44	59.34	7.05	21.44	1.225713833	0.048297087
SAUSA300_RS12140	SAUSA300_2202	*rplW*	50S ribosomal protein L23	300.74	391.01	55.07	115.75	1.21705224	0.043626347

Genes downregulated in GSH when compared to CSSC

Locus	Old locus	Gene	Product	TPM.1 GSH	TPM.2 GSH	TPM.1 CSSC	TPM.2 CSSC	DE Log_2 FC	DE Adj. *P*-value
SAUSA300_RS03005		*vraX*	C1q-binding complement inhibitor VraX	7355.24	5156.82	130098.29	60616.24	-3.967945975	1.11797E-09
SAUSA300_RS13040	SAUSA300_2361		putative metal homeostasis protein	4606.12	5956.22	51134.91	41439.61	-3.48392362	1.7629E-09

Table B-3 (cont'd)

SAUSA300_RS03000			hypothetical protein	278.92	126	2775.63	1589.92	-3.478210201	2.09417E-07
SAUSA300_RS04580	SAUSA300_0848		FAD/NAD(P)-binding protein	8.92	9.34	29.4	171.15	-3.296989547	2.82912E-09
SAUSA300_RS12890	SAUSA300_2333		nitrate/nitrite transporter	20.71	16.94	112.39	200.42	-3.275833554	7.74351E-10
SAUSA300_RS13360	SAUSA300_2413	*cntL*	D-histidine (S)-2-aminobutanoyltransferase CntL	5.63	10.01	42.35	67.31	-3.17898958	1.11797E-09
SAUSA300_RS15375			hypothetical protein	127.45	127.38	1755.08	300.14	-3.153523215	2.80009E-05
SAUSA300_RS13860	SAUSA300_2495	*copZ*	copper chaperone CopZ	1014.44	1716.65	10217.43	5935.91	-3.018544811	1.92626E-06
SAUSA300_RS06690	SAUSA300_1234	*rpsN*	30S ribosomal protein S14	254.16	210.76	991.64	2246.49	-3.005106974	5.57662E-09
SAUSA300_RS10485			hypothetical protein	37.25	52.36	375.59	160.57	-2.983464068	1.22502E-05
SAUSA300_RS01625	SAUSA300_0305		formate/nitrite transporter family protein	96.03	78.13	429.39	544.99	-2.826851365	5.35039E-07
SAUSA300_RS13325	SAUSA300_2406		MFS transporter	91.76	56.32	310.49	534.53	-2.73389307	1.70962E-06

Table B-3 (cont'd)

SAUSA300_RS13340	SAUSA300_2409		ABC transporter permease	6.94	6.37	20.31	54.35	-2.695416261	3.1823E-07
SAUSA300_RS10275	SAUSA300_1878	*rlmD*	23S rRNA (uracil(1939)-C(5))-methyltransferase RlmD	10.55	25.98	86.77	64.72	-2.59701828	6.42746E-05
SAUSA300_RS07015	SAUSA300_1291		amidohydrolase	14.52	20.48	63.58	90.07	-2.592510948	1.48713E-06
SAUSA300_RS07010	SAUSA300_1290	*dapD*	2,3,4,5-tetrahydropyridine-2,6-dicarboxylate N-acetyltransferase	147.91	82.44	455.49	710.32	-2.577810751	1.80121E-05
SAUSA300_RS13355	SAUSA300_2412	*cntM*	staphylopine dehydrogenase CntM	4.91	7.1	16.89	38.39	-2.556123075	5.35039E-07
SAUSA300_RS08880	SAUSA300_1628		amino acid permease	44.79	44.97	113.06	312.07	-2.497406008	1.33354E-06
SAUSA300_RS14175	SAUSA300_2551	*nrdD*	anaerobic ribonucleoside-triphosphate reductase	6.63	12.59	34.12	39.52	-2.463040159	2.44652E-05
SAUSA300_RS01635	SAUSA300_0307		5'-nucleotidase, lipoprotein e(P4) family	43.27	35.25	160.97	150.13	-2.430087067	0.000106264
SAUSA300_RS13850	SAUSA300_2493	*cwrA*	cell wall inhibition responsive protein CwrA	620.28	482.23	3279.08	941.3	-2.385901587	0.001962663
SAUSA300_RS13765	SAUSA300_2481		sterile α motif-like domain-containing protein	5849.07	9772.13	34671.29	16151.83	-2.308962369	0.001229708

Table B-3 (cont'd)

SAUSA300_RS14170	SAUSA300_2550	*nrdG*	anaerobic ribonucleoside-triphosphate reductase activating protein	20.93	31.36	89.47	81	-2.272174034	0.000295853
SAUSA300_RS09670	SAUSA300_1767		gallidermin/nisin family lantibiotic	16.77	15.01	68.29	38.64	-2.247279 71	0.001769395
SAUSA300_RS12480	SAUSA300_2259		LCP family protein	35.78	48.58	113.18	157.63	-2.194338867	0.00010572
SAUSA300_RS06590	SAUSA300_1215		hypothetical protein	48.95	74.96	241.93	125.4	-2.185736423	0.002104691
SAUSA300_RS11550	SAUSA300_2097		SDR family oxidoreductase	15.49	14.45	31.72	75.47	-2.158185258	9.08117E-05
SAUSA300_RS15795		*pepA1*	type I toxin-antitoxin system Fst family toxin PepA1	715.07	553.18	2456.95	1290.29	-2.102721683	0.003666205
SAUSA300_RS07025	SAUSA300_1293	*lysA*	diaminopimelate decarboxylase	74.55	150.89	195.47	534.7	-2.075782801	0.000150994
SAUSA300_RS13345	SAUSA300_2410		ABC transporter permease	34.71	39.89	59.12	204.03	-2.068669945	0.000155603
SAUSA300_RS00400	SAUSA300_0079		YdhK family protein	94.18	273.67	361.26	716.43	-2.025052602	0.000847597
SAUSA300_RS01990	SAUSA300_0374		GlsB/YeaQ/YmgE family stress response membrane protein	2038.13	2912.41	6286.49	7095.9	-2.015356648	0.000920149

Table B-3 (cont'd)

SAUSA300_RS01265	SAUSA300_0237		nucleoside hydrolase	21.77	15.4	50.02	59.68	-2.006858994	0.001769395
SAUSA300_RS13280	SAUSA300_2398	*fetB*	iron export ABC transporter permease subunit FetB	38.38	40.36	106.82	105.33	-1.989683824	0.001769395
SAUSA300_RS09355	SAUSA300_1712	*ribE*	6,7-dimethyl-8-ribityllumazine synthase	105.47	96.68	240.59	334.73	-1.985867081	0.000923237
SAUSA300_RS12545	SAUSA300_2269		hypothetical protein	243.57	181.89	573.51	583.69	-1.942853336	0.003061771
SAUSA300_RS05185	SAUSA300_0964		DUF5011 domain-containing protein	1499.07	1054.32	4004.37	2605.7	-1.920714136	0.007648851
SAUSA300_RS13330	SAUSA300_2407		ABC transporter ATP-binding protein	9.03	10.4	11.71	53.39	-1.903394709	0.001594128
SAUSA300_RS13725	SAUSA300_2473		alpha/beta hydrolase	99.78	68.21	212.77	237.78	-1.894908447	0.003781697
SAUSA300_RS06940	SAUSA300_1278	*pepF*	oligoendopeptidase F	97.95	85.16	207.72	271.22	-1.882492346	0.002267767
SAUSA300_RS13855	SAUSA300_2494		heavy metal translocating P-type ATPase	152.55	175.07	318.07	537.55	-1.874719351	0.000950944
SAUSA300_RS04855	SAUSA300_0902	*pepF*	oligoendopeptidase F	35.3	79.69	87.93	218.14	-1.851384637	0.001387792

Table B-3 (cont'd)

SAUSA300_RS14010	SAUSA300_2525		fructosamine kinase family protein	27.65	23	62.37	62.14	-1.837255588	0.005217474
SAUSA300_RS05795	SAUSA300_1068		beta-class phenol-soluble modulin	1868.35	569.95	3464.54	3534.23	-1.828687326	0.01604228
SAUSA300_RS15490			type I toxin-antitoxin system toxin PepG1	775.36	570.24	2420.73	678.54	-1.814502823	0.027218672
SAUSA300_RS13645	SAUSA300_2460		GNAT family N-acetyltransferase	101.29	90.05	252.13	188.12	-1.802404738	0.010034607
SAUSA300_RS12865	SAUSA300_2328		DUF4889 domain-containing protein	434.69	380.4	1025.36	853.36	-1.792489741	0.0087662
SAUSA300_RS05995	SAUSA300_1107		TM2 domain-containing protein	1924.53	2043.23	5682.01	2971.77	-1.792302309	0.014935747
SAUSA300_RS04765	SAUSA300_0884		YjzD family protein	684.43	791.23	1986.21	1210.13	-1.784465382	0.012533987
SAUSA300_RS14670	SAUSA300_2642		DUF3147 family protein	8.84	5.38	16.61	19.99	-1.784354321	0.010137322
SAUSA300_RS02195	SAUSA300_0409	*spn*	myeloperoxidase inhibitor SPIN	1850.15	1455.3	4360.22	3178.19	-1.777678341	0.01218702
SAUSA300_RS04565	SAUSA300_0845		M17 family metallopeptidase	51.4	48.49	93.39	150.85	-1.768959834	0.002862569

Table B-3 (cont'd)

SAUSA300_RS10185	SAUSA300_1865	*vraR*	two-component system response regulator VraR	108.18	172.79	277.59	350.5	-1.766155442	0.003682729
SAUSA300_RS01620	SAUSA300_0304		DUF4064 domain-containing protein	23.16	30.35	41.54	89.51	-1.743647507	0.002030812
SAUSA300_RS15740			phenol-soluble modulin PSM-alpha-1	1137.55	579.15	1294.02	3576.07	-1.701514808	0.010137322
SAUSA300_RS09140	SAUSA300_1674		trypsin-like peptidase domain-containing protein	146.69	172.07	242.45	500.75	-1.68447348	0.002757425
SAUSA300_RS00995	SAUSA300_0190		alpha-keto acid decarboxylase family protein	15.79	9.96	25.77	34.11	-1.671760935	0.012201753
SAUSA300_RS01235	SAUSA300_0233		hypothetical protein	18.92	37.34	48.66	69.56	-1.657631234	0.008917687
SAUSA300_RS10555			hypothetical protein	778.61	395.61	1740.21	716.33	-1.646395888	0.043970121
SAUSA300_RS13045	SAUSA300_2362		2,3-diphosphoglycerate-dependent phosphoglycerate mutase	1347.72	1092.58	1514.2	4828.17	-1.644032898	0.006310057
SAUSA300_RS06715			DNA damage-induced cell division inhibitor SosA	30.21	39.84	75.14	62.69	-1.641393003	0.017091893
SAUSA300_RS12715			hypothetical protein	38.89	63.88	113.65	82.31	-1.634774724	0.021751487

Table B-3 (cont'd)

SAUSA300_RS14565	SAUSA300_2621		SMP-30/gluconolactonase/LRE family protein	11.83	13.89	27.91	22.36	-1.628508384	0.019048836
SAUSA300_RS01090	SAUSA300_0207		M23 family metallopeptidase	48.53	29.99	80.85	88.84	-1.611637437	0.020028183
SAUSA300_RS03335	SAUSA300_0622		M50 family metallopeptidase	81.56	50.23	140.33	140.73	-1.611629485	0.021751487
SAUSA300_RS14075	SAUSA300_2537		L-lactate dehydrogenase	166.32	128.21	241.49	410.57	-1.596559574	0.010525476
SAUSA300_RS13385	SAUSA300_2418		carboxymuconolactone decarboxylase family protein	130.55	127.8	235.12	291.71	-1.596256095	0.012187 02
SAUSA300_RS00960	SAUSA300_0183		YagU family protein	655.29	562.26	1441.83	854.01	-1.582709357	0.035515 08
SAUSA300_RS09425	SAUSA300_1725		transaldolase	260.88	205.76	368.46	647.26	-1.571635626	0.011356589
SAUSA300_RS12970			hypothetical protein	33.77	46.81	81.4	67.56	-1.567157838	0.024819405
SAUSA300_RS06685	SAUSA300_1233	*rpmG*	50S ribosomal protein L33	6062.78	8757.21	16477.46	9467.32	-1.557800202	0.036577794
SAUSA300_RS03960	SAUSA300_0736	*raiA*	ribosome-associated translation inhibitor RaiA	7751.35	7263.3	17578.62	9706.41	-1.557028276	0.039800629

Table B-3 (cont'd)

SAUSA300_RS04760	SAUSA300_0883		MAP domain-containing protein	85.49	70.38	121.11	211.71	-1.554299896	0.01218702
SAUSA300_RS10805			transcriptional regulator	28.08	25.44	43.65	67.39	-1.546395517	0.015399326
SAUSA300_RS07035	SAUSA300_1295	*cspA*	cold shock protein CspA	25739.07	32953.44	65893.82	36585.83	-1.545899549	0.039345525
SAUSA300_RS04990	SAUSA300_0929		IDEAL domain-containing protein	1430.09	1320.39	2511.05	2756.31	-1.531784305	0.020157954
SAUSA300_RS11520	SAUSA300_2091	*deoD*	purine-nucleoside phosphorylase	605.71	750.39	887.3	1889.62	-1.515711571	0.008215915
SAUSA300_RS06835	SAUSA300_1258		2-hydroxymuconate tautomerase	1261.11	1709.56	3231.43	1800.33	-1.514859276	0.043970121
SAUSA300_RS05195	SAUSA300_0966	*purE*	5-(carboxyamino)imidazole ribonucleotide mutase	11.98	16.99	17.97	42.28	-1.512944011	0.010034607
SAUSA300_RS12780	SAUSA300_2313		L-lactate permease	386.38	788.45	887.06	1282.53	-1.51253439	0.015456886
SAUSA300_RS01560	SAUSA300_0292		hypothetical protein	109.61	156.46	274.73	179.25	-1.510704485	0.039306475
SAUSA300_RS15735			phenol-soluble modulin PSM-alpha-2	1729.12	776.91	1675.5	4447.18	-1.502592842	0.031094167

Table B-3 (cont'd)

SAUSA300_RS04210			hypothetical protein	130.44	109.16	247.64	182.79	-1.494651806	0.040816815
SAUSA300_RS12940	SAUSA300_2344	*cobA*	uroporphyrinogen-III C-methyltransferase	10.7	10.23	17.6	21.02	-1.467142223	0.027218672
SAUSA300_RS07160	SAUSA300_1314		YozE family protein	237.97	282.19	397.04	556.21	-1.463120185	0.018505881
SAUSA300_RS02365	SAUSA300_0442		YibE/F family protein	153.15	96.62	216.84	251.25	-1.432737656	0.040816815
SAUSA300_RS04030	SAUSA300_0747	*trxB*	thioredoxin-disulfide reductase	108.6	128.63	142.25	317.59	-1.425829929	0.013662837
SAUSA300_RS09030			hypothetical protein	53.77	91.22	107.47	144.25	-1.424645271	0.027904275
SAUSA300_RS12420			hypothetical protein	397.77	556.75	836.48	685.19	-1.400678637	0.047533674
SAUSA300_RS14620	SAUSA300_2632		HdeD family acid-resistance protein	96.03	76.17	130.29	182.16	-1.392248821	0.035600642
SAUSA300_RS09800	SAUSA300_1790		peptidylprolyl isomerase	409.01	527.86	476.97	1357.86	-1.382544145	0.017038754
SAUSA300_RS02965	SAUSA300_0556	*hxlB*	6-phospho-3-hexuloisomerase	23.35	63	52.33	96.07	-1.369305342	0.03661048

Table B-3 (cont'd)

SAUSA300_RS04985	SAUSA300_0928		competence protein ComK	17.45	13.42	19.18	40.77	-1.368456829	0.033549663
SAUSA300_RS04080	SAUSA300_0756	*gap*	type I glyceraldehyde-3-phosphate dehydrogenase	1232.21	2113.44	2006.84	3819.2	-1.365054426	0.021770348
SAUSA300_RS05095	SAUSA300_0948	*menB*	1,4-dihydroxy-2-naphthoyl-CoA synthase	293.47	269.29	423.47	509.88	-1.333613795	0.046427827
SAUSA300_RS11560	SAUSA300_2099	*czrB*	CDF family zinc efflux transporter CzrB	533.54	691.02	759.56	1273.14	-1.308531176	0.031701317
SAUSA300_RS07000	SAUSA300_1288	*dapA*	4-hydroxy-tetrahydrodipicolinate synthase	16.22	43.3	33.36	64.28	-1.298963468	0.047684211
SAUSA300_RS04245	SAUSA300_0786		organic hydroperoxide resistance protein	64.77	62.98	75.88	146.19	-1.293856257	0.036752967
SAUSA300_RS08745			hypothetical protein	346.85	345.68	424.38	756.5	-1.292800049	0.03733
SAUSA300_RS07165	SAUSA300_1315		PTS glucose transporter subunit IIA	235.02	286.37	315.14	535.94	-1.275878242	0.03733
SAUSA300_RS01250	SAUSA300_0235		L-lactate dehydrogenase	2378.38	2353.91	2610.86	5659.02	-1.275428749	0.036430885
SAUSA300_RS03665	SAUSA300_0683		DeoR/GlpR family DNA-binding transcription regulator	104.08	141.33	151.47	239.39	-1.273283026	0.040238276

Table B-3 (cont'd)

SAUSA300_RS05540	SAUSA300_1029	*isdA*	LPXTG-anchored heme-scavenging protein IsdA	247.96	244.84	297.79	505.14	-1.246621213	0.047533674
SAUSA300_RS11300	SAUSA300_2052		single-stranded DNA-binding protein	60.13	62.2	73.21	125.85	-1.245357734	0.047684211
SAUSA300_RS08320	SAUSA300_1525		glycine--tRNA ligase	405.39	572.44	460.2	1101.39	-1.176211964	0.04843413

Table B-4. Sodium thiosulfate (sTS) differentially expressed genes.

Genes upregulated in sTS when compared to CSSC

Locus	Old locus	Gene	Product	TPM. 1 sTS	TPM. 2 sTS	TPM. 1 CSSC	TPM. 2 CSSC	DE Log2 FC	DE Adj. *P*-value
SAUSA300_RS00930	SAUSA300_0177		acyl-CoA/acyl-ACP dehydrogenase	166.22	182.5	2.69	9.11	3.975153529	5.97E-23
SAUSA300_RS10250	SAUSA300_1874	*ftnA*	H-type ferritin FtnA	4777.36	5582.06	122.59	214.34	3.844318382	8.99E-22
SAUSA300_RS10920	SAUSA300_1986		nitroreductase family protein	251.11	259.56	5.47	16.95	3.610523144	1.63E-19
SAUSA300_RS04665	SAUSA300_0864		argininosuccinate synthase	26.22	42.8	0.59	2.39	3.596379992	1.94E-15
SAUSA300_RS00915	SAUSA300_0174		ABC transporter ATP-binding protein	34.96	37.48	1.31	1.85	3.34231159	1.77E-13
SAUSA300_RS11935	SAUSA300_2165	*budA*	acetolactate decarboxylase	95.54	152.69	4.02	10.73	3.126458411	9.50E-14
SAUSA300_RS00925	SAUSA300_0176		ABC transporter permease	80.18	90.47	4.22	2.74	3.098636848	1.70E-08
SAUSA300_RS02330	SAUSA300_0435		methionine ABC transporter ATP-binding protein	182.15	117.61	6.07	13.82	2.95296498	1.52E-11
SAUSA300_RS10255			hypothetical protein	59.69	130.21	3.61	8.17	2.905815163	4.00E-08
SAUSA300_RS13755	SAUSA300_2479	*cidA*	holin-like murein hydrolase modulator CidA	282.2	243.42	10.97	26.05	2.90161874	1.35E-12
SAUSA300_RS13745	SAUSA300_2477		pyruvate oxidase	334.37	317.48	16.24	30.98	2.797331264	7.44E-12
SAUSA300_RS11605	SAUSA300_2105		PTS mannitol transporter subunit IICB	42.33	265.36	3.52	19.81	2.697969241	2.47E-05
SAUSA300_RS03085	SAUSA300_0577		redox-sensitive transcriptional regulator HypR	137.39	205.18	12.24	7.56	2.612761904	5.59E-06

Table B-4 (Cont'd)

SAUSA300_RS02335	SAUSA300_0436		methionine ABC transporter permease	167.18	115.53	4.85	23.05	2.573132474	1.07E-07
SAUSA300_RS00910	SAUSA300_0173		DUF4242 domain-containing protein	398.39	264.86	14.98	49.04	2.546576593	1.70E-08
SAUSA300_RS13025	SAUSA300_2359		transporter substrate-binding domain-containing protein	402	472.45	19.34	69.69	2.502235403	3.10E-09
SAUSA300_RS01060	SAUSA300_0201		ABC transporter permease	58.87	34.05	3.3	3.88	2.500861509	1.50E-06
SAUSA300_RS11940	SAUSA300_2166	*alsS*	acetolactate synthase AlsS	63.74	64.68	2.66	11.08	2.456850704	3.47E-08
SAUSA300_RS00920	SAUSA300_0175		ABC transporter substrate-binding protein	30.77	32.14	2.69	2.58	2.331970676	7.16E-06
SAUSA300_RS02340	SAUSA300_0437	*gmpC*	dipeptide ABC transporter glycylmethionine-binding lipoprotein	818.78	605.64	30.16	144.44	2.298614243	2.06E-06
SAUSA300_RS09895	SAUSA300_1808		ABC transporter permease subunit	30.4	59.36	1.67	9.24	2.268943961	1.29E-05
SAUSA300_RS01215	SAUSA300_0229		acyl CoA:acetate/3-ketoacid CoA transferase	15.25	34.63	1.58	3.76	2.258843535	3.99E-06
SAUSA300_RS02345	SAUSA300_0438	*aaa*	autolysin/adhesin Aaa	472.91	464.3	32.67	82.52	2.170454206	1.29E-07
SAUSA300_RS04425	SAUSA300_0821		SUF system NifU family Fe-S cluster assembly protein	38.65	47.9	2.17	9.09	2.160861821	5.46E-06
SAUSA300_RS11740	SAUSA300_2132		hypothetical protein	560.61	1318.04	76.55	120.09	2.152383371	2.11E-05
SAUSA300_RS13910	SAUSA300_2505		GNAT family N-acetyltransferase	28	26.06	0.55	7	2.131333234	0.000552202
SAUSA300_RS07500	SAUSA300_1373		ferredoxin	2767.83	2819.97	274.46	309.79	2.09610162	2.11E-05
SAUSA300_RS06580	SAUSA300_1213		hypothetical protein	56.86	35.1	0.47	12.46	2.088354863	0.003000985

Table B-4 (Cont'd)

SAUSA300_RS05865	SAUSA300_1082		YggS family pyridoxal phosphate-dependent enzyme	86.4	143.38	7.63	23.43	2.053900828	5.29E-06
SAUSA300_RS04410	SAUSA300_0818	*sufC*	Fe-S cluster assembly ATPase SufC	209.2	187.03	9.8	48.93	2.049308555	2.44E-05
SAUSA300_RS08560	SAUSA300_1570		peptidase U32 family protein	20.05	28.31	1.26	5.73	2.028225132	3.36E-05
SAUSA300_RS03730	SAUSA300_0695	*queE*	7-carboxy-7-deazaguanine synthase QueE	26.98	35.96	1.9	7.02	2.025380044	1.29E-05
SAUSA300_RS06505			hypothetical protein	22.5	14.97	0.61	4.2	2.016536706	0.003526285
SAUSA300_RS01075	SAUSA300_0204	*ggt*	γ-glutamyltransferase	49.01	42.45	4.18	7.39	2.012821806	6.77E-06
SAUSA300_RS02320	SAUSA300_0433		cysteine synthase family protein	23.84	24.3	2.64	2.54	2.001501731	0.00017793
SAUSA300_RS08565	SAUSA300_1571		methyltransferase domain-containing protein	23.22	32.38	1.63	6.46	1.99110769	3.27E-05
SAUSA300_RS02535	SAUSA300_0472	*ispE*	4-(cytidine 5'-diphospho)-2-C-methyl-D-erythritol kinase	115.46	162.67	8.1	34.39	1.968938636	2.51E-05
SAUSA300_RS08015	SAUSA300_1468	*recN*	DNA repair protein RecN	87.27	75.22	4.41	21.76	1.937444192	7.31E-05
SAUSA300_RS05880	SAUSA300_1085		RNA-binding protein	257.23	327.74	16.44	77.46	1.92683528	5.07E-05
SAUSA300_RS05300	SAUSA300_0985	*nrdH*	glutaredoxin-like protein NrdH	257.89	278.21	23.84	53.83	1.907622231	7.77E-06
SAUSA300_RS06500	SAUSA300_1203		hypothetical protein	31.73	30.95	1.84	7.85	1.894343714	0.000357239
SAUSA300_RS01065	SAUSA300_0202		ABC transporter permease	21.04	14.22	1.75	3.11	1.888041935	0.000125814
SAUSA300_RS07495	SAUSA300_1372		helix-turn-helix domain-containing protein	167.96	175.45	17.77	29.53	1.875386447	2.63E-05

Table B-4 (Cont'd)

SAUSA300_RS03080	SAUSA300_0576		hypothiocyanous acid reductase MerA	274.24	263.92	32.03	32.87	1.87093699	0.000299457
SAUSA300_RS12110	SAUSA300_2196	*rpmC*	50S ribosomal protein L29	202	193.75	14.13	49.61	1.870234088	3.36E-05
SAUSA300_RS07420	SAUSA300_1361		heptaprenyl diphosphate synthase component 1	152.81	157.99	6.16	48.55	1.857742232	0.000902686
SAUSA300_RS09470	SAUSA300_1731	*pckA*	phosphoenolpyruvate carboxykinase (ATP)	24.6	74.72	4.33	9.46	1.852519043	0.000616728
SAUSA300_RS07030	SAUSA300_1294	*msaC*	sarA expression modulator MsaC	22.61	23.86	2.12	4.81	1.845486059	0.000122678
SAUSA300_RS06575	SAUSA300_1212		polymorphic toxin type 50 domain-containing protein	94.6	73.27	2.68	27.94	1.815437068	0.003210931
SAUSA300_RS09400	SAUSA300_1721		hypothetical protein	394.34	368.21	17.92	120.1	1.81272787	0.000758264
SAUSA300_RS06390	SAUSA300_1182		2-oxoacid:acceptor oxidoreductase subunit alpha	21.84	28.36	1.98	6.27	1.812403244	4.40E-05
SAUSA300_RS05610	SAUSA300_1042	*polX*	DNA polymerase/3'-5' exonuclease PolX	12.71	19.27	0.96	4.52	1.807853608	0.00031034
SAUSA300_RS06610	SAUSA300_1219		sensor histidine kinase	18.47	19.41	0.93	5.8	1.803045824	0.000704809
SAUSA300_RS12105	SAUSA300_2195	*rpsQ*	30S ribosomal protein S17	244.44	209.29	20.36	53.63	1.792468104	4.66E-05
SAUSA300_RS02845	SAUSA300_0532	*fusA*	elongation factor G	1115.28	1446.07	121.77	295.86	1.764528575	2.94E-05
SAUSA300_RS11585			hypothetical protein	23.13	23.94	1.45	6.13	1.734975149	0.007131029
SAUSA300_RS08285	SAUSA300_1518		DEAD/DEAH box helicase	70.35	99.91	3.81	28.93	1.728418368	0.00220313
SAUSA300_RS06535	SAUSA300_1208		hypothetical protein	39.85	28.58	3.69	7.04	1.727369268	0.000893544

Table B-4 (Cont'd)

SAUSA300_RS12045	SAUSA300_2183		adenylate kinase	159.09	169.86	17.28	36.57	1.723116664	6.26E-05
SAUSA300_RS09395	SAUSA300_1720		N-acetylglucosaminidase	713.02	690.23	56.98	199.5	1.712393268	0.00011345
SAUSA300_RS08400	SAUSA300_1541	*grpE*	nucleotide exchange factor GrpE	66.94	91.39	4.95	24.8	1.712372773	0.000634316
SAUSA300_RS04415	SAUSA300_0819	*sufD*	Fe-S cluster assembly protein SufD	62.98	67.76	5.79	17.93	1.68868279	0.00010867
SAUSA300_RS01055	SAUSA300_0200		ABC transporter ATP-binding protein	83.03	73.92	9.74	14.41	1.68588224	0.000393937
SAUSA300_RS08430	SAUSA300_1546	*holA*	DNA polymerase III subunit delta	47.29	70.24	4.79	16.68	1.68398412	0.000268858
SAUSA300_RS11580	SAUSA300_2101		SAP domain-containing protein	35.61	32.52	1.47	12.29	1.67814992	0.004011335
SAUSA300_RS05615	SAUSA300_1043		endonuclease MutS2	16.87	19.65	1.13	6.14	1.652461587	0.001302251
SAUSA300_RS06000	SAUSA300_1108		peptide deformylase	17.67	21.98	1.1	6.63	1.652173429	0.002996801
SAUSA300_RS07300	SAUSA300_1339		YppE family protein	103.26	123.55	6.7	38.94	1.645638316	0.001749293
SAUSA300_RS04145	SAUSA300_0769		DUF5067 domain-containing protein	23.67	17.71	0.43	8.37	1.617434315	0.021566263
SAUSA300_RS12020	SAUSA300_2178		DNA-directed RNA polymerase subunit alpha	241.15	327.11	27.47	79.22	1.616044804	0.00021503
SAUSA300_RS04800	SAUSA300_0890		ATP-binding cassette domain-containing protein	33.2	26.45	3.17	7.76	1.606820984	0.000538775
SAUSA300_RS06470	SAUSA300_1198	*hflX*	GTPase HflX	13.96	20.11	1.23	5.57	1.602081278	0.001606474
SAUSA300_RS08765	SAUSA300_1609		A24 family peptidase	15	13.39	1.72	3.11	1.601724494	0.001404406

Table B-4 (Cont'd)

SAUSA300_RS09505	SAUSA300_1738		DUF4909 domain-containing protein	29.17	21.11	3.24	5.12	1.600583121	0.002224654
SAUSA300_RS10970	SAUSA300_1995		LacI family DNA-binding transcriptional regulator	24.2	54.57	2.24	13.74	1.596151079	0.005972472
SAUSA300_RS11965	SAUSA300_2169		DUF6414 family protein	23.35	23.96	0.86	9.3	1.593421868	0.010578232
SAUSA300_RS06635	SAUSA300_1224		hypothetical protein	126.41	182.58	18.86	34.11	1.593057072	0.000529061
SAUSA300_RS13020	SAUSA300_2358		amino acid ABC transporter permease	282.36	411.6	19.62	127.31	1.590410837	0.003709448
SAUSA300_RS03740	SAUSA300_0697	*queC*	7-cyano-7-deazaguanine synthase QueC	11.34	14.63	1.12	3.89	1.574831082	0.001831038
SAUSA300_RS03655	SAUSA300_0681		hypothetical protein	379.98	213.74	35.4	71.4	1.573087702	0.001783967
SAUSA300_RS02325	SAUSA300_0434		bifunctional cystathionine γ-lyase/homocysteine desulfhydrase	55.47	65.41	6.96	15.5	1.562598853	0.000357239
SAUSA300_RS14245	SAUSA300_2560		hypothetical protein	38.03	46.95	2.45	15.39	1.558169728	0.00617418
SAUSA300_RS07325	SAUSA300_1343	*nth*	endonuclease III	64.8	87.84	3.97	29.49	1.553667971	0.006569744
SAUSA300_RS06615	SAUSA300_1220		response regulator transcription factor	32.09	37.38	2.75	11.65	1.552786993	0.001657565
SAUSA300_RS08875	SAUSA300_1627	*infC*	translation initiation factor IF-3	553.3	949.95	69.57	229.93	1.550780996	0.001005053
SAUSA300_RS05040	SAUSA300_0938		hypothetical protein	43.33	39.13	1.59	16.71	1.541104259	0.013906827
SAUSA300_RS12025	SAUSA300_2179	*rpsK*	30S ribosomal protein S11	151.2	203.18	20.99	45.01	1.539937665	0.000550683
SAUSA300_RS02035	SAUSA300_0382		L-cystine transporter	862.92	768.97	127.04	125.62	1.528200303	0.004872848

Table B-4 (Cont'd)

SAUSA300_RS02815	SAUSA300_0526		class I SAM-dependent methyltransferase	78.73	103.41	6.44	33.14	1.528094211	0.002980786
SAUSA300_RS14655	SAUSA300_2639		cold-shock protein	127992.86	139110.15	15403.29	36858.2	1.520163913	0.000388284
SAUSA300_RS10985	SAUSA300_1998		YeeE/YedE family protein	50.99	41.39	4.7	14.19	1.51993081	0.001033925
SAUSA300_RS03445	SAUSA300_0642		hypothetical protein	257.61	251.32	16.71	97.23	1.519712443	0.004102487
SAUSA300_RS05600	SAUSA300_1040	*zapA*	cell division protein ZapA	237.88	262.88	20.25	87.95	1.517895145	0.00172398
SAUSA300_RS09835	SAUSA300_1797		helix-turn-helix transcriptional regulator	449.17	597.96	63.39	137.04	1.508302565	0.000605046
SAUSA300_RS05135	SAUSA300_0955		bifunctional autolysin	147.89	156.65	21.05	33.47	1.505201421	0.001197262
SAUSA300_RS07205	SAUSA300_1323		NifU N-terminal domain-containing protein	46.86	50.74	3.82	17.28	1.498358274	0.003835402
SAUSA300_RS08305	SAUSA300_1522	*dnaG*	DNA primase	64.85	99.73	6.34	30.02	1.488297936	0.003419209
SAUSA300_RS05360	SAUSA300_0995		dihydrolipoamide acetyltransferase family protein	85.77	122.32	14.37	23.34	1.481352945	0.001759275
SAUSA300_RS14570	SAUSA300_2622		rhodanese-related sulfurtransferase	245.63	271.2	25.72	85.02	1.480012125	0.000909205
SAUSA300_RS04660	SAUSA300_0863	*argH*	argininosuccinate lyase	31.85	95.95	7.81	15.19	1.478895537	0.008440785
SAUSA300_RS08955	SAUSA300_1641		citrate synthase	43.32	77.93	6.68	17.62	1.478202694	0.001906952
SAUSA300_RS11415	SAUSA300_2073		thymidine kinase	49.56	97.11	5.39	26.81	1.477917301	0.0065615

Table B-4 (Cont'd)

SAUSA300_RS10440	SAUSA300_1907		DUF1700 domain-containing protein	58.49	66.18	3.85	25.08	1.471677067	0.007713829
SAUSA300_RS04640	SAUSA300_0860		ornithine--oxo-acid transaminase	17.22	21.37	2.03	6.05	1.469146272	0.001533869
SAUSA300_RS09830	SAUSA300_1796		DUF445 domain-containing protein	117.02	120.44	7.76	47.79	1.467489302	0.00659566
SAUSA300_RS12845	SAUSA300_2324		sucrose-specific PTS transporter subunit IIBC	46.88	101.45	9.24	19.02	1.456119968	0.004064768
SAUSA300_RS07330	SAUSA300_1344		DnaD domain-containing protein	47.91	80.86	5.1	23.78	1.451306077	0.005335616
SAUSA300_RS04390	SAUSA300_0814		Abi family protein	549.34	623.37	29.73	254.5	1.450299962	0.014178774
SAUSA300_RS07905	SAUSA300_1448		Fur family transcriptional regulator	1004.45	1049.92	138.18	264.89	1.446574906	0.001194478
SAUSA300_RS06110	SAUSA300_1129		putative DNA-binding protein	22.85	29.81	1.68	10.38	1.443984846	0.011462055
SAUSA300_RS08030	SAUSA300_1471		exodeoxyribonuclease VII small subunit	45.76	47.16	2.18	19.9	1.442471384	0.018971358
SAUSA300_RS02530	SAUSA300_0471		Veg family protein	6854.46	5742.38	861.02	1623.4	1.437194902	0.0017702
SAUSA300_RS03690	SAUSA300_0687		hemolysin family protein	518.55	571.66	39.62	218.92	1.436842442	0.005868545
SAUSA300_RS08830	SAUSA300_1620	*yihA*	ribosome biogenesis GTP-binding protein YihA/YsxC	25.87	31.59	2.65	10.14	1.433920608	0.00365079
SAUSA300_RS00935	SAUSA300_0178		DUF2294 domain-containing protein	699.17	635.15	92.52	169.33	1.433256821	0.001759275
SAUSA300_RS01475	SAUSA300_0275		DUF5079 family protein	16.09	13.71	0.96	6.08	1.424540089	0.013343771
SAUSA300_RS06030	SAUSA300_1114	*rsgA*	ribosome small subunit-dependent GTPase A	26.91	41.89	2.17	14.22	1.420277101	0.012219224

Table B-4 (Cont'd)

SAUSA300_RS02630	SAUSA300_0490	*hslO*	Hsp33 family molecular chaperone HslO	26.36	51.21	3.45	13.85	1.419876334	0.006705135
SAUSA300_RS08405	SAUSA300_1542	*hrcA*	heat-inducible transcriptional repressor HrcA	64.48	78.31	7.29	24.75	1.414974279	0.002020778
SAUSA300_RS16000			minor capsid protein	64.77	51.67	5.38	21.52	1.414265218	0.004559983
SAUSA300_RS00010	SAUSA300_0001	*dnaA*	chromosomal replication initiator protein DnaA	67.83	84.14	6.12	29.82	1.413894401	0.00521982
SAUSA300_RS09815	SAUSA300_1793		exonuclease SbcCD subunit D	149.25	133.02	10.9	57.23	1.409258628	0.006866043
SAUSA300_RS08175	SAUSA300_1498	*gcvT*	glycine cleavage system aminomethyltransferase GcvT	20.75	28.44	2.29	8.93	1.405429661	0.004182027
SAUSA300_RS05640	SAUSA300_1047	*sdhA*	succinate dehydrogenase flavoprotein subunit	80.31	159.32	14.37	35.52	1.402206756	0.004148534
SAUSA300_RS03170	SAUSA300_0590		flavodoxin family protein	168.71	353.81	32.37	74.97	1.39571506	0.005254432
SAUSA300_RS06055	SAUSA300_1119	*fakA*	fatty acid kinase catalytic subunit FakA	300.4	414.08	34.03	132	1.394456625	0.003388922
SAUSA300_RS10245	SAUSA300_1873	*murT*	lipid II isoglutaminyl synthase subunit MurT	47.47	63.41	5.4	20.43	1.383188175	0.003741699
SAUSA300_RS06015	SAUSA300_1111	*rlmN*	23S rRNA (adenine(2503)-C(2))-methyltransferase RlmN	30.99	24.58	2.2	11.44	1.37462649	0.010331 72
SAUSA300_RS07885	SAUSA300_1444	*scpB*	SMC-Scp complex subunit ScpB	53.91	96.87	6.52	29.18	1.369529428	0.009255663
SAUSA300_RS10510			hypothetical protein	570.15	437.9	47.79	197.93	1.355984544	0.006946407
SAUSA300_RS12075	SAUSA300_2189	*rplF*	50S ribosomal protein L6	278.74	302.35	43.19	76.27	1.35369998	0.003358653

Table B-4 (Cont'd)

SAUSA300_RS07055	SAUSA300_1298		5-bromo-4-chloroindolyl phosphate hydrolysis family protein	90.72	120.45	9.78	41.59	1.347639201	0.006393396
SAUSA300_RS08555	SAUSA300_1569		U32 family peptidase	30.94	38.71	3.9	12.58	1.328773323	0.004179148
SAUSA300_RS08475	SAUSA300_1555	*aroE*	shikimate dehydrogenase	20.01	19.31	2.41	6.61	1.328408177	0.005343835
SAUSA300_RS13525	SAUSA300_2440	*fnbB*	fibronectin-binding protein FnbB	33.42	36.99	5.83	8.01	1.325807162	0.007685236
SAUSA300_RS03525	SAUSA300_0657		DUF402 domain-containing protein	131.95	119.81	10.61	53.72	1.324846698	0.010740075
SAUSA300_RS10880			hypothetical protein	28.16	23.59	2.18	10.71	1.323400914	0.015076794
SAUSA300_RS13770	SAUSA300_2482		CHAP domain-containing protein	327.51	475.05	69.74	79.07	1.321758295	0.013171009
SAUSA300_RS03075	SAUSA300_0575		DUF1450 domain-containing protein	136.04	155.43	16.77	52.54	1.320392738	0.004002855
SAUSA300_RS12090	SAUSA300_2192	*rplE*	50S ribosomal protein L5	241.32	261.54	35.53	75.61	1.316847299	0.003248204
SAUSA300_RS09175	SAUSA300_1680		hypothetical protein	28.85	44.37	3.77	13.81	1.316413745	0.008367857
SAUSA300_RS06160	SAUSA300_1138	*sucC*	ADP-forming succinate--CoA ligase subunit β	39.79	75.45	5.34	22.88	1.316067708	0.012297821
SAUSA300_RS14005	SAUSA300_2524		TIGR04197 family type VII secretion effector	10.94	13.69	1.2	4.49	1.31119586	0.026708744
SAUSA300_RS08020	SAUSA300_1469	*argR*	transcriptional regulator ArgR	254.79	197.21	33.1	66.06	1.310396701	0.005868545
SAUSA300_RS12465			hypothetical protein	79.82	68.58	6.51	31.23	1.307818655	0.013808772
SAUSA300_RS04920	SAUSA300_0915		esterase family protein	28.33	35.56	2.92	13.15	1.306127155	0.010544027

Table B-4 (Cont'd)

SAUSA300_RS06570	SAUSA300_1211		hypothetical protein	198.09	152.7	16.71	72.57	1.299124566	0.011886151
SAUSA300_RS06655	SAUSA300_1228	*thrB*	homoserine kinase	39	34.08	4.04	14.12	1.288882425	0.007685236
SAUSA300_RS07355	SAUSA300_1349	*bshA*	N-acetyl-alpha-D-glucosaminyl L-malate synthase BshA	21.75	29.74	2.94	9.58	1.28633838	0.00702676
SAUSA300_RS00405			hypothetical protein	42.06	41.68	2.57	19.13	1.285264513	0.037556934
SAUSA300_RS02780	SAUSA300_0519		RNA polymerase sigma factor	12.82	11.18	1.2	4.68	1.284738694	0.017956927
SAUSA300_RS07450			hypothetical protein	38.79	36.93	5.6	11.16	1.28448471	0.013171009
SAUSA300_RS08900	SAUSA300_1631		replication initiation and membrane attachment family protein	44.25	49.64	4.2	20.37	1.280018335	0.012297821
SAUSA300_RS06625	SAUSA300_1222		thermonuclease family protein	47.49	55.81	4.64	22.12	1.279999427	0.013151395
SAUSA300_RS02840	SAUSA300_0531	*rpsG*	30S ribosomal protein S7	974.86	1209.2	162.63	325.5	1.277221364	0.004752685
SAUSA300_RS10445	SAUSA300_1908		membrane protein	67.43	75.87	5.72	32.43	1.276273141	0.018329865
SAUSA300_RS08295	SAUSA300_1520		tRNA (adenine(22)-N(1))-methyltransferase TrmK	21.48	25.09	1.83	10.5	1.267260338	0.021818 12
SAUSA300_RS06425	SAUSA300_1189	*mutL*	DNA mismatch repair endonuclease MutL	25.06	21.63	1.63	11.25	1.262983714	0.029577139
SAUSA300_RS07310	SAUSA300_1340	*recU*	Holliday junction resolvase RecU	96.49	110.36	12.52	38.73	1.261666313	0.005882961
SAUSA300_RS12115	SAUSA300_2197	*rplP*	50S ribosomal protein L16	219.55	216.18	34.63	62.4	1.254890186	0.007228347

Table B-4 (Cont'd)

SAUSA300_RS07415	SAUSA300_1360		demethylmenaquinone methyltransferase	100.37	106.38	7.9	48.88	1.254021602	0.023354301
SAUSA300_RS03560	SAUSA300_0663		hypothetical protein	149.88	205.1	10.32	88.81	1.25384121	0.040617602
SAUSA300_RS12085	SAUSA300_2191		type Z 30S ribosomal protein S14	354.72	342.18	58.41	92.01	1.252383913	0.009994056
SAUSA300_RS06225			hypothetical protein	364.19	664.67	71.03	167.17	1.250373186	0.010677443
SAUSA300_RS06205	SAUSA300_1147	*hslU*	ATP-dependent protease ATPase subunit HslU	61.98	88.15	8.16	30.34	1.247877063	0.009638217
SAUSA300_RS02720	SAUSA300_0508		UvrB/UvrC motif-containing protein	20.17	22.87	1.86	9.58	1.244763755	0.022624056
SAUSA300_RS14280	SAUSA300_2567	*arcC*	carbamate kinase	28.35	41.97	3.63	14.53	1.244717224	0.013177658
SAUSA300_RS03505	SAUSA300_0654	*sarX*	HTH-type transcriptional regulator SarX	32.61	33.33	4.17	12.09	1.241607397	0.011218307
SAUSA300_RS08920	SAUSA300_1635	*mutM*	bifunctional DNA-formamidopyrimidine glycosylase/DNA-(apurinic or apyrimidinic site) lyase	31.42	39.7	3.16	15.97	1.239891761	0.019075819
SAUSA300_RS04420	SAUSA300_0820		cysteine desulfurase	50.91	53.67	7.1	18.45	1.23887863	0.006064628
SAUSA300_RS08265	SAUSA300_1514		Fur family transcriptional regulator	52.06	34.23	5.53	16.08	1.225087199	0.017956927
SAUSA300_RS12095	SAUSA300_2193	*rplX*	50S ribosomal protein L24	260.5	225.81	41.81	65.15	1.224551786	0.013171009
SAUSA300_RS14320	SAUSA300_2574		hypothetical protein	15.17	23.43	1.76	8.39	1.22435182	0.029445073
SAUSA300_RS10145	SAUSA300_1857		SE1561 family protein	318.39	292.23	35.05	125.05	1.222208253	0.010896691

Table B-4 (Cont'd)

SAUSA300_RS14680	SAUSA300_2644	*rsmG*	16S rRNA (guanine(527)-N(7))-methyltransferase RsmG	18.02	22.15	2.46	7.7	1.221177741	0.012297821
SAUSA300_RS02315	SAUSA300_0432		sodium-dependent transporter	87.06	133.5	16.69	35.07	1.213364032	0.009638217
SAUSA300_RS12670	SAUSA300_2293	*corA*	magnesium/cobalt transporter CorA	29.36	32	2.08	15.47	1.213160134	0.040617602
SAUSA300_RS02835	SAUSA300_0530	*rpsL*	30S ribosomal protein S12	735.55	965.43	114.35	311.34	1.212672535	0.007131029
SAUSA300_RS10470	SAUSA300_1913	*pmtA*	phenol-soluble modulin export ABC transporter ATP-binding protein PmtA	41.88	54.31	5.71	19.38	1.206438904	0.011021615
SAUSA300_RS14240	SAUSA300_2559	*nsaR*	nisin susceptibility-associated two-component system response regulator NsaR	22.89	34.37	3.63	10.86	1.202127945	0.014199959
SAUSA300_RS06195	SAUSA300_1145	*xerC*	tyrosine recombinase XerC	84.99	86.97	7.95	40.15	1.201073232	0.021708573
SAUSA300_RS00220	SAUSA300_0041		hypothetical protein	19.36	14.3	1.17	8.53	1.199774158	0.048851336
SAUSA300_RS03735	SAUSA300_0696	*queD*	6-carboxytetrahydropterin synthase QueD	19.96	24.37	3.84	6.07	1.198927896	0.022523689
SAUSA300_RS02830	SAUSA300_0529		ribosomal L7Ae/L30e/S12e/Gadd45 family protein	511.03	693.13	97.37	182.64	1.196781397	0.010544027
SAUSA300_RS12475	SAUSA300_2258	*fdhF*	formate dehydrogenase subunit α	20.81	29.08	2.52	11.14	1.19365517	0.019075819
SAUSA300_RS07410	SAUSA300_1359		polyprenyl synthetase family protein	80.36	99.88	13.46	30.66	1.193036326	0.008587112
SAUSA300_RS12040	SAUSA300_2182	*infA*	translation initiation factor IF-1	135.03	118.68	19.89	41.42	1.189494372	0.012784 97

Table B-4 (Cont'd)

SAUSA300_RS03500	SAUSA300_0653		AraC family transcriptional regulator	27.41	29.36	3.45	11.73	1.184023304	0.011714796
SAUSA300_RS02185	SAUSA300_0407		superantigen-like protein SSL11	12.71	19.49	2.18	5.91	1.181097954	0.02045461
SAUSA300_RS12150	SAUSA300_2204	*rplC*	50S ribosomal protein L3	100.3	140.34	18.58	39.74	1.180865562	0.010918646
SAUSA300_RS02615	SAUSA300_0487	*tilS*	tRNA lysidine(34) synthetase TilS	30.35	41	3.81	15.72	1.180486675	0.01850741
SAUSA300_RS03785	SAUSA300_0704		ABC-F family ATP-binding cassette domain-containing protein	44.03	56.46	4.2	24.78	1.176623601	0.033205504
SAUSA300_RS12080	SAUSA300_2190	*rpsH*	30S ribosomal protein S8	341.79	321.9	62.37	82.95	1.174216686	0.022233967
SAUSA300_RS15905			hypothetical protein	194.38	167.85	17.01	86.2	1.170149598	0.031065572
SAUSA300_RS05430	SAUSA300_1009	*typA*	translational GTPase TypA	71.33	72.44	10.76	25.73	1.166293484	0.009638217
SAUSA300_RS09695	SAUSA300_1771		DUF1828 domain-containing protein	119.66	111.16	9.95	58.37	1.152749612	0.037717454
SAUSA300_RS12320	SAUSA300_2231	*fdhD*	formate dehydrogenase accessory sulfurtransferase FdhD	148.55	252.62	28.69	73.94	1.149986618	0.016791141
SAUSA300_RS11025	SAUSA300_2005	*tsaE*	tRNA (adenosine(37)-N6)-threonylcarbamoyltransferase complex ATPase subunit type 1 TsaE	24.98	35.4	2.57	14.83	1.148885744	0.045211561
SAUSA300_RS05375	SAUSA300_0998		XRE family transcriptional regulator	31.74	28.04	3.57	12.93	1.147416438	0.02373368
SAUSA300_RS10475	SAUSA300_1914		GntR family transcriptional regulator	50.96	54.39	8.23	18.34	1.14738694	0.015563226

Table B-4 (Cont'd)

SAUSA300_RS00135	SAUSA300_0026	*rlmH*	23S rRNA (pseudouridine(1915)-N(3))-methyltransferase RlmH	81.39	82.53	10.08	35.28	1.143342514	0.017545434
SAUSA300_RS05520	SAUSA300_1026		DUF177 domain-containing protein	1408.85	1628.89	153.02	729.17	1.142321273	0.026375528
SAUSA300_RS06185	SAUSA300_1143	*topA*	type I DNA topoisomerase	22.38	28.69	2.93	11.36	1.142306307	0.020254051
SAUSA300_RS11135	SAUSA300_2025		PP2C family protein-serine/threonine phosphatase	90.66	96.43	7.51	48.79	1.140625951	0.045722533
SAUSA300_RS04070	SAUSA300_0754		DUF4887 domain-containing protein	31.57	46.65	3.56	19.17	1.137056414	0.040902383
SAUSA300_RS08465	SAUSA300_1553	*nadD*	nicotinate (nicotinamide) nucleotide adenylyltransferase	34.8	40.1	3.4	18.51	1.136999294	0.038664002
SAUSA300_RS06060	SAUSA300_1120	*recG*	ATP-dependent DNA helicase RecG	22.94	27.39	2.75	11.61	1.136698 83	0.023385793
SAUSA300_RS06750	SAUSA300_1243		exonuclease subunit SbcC	35.47	26.68	4.61	11.82	1.133667703	0.018329227
SAUSA300_RS10980	SAUSA300_1997		sulfurtransferase TusA family protein	238.49	174.32	39.77	54.14	1.133582231	0.035077 68
SAUSA300_RS06270	SAUSA300_1158	*rimP*	ribosome maturation factor RimP	44.55	52.1	4.81	23.17	1.131858283	0.033082679
SAUSA300_RS05255	SAUSA300_0978		ABC transporter ATP-binding protein	25.48	34.9	3.08	14.38	1.128877854	0.031545527
SAUSA300_RS00415	SAUSA300_0081		TIGR04141 family sporadically distributed protein	26.27	28.9	2.61	13.76	1.125988829	0.036477 48
SAUSA300_RS04805	SAUSA300_0891		peptide ABC transporter substrate-binding protein	164.14	162.96	17.14	79.74	1.115766728	0.030017983

Table B-4 (Cont'd)

SAUSA300_RS12850	SAUSA300_2325		YbgA family protein	1266.06	1099.47	186.43	436.86	1.113251503	0.015836168
SAUSA300_RS12070	SAUSA300_2188	*rplR*	50S ribosomal protein L18	337.86	370.31	67.79	97.07	1.113241203	0.027131822
SAUSA300_RS03360	SAUSA300_0627		glycosyltransferase family A protein	75.41	99.25	8.99	42.82	1.105268315	0.034605756
SAUSA300_RS06405	SAUSA300_1185	*miaB*	tRNA (N6-isopentenyl adenosine(37)-C2)-methylthiotransferase MiaB	29.59	31.52	2.91	15.56	1.10340263	0.041811058
SAUSA300_RS02095	SAUSA300_0392		hypothetical protein	57.45	71.76	12.74	17.62	1.089216778	0.046819375
SAUSA300_RS06065	SAUSA300_1121	*fapR*	transcription factor FapR	30.23	53.79	6.74	14.99	1.083891117	0.033671936
SAUSA300_RS01160	SAUSA300_0221	*pflA*	pyruvate formate-lyase-activating protein	122.11	183.25	25.7	52.94	1.08216605	0.023291555
SAUSA300_RS05810	SAUSA300_1071	*bshC*	bacillithiol biosynthesis cysteine-adding enzymeBshC	44.68	78.38	9.52	23.21	1.078932507	0.02856935
SAUSA300_RS09810	SAUSA300_1792		AAA family ATPase	74.69	76.48	7.93	38.54	1.072779291	0.040617602
SAUSA300_RS02020	SAUSA300_0379	*ahpF*	alkyl hydroperoxide reductase subunit F	642.39	954.36	147.53	247.96	1.069844011	0.030156128
SAUSA300_RS05515	SAUSA300_1025		nucleotidyltransferase	22.61	35.18	3.63	13.25	1.057905641	0.037891511
SAUSA300_RS07350	SAUSA300_1348		CCA tRNA nucleotidyltransferase	18.14	20.57	3.12	7.55	1.047992951	0.027808317
SAUSA300_RS09220	SAUSA300_1687		DNA translocase FtsK	21.23	23.84	3.07	10.24	1.045253893	0.027886142
SAUSA300_RS09260	SAUSA300_1695		phosphotransferase family protein	383.86	419.38	42.82	209.49	1.04345534	0.047336317

Table B-4 (Cont'd)

SAUSA300_RS08000	SAUSA300_1465	*hemE*	alpha-ketoacid dehydrogenase subunit beta	35.74	46.72	6.11	17.44	1.041265361	0.02841327
SAUSA300_RS09760	SAUSA300_1783		uroporphyrinogen decarboxylase	27.93	34.77	3.77	15.39	1.032689086	0.043331707
SAUSA300_RS08445	SAUSA300_1549		ComEA family DNA-binding protein	11.26	13.04	1.76	5.24	1.027530569	0.047629476
SAUSA300_RS09570	SAUSA300_1749		DUF1433 domain-containing protein	54.34	42.18	7.05	21.44	1.021661185	0.045862518

Genes downregulated in sTS when compared to CSSC

Locus	Old locus	Gene	Product	TPM.1 sTS	TPM.2 sTS	TPM.1 CSSC	TPM.2 CSSC	DE Log2 FC	DE Adjusted *P*-value
SAUSA300_RS13360	SAUSA300_2413	*cntL*	D-histidine (S)-2-aminobutanoyltransferase CntL	2.8	1.24	42.35	67.31	-5.084086128	5.27E-26
SAUSA300_RS13040	SAUSA300_2361		putative metal homeostasis protein	2490.1	1355.85	51134.91	41439.61	-5.024874151	4.53E-22
SAUSA300_RS13355	SAUSA300_2412	*cntM*	staphylopine dehydrogenase CntM	1.51	0.99	16.89	38.39	-4.831891364	1.58E-29
SAUSA300_RS13325	SAUSA300_2406		MFS transporter	24.57	23.55	310.49	534.53	-4.662309168	9.76E-31
SAUSA300_RS04580	SAUSA300_0848		FAD/NAD(P)-binding protein	6.41	3.17	29.4	171.15	-4.368667787	7.41E-18
SAUSA300_RS06690	SAUSA300_1234	*rpsN*	30S ribosomal protein S14	142.38	80.88	991.64	2246.49	-4.253496035	2.38E-22

Table B-4 (Cont'd)

SAUSA300_RS01635	SAUSA300_0307		5'-nucleotidase, lipoprotein e(P4) family	12.1	13.51	160.97	150.13	-4.22739216	1.39E-18
SAUSA300_RS03000			hypothetical protein	188.34	169.37	2775.63	1589.92	-4.217603633	1.13E-14
SAUSA300_RS13340	SAUSA300_2409		ABC transporter permease	2.99	2.36	20.31	54.35	-4.199861087	4.75E-24
SAUSA300_RS03005		*vraX*	C1q-binding complement inhibitor VraX	6898.76	9175.19	130098.29	60616.24	-4.184492053	1.84E-13
SAUSA300_RS05540	SAUSA300_1029	*isdA*	LPXTG-anchored heme-scavenging protein IsdA	43.4	64.41	297.79	505.14	-3.514307723	4.09E-17
SAUSA300_RS13330	SAUSA300_2407		ABC transporter ATP-binding protein	3.45	3.47	11.71	53.39	-3.50199193	1.02E-14
SAUSA300_RS08880	SAUSA300_1628		amino acid permease	21.66	33.49	113.06	312.07	-3.435439103	1.97E-17
SAUSA300_RS13345	SAUSA300_2410		ABC transporter permease	18.61	12.47	59.12	204.03	-3.434548452	4.00E-15
SAUSA300_RS13350	SAUSA300_2411	*cntA*	staphylopine-dependent metal ABC transporter substrate-binding protein CntA	15.32	11.36	38.2	205.11	-3.386083399	7.58E-13
SAUSA300_RS09355	SAUSA300_1712	*ribE*	6,7-dimethyl-8-ribityllumazine synthase	54.44	42.98	240.59	334.73	-3.208032845	7.65E-13

Table B-4 (Cont'd)

SAUSA300_RS03315	SAUSA300_0618		metal ABC transporter substrate-binding protein	258.97	206.02	519.68	2555.86	-3.002466305	7.55E-11
SAUSA300_RS15375			hypothetical protein	240.53	184.21	1755.08	300.14	-2.977529774	2.63E-05
SAUSA300_RS15090			phenol-soluble modulin PSM-alpha-3	512.32	700.74	1880.69	4471.81	-2.959942807	1.13E-13
SAUSA300_RS15730			phenol-soluble modulin PSM-alpha-4	420.56	500.1	1439.61	3355.4	-2.956950307	7.48E-14
SAUSA300_RS15740			phenol-soluble modulin PSM-alpha-1	417.86	484.5	1294.02	3576.07	-2.955553758	7.92E-14
SAUSA300_RS12980	SAUSA300_2351	*adcA*	zinc ABC transporter substrate-binding lipoprotein AdcA	46.68	20.89	56.86	466.55	-2.952860287	3.23E-07
SAUSA300_RS15795		*pepA1*	type I toxin-antitoxin system Fst family toxin PepA1	440.19	391.97	2456.95	1290.29	-2.952268106	4.30E-07
SAUSA300_RS03665	SAUSA300_0683		DeoR/GlpR family DNA-binding transcription regulator	41.8	38.4	151.47	239.39	-2.943524601	5.60E-12
SAUSA300_RS15735			phenol-soluble modulin PSM-alpha-2	520.36	645.79	1675.5	4447.18	-2.931688449	1.13E-13
SAUSA300_RS00605	SAUSA300_0117	*sirA*	staphyloferrin B ABC transporter substrate-binding protein SirA	26.01	28.78	74.07	209.8	-2.890004889	2.89E-13

Table B-4 (Cont'd)

SAUSA300_RS13045	SAUSA300_2362		2,3-diphosphoglycerate-dependent phosphoglycerate mutase	618.45	564.86	1514.2	4828.17	-2.887349944	1.17E-12
SAUSA300_RS13850	SAUSA300_2493	*cwrA*	cell wall inhibition responsive protein CwrA	543.67	434.08	3279.08	941.3	-2.884622592	1.27E-05
SAUSA300_RS02195	SAUSA300_0409	*spn*	myeloperoxidase inhibitor SPIN	1033.96	769.97	4360.22	3178.19	-2.826992551	2.52E-07
SAUSA300_RS10530	SAUSA300_1920		chemotaxis-inhibiting protein CHIPS	755.37	557.66	1791.56	4444.32	-2.777613179	3.14E-11
SAUSA300_RS07015	SAUSA300_1291		amidohydrolase	19.38	18.26	63.58	90.07	-2.727134119	9.87E-10
SAUSA300_RS10275	SAUSA300_1878	*rlmD*	23S rRNA (uracil(1939)-C(5))-methyltransferase RlmD	17.23	22.95	86.77	64.72	-2.720040553	4.94E-07
SAUSA300_RS05795	SAUSA300_1068		beta-class phenol-soluble modulin	736.3	1082.15	3464.54	3534.23	-2.714539171	4.36E-08
SAUSA300_RS10485			hypothetical protein	71.49	73.87	375.59	160.57	-2.704770409	1.29E-05
SAUSA300_RS07010	SAUSA300_1290	*dapD*	2,3,4,5-tetrahydropyridine-2,6-dicarboxylate N-acetyltransferase	155.11	130.25	455.49	710.32	-2.702224538	7.26E-10
SAUSA300_RS01625	SAUSA300_0305		formate/nitrite transporter family protein	142.2	110.14	429.39	544.99	-2.657219054	1.82E-08

Table B-4 (Cont'd)

SAUSA300_RS03320	SAUSA300_0619		metal ABC transporter permease	91.33	78.8	167.19	603.2	-2.611758841	1.04E-09
SAUSA300_RS01620	SAUSA300_0304		DUF4064 domain-containing protein	16.7	15.97	41.54	89.51	-2.604771522	4.31E-10
SAUSA300_RS05570	SAUSA300_1035	*isdG*	staphylobilin-forming heme oxygenase IsdG	22.02	17.34	65.99	76.77	-2.579655241	1.85E-07
SAUSA300_RS15490			type I toxin-antitoxin system toxin PepG1	477.23	455.28	2420.73	678.54	-2.577771179	0.000116514
SAUSA300_RS05790	SAUSA300_1067		beta-class phenol-soluble modulin	1106.64	1728.55	4820.71	4917	-2.563896531	3.54E-07
SAUSA300_RS11570			hypothetical protein	5681.91	4107.36	21374.9	10774.7	-2.540979248	2.83E-05
SAUSA300_RS09670	SAUSA300_1767		gallidermin/nisin family lantibiotic	15.98	16.3	68.29	38.64	-2.534092969	2.65E-05
SAUSA300_RS01970	SAUSA300_0370	*selX*	staphylococcal enterotoxin-like toxin X	23.17	18.95	46.85	118.55	-2.522882501	1.94E-09
SAUSA300_RS03960	SAUSA300_0736	*raiA*	ribosome-associated translation inhibitor RaiA	4599.5	3956.35	17578.62	9706.41	-2.512502454	2.11E-05
SAUSA300_RS10555			hypothetical protein	414.3	365.63	1740.21	716.33	-2.508266241	6.60E-05

Table B-4 (Cont'd)

SAUSA300_RS11560	SAUSA300_2099	*czrB*	CDF family zinc efflux transporter CzrB	141.8	424.63	759.56	1273.14	-2.481461542	2.17E-06
SAUSA300_RS12545	SAUSA300_2269		hypothetical protein	191.99	166.1	573.51	583.69	-2.466327657	9.67E-07
SAUSA300_RS12715			hypothetical protein	33.08	30.07	113.65	82.31	-2.439049512	1.65E-05
SAUSA300_RS04395	SAUSA300_0815		DUF4888 domain-containing protein	69.18	67.74	84.03	531.89	-2.419905295	1.88E-06
SAUSA300_RS06940	SAUSA300_1278	*pepF*	oligoendopeptidase F	77.16	80.38	207.72	271.22	-2.355707981	3.51E-07
SAUSA300_RS07025	SAUSA300_1293	*lysA*	diaminopimelate decarboxylase	104.32	105.7	195.47	534.7	-2.355706834	6.34E-09
SAUSA300_RS04855	SAUSA300_0902	*pepF*	oligoendopeptidase F	42.9	53.23	87.93	218.14	-2.271933875	2.39E-08
SAUSA300_RS14010	SAUSA300_2525		fructosamine kinase family protein	24.57	20.05	62.37	62.14	-2.268664211	1.21E-05
SAUSA300_RS12865	SAUSA300_2328		DUF4889 domain-containing protein	390.68	307.86	1025.36	853.36	-2.247029225	3.44E-05
SAUSA300_RS05185	SAUSA300_0964		DUF5011 domain-containing protein	1344.95	1198.29	4004.37	2605.7	-2.240557187	9.67E-05

Table B-4 (Cont'd)

SAUSA300_RS00130	SAUSA300_0025	*adsA*	LPXTG-anchored adenosine synthase AdsA	4.83	4.47	11.14	14.81	-2.224498518	2.82E-06
SAUSA300_RS10185	SAUSA300_1865	*vraR*	two-component system response regulator VraR	111.81	117.53	277.59	350.5	-2.222222326	2.51E-06
SAUSA300_RS02705	SAUSA300_0505	*pdxT*	pyridoxal 5'-phosphate synthase glutaminase subunit PdxT	208.5	233.65	367.74	991.65	-2.197436211	7.09E-08
SAUSA300_RS04165	SAUSA300_0772	*clfA*	MSCRAMM family adhesin clumping factor ClfA	20.79	30.17	40.34	118.93	-2.194119213	2.33E-07
SAUSA300_RS13765	SAUSA300_2481		sterile alpha motif-like domain-containing protein	11244.19	9876.44	34671.29	16151.83	-2.168418284	0.000529061
SAUSA300_RS02365	SAUSA300_0442		YibE/F family protein	87.7	92.56	216.84	251.25	-2.167103753	8.38E-06
SAUSA300_RS10525	SAUSA300_1919	*scn*	complement inhibitor SCIN-A	3693.57	3390.7	7817.15	11222.06	-2.164778699	2.32E-06
SAUSA300_RS04565	SAUSA300_0845		M17 family metallopeptidase	44.82	45.34	93.39	150.85	-2.154971493	1.02E-06
SAUSA300_RS12480	SAUSA300_2259		LCP family protein	48.31	58.68	113.18	157.63	-2.101833959	5.48E-06
SAUSA300_RS03325	SAUSA300_0620		metal ABC transporter ATP-binding protein	378.55	283.98	422.23	1700.83	-2.097167098	6.77E-06

Table B-4 (Cont'd)

SAUSA300_RS06485	SAUSA300_1201	*glnA*	type I glutamate--ammonia ligase	341.1	347.9	459.62	1631.59	-2.088957463	1.34E-06
SAUSA300_RS12430	SAUSA300_2251		NAD/NADP-dependent octopine/nopaline dehydrogenase family protein	22.26	24.63	33.52	102.18	-2.074184097	8.89E-07
SAUSA300_RS11550	SAUSA300_2097		SDR family oxidoreductase	15.39	23.74	31.72	75.47	-2.073058115	2.11E-06
SAUSA300_RS04765	SAUSA300_0884		YjzD family protein	740.03	669.63	1986.21	1210.13	-2.072766933	0.00045621
SAUSA300_RS00215	SAUSA300_0040		hypothetical protein	5.84	7.06	16.36	14.43	-2.058583378	0.000317197
SAUSA300_RS13725	SAUSA300_2473		alpha/beta hydrolase	87.49	105.79	212.77	237.78	-2.035252592	3.94E-05
SAUSA300_RS13645	SAUSA300_2460		GNAT family N-acetyltransferase	106.56	94.05	252.13	188.12	-2.003367465	0.000411997
SAUSA300_RS03025	SAUSA300_0565		DUF423 domain-containing protein	70.71	78.56	171.64	157.52	-1.990628548	0.00017566
SAUSA300_RS05995	SAUSA300_1107		TM2 domain-containing protein	2190.76	1945.41	5682.01	2971.77	-1.984113099	0.001351833
SAUSA300_RS14175	SAUSA300_2551	*nrdD*	anaerobic ribonucleoside-triphosphate reductase	17.67	14.68	34.12	39.52	-1.976282154	8.36E-05

Table B-4 (Cont'd)

SAUSA300_RS01990	SAUSA300_0374		GlsB/YeaQ/YmgE family stress response membrane protein	2666.59	3344.13	6286.49	7095.9	-1.974138146	6.84E-05
SAUSA300_RS11520	SAUSA300_2091	*deoD*	purine-nucleoside phosphorylase	510.44	622.99	887.3	1889.62	-1.95839709	2.99E-06
SAUSA300_RS09015	SAUSA300_1652		universal stress protein	1143.03	989.51	2394.1	2210.15	-1.952065351	0.000256582
SAUSA300_RS16020			hypothetical protein	6646.76	5039.17	11754.97	14607.47	-1.94536573	9.04E-05
SAUSA300_RS09140	SAUSA300_1674		trypsin-like peptidase domain-containing protein	137.65	170.54	242.45	500.75	-1.945099422	4.14E-06
SAUSA300_RS01265	SAUSA300_0237		nucleoside hydrolase	25.16	24.34	50.02	59.68	-1.944052105	8.11E-05
SAUSA300_RS03335	SAUSA300_0622		M50 family metallopeptidase	61.66	69.85	140.33	140.73	-1.936603756	0.000179051
SAUSA300_RS14565	SAUSA300_2621		SMP-30/gluconolactonase/LRE family protein	11.04	13.25	27.91	22.36	-1.926173373	0.000573173
SAUSA300_RS06685	SAUSA300_1233	*rpmG*	50S ribosomal protein L33	7750.21	5201.14	16477.46	9467.32	-1.900792019	0.00218641
SAUSA300_RS14075	SAUSA300_2537		L-lactate dehydrogenase	153.26	133.22	241.49	410.57	-1.898492363	2.42E-05

Table B-4 (Cont'd)

SAUSA300_RS14670	SAUSA300_2642		DUF3147 family protein	11.3	4.5	16.61	19.99	-1.897774308	0.00157865
SAUSA300_RS09800	SAUSA300_1790		peptidylprolyl isomerase	361.94	372.49	476.97	1357.86	-1.894978207	6.32E-06
SAUSA300_RS13385	SAUSA300_2418		carboxymuconolactone decarboxylase family protein	109.83	138.64	235.12	291.71	-1.889078501	0.000103575
SAUSA300_RS08745			hypothetical protein	275.34	252.35	424.38	756.5	-1.865833571	2.68E-05
SAUSA300_RS13280	SAUSA300_2398	*fetB*	iron export ABC transporter permease subunit FetB	44.21	61.64	106.82	105.33	-1.859001088	0.000434876
SAUSA300_RS07195	SAUSA300_1321		bacilliredoxin BrxA	193.91	182.28	436.66	287.71	-1.856049223	0.001666507
SAUSA300_RS13975	SAUSA300_2518		alpha/beta hydrolase	18.41	17.86	28.75	51.73	-1.852317746	3.15E-05
SAUSA300_RS02890	SAUSA300_0541		deoxynucleoside kinase	134.85	145.95	239.82	357.12	-1.849793208	5.42E-05
SAUSA300_RS05095	SAUSA300_0948	*menB*	1,4-dihydroxy-2-naphthoyl-CoA synthase	245.75	209.05	423.47	509.88	-1.834799054	0.000234875
SAUSA300_RS10505	SAUSA300_1918		phospholipase	79.67	65.4	114.49	203.59	-1.828037314	6.60E-05

Table B-4 (Cont'd)

SAUSA300_RS04985	SAUSA300_0928		competence protein ComK	12.7	14.15	19.18	40.77	-1.819591096	3.36E-05
SAUSA300_RS07460	SAUSA300_1366		hypothetical protein	51.89	51.31	99.36	105.22	-1.807348439	0.000634316
SAUSA300_RS08320	SAUSA300_1525		glycine--tRNA ligase	326.21	369.09	460.2	1101.39	-1.805508328	1.56E-05
SAUSA300_RS04185	SAUSA300_0776		thermonuclease family protein	42.25	32.93	55.04	109.15	-1.792396052	7.24E-05
SAUSA300_RS04760	SAUSA300_0883		MAP domain-containing protein	70.88	89.42	121.11	211.71	-1.782988447	6.24E-05
SAUSA300_RS01655	SAUSA300_0310		PTS sugar transporter subunit IIC	215.89	191.53	354.35	455.82	-1.782003764	0.000262324
SAUSA300_RS00885	SAUSA300_0168	*isdI*	staphylobilin-forming heme oxygenase IsdI	65.39	59.74	108.81	139.86	-1.779195165	0.000299457
SAUSA300_RS14620	SAUSA300_2632		HdeD family acid-resistance protein	68.13	89.51	130.29	182.16	-1.773810679	0.0001905
SAUSA300_RS03030	SAUSA300_0566		amino acid permease	45.43	50.53	58.42	156.54	-1.767434199	2.70E-05
SAUSA300_RS00705	SAUSA300_0135		superoxide dismutase	265.49	304.7	528.37	543.46	-1.764391635	0.000670455

Table B-4 (Cont'd)

SAUSA300_RS02710	SAUSA300_0506		NupC/NupG family nucleoside CNT transporter	217.63	218.71	399.73	417.86	-1.751889824	0.000704809
SAUSA300_RS05245	SAUSA300_0976	*purD*	phosphoribosylamine--glycine ligase	45.13	49.13	68	118.94	-1.717598011	0.00010867
SAUSA300_RS03405	SAUSA300_0635		iron ABC transporter permease	75.53	67.21	109.02	170.19	-1.715867328	0.000223999
SAUSA300_RS07035	SAUSA300_1295	*cspA*	cold shock protein CspA	35505.41	24378.62	65893.82	36585.83	-1.706968213	0.007102539
SAUSA300_RS03635			hypothetical protein	118.33	113.91	207.18	212.52	-1.703052969	0.001262424
SAUSA300_RS07000	SAUSA300_1288	*dapA*	4-hydroxy-tetrahydrodipicolinate synthase	21.44	27.9	33.36	64.28	-1.692306711	0.000130572
SAUSA300_RS14170	SAUSA300_2550	*nrdG*	anaerobic ribonucleoside-triphosphate reductase activating protein	50.48	46.12	89.47	81	-1.691215066	0.002137734
SAUSA300_RS07160	SAUSA300_1314		YozE family protein	228.8	284.07	397.04	556.21	-1.686713441	0.000403211
SAUSA300_RS05340	SAUSA300_0991	*def*	peptide deformylase	239.26	284.4	332.95	694.29	-1.660757846	0.00010867
SAUSA300_RS14595	SAUSA300_2627		anion permease	120.67	108.5	191.18	213.23	-1.653514614	0.001374985

Table B-4 (Cont'd)

SAUSA300_RS04490	SAUSA300_0832	DUF86 domain-containing protein	44.88	45.73	67.64	97.59	-1.644470596	0.000573173
SAUSA300_RS04990	SAUSA300_0929	IDEAL domain-containing protein	1983.26	903.46	2511.05	2756.31	-1.640969217	0.004874 3
SAUSA300_RS10805		transcriptional regulator	30.13	30.49	43.65	67.39	-1.622088691	0.000887659
SAUSA300_RS06775	SAUSA300_1248	HesB/YadR/YfhF family protein	263.77	233.96	470.69	336.43	-1.620107987	0.006175256
SAUSA300_RS06835	SAUSA300_1258	2-hydroxymuconate tautomerase	1764.03	1415.14	3231.43	1800.33	-1.617697923	0.010331 72
SAUSA300_RS03035	SAUSA300_0567	threonine/serine exporter family protein	117.79	120.91	197.42	194.07	-1.587349791	0.003226298
SAUSA300_RS01090	SAUSA300_0207	M23 family metallopeptidase	48.26	53.9	80.85	88.84	-1.584196156	0.002339682
SAUSA300_RS04400	SAUSA300_0816	CsbD family protein	9469.14	12657.73	14167.41	25661.71	-1.584100205	0.000414747
SAUSA300_RS13155	SAUSA300_2378	membrane protein	85.53	111.63	91.35	306.56	-1.561080472	0.000496699
SAUSA300_RS10175	SAUSA300_1863	YtxH domain-containing protein	868.92	894.3	1264.96	1649.91	-1.540443059	0.001749293

Table B-4 (Cont'd)

SAUSA300_RS09040	SAUSA300_1656		universal stress protein	4000.78	4549.22	7380.44	5519.76	-1.531998422	0.008598472
SAUSA300_RS09440	SAUSA300_1726		CrcB family protein	20.91	21.89	30.37	39.66	-1.51521988	0.002996801
SAUSA300_RS03590	SAUSA300_0669		undecaprenyl-diphosphate phosphatase	143.51	169.22	193.67	334.22	-1.50631627	0.000902686
SAUSA300_RS14335	SAUSA300_2577	*manA*	mannose-6-phosphate isomerase, class I	35.29	38.3	51.85	64.49	-1.491225148	0.00320824
SAUSA300_RS04705	SAUSA300_0872		YisL family protein	177.63	150.33	234.22	286.46	-1.488899692	0.003891948
SAUSA300_RS04210			hypothetical protein	142.88	151.88	247.64	182.79	-1.485921019	0.011886151
SAUSA300_RS01890	SAUSA300_0356		cyclase family protein	35.26	39.75	52.5	62.54	-1.460960702	0.004533387
SAUSA300_RS05490	SAUSA300_1020		glycerophosphodiester phosphodiesterase	64.71	71.26	81.7	139	-1.453651462	0.001576888
SAUSA300_RS12820	SAUSA300_2320		DUF2871 domain-containing protein	300.47	267.74	471.95	326.05	-1.440472531	0.017451703
SAUSA300_RS07815	SAUSA300_1432		hypothetical protein	466.74	369.1	688.09	481.45	-1.426868523	0.019203661

Table B-4 (Cont'd)

SAUSA300_RS04685	SAUSA300_0868	*lepB*	signal peptidase I	215.3	244.14	324.62	340.62	-1.414555238	0.008097902
SAUSA300_RS12720	SAUSA300_2302		glycopeptide resistance protein TcaA	67.27	73.15	91.37	118.42	-1.40813734	0.0048743
SAUSA300_RS05680	SAUSA300_1053		formyl peptide receptor-like 1 inhibitory protein	103.34	135.89	163.96	177.55	-1.391949937	0.009159035
SAUSA300_RS14345	SAUSA300_2579		amidase domain-containing protein	61.69	65.69	72.91	124.99	-1.391829312	0.002522619
SAUSA300_RS12500	SAUSA300_2262	*sdpB*	CPBP family intramembrane glutamic endopeptidaseSdpB	115.62	131.32	138.46	245.35	-1.386155028	0.002424322
SAUSA300_RS06715			DNA damage-induced cell division inhibitor SosA	54.17	45.09	75.14	62.69	-1.382950861	0.019075819
SAUSA300_RS04720	SAUSA300_0875		metal-sulfur cluster assembly factor	2157.52	1858.45	3013.21	2486.78	-1.376334008	0.017956927
SAUSA300_RS05060			SAR1012 family small protein	117.31	122.81	157.56	189.8	-1.374804231	0.008367857
SAUSA300_RS01985	SAUSA300_0373		helix-turn-helix transcriptional regulator	528.79	356.82	674.57	540.83	-1.368071835	0.022823811
SAUSA300_RS10205	SAUSA300_1869	*map*	type I methionyl aminopeptidase	315.99	346.41	395.43	573.91	-1.354493125	0.00521982

Table B-4 (Cont'd)

SAUSA300_RS03045	SAUSA300_0569		heme-dependent peroxidase	408.44	464.95	547.41	699.71	-1.353228586	0.0071872
SAUSA300_RS00580	SAUSA300_0112		L-lactate permease	80.31	80.81	90.96	151.22	-1.352592372	0.003891948
SAUSA300_RS03825	SAUSA300_0712		peptide MFS transporter	361.77	349.19	446.1	552.59	-1.331649516	0.009270639
SAUSA300_RS04710	SAUSA300_0873		CoA-disulfide reductase	260.29	284.82	334.67	430.34	-1.327296927	0.008508348
SAUSA300_RS02430	SAUSA300_0454	*recR*	recombination mediator RecR	280.45	259.58	313.93	467.63	-1.324897022	0.006623051
SAUSA300_RS01560	SAUSA300_0292		hypothetical protein	194.91	162.79	274.73	179.25	-1.313861922	0.036533213
SAUSA300_RS09770	SAUSA300_1784	*traP*	signal transduction protein TRAP	1852.02	1751.65	2359.68	2513.71	-1.313810591	0.014563041
SAUSA300_RS02350	SAUSA300_0439		hypothetical protein	338.47	329.48	489.06	365.53	-1.310934537	0.029178439
SAUSA300_RS12530			hypothetical protein	134.68	141.35	174.82	202.07	-1.3101686	0.012913273
SAUSA300_RS09165	SAUSA300_1678		formate--tetrahydrofolate ligase	44.61	61.74	45.4	123.55	-1.30030608	0.003965203

Table B-4 (Cont'd)

SAUSA300_RS11360	SAUSA300_2063	*atpE*	F0F1 ATP synthase subunit C	123.74	133.08	148.28	212.29	-1.29800933	0.008599868
SAUSA300_RS03010	SAUSA300_0562	*thiD*	bifunctional hydroxymethylpyrimidine kinase/phosphomethylpyrimidine kinase	261.8	257.99	271.97	490.49	-1.297532703	0.004904817
SAUSA300_RS10935	SAUSA300_1989	*agrB*	accessory gene regulator AgrB	857.02	1101.23	1150.16	1544.07	-1.295519826	0.009638217
SAUSA300_RS05160	SAUSA300_0960	*qoxD*	cytochrome aa3 quinol oxidase subunit IV	1183.89	1388.16	1833.15	1402.26	-1.292802829	0.030017983
SAUSA300_RS14020	SAUSA300_2527		hypothetical protein	195.43	178.91	234.55	255.04	-1.261693849	0.020068907
SAUSA300_RS11310	SAUSA300_2054	*fabZ*	3-hydroxyacyl-ACP dehydratase FabZ	266.26	297.19	334.11	388.37	-1.23030086	0.019632788
SAUSA300_RS06360	SAUSA300_1176	*pgsA*	CDP-diacylglycerol--glycerol-3-phosphate 3-phosphatidyltransferase	286.65	259.49	332.74	348.56	-1.207979469	0.028796897
SAUSA300_RS09030			hypothetical protein	97.19	97.14	107.47	144.25	-1.196443392	0.021841334
SAUSA300_RS05470	SAUSA300_1017		DUF420 domain-containing protein	216.93	251.59	290.01	273.89	-1.19322767	0.035325655
SAUSA300_RS05050	SAUSA300_0940		DoxX family protein	613.49	450.74	674.12	617.32	-1.188234093	0.043394609

Table B-4 (Cont'd)

SAUSA300_RS13290	SAUSA300_2400		M42 family metallopeptidase	93.53	102.65	107.51	141.03	-1.185015768	0.020256411
SAUSA300_RS14105	SAUSA300_2541	*lqo*	L-lactate dehydrogenase (quinone)	854.76	1163.52	1221.75	1179.67	-1.178605822	0.037556934
SAUSA300_RS01870	SAUSA300_0353		ABC-2 transporter permease	127.18	125.67	153.17	147	-1.165101924	0.040283358
SAUSA300_RS05075	SAUSA300_0944		1,4-dihydroxy-2-naphthoate polyprenyltransferase	144.04	152.14	165.23	195.88	-1.15665721	0.029271275
SAUSA300_RS04575	SAUSA300_0847		PaaI family thioesterase	271.11	246.89	284.21	333.56	-1.122290299	0.037490909
SAUSA300_RS04545	SAUSA300_0841		NAD(P)/FAD-dependent oxidoreductase	225.3	213.5	235.12	287.7	-1.113804911	0.035548336
SAUSA300_RS11600	SAUSA300_2104	*glmS*	glutamine--fructose-6-phosphate transaminase (isomerizing)	88.9	132.72	96.78	188.62	-1.111734202	0.019413764
SAUSA300_RS10940	SAUSA300_1990		cyclic lactone autoinducer peptide	702.34	960.66	732.35	1307.69	-1.06846588	0.026476425
SAUSA300_RS11495	SAUSA300_2088		S-ribosylhomocysteine lyase	522.71	538.77	545.39	657.2	-1.054221759	0.048463664

Table B-5. Transporters differentially expressed in GSH, GSSG, and sTS.

Locus	Old locus	Gene	Product	DE Log_2 FC	DE Adj. *P*-value
Differentially expressed transporters in GSH					
SAUSA300_RS00925	SAUSA300_0176		ABC transporter permease	3.125833599	5.35039E-07
SAUSA300_RS00915	SAUSA300_0174		ABC transporter ATP-binding protein	2.989014416	3.54407E-07
SAUSA300_RS02340	SAUSA300_0437	*gmpC*	dipeptide ABC transporter glycylmethionine-binding lipoprotein	2.315679543	4.10697E-05
SAUSA300_RS02330	SAUSA300_0435		methionine ABC transporter ATP-binding protein	2.290401543	1.35302E-05
SAUSA300_RS00920	SAUSA300_0175		ABC transporter substrate-binding protein	2.282409423	0.000547181
SAUSA300_RS02335	SAUSA300_0436		methionine ABC transporter permease	1.995195436	0.001769395
SAUSA300_RS02315	SAUSA300_0432		sodium-dependent transporter	1.950671187	0.001418977
SAUSA300_RS02035	SAUSA300_0382		L-cystine transporter	1.838262363	0.00898218
SAUSA300_RS13025	SAUSA300_2359		transporter substrate-binding domain-containing protein	1.753694235	0.002677665
SAUSA300_RS01440	SAUSA300_0268		MFS transporter	1.728656723	0.013484163
SAUSA300_RS01055	SAUSA300_0200		ABC transporter ATP-binding protein	1.667394083	0.01218702
SAUSA300_RS01060	SAUSA300_0201		ABC transporter permease	1.524008315	0.020157954
SAUSA300_RS10985	SAUSA300_1998		YeeE/YedE family protein	1.304988845	0.030246065
SAUSA300_RS12890	SAUSA300_2333		nitrate/nitrite transporter	-3.275833554	7.74351E-10

Table B-5 (cont'd)

SAUSA300_RS01625	SAUSA300_0305		formate/nitrite transporter family protein	-2.826851365	5.35039E-07
SAUSA300_RS13325	SAUSA300_2406		MFS transporter	-2.73389307	1.70962E-06
SAUSA300_RS13340	SAUSA300_2409		ABC transporter permease	-2.695416261	3.1823E-07
SAUSA300_RS08880	SAUSA300_1628		amino acid permease	-2.497406008	1.33354E-06
SAUSA300_RS13345	SAUSA300_2410		ABC transporter permease	-2.068669945	0.000155603
SAUSA300_RS13280	SAUSA300_2398	*fetB*	iron export ABC transporter permease subunit FetB	-1.989683824	0.001769395
SAUSA300_RS13330	SAUSA300_2407		ABC transporter ATP-binding protein	-1.903394709	0.001594128
SAUSA300_RS12780	SAUSA300_2313		L-lactate permease	-1.51253439	0.015456886
SAUSA300_RS11560	SAUSA300_2099	*czrB*	CDF family zinc efflux transporter CzrB	-1.308531176	0.031701317
SAUSA300_RS07165	SAUSA300_1315		PTS glucose transporter subunit IIA	-1.275878242	0.03733
Differentially expressed transporters in GSSG					
SAUSA300_RS00925	SAUSA300_0176		ABC transporter permease	3.303313167	9.01551E-10
SAUSA300_RS00915	SAUSA300_0174		ABC transporter ATP-binding protein	2.830762445	9.05749E-09
SAUSA300_RS02340	SAUSA300_0437	*gmpC*	dipeptide ABC transporter glycylmethionine-binding lipoprotein	2.654314417	9.05749E-09
SAUSA300_RS00920	SAUSA300_0175		ABC transporter substrate-binding protein	2.408938291	4.67518E-06
SAUSA300_RS02035	SAUSA300_0382		L-cystine transporter	2.306320567	1.28398E-05

Table B-5 (cont'd)

SAUSA300_RS10985	SAUSA300_1998		YeeE/YedE family protein	2.196473104	7.51319E-07
SAUSA300_RS01055	SAUSA300_0200		ABC transporter ATP-binding protein	2.136824537	6.18049E-06
SAUSA300_RS02315	SAUSA300_0432		sodium-dependent transporter	2.108173714	2.0706E-06
SAUSA300_RS02335	SAUSA300_0436		methionine ABC transporter permease	1.986024342	5.44287E-05
SAUSA300_RS02330	SAUSA300_0435		methionine ABC transporter ATP-binding protein	1.982114069	7.69607E-06
SAUSA300_RS13025	SAUSA300_2359		transporter substrate-binding domain-containing protein	1.868432696	5.3321E-05
SAUSA300_RS01060	SAUSA300_0201		ABC transporter permease	1.815353512	0.000587577
SAUSA300_RS01440	SAUSA300_0268		MFS transporter	1.732819023	0.000196649
SAUSA300_RS03880	SAUSA300_0721		siderophore ABC transporter substrate-binding protein	1.435417673	0.021157034
SAUSA300_RS13020	SAUSA300_2358		amino acid ABC transporter permease	1.377126022	0.040614674
SAUSA300_RS13015	SAUSA300_2357		amino acid ABC transporter ATP-binding protein	1.279374623	0.013517702
SAUSA300_RS13340	SAUSA300_2409		ABC transporter ATP-binding protein	-2.76312879	3.44703E-09
SAUSA300_RS06690	SAUSA300_1234	*rpsN*	ABC transporter permease	-2.642568704	3.35575E-08
SAUSA300_RS07010	SAUSA300_1290	*dapD*	amino acid permease	-2.520651649	2.56794E-08
SAUSA300_RS07015	SAUSA300_1291		MFS transporter	-2.326963795	6.21097E-07

Table B-5 (cont'd)

SAUSA300_RS01625	SAUSA300_0305		nitrate/nitrite transporter	-2.081032901	1.90088E-05
SAUSA300_RS05195	SAUSA300_0966	*purE*	formate/nitrite transporter family protein	-2.066362184	7.22394E-06
SAUSA300_RS13345	SAUSA300_2410		staphylopine-dependent metal ABC transporter substrate-binding protein CntA	-1.806048803	0.00029532
SAUSA300_RS13860	SAUSA300_2495	*copZ*	ABC transporter permease	-1.799606649	0.004998035
SAUSA300_RS14075	SAUSA300_2537		L-lactate permease	-1.396183733	0.005316458
Differentially expressed transporters in sTS					
SAUSA300_RS00915	SAUSA300_0174		ABC transporter ATP-binding protein	3.34231159	1.77E-13
SAUSA300_RS00925	SAUSA300_0176		ABC transporter permease	3.098636848	1.70E-08
SAUSA300_RS02330	SAUSA300_0435		methionine ABC transporter ATP-binding protein	2.95296498	1.52E-11
SAUSA300_RS11605	SAUSA300_2105		PTS mannitol transporter subunit IICB	2.697969241	2.47E-05
SAUSA300_RS02335	SAUSA300_0436		methionine ABC transporter permease	2.573132474	1.07E-07
SAUSA300_RS13025	SAUSA300_2359		transporter substrate-binding domain-containing protein	2.502235403	3.10E-09
SAUSA300_RS01060	SAUSA300_0201		ABC transporter permease	2.500861509	1.50E-06
SAUSA300_RS00920	SAUSA300_0175		ABC transporter substrate-binding protein	2.331970676	7.16E-06
SAUSA300_RS02340	SAUSA300_0437	*gmpC*	dipeptide ABC transporter glycylmethionine-binding lipoprotein	2.298614243	2.06E-06

Table B-5 (cont'd)

SAUSA300_RS09895	SAUSA300_1808		ABC transporter permease subunit	2.268943961	1.29E-05
SAUSA300_RS01065	SAUSA300_0202		ABC transporter permease	1.888041935	0.000125814
SAUSA300_RS01055	SAUSA300_0200		ABC transporter ATP-binding protein	1.68588224	0.000393937
SAUSA300_RS13020	SAUSA300_2358		amino acid ABC transporter permease	1.590410837	0.003709448
SAUSA300_RS02035	SAUSA300_0382		L-cystine transporter	1.528200303	0.004872848
SAUSA300_RS10985	SAUSA300_1998		YeeE/YedE family protein	1.51993081	0.001033925
SAUSA300_RS12845	SAUSA300_2324		sucrose-specific PTS transporter subunit IIBC	1.456119968	0.004064768
SAUSA300_RS02315	SAUSA300_0432		sodium-dependent transporter	1.213364032	0.009638217
SAUSA300_RS12670	SAUSA300_2293	*corA*	magnesium/cobalt transporter CorA	1.213160134	0.040617602
SAUSA300_RS10470	SAUSA300_1913	*pmtA*	phenol-soluble modulin export ABC transporter ATP-binding protein PmtA	1.206438904	0.011021615
SAUSA300_RS05255	SAUSA300_0978		ABC transporter ATP-binding protein	1.128877854	0.031545527
SAUSA300_RS04805	SAUSA300_0891		peptide ABC transporter substrate-binding protein	1.115766728	0.030017983
SAUSA300_RS13325	SAUSA300_2406		MFS transporter	-4.662309168	9.76E-31
SAUSA300_RS13340	SAUSA300_2409		ABC transporter permease	-4.199861087	4.75E-24
SAUSA300_RS13330	SAUSA300_2407		ABC transporter ATP-binding protein	-3.50199193	1.02E-14

Table B-5 (cont'd)

SAUSA300_RS08880	SAUSA300_1628		amino acid permease	-3.435439103	1.97E-17
SAUSA300_RS13345	SAUSA300_2410		ABC transporter permease	-3.434548452	4.00E-15
SAUSA300_RS13350	SAUSA300_2411	*cntA*	staphylopine-dependent metal ABC transporter substrate-binding protein CntA	-3.386083399	7.58E-13
SAUSA300_RS03315	SAUSA300_0618		metal ABC transporter substrate-binding protein	-3.002466305	7.55E-11
SAUSA300_RS12980	SAUSA300_2351	*adcA*	zinc ABC transporter substrate-binding lipoprotein AdcA	-2.952860287	3.23E-07
SAUSA300_RS00605	SAUSA300_0117	*sirA*	staphyloferrin B ABC transporter substrate-binding protein SirA	-2.890004889	2.89E-13
SAUSA300_RS01625	SAUSA300_0305		formate/nitrite transporter family protein	-2.657219054	1.82E-08
SAUSA300_RS03320	SAUSA300_0619		metal ABC transporter permease	-2.611758841	1.04E-09
SAUSA300_RS11560	SAUSA300_2099	*czrB*	CDF family zinc efflux transporter CzrB	-2.481461542	2.17E-06
SAUSA300_RS03325	SAUSA300_0620		metal ABC transporter ATP-binding protein	-2.097167098	6.77E-06
SAUSA300_RS13280	SAUSA300_2398	*fetB*	iron export ABC transporter permease subunit FetB	-1.859001088	0.000434876
SAUSA300_RS01655	SAUSA300_0310		PTS sugar transporter subunit IIC	-1.782003764	0.000262324
SAUSA300_RS03030	SAUSA300_0566		amino acid permease	-1.767434199	2.70E-05
SAUSA300_RS02710	SAUSA300_0506		NupC/NupG family nucleoside CNT transporter	-1.751889824	0.000704809
SAUSA300_RS03405	SAUSA300_0635		iron ABC transporter permease	-1.715867328	0.000223999

Table B-5 (cont'd)

SAUSA300_RS14595	SAUSA300_2627	anion permease	-1.653514614	0.001374985
SAUSA300_RS00580	SAUSA300_0112	L-lactate permease	-1.352592372	0.003891948
SAUSA300_RS03825	SAUSA300_0712	peptide MFS transporter	-1.331649516	0.009270639
SAUSA300_RS01870	SAUSA300_0353	ABC-2 transporter permease	-1.165101924	0.040283358